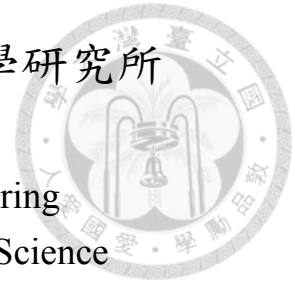國立臺灣大學電機資訊學院電信工程學研究所
博士論文
Graduate Institute of Communication Engineering
College of Electrical Engineering and Computer Science
National Taiwan University
Doctoral Dissertation

以賽局理論為基礎的無線網路資源管理機制
Game-Theoretic Resource Management in Wireless Networks

王志宇
Chih-Yu Wang

指導教授：魏宏宇博士和劉國瑞博士
Advisor: Hung-Yu Wei, Ph.D. and K.J. Ray Liu, Ph.D.

中華民國 102 年 6 月
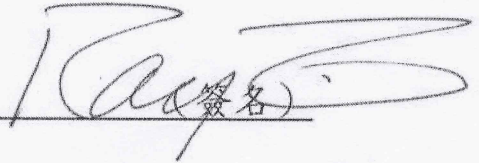June, 2013

國立臺灣大學博士學位論文
口試委員會審定書

以賽局理論為基礎的無線網路資源管理機制
Game-Theoretic Resource Management in Wireless Networks

本論文係王志宇君（D96942027）在國立臺灣大學電信工程學研究所完成之博士學位論文，於民國102年 6 月 19 日承下列考試委員審查通過及口試及格，特此證明

口試委員：

（指導教授）

所　　長　_____（簽名）

致謝

中文摘要

次世代無線廣域網路 (WWAN) 通訊標準，如 IEEE 制定的 802.16 (WiMAX) 和 3GPP 制定的 LTE-Advanced 標準，由於其承諾將達成由 ITU-R 所規畫的 4G 無線網路願境而在近期獲得眾多的關注。然而，在無線網路可用資源日趨匱乏的情況下，這些通訊標準採用了大量新技術以提升資源的使用效率。然而，在現實的各種限制下，這些新技術依然要面臨以有限的計算資源和處理時間內進行資源分配最佳化的挑戰。

無線網路裡的資源管理問題的困難點在於他們牽扯到參與者的自私行為與其之間的競爭關係。在無線網路的資源分配問題裡，由於資源有限，當有一參與者 (如手機、平板和基地台等) 取得較多資源時，其他參與者往往會失去部分資源。此特性使其問題自然的出現了競爭行為。當參與者受控或本身即為使用者時，我們可假定此類參與者為理性行為者，而理性行為者在競爭環境下往往會表現出自私的行為。此類行為和傳統處理資源分配問題的最佳化解法下假定所有參與者皆為了某共同目標而遵守系統指令相違背。若放任此類自私行為不管，傳統解法往往會面臨參與者行為不符預期且系統效能不彰的問題。近年來，將賽局理論應用於無線網路資源分配理論的相關研究日漸熱門。賽局理論是一套用來分析玩家之間的互動 (如競爭行為) 的數學理論工具。我們可以從賽局理論的角度來看待傳統的資源分配管理問題，並藉由賽局理論的分析和理論基礎提出嶄新的解決方案。此類方案應保持合理的效能、實作性，並能夠對自私行為進行有效的控管。

在本論文中，我們將探討異質網路、裝置對裝置通訊、以及群體廣播等最新的網路系統，將針對各個系統裡的資源管理問題，提出新穎的以賽局理論為基礎的方法論。我們所探討的系統都存在明顯的競爭環境，並在我們的分析中發現了有害的自私行為。因此，我們根據分析的結果和各個系統的特性，分別提出了可以有效管制自私行為的新穎解決方案。我們透過理論證明或模擬實驗的方式，驗證了這些解決方案在管制自私行為的同時，也保證了合理的系統效能和實作性。

在異質網路中，我們首先探討了微型基地台的涵蓋範圍問題，我們首先觀察到在此類問題中，微型基地台從自私使用者所收集到的資訊可能會有謊報而無法反映系統現況的問題。針對此類自私行為，我們提出了以投票機制為基礎的賽局機制設計，藉此確保自私使用者會選擇誠實回報他們所觀察到的系統狀況。接下來，我們分析在異質網路裡的微型基地台定價問題。我們證明了藉由最佳的差異化合約設計和微型基地台之間的搭配，我們可以有效地提升無線網路系統的服務品質，同時系統服務商的利潤也有顯著的提升。最後，我們探討頻帶集成的最佳規畫與設定問題。我們注意到在此類問題中，基地台一樣需要從使用者收集其心目中的服務質量需求，而自私的使用者一樣有可

能會藉由謊報而獲得不正當的利益。針對此問題，我們提出了以拍賣機制為基礎的設計，並以理論證明了自私使用者在此機制下會誠實地回報他們的服務質量需求。

在裝置對裝置通訊系統中，我們觀察到此類系統的點對點傳輸特性讓使用者更容易謊報他們所觀察到的資訊。同時，我們也注意到此類系統的傳輸品質可以藉由簡單的資源交換機制獲得提升。從這兩點出發，我們提出了以交換機制為基礎的賽局機制設計。此設計的運算複雜度低，達到的資源分配結果滿足柏拉圖最適，同時也保證了使用者會誠實地向基地台回報他們所觀察到的資訊。

最後，在群體廣播系統裡，我們首先討論了一個較抽象的社會學習與網路外部性問題。我們提出了一個新的賽局模型：中國餐廳賽局以處理這個問題。藉由分析這個賽局，我們可以預期自私使用者在有網路外部性的網路裡的最佳決策。從這個賽局模型出發，我們探討了在可伸縮編碼群體廣播系統裡的使用者影片訂閱問題。我們認為此類問題其實是一個網路裡的決策問題，並可以使用我們的中國餐廳賽局來分析。以此為出發點，我們提出了一個多維馬爾可夫決策過程來描述此系統的長期效能演進。我們的分析顯示，當我們在系統套用最佳定價時，我們不只最大化系統服務商的利潤，同時也提升了整個系統的社會福利。
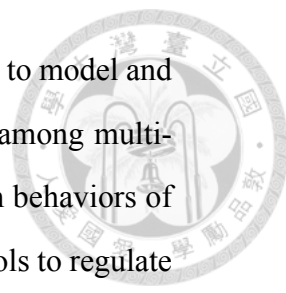
關鍵字：無線網路、資源管理、賽局理論、異質網路、裝置對裝置通訊、群體廣播、自私行為

Abstract

Next-generation wireless wide-area network (WWAN) standards, such as IEEE 802.16 and 3GPP LTE-Advanced, raised lots of attentions in these days since they are established for achieving the 4G standard requirements proposed by ITU-R [1], which illustrates a colorful vision for the future wireless communication. Nevertheless, the resource for wireless networking, such as spectrum, is very limited and difficult to expand. In order to fulfill this vision with limited resource, these new wireless standards introduce numerous advanced techniques to increase the resource utilization efficiency. Most challenges in these techniques can be transformed into resource allocation problems under the resource limitation constraints.
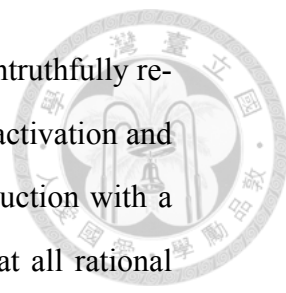
The resource management problems in wireless networks are difficult since they involve complex competitions and selfish behaviors from participants in the wireless networks. An operation that increases the participant's allocated resource inevitably reduces the resource for other participants, which results in competitions. Additionally, when the participants are or controlled by real humans, we can fairly assume that these participants are rational and therefore selfish. The competition effect and selfishness of participants in wireless networks imposes an serious threat to all existing solutions which are based on traditional perspectives, which usually inherent an assumption that all participants faithfully follow the orders of the system for some global objective. In recent years, researchers discovered that game theory is suitable for analyzing the wireless networking systems, especially for resource man-

agement problems. Game theory is a mathematical tool applied to model and to analyze the outcome of interactions, such as competitions, among multiple decision-makers. It can help analyze and predict the selfish behaviors of participants in wireless networks. It also provides a series of tools to regulate those undesired selfish behaviors and eliminate the performance degradation from the competition effects. By introducing game-theoretic approaches, we can propose novel solutions that are efficient, practical, and robust to the selfish behaviors of participants in wireless networks.

In this dissertation, we propose novel game-theoretic approaches to several resource management problems in the state-of-the-art wireless systems, which are heterogeneous networks, D2D communication, and multicasting system. Given the analysis based on game theory, we identify the potential threats from selfishness and propose novel solutions to each problem in order to address the selfish behaviors of participants while keeping reasonable efficiency and practicability. Extensive simulations are also executed for evaluating the performance of each proposed solutions.

In heterogeneous networks, we first study the femtocell coverage control problem. We first identify that the system information collected from them does not necessarily reflect the true status of the system due to the selfish nature of mobile stations. Thus, we design FEmtocell Virtual Election Rule (FEVER), a voting based mechanism that not only is proved to be truthful and has low implementation complexity, but also strikes a balance between efficiency and fairness to meet the different needs. Then, we study the femtocell service price problem in heterogeneous network. Femtocell technology can be used to improve service quality and increase profit by attracting customers. Meanwhile, differentiated contracts for different types of users also show great potential for profit increase. We show that by applying differentiated contracts in femtocell service. The profits of service providers can be significantly increased. Finally, we study the carrier aggregation mechanism

in LTE-Advanced system. We observe that selfish users may untruthfully report their QoS requirements in order to manipulate the carrier activation and resource block allocation. Therefore, we propose a truthful auction with a greedy resource allocation algorithm in order to guarantee that all rational UEs truthfully report their QoS requirements.

In D2D communication system, we observe that the ad-hoc characteristic of D2D communication poses the truth-telling issue into the system. Additionally, we find out that that the transmission quality in D2D communications can be significantly improved through a proper resource exchange. Based on this observation, we propose a Trader-assisted Resource Exchange (T-REX) mechanism, an exchange-based mechanism that converges in polynomial time and achieves Pareto optimal. We prove that all rational D2D pairs will truthfully report their information when the trader preference functions are properly designed.

Finally, in the multicastins system, we first discuss the general social learning problem in a network with exteranlity effects. We propose a game-theoretic framework called Chinese restaurant game. Through analyzing the Chinese restaurant game, we derive the optimal strategy of each agent and provide a recursive method to achieve the optimal strategy. Based on this framework, we analyze the scalable video coding multicasting system, which is an effective solution for video streaming services in wireless networks. We observe that the requests from users in such a system in fact is a social decision making problem and can be formulated with Chinese restaurant game. We propose a stochastic framework based on Multi-dimensional Markov Decision Process (M-MDP) to evaluate the corresponding system efficiency. We show that the optimal pricing strategy, which maximizes the expected revenue of the service provider, also increases the social welfare of the system.
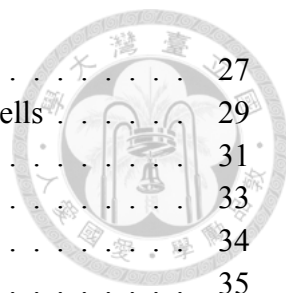
Keywords: wireless networks, resource management, game theory, heterogeneous network, device-to-device communication, multicast, selfish
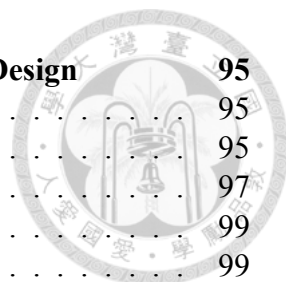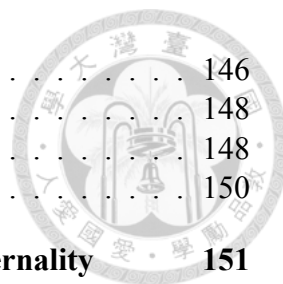
Contents

List of Figures

List of Tables

Chapter 1

Introduction

1.1 Motivation

Wireless networking experiences significant technique advances in recent decades. These advances, along with the accelerating deployments in all developed and most developing countries, is pushed by the increasing demands from the mass all over the world. Next-generation wireless wide-area network (WWAN) standards, such as IEEE 802.16 and 3GPP LTE-Advanced, raised most attentions in these days since they are established for achieving the 4G standard requirements proposed by ITU-R [1], which illustrates a colorful vision for the future wireless communication in every place, every moment. Nevertheless, the resource for wireless networking, such as spectrum, is very limited and difficult to expand. In order to fulfill this vision with limited resource, these new wireless standards introduces numerous advanced techniques, such as multi-input-multi-output (MIMO), orthogonal frequency-division multiple access (OFDMA), carrier aggregation (CA), heterogeneous networks, device-to-device (D2D) communications, multicasting/broadcasting services, and so on. Some of them are used for achieving ultra-high throughput, some are for maintaining service quality, and some are for increasing resource utilization efficiency. These techniques are technically guaranteed to boost the service quality of next generation wireless communications. Nevertheless, challenges still exist in applying these techniques in real world scenarios.
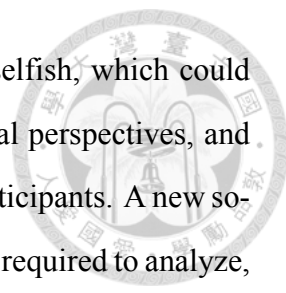
Traditionally, the challenges in applying these techniques are from two perspectives:

practicability and optimality, under the resource constraints. The practicability of a technique usually is the first to be addressed since a technique without a practical realization or implementation cannot be applied in real world at all. Optimality issue arises when we are interested in the optimal configuration in order to achieve the optimal yet theoretic performance. In many scenarios, there is a tradeoff between the solutions from these two perspectives. Most researchers focus on seeking a practical yet efficient solution for implementing the techniques. Nevertheless, all solutions are under the constraints of limited resource in wireless networks. Most challenges then can be transformed into a resource management problem: given the available resource, how and on what degrees the new technique can help improve the network performance?

We observe that there are some common characteristics in wireless network resource management problems. Let's consider a typical wireless network with user devices (mobilephones, tablets, etc.) and infrastructures (base stations, core networks, etc.) interact with each other through wireless communications. A participant's operation, such as requesting resource, reporting QoS requirements, or determining transmission power, may not only influence the service quality experienced by herself but also affects the ones experienced by others in the same network. Additionally, when the participants are controlled by real humans, we can fairly assume that these participants are rational. A rational participant's objective is to maximize her utility, which could be related to her experienced service quality, data delivery/reception amount, or even revenue/profit in the system. Given the fact that the resource is limited in wireless networks, an operation that increases the participant's allocated resource inevitably reduces the resource for other participants, and therefore degrades the service quality. The competition among the participants forms naturally. Combining the competition effect and rationality of participants together, the operations of these participants become selfish in wireless networks.
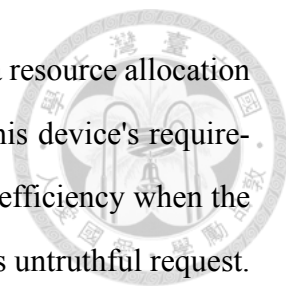
The selfishness of participants in wireless networks imposes an serious threat to all existing solutions which are based on traditional perspectives, especially for resource management problems. The solutions from traditional perspectives usually inherent an assumption that all participants faithfully follow the orders of the system for some global

objective. This assumption becomes invalid when participants are selfish, which could lead to 1) undesired operations which are unexpected from traditional perspectives, and 2) degraded system performance due to fierce competitions among participants. A new solution concept for wireless network resource management problems is required to analyze, predict, or even regulate these selfish behaviors in order to prevent undesired performance degradation.

Game-theoretic approach, a new perspective for wireless networking problems, can help analyze and predict the selfish behaviors of participants in wireless networks. Game theory is a mathematical tool applied to model and to analyze the outcome of interactions among multiple decision-makers. It has been shown to be a powerful tool for analyzing complex interactive system in economic and politic. Additionally, it also provides a series of tools to regulate those undesired selfish behaviors and eliminate the performance degradation from the competition effects. In recent years, researchers discovered that game theory is also suitable for analyzing the wireless networking systems. Recalling a typical wireless network with various participants interact with each other through wireless communications by following designed protocols. Some or all participants can be considered as players in the game, while the wireless communication techniques and designed protocols can be considered as the game rules. Finally, the service quality or performance experienced by participants can be considered their utility in the game. Following this formulation, we transform a wireless network resource management problem into a game. The behaviors of selfish participants can then be studied through the well-established solution concepts in game theory, such as best responses and Nash equilibrium. The undesired behaviors, such as untruthful information report, unfair competition, and other cheating actions, can then be identified.

By introducing game-theoretic approaches into the wireless network resource management problems, we potentially can propose novel solutions that are efficient, practical, and robust to the selfish behaviors of participants in wireless networks. Those undesired behaviors in wireless networks that are identified through game-theoretic analysis could be regulated by powerful tools provided in game theory. For instance, a device may request
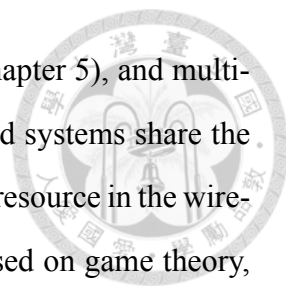
some resource with an amount exceeding the amount she required in a resource allocation process. Such a selfish behavior may increase the probability that this device's requirement is satisfied, but it also degrades the overall resource utilization efficiency when the resulting resource allocation deviates from the optimal one due to this untruthful request. A game-theoretic pricing design can be implemented in the resource allocation process to prevent such an issue. Through imposing a proper price on the resource, the requests from the devices will more likely reflect their true requirements since increasing their demands also lead to higher payment to them. Various game-theoretic techniques, such as voting, pricing, auction, and so on, can be applied on various resource management problems in wireless networks in order to regulate the undesired selfish behaviors and increase the system efficiency. Nevertheless, most of them also require further expansion or modifications in order to satisfy the practicability constraints in wireless networks.

Our objective is to understand the applications of game theory in various state-of-the-art wireless networks, such as heterogeneous networks, device-to-device communications, and multicasting system. In each system, we formulate the critical resource management problem as a game, and then identify the potential selfish and undesired behaviors of participants through game-theoretic analysis. Finally, we propose novel solutions to regulate these behaviors in order to increase the system efficiency while satisfying the practicability constraints. Both the theoretic improvements and limitations of game theory in different wireless network resource management problems will be thoroughly studied in this dissertation. In general, we show that game-theoretic approaches indeed benefit the wireless network by providing efficient, practical, and robust solutions to various resource management problems.

1.2 Dissertation Outline

In this dissertation, we first provide brief preliminaries on the wireless systems we would like to investigate and the basic game theory concepts we would apply in Chapter 1.4. Then, we propose novel game-theoretic approaches to several resource management problems in the state-of-the-art wireless systems in the following chapters, which are het-

erogeneous networks (Chapter 2, 3, and 4), D2D communication (Chapter 5), and multi-casting system with social learning (Chapter 6 and 7). All the studied systems share the same characteristic that devices may selfishly compete for the limited resource in the wireless system, as we illustrated in each chapter. Given the analysis based on game theory, we then propose novel solutions to each problem in order to address the selfish behaviors of participants while keeping reasonable efficiency and practicability. Finally, we draw our conclusions in Chapter 8.
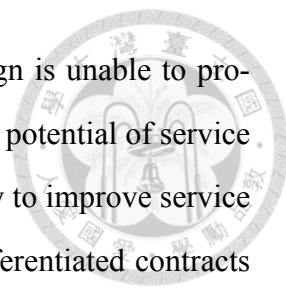
1.2.1 Cell-Breathing in Heterogeneous Networks: A Voting Approach (Chapter 2)

Overlay macrocell-femtocell system, a popular type of heterogeneous network, aims to increase the system capacity with a low-cost infrastructure. To construct such an infrastructure, we need to solve some existing problems. First, there is a tradeoff between femtocell coverage and overall system throughput, which we defined as the cell-breathing phenomenon. In light of this, we propose a femtocell downlink cell-breathing control framework to strike a balance between the coverage and data rate. Second, due to the selfish nature of mobile stations, the system information collected from them does not necessarily reflect the true status of the system. Thus, we design FEmtocell Virtual Election Rule (FEVER), a voting based direct mechanism that only requires users to report their channel quality information to the femtocell base station. Not only is it proved to be truthful and has low implementation complexity, but also strikes a balance between efficiency and fairness to meet the different needs. The simulation results verify the enhanced system performance under FEVER mechanism.

1.2.2 Service Price in Heterogeneous Networks: Optimal Contract Design (Chapter 3)

Most service providers offer an unlimited data service plan under a flat, fixed-rate contract to meet the huge demand. However, because service quality and user experience can

vary dramatically in wireless communications, such a contract design is unable to provide equal service quality for all users, which greatly limits the profit potential of service providers. As a result, mobile industries look to femtocell technology to improve service quality and increase profit by attracting customers. Meanwhile, differentiated contracts for different types of users also show great potential for profit increase. In this chapter, we investigate unlimited data service plans in terms of enhancements from both femtocell systems and differentiated contracts. The incentive compatibility (IC) issue in differentiated contract design is considered under the overlay macrocell-femtocell system in both split-spectrum and shared-spectrum models. The profits under optimal differentiated contracts, with and without the IC condition are compared to traditional flat fee contracts, and numerical results show that optimal differentiated contracts indeed generate more profits and serve more users.

1.2.3 Carrier Aggregation in LTE-Advanced System: An Auction Design (Chapter 4)

Carrier aggregation is introduced in LTE-Advanced for aggregating non-contiguous spectrum into a virtual carrier. UEs with carrier aggregation capability can increase their peak data rates by transmitting through the aggregated virtual carrier that virtually provides a larger transmission bandwidth. Nevertheless, it deserves further study on how carrier aggregation should be implemented and configured in order to address the diverse carrier quality experienced by UEs and their heterogeneous QoS requirements efficiently. Additionally, most existing resource allocation methods relies on the assumption that UEs always report their information truthfully, which may be unrealistic when UEs are rational from a game-theoretic perspective. In order to address the preceding concerns, we provide a utility-based game-theoretic approach to the carrier aggregation design in LTE-Advanced system. We first formulate the resource allocation problem in carrier aggregation as a non-linear optimization problem, which is proved to be NP-hard. Then, we propose a truthful auction with a greedy resource allocation algorithm in order to 1) find an efficient carrier activation and resource allocation solution under the QoS requirements

of UEs, and 2) guarantee that all rational UEs truthfully report their QoS requirements. Finally, we conduct extensive simulations in order to evaluate the system performance of the proposed auction design.

1.2.4 Device-to-Device Communications in LTE-Advanced System: A Resource Exchange Approach (Chapter 5)

Device-to-Device (D2D) communication could improve the efficiency of resource utilization in cellular networks by allowing nearby devices to communicate directly with each other. Nevertheless, one main challenge in D2D communication is resource allocation, given the diverse channel qualities of D2D devices. Additionally, when D2D devices and users are rational, then from a game-theoretic perspective, the ad-hoc characteristic of D2D communication poses the truth-telling issue into the system.

We observed that the transmission quality in D2D communications can be significantly improved through a proper resource exchange. Based on this observation, we propose a novel D2D resource allocation framework for an LTE- Advanced system. We theoretically prove that any arbitrary algorithm, either distributed or centralized, will converge in the proposed framework whenever all performed exchanges are beneficial. Based on the concept of beneficial exchange, we propose a Trader-assisted Resource Exchange (T-REX) mechanism, an exchange-based mechanism that converges in polynomial time and achieves Pareto optimal, as an efficient and flexible solution to the D2D resource allocation problem. The eNodeB regulates the D2D resource allocation through designing the trader preference functions in the T-REX mechanism. By applying game-theoretic analysis to the D2D communication system, we prove that all rational D2D pairs will truthfully report their information when the trader preference functions are properly designed. Finally, our simulation results show that the proposed T-REX mechanism significantly mitigates the interference experienced by D2D devices in LTE-Advanced systems.
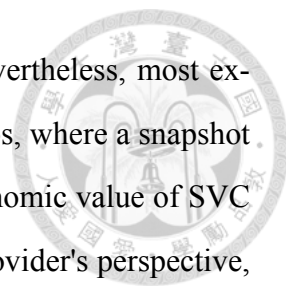
1.2.5 Chinese Restaurant Game: Social Learning vs. Network Externality (Chapter 6)
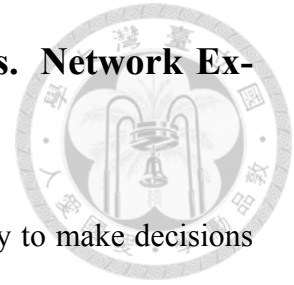
In a social network, agents are intelligent and have the capability to make decisions to maximize their utilities. They can either make wise decisions by taking advantages of other agents' experiences through learning, or make decisions earlier to avoid competitions from huge crowds. Both these two effects, social learning and negative network externality, play important roles in the decision process of an agent. While there are existing works on either social learning or negative network externality, a general study on considering both effects is still limited. We find that Chinese restaurant process, a popular random process, provides a well-defined structure to model the decision process of an agent under these two effects. By introducing the strategic behavior into the non-strategic Chinese restaurant process, we propose a new game, called Chinese Restaurant Game, to formulate the social learning problem with negative network externality. Through analyzing the proposed Chinese restaurant game, we derive the optimal strategy of each agent and provide a recursive method to achieve the optimal strategy. How social learning and negative network externality influence each other under various settings is studied through simulations. We also illustrate the spectrum access problem in cognitive radio networks as one of the application of Chinese restaurant game. We find that the proposed Chinese restaurant game theoretic approach indeed helps users make better decisions and improves the overall system performance.

1.2.6 Stochastic SVC Multicasting model using Chinese Restaurant Game (Chapter 7)

Heterogeneous multimedia content delivery over wireless networks is an important yet challenging issue. One of the challenges is maintaining the quality of service due to the scarce resource in wireless communications and heavy loadings from heterogeneous demands. A promising solution is combining multicasting and scalable video coding (SVC) techniques via cross-layer design which has been shown to be effectively enhancing the

quality of multimedia content delivery service in the literature. Nevertheless, most existing works on SVC multicasting system focus on the static scenarios, where a snapshot of user demands is given and remains the same. In addition, the economic value of SVC multicasting system, which is an important issue from the service provider's perspective, has seldom been explored. In this work, we study a subscription-based SVC multicasting system with stochastic user arrival and heterogeneous user preferences. A stochastic framework based on Multi-dimensional Markov Decision Process (M-MDP) is proposed to study the negative network externality existing in the proposed system and theoretically evaluate the corresponding system efficiency. A game-theoretic analysis is conducted to understand the rational demands from heterogeneous users under different subscription pricing schemes. By transforming the original dynamic and complex M-MDP revenue optimization problem into a traditional average-reward MDP problem, we show that the optimal pricing strategy which maximizes the expected revenue of the service provider can be derived efficiently. Moreover, the overall user's valuation on the system, e.g., social welfare, is maximized under such an optimal pricing strategy. Finally, the efficiency of the proposed solutions is evaluated through simulations.

1.3 Contributions of Dissertation

In summary, we made the following contributions in this dissertation:

Heterogeneous Networks

1. We are the first to study the cell-breathing phenomenon in heterogeneous networks. We propose a novel femtocell cell-breathing control framework for managing the load-balancing and coverage control among overlay cells.

2. Based on the cell-breathing framework, we formulate a game-theoretical model for discussing the cheating issue in overlay network with selfish mobile stations. We introduce the concept of voting theory into the cell-breathing control framework. The proposed voting-based FEVER mechanism is proved to be truthful. This truth-

ful strategies form a dominant-strategy Nash Equilibrium in FEVER mechanism, which can be easily implemented. In addition, we prove that FEVER mechanism offers the flexibility to strike a balance between capacity efficiency and allocation fairness.
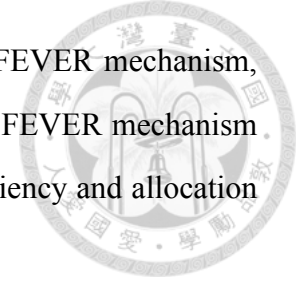
3. We propose a novel wireless service differentiation framework to investigate the profit service providers make under a variety of differentiated contracts in the heterogeneous system. This framework addresses the differences between wireless service quality among users, which is the basis of the service differentiation.

4. We draw a comparison between the shared-spectrum and split-spectrum systems in our service differentiation framework and have derived the optimal (profit maximizing) contracts under three schemes: flat fee contracts, differentiated contracts without incentive compatible concerns, and incentive compatible differentiated contracts. In a split-spectrum system, it is difficult to further extract profits from MSs as the only incentive compatible contract is a flat fee one. By contrast, in a shared-spectrum system, there are differentiated contracts generating profits by raising service prices for the MSs with good service qualities in femtocells, while providing cheaper prices to other MSs with poor service qualities.

5. We address the heterogeneous characteristics of carrier quality, coverage, and UE QoS requirements in the proposed game-theoretic approach to carrier aggregation mechanism. We make use of the carrier aggregation to enhance the system performance by satisfying the QoS requirements of UEs more efficiently. Specifically, we consider two type of UEs, throughput-sensitive and delay-sensitive UEs, in this work. The proposed solution effectively reduces the delay for delay-sensitive UEs while satisfying the throughput requirements of throughput-sensitive UEs. Additionally, we propose a truthful auction design specifically for the heterogeneous carrier quality and QoS requirements of UEs. We theoretically prove that the proposed design indeed provides proper incentive for the UEs to truthfully report their QoS requirements.

6. All proposed solutions for each problem in heterogeneous networks are evaluated through extensive simulations in our LTE-Advances simulator, which uses the models and parameters suggested in 4G evaluation document [1] and 3GPP LTE standard [2].
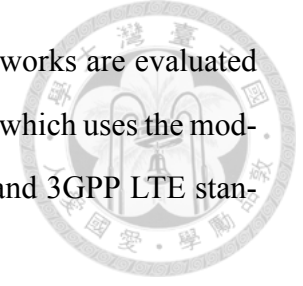
Device-to-device Communication

1. We propose a novel LTE-Advanced D2D resource allocation framework based on the resource exchange approach. We reuse most existing LTE-Advanced components and followed the same signalling flow logic in order to minimize the protocol impacts.

2. We theoretically prove that the resource exchange approach is equivalent to the traditional resource allocation approach in the solution feasibility. Additionally, we prove that any arbitrary algorithm, either distributed or centralized, will converge in the proposed framework whenever all exchanges are beneficial. To the best of our knowledge, we are the first group to present the resource exchange approach to the D2D resource allocation problem.

3. We propose the Trader-assisted Resource Exchange (T-REX) mechanism as an efficient and flexible solution to the D2D resource allocation problem in the proposed framework. The T-REX mechanism identifies the beneficial exchanges through analyzing the corresponding exchange graph. The algorithm's complexity is polynomial, which makes it a practical solution to large-scale D2D networks. In addition, the derived allocation is Pareto optimal; therefore, the efficiency is guaranteed. In addition, we prove that the T-REX mechanism is strategy-proof when the trader preference functions are properly designed.

4. All the proposed solutions were evaluated through the proposed LTE-Advanced D2D simulator, which uses the models and parameters suggested in the latest 3GPP technical contribution [3]. Our simulation results showed that the proposed T-REX mechanism significantly mitigates the interference experienced by D2D devices.

Additionally, the convergence of the proposed framework is verified and evaluated in the simulations.

Social Learning and Multicasting System

1. We propose a novel game, called **Chinese Restaurant Game**, to formulate the social learning problem with negative network externality by introducing the strategic behavior into the non-strategic Chinese restaurant process. Through analyzing the Chinese restaurant game, we observe that the timing of making decision significantly influences a participant's utility. We show that there exists a tradeoff between two contradictory advantages, which are making decisions earlier for choosing better actions and making decisions later for learning more accurate believes.

2. Chinese restaurant game is general enough to model various learning and decision making problems in social network, cloud computing, and wireless networks. We demonstrate how the model can be applied in real applications by studying the channel access and sensing problems in cognitive radio network. Through simulations, we show that both the sensing accuracy and utilities of network users are enhanced by applying the best strategies derived from Chinese restaurant game.

3. We develop a Markov decision process based stochastic framework to analyze the resource allocation in a SVC multicasting system with heterogeneous user demands. By considering the stochastic user arrival, such a framework is more general than the existing snapshot-based approaches in the literature.

4. We propose a game-theoretic model, which is based on Chinese restaurant game, to analyze the behaviors of heterogeneous users. We study how rational and intelligent users submit their demands, i.e., subscriptions, under two pricing schemes: one-time charge scheme and per-slot charge scheme, and derive the equilibrium conditions of the game. To the best of our knowledge, this is the first work bringing game theoretic analysis to the SVC multicasting system.

5. We theoretically evaluate the economic value of the SVC multicasting system. Specifically, we investigate the revenue-maximized policy and pricing strategies in both one-time charge and per-slot charge schemes. We propose an efficient algorithm to derive the optimal policy and pricing strategies of the SVC multicasting system. Both theory and simulation results confirm that the derived solution not only maximizes the expected revenue but also optimizes the social welfare.
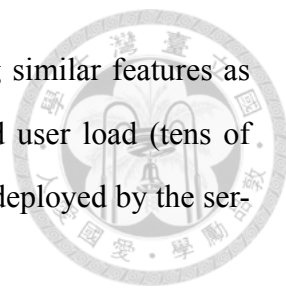
1.4 Preliminaries

1.4.1 4G Heterogeneous Networks

High system capacity is one of the fundamental requirements of wireless communication system. Various techniques have been proposed in WiMAX and LTE-Advanced (LTE-A) for enhancing the quality and transmission capacity such as Multi-Input Multiple-Output (MIMO), Carrier Aggregation (CA), and other techniques [4]. While most advanced signal and transmission techniques potentially enhance the performance of wireless systems [4], they eventually reach the theoretical limitation due to the physical laws: the signal quality. Most of next generation wireless networks are planned to operate in high frequency spectrum. In such spectrum, the signals will degrade significantly in long distance and indoor environments. This suggests that more areas will experience weak signal receptions unless the network deployment is densified.

In order to boost network capacity in a flexible and cost-efficient manner, the concept of Heterogeneous Networks (HetNets) has been introduced in LTE-A standard [5]. A heterogeneous network consists of macrocells, which are deployed for serving large coverage areas, and low-power and low-cost nodes such as picocells, femtocells, relay nodes, or remote radio heads (RRHs), which provide services in areas with dedicated capacity. The wireless signal quality can be greatly enhanced through the assistance from the low-power nodes when they are properly deployed in the coverage holes in the macrocells. Additionally, these low-cost nodes are more economically attractive as they usually require lower-cost infrastructure and lower requirements in terms of backhaul connections.

A typical HetNet in LTE-A is composed of lower-power base stations (BSs) underlying in the existing macrocell system. These small BSs are intended to increase the signal strength, offload the macrocells, and enhance the spectrum utilization. The deployment of HetNets can be planned and conducted by the service provider in advance, or requested and deployed by users themselves. The service area and operating spectrum of the small cells is usually partly or fully overlapping with the macrocell. Heterogeneous small cell base stations have been introduced in HetNets [5]. We briefly state as follows:

- **Picocells** are low-power (23 to 30dBm) cell towers providing similar features as macrocells except smaller coverage (hundreds of meters) and user load (tens of users). They use the same backhaul as the macrocells and are deployed by the service provider.

- **Relays** are small stations that deliver the data between macrocells and MSs in a multi-hop over-the-air scheme. They are mostly deployed by the service provider in order to extend the coverage of existing networks. A relay requires over-the-air backhaul capacity between macrocell BS and uses a similar transmit power as picocells.

- **RRHs** are radio control units that are connected directly to the macrocells through fibers but deployed with a distance from the macrocell BS. The macrocell has full control on the RRHs and operate them as its own wireless interface.

- **Femtocells** are also known as Home eNode Bs (HeNBs) in LTE systems [6]. A femtocell BS (femtoBS) can be regarded as a simple, low-transmission power (i.e. 23 dBm or less) base station installed by users in an unplanned manner. Through the deployment of femtoBSs, subscribers are able to access to networks via broadband backhaul. That is, femtocells may utilize Internet protocol (IP) and flat base station architectures. FemtoBSs may operate in open-access, closed-subscribed group (CSG), or hybrid-access scheme, depending on the choice of the cell owner.

In these possible choices of small cells, the femtocell has the following advantages: It increases indoor signal coverage and system capacity on demands, providing higher link quality with lower transmission power, and utilizes the existing broadband connection as its backhaul. Nevertheless, the femtocell system faces several challenges. Intercell interference, one of the most severe issues, takes place since femtoBSs typically operate in a licensed spectrum. Therefore, their coverage overlaps with other base stations in the same spectrum, as shown in Fig. 1.1, in which networks often suffer from interference. Additionally, the backhaul may also be an issue since it is likely that the femtocell operates in a broadband connection with limited quality of service (QoS), such as significant long
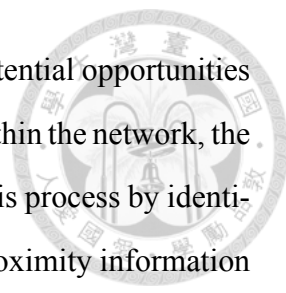
Figure 1.1: An illustration of Interference in Heterogeneous Networks

delay. The low QoS of relied connections may limit the ability of the service provider to control the femtocells in real time.

1.4.2 Device-to-Device Communications

Heterogeneous networks basically make use of the proximity gain from the user device to the base stations of small cells. There is another way to make use of the proximity gain by implementing device-to-device (D2D) communication [7] in cellular system. Traditionally, two cellular devices communicate with each other through multi-hop transmission, with base stations (BSs) as their intermediate infrastructure. Such a transmission scenario is inefficient in terms of both resource utilization and transmission delay when these two devices are in close proximity to each other. In D2D communication, two nearby devices to communicate with each other directly. This approach improves the transmission quality from the proximity [8], reduces the transmission delay by utilizing one-hop direct connection instead of two-hop cellular connection, and provides an extra dimension for resource reuse in the cellar system. 3GPP has begun to examine the service requirement for Proximity-based Services (ProSe), which is the D2D communications for LTE-Advanced, and then has started ProSe radio access network standardization recently [9]. Four service scenarios are considered: whether the devices are within and out of network coverage, and whether the devices are allowed to discover nearby devices only or could utilize direct communications with each others.

There are two major challenges in D2D communication: peer discovery and resource
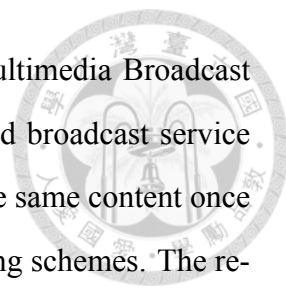
allocation [7]. D2D devices should have the ability to discover the potential opportunities to execute D2D communication with their peers. When devices are within the network, the BSs, or evolved Node-B (eNB) in LTE system, could participate in this process by identifying potential D2D pairs or providing (approximate) location and proximity information to devices. When devices are out of the network coverage, a distributed peer discovery function is necessary. Nevertheless, the accurate channel gain still needs to be measured through a proximity signalling technique, which requires further studies.

Resource allocation is another key challenge in D2D communications in a cellular system [7]. As specified by [7], D2D communications can be executed in unlicensed or licensed spectra. Although the former choice could utilize the existing wireless technology such as Wi-Fi and Bluetooth, it is relatively unreliable due to its openness to other out-of-system devices. For the latter choice, in which the resources utilized by D2D communications are dedicated resources (spectrum, resource blocks, etc.) licensed to the cellular system or a specific purpose (public safety, for instance) [10]. When devcies are within the network coverage, the BSs should regulate the resource allocation of D2D communications in order to prevent undesired interference to existing cellular users, and enhance resource utilization efficiency. When devices are out of the network coverage, they should have the ability to identify the available resource and reduce the potential interference to other devices in a distributed fashion.

1.4.3 Multimedia Multicasting System

Multimedia service is one of the most popular and fast growing applications in wireless networks. It is also the most challenging one since the loading generated by the multimedia content is much heavier than other services, along with more strict QoS requirements such as short delays. In some application scenarios, such as live broadcast streaming [11] or Internet protocol TV [12, 13], users in the same network request for the same multimedia content. In such scenarios, multicasting services could be applied to efficiently deliver the content to multiple users by making use the broadcasting characteristic of wireless communications.

The multicasting service has been standardized as Enhanced Multimedia Broadcast Multicast Services (E-MBMS) in LTE and Multimedia multicast and broadcast service (MBS) in WiMAX. The basic concept of multcasting is delivering the same content once to multiple users at once using relatively robust modulation and coding schemes. The resource for multicasting service could be either predefined in order to prevent unnecessary interference to existing unicast services, or opportunistically reuse when the interference is tolerable.

How the resource should be allocated for such an service is the main challenge and has been explored by numerous researchers. In brief, the resource should be efficiently allocated to different multicast group, which is determined by the demands, according to the diverse transmission quality experienced by users. Additionally, the service should have minimal impact on other traditional unicast services, which imposes a (dynamic) resource constraint on the multicasting service. Most researchers agree that a cross-layer design between wireless communication layer and application layer is necessary since the service quality highly depends on the quality of received multimedia content and preferences of users, which cannot be linked to the wireless communication performance in a straight-forward way. For instance, the users may be heterogeneous in experienced transmission quality, device capability, or preference on the video content/quality, which should be taken into account when configuring the mutlicasting service. The relation of wireless transmission performance to the multimedia content quality should also be carefully addressed in the cross-layer design. The relation usually depends on the multimedia encoding/decoding technique applied in the application layer. For instance, scalable video coding (SVC) [14] encodes a video into multiple layers. A basic-quality video can be derived by decoding the basic layer along, while higher quality video can be derived by decoding multiple layers in sequential order. This characteristic makes it a perfect match to multmedia multicasting service providing multiple qualities of multimedia contents.

1.4.4   Game Theory

Basic Game Elements

Game theory is a powerful tool applied to model and to analyze the outcome of inter-actions among multiple decision-makers. A traditional game consists of three basic elements: **players**, **strategies**, and **utilities**. Players are the participants and decision makers in the game. They can take some predefined **actions** to affect the interaction with other players and make influence on the final game result. Players are individual decision makers - given specified information (game rules, state of the system, applied actions of other players, etc) of the game, they apply strategies to decide the actions (reactions) taken in the game. Formally speaking, strategies are functions that map collected information to applied actions. The set of all possible strategies is defined as a strategy space, and the set of a possible combination of each player's strategy is called a strategy profile.

Given this information, players may apply different strategies when making decisions. With strategy profiles and related arguments, the game structure will produce a corresponding outcome. Outcomes can be considered as the results produced by an input strategy profile, which may carry different implications to different players. A player's evaluation of the outcome is given by a utility function. Utility functions, as quantified evaluations to the outcomes of a game, map the outcomes into real-value spaces. Since different game strategies may bring out different outcomes, we can see the element of utility as a function of a strategy evaluation. Under the framework of a game theory, the behavior of players' interactions can be properly modeled. The process may be also helpful to supply insights into the problems we investigate. For researchers in communication areas, game theory is very useful to analyze problems involving interactions among elements in the system, the resource allocation problem particularly.

In most cases, we assume that all players are rational. Thus, they tend to adopt strategy that can maximize their utility. In such games, every player is trying to maximize their own utility. Furthermore, if the players refuse to collude with each other, the game can be modeled as a non-cooperative game. In most game models, the purpose of the theoretic analysis is to find out the equilibrium, namely, the most likely produced outcome of a

steady state in the system.

Strategic Game and Nash Equilibrium

A strategic game is a type of games that all players behave simultaneously with perfect knowledge on other players' possible actions. Specifically, suppose that there is a game that involves two or more players, in which each player is assumed to know the actions of the other players. All players choose their actions simultaneously, and then the outcome of the game is also settled. In such a case, a rational player should predict what actions other players will choose <u>before</u> she chooses her action.

The expected outcome of the game can be found through finding the Nash equilibrium. Let's assume that there exists an action profile that after each player has chosen her action accordingly, no player can increase her utility from changing her action when other players' actions remain unchanged. If such an action profile is applied, no players have the incentive to deviate from the applied action since the deviation gives her equal or less utility. When the above conditions are met, the action profile constitutes a Nash equilibrium.

Using a typical HetNet system as an example, femtocells can be considered as the players in the strategic game, while their actions are their applied transmission power, occupied resources, or other operations that will potentially influence the service quality of other cells. Then, a femtocell's utility can be defined as the service quality, such as the throughput or delay time, experienced by UEs in the cell. An example is illustrated in Fig. 1.2, where multiple femtoBSs are determining their transmission power. Given other femtocell's transmission power, a femtocell may have her optimal transmission power that maximizes her utility. In such an approach, we would like to identify the stable outcome of the game, that is, the Nash equilibrium in the HetNet.

Strategic game approach is straight forwarding, but the results may not be appealing: the Nash equilibrium can be an inefficient outcome comparing to the optimal solution due to the competitive effect in strategic game. Some regulation designs, such as penalties on the femtocells, may be necessary to improve the system performance.

Figure 1.2: Strategic Game Approach to Heterogeneous Networks

Stackelberg Game and Subgame-Perfect Nash Equilibrium

The Stackelberg game is a sequential game specifically for the systems with hierarchical structure, which is a natural approach to the resource allocation in HetNets. In a Stackelberg game, two types of players, leaders and followers, are defined. In the game process, the leader should apply or announce her action first. Then, the followers response to the leader's action accordingly. Since all players are rational, the followers should choose their actions that maximize their own utility. By using this insight, the leader can predict the rational responses of the followers if she chooses certain actions. The leader then can choose her action that maximize her own utility based on her analysis on the rational response of the followers. The leaders, which should be macrocells in HetNets, have the advantages to apply their actions wisely before the followers, which are the femtocells in HetNets (Fig. 1.3). By strategically determining their applied action, the macrocells can lead the game to their desired outcome when they have enough information to predict the response of the femtocells in HetNets.

In a Stackelberg game, we will study the subgame perfect Nash equilibrium. Subgame perfect Nash equilibrium is a popular refinement to the Nash equilibrium under the sequential game. It guarantees that all players choose strategies rationally in every possible
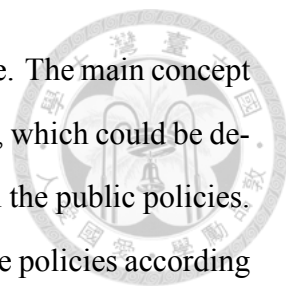
Figure 1.3: Stackelberg Game Approach to Heterogeneous Networks

subgame. A subgame is a part of the original game. In a typical leader-follower Stackelberg game, there are two subgames: the follower subgame and the leader subgame. The subgame perfect Nash equilibrium in Stackelber game can be found through backward induction: the Nash equilibrium of subgames in the follower subgame, in every possible outcome of the leader subgame, is derived first. Then, taking the Nash equilibrium of the follower subgame as the predicted responses of followers, the leader chooses her best strategy that maximize her expected utility in the leader subgame. The subgame perfect Nash equilibrium is then derived by combing the Nash equilibrium of follower subgame and the best responses of the leaders.

Stackelberg game is ideal for system involving central authority or hierarchical structures, such as HetNets consists of both macrocell and femtocells. Nevertheless, the requirements to fully understand the response of femtocells given any possible action of macrocell in Stackelberg game may be impractical when the HetNet is complex. In such a case, learning techniques, such as reinforcement learning, could be applied to help macrocell find her best strategy in the Stackelberg game.

Voting and Truth-telling

Voting is an important research topic in economics and politics. It is commonly used in today's society for determining important choice or policy which affects the mass, espe-

cially when individuals may have different preferences on the outcome. The main concept of voting that all voters have their own preferences on several policies, which could be defined in ranks. A voting is hold to aggregate all voter's preferences on the public policies. Then, a predefined voting rule determined the social preferences on the policies according to the aggregated preferences. This approach may be suitable for wireless networks when determining system parameters or choosing a configuration profile. The voters, which are the participants in the wireless network, deliver their preferences on the parameter/ configuration through feedback or control channels. The authority than determine the configuration according to the aggregated preferences.

The voting rule a critical design in voting. The most commonly used voting rule is the majority rule, which chooses the policy that most voters vote for. The concept is straightforward and easy to be implemented in real world, which makes it a popular choice of voting rules. Unfortunately, the majority rule has been proved to be untruthful and easy to be manipulated, which means that the outcome may be unfair and even not reflect the true preferences of majority. In addition, it has been shown by Arrow [15] that it is impossible to construct a voting rule that is non-dictatorship, Pareto efficient, and independence of irrelevant alternatives when voters could choose any of possible preferences on the policies, which means that unless the voting rule is dictatorship or inefficient, there always exists a method for voters to manipulate the outcome to their preferred one by alternate the reported preferences. The theorem therefore suggests that a truthful, non-dictatorship, and efficient voting rule only exists in a system with some restrictions on the preferences of voters.

Median Voter Scheme (MVS) is a popular truthful voting design. It is used to choose a public policy $r \in \mathbf{R}$ that can be one-to-one transformed into a real value set $\bar{R} \subset [0, 1]$. The procedure of MVS is as follows:

1. The election holder announces what order of the sorted votes he will choose (the median one, for instance.)

2. All voters vote for their most preferred policy v_i.

3. The election holder chooses the votes according to the rule he claimed before as the output of the election

Mathematically, given a sorted vote set $V = \{v | v_i \leq v_j \forall i < j\}$ in ascending order and a predetermined selected vote order κ, the output of MVS is v_κ. MVS is proved to be truthful when the preferences of voters are single-peaked, which means that a voter's preference on a policy v_i' is less when its distance to her most preferred one is larger. Such a preference structure is common in real word applications, such as the location of a hospital on the street, or the coverage of a cell, as we will illustrated in Chapter 2.

Mechanism Design

Mechanism design is a branch of game theory. System designers apply the techniques to design an algorithm or a procedure to achieve some good properties in the system . By using the techniques of mechanism design, the system can achieve several desirable properties. For example, the property of social welfare maximizes the utility summation of all players. Note that such rules are not against the players' nature of rationality and selfishness. That is, the players' decisions are still based on their own profits under the setup. Since mechanism design provides a set of elegant tools for a general system design, it is fairly suitable to apply the concept to wireless communication protocols or algorithm designs, especially when the element of players' interactions involves.

Vickrey−Clarke−Groves (VCG) mechanism is one of the most successful mechanism as it guarantees the truthful Nash equilibrium and achieves the optimal resource allocation at the same time. Nevertheless, the VCG mechanism has an unacceptably high complexity when the allocation problem is NP-hard, which make it impractical in some models.

In HetNets, for instance, mechanism design can be a powerful tool when the service provider or base stations would like to improve the efficiency of a system with rational players or prevent undesired cheating behaviors from the user devices. In a typical carrier assignment problem in cellular networks, for instance, the base station may request the carrier quality and QoS requirements of user devices in order to determine the efficient allocation. A user, if rational, may manipulate the allocation by reporting their information

untruthfully. When the manipulated allocation is more desired by the user, such as more assigned carriers and resource blocks, she then has the incentive to report information untruthfully. In such a case, mechanism design can take place to prevent these undesired outcomes.
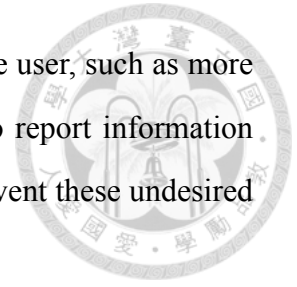
Chapter 2
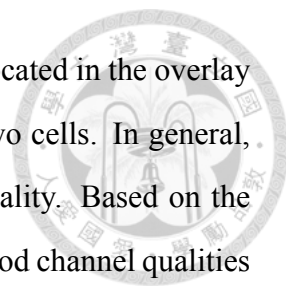
Cell-Breathing in Heterogeneous Networks: A Voting Approach

2.1 Introduction

Overlay macrocell-femtocell system aims to enhance the system capacity in a low-cost and self-organized manner [16]. A femtocell base station (BS) with low transmission power can be installed in indoor or natural environments to overcome macrocell's severe signal degradations. Since the mobile stations (MSes) in these environments are at relatively shorter distances from the femtocell than the macrocell, their signal qualities are enhanced with the lower radio propagation loss. Thus, the cellular system capacity is enhanced by the femtocell. In practical implementation, femtocell BSes are usually deployed by users themselves in an unplanned manner, and operate through existing personal broadband connections. These connections with limited data rates will be used as backhaul links of femtocells. Hence, the femtocell system should be self-organized in order to prevent unnecessary interference and resource wastes [17].

2.1.1 Cell-Breathing Phenomenon in Overlay System

Regarding efficiency, there is a tradeoff between system throughput and coverage in downlink scheme of overlay macrocell-femtocell system. We may examine an overlay

system with one macrocell and one femtocell as an example. MSes located in the overlay section of both cells can freely choose the serving cell from these two cells. In general, MSes' choices on the cells mainly depend on the offered service quality. Based on the system efficiency perspective, only a limited number of MSes with good channel qualities are supposed to be served by the femtocell. Other MSes should be served by the macrocell in order to preserve the limited femtocell resources.

The limitations on the femtocell resources come from two parts: wired backhaul data rate and wireless resources. The wired backhaul data rate becomes the limitation when femtocells operate through existing broadband connections with limited data rate compared to the macrocells deployed by the service operators. The wireless resources becomes the limitation when femtocells is only allowed to use limited wireless resources such as spectrum or access time since they usually operate in a lower coverage and loading on average comparing to the macrocells. Note that both limitations can be considered as the constraints on the capacity of the femtocells.

The cell-breathing phenomenon in overlay macrocell-femtocell system arises when the femtocell backhaul data rate becomes the stricter constraint of the femtocell throughput. When the backhaul data rate is the stricter constraints, those MSs served by the femtocell may experience a low throughput. It happens when the coverage of the femtocell is not properly configured. We illustrate an example in Fig. 2.1, where an overlay macrocell-femtocell system is serving five MSes. The femtocell BS has a 3Mbps backhaul connection. When the femtocell BS's downlink transmission power is P_1, it provides a small coverage and therefore only serves two MSes. Each of the MSes has a throughput of 1.5Mbps. The total backhaul data rate, which is 3Mbps, has been allocated to these two MSes. For other MSes, they are served by the macrocells. The overall achieved system throughput under P_1 is 5.4Mbps. Then, when the femtocell BS increases its downlink power from P_1 to $P_2(P_2 > P_1)$, the coverage of the femtocell increases. Four, instead of two, MSes can be served by the femtocell. The newly joined MSes will choose the femtocell as their serving cell since the femtocell provides a higher expected throughput ($0.5Mbps$) to them. Nevertheless, the original two MSes experience a lower throughput

Figure 2.1: Downlink Cell-breathing in an overlay macrocell-femtocell system

comparing to the data rate under P_1, which is because the overall femtocell throughput is constrained by the limited backhaul data rate. In such a case, the overall achieved system throughput is reduced to $3Mbps + 2Mbps = 5Mbps$. The efficiency loss is due to the unbalanced loading between the macrocell and femtocell. The increased femtocell coverage benefits some MSes originally served by the macrocell but degrades the data rates of other MSes who are already served by the femtocell. The backhaul resource utilization turns out to be inefficient when too many MSes choose to be served by the femtocell. In short, increasing femtocell downlink transmission power may result in the degradation of MSes' downlink throughput and impair the utilitarian of the overall system resource.

2.1.2 Selfish Behavior of MSes in Self-organized Femtocells
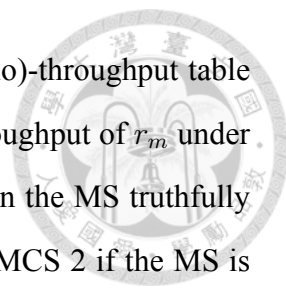
Because of femtocell's unplanned deployment characteristic, traditional optimization techniques cannot be applied before installations. Thus, femtocell system should be designed as a self-organized system. When the femtocell BS tries to organize and decide proper system parameters, such as downlink transmission power, comprehensive information on the overlay system, including the backhaul data rate and downlink channel quality information (CQI) of MSes, is required. To collect downlink CQI of MSes, the femtocell BS needs to request a CQI report from the MS to derive the information. However, since the choice of downlink transmission power is related to the CQI reported by MSes, this

Figure 2.2: Selfish Behaviors of MSes under traditional access policy

creates an issue in the self-organized system: selfish behavior of MSes.

Because MSes are distributed devices controlled by users, they are assumed selfish. Their behavior is based on their own benefits, which may be conflicted with the system optimization objective. In the femtocell system we discussed in the previous paragraph, there is a chance that MSes may report unauthentic CQI that does not reflect the true channel state but can persuade the femtocell to make the action that enhances the cheating MSes' benefits when the accessing rule is not properly designed.

Let us consider two traditional access policies and see how selfish MSes may choose to report fake CQI here: 1) The femtocell chooses to serve k MSes with worst channel qualities in macrocell. The femtocell downlink transmission power will then be adjusted to allow those users to be served by the femtocell. When an MS is selfish, it has the incentive to report a lower channel quality in CQI report since this fake report increases the probability that it can be served by the femtocell. 2) The femtocell chooses to serve k MSes with highest channel qualities in femtocell. In this case, MSes tend to report higher channel quality in CQI reports in order to increase the probability to be served by the femtocell. Specifically, a selfish MS tends to report an untruthful SNR in the CQI report which is a higher SNR that leads to the same modulation and coding scheme (MCS) as the one if the true SINR is reported. By reporting a higher SINR, the probability to be served by the femtocell increases, while the resulting throughput is still higher than the one under the macrocell.
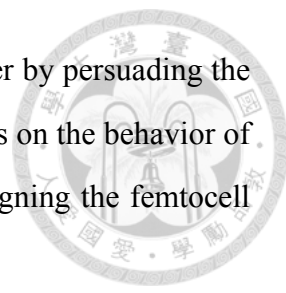
We illustrate a typical SINR(signal-to-interference-and-noise ratio)-throughput table in Fig. 2.2 as an example. Let us assume that a certain MS has a throughput of r_m under the macrocell service, and its SINR under the femtocell is Q_1. When the MS truthfully reports Q_1 in the SINR report, the MCS the femtocell will apply is MCS 2 if the MS is selected, and the resulting throughput is r_1 if no other constraint is imposed. Nevertheless, if the MS untruthfully report Q_2 instead of Q_1 in the SINR report, the resulting MCS is still MCS 2, and the resulting throughput remains r_1 since its true SINR is Q_1. This untruthful report does not degrade the throughput of the MS under the femtocell. Additionally, it increases the probability of the MS being served by the femtocell. Therefore, the rational MS has the incentive to cheat by reporting Q_2 instead of Q_1 in its SINR report.

In the above examples, we observe that rational MSes are likely to be cheated under traditional access policy. When the collected information does not reflect the true system status, the decision of the femtocell will deviate from the optimization choice due to the selfish behavior of MSes, which is not a desired situation from the system optimization perspective.

2.1.3 Subscriber Group Modes

Subscriber group mode is another important characteristic in the self-organized femtocell system. Since femtocell BSes are purchased and deployed by home or corporation users, these users may not be willing to share the service with other foreign users. Thus, a subscriber group can be optionally defined in the femtocell for access control. Three subscriber group modes are defined in the femtocell system: Open Subscriber Group (OSG), Closed Subscriber Group (CSG), and Hybrid mode [18]. In OSG mode, all users are allowed to access the femtocell service. In contrast, a femtocell in CSG mode only allows access to users in the subscriber group. As a balanced design between OSG and CSG, in Hybrid mode subscriber group users can access the femtocell service at any time, while non-subscriber group users can access it under a lower priority.

Although Hybrid mode offers a flexible resource allocation approach, the selfish behavior of MSes becomes a more serious issue under Hybrid mode because of different
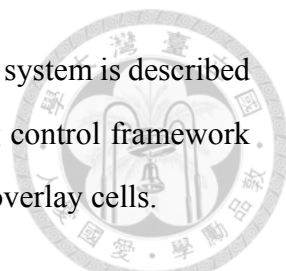
types of MSes. Different types of MSes may compete with each other by persuading the femtocell favoring one of the groups and blocking the other. Analysis on the behavior of MSes under different subscriber group modes is required when designing the femtocell self-organized mechanism.

In this work, we analyze the cell-breathing phenomenon resulting from the femtocell downlink power control through the proposed femtocell cell-breathing control framework. Due to the selfish behavior of MSes in a wireless network, we need a truthful CQI collecting mechanism to ensure the authenticity of the reported CQI from MSes. In addition, the mechanism should be functional in an environment lacking of an information sharing process among MSes since such a process is not available in general wide-area wireless network. To address these two requirements, we propose a **voting based FEmtocell Virtual Election Rule (FEVER)** mechanism, which only requires MSes to report their own private CQI to the femtocell. Voting, which has been popularly used in our daily life and well-studied in politic and economic areas, is an effective method to determine policies related to mass publics [19]. In voting process, the opinions of voters on a policy are collected through the voting process held by the authority, and the decision will be made based on the collected votes and predefined voting rules. We observe that this process highly matches our cell-breathing control framework - the femtocell's transmission power should be determined by the information (opinions) provided by the MSes. We prove that in FEVER mechanism, all MSes truthfully report their CQI without the incentive to manipulate. Additionally, FEVER mechanism provides the flexibility to satisfy different requirements in the balance between efficiency and fairness.

Finally, for the three subscriber group modes defined in femtocell system, we propose the Subscriber Group FEVER (SG-FEVER) mechanism. The objectives of SG-fever are: 1) ensuring the service quality of subscriber group users, and 2) maintaining the truthful characteristic of FEVER mechanism. We prove that SG-FEVER mechanism fulfill above two objectives, and it also inherits the flexibility of FEVER mechanism to strike a balance between efficiency and fairness.

The main contributions of this chapter are listed as follows.

1. The cell-breathing phenomenon in overlay macrocell-femtocell system is described and investigated. We propose a novel femtocell cell-breathing control framework for managing the load-balancing and coverage control among overlay cells.

2. We formulate a game-theoretical model for discussing the cheating issue in overlay network with selfish mobile stations. We introduce the concept of voting theory into the cell-breathing control framework. The proposed voting-based FEVER mechanism is proved to be truthful. This truthful strategies form a dominant-strategy Nash Equilibrium in FEVER mechanism, which can be easily implemented. In addition, we prove that FEVER mechanism offers the flexibility to strike a balance between capacity efficiency and allocation fairness.

3. For evaluating the system performance, a LTE overlay network simulator is implemented with realistic radio propagation and modulation models [1] [20]. The efficiency and fairness under different parameter settings in FEVER mechanism is verified through simulations. We further investigate and compare the three subscriber group modes under SG-FEVER mechanism with the LTE simulator. The characteristics of these three modes are demonstrated in realistic simulations.

2.2 Femtocell Cell-Breathing Framework

We start from an overlay macrocell-femtocell system. A macrocell BS serves MSes in its coverage area. One femtocell BS is located in the macrocell's coverage area, with one coverage area overlapping with the former one. Both BSes are operating with backhaul connections with certain data rates. For analysis simplification, the macrocell and femtocell use different spectrums in our model, so there is no inter-cell interference issue in the overlay system. Note that the main conclusion of this chapter is not affected even the cells share the same spectrum, which is discussed in Section 2.4.

We are focusing on the downlink wireless transmission of MSes in this chapter. There are N MSes $M_i \in S$ in the coverage of femtocell. An MS can be served by either the macrocell or femtocell. We denote the set of MSes served by the macrocell and the fem-

tocell by S_m and S_f, respectively. For a given cell $j = \{f, m\}$, the BS transmits downlink data to MSes by a power P_j in a carrier. For an MS M_i served by the cell j, its downlink SINR is $\eta_{i,j} = \frac{P_j G_{i,j}}{N_0 + I_{i,j}}$ where $G_{i,j}$ is the signal loss rate from cell j to M_i, N_0 is the background white noise, and $I_{i,j}$ is the location-dependent interference. We use $L_{i,j} = \frac{G_{i,j}}{N_0 + I_{i,j}}|_{j=\{m,f\}} \in \Lambda$ to denote the channel quality information (CQI) of M_i in cell j, where Λ is the universal set of CQI. For a given SINR $\eta_{i,j}$, we denote the wireless data rate from cell j to M_i by $\Gamma(\eta_{i,j})$, which is the PHY transmission rate in a typical wireless communication system. We assume $\Gamma(\cdot)$ is an increasing function, which is true in most modulation schemes.

2.2.1 Cell-Breathing Phenomenon

Given the same network scenario (macrocell BS's downlink power, all MSes' signal loss rates, etc), when the femtocell BS increases its downlink power P_f, we observe that there are two opposite influences on the MSes. On one hand, it enhances the wireless transmission qualities of MSes served by the femtocell. To be specific, an MS M_i's SINR $\eta_{i,f} = P_f L_{i,f}$ increases linearly with P_f, and its wireless data rate $\Gamma(\eta_{i,f})$ increases with P_f because $\Gamma(\eta_{i,f})$ is an increasing function (For convenience, we denote $\Gamma(P_f L_{i,f})$ by $\Gamma_{i,f}(P_f)$). On the other hand, because the downlink transmission in the femtocell is enhanced, some MSes may choose to select the femtocell instead of macrocell as their serving cell. Thus, MSes already served by the femtocell may have a lower expected throughput due to the joining of new MSes. The **cell-breathing phenomenon** is composed of these two effects. Note that this is different from the cell-breathing in CDMA system [21]. In the case of CDMA cell-breathing, an increase in the cell coverage results in a decrease in the cell's capacity due to interference among MSes in the same cell. In contrast, in OFDMA system the overall throughput in general increases with the transmission power until it is constrained by the wired backhaul data rate. However, the overlay system throughput may decrease when the femtocell's coverage increases since MSes may inefficiently choose the femtocell as their serving cell and therefore reduce the overall resource utilization.

Figure 2.3: Femtocell Cell-Breathing Control Framework

Additionally, the coverage of a femtocell should be self-organized according to the current cell deployment and resource availability of the overlay system. In traditional cellular networks, the cell coverage is usually properly planned by telecom operator in advance. On the contrary, femtocell base stations are typically deployed in an unplanned manner [16, 17]. In this chapter, we assume that the femtocell has been deployed by the user, and therefore the cell deployment is given in advance. In such a scenario, we consider the self-organized femtocell coverage control problem given that the femtocell base stations are already deployed. The optimal cell planning, which is another interesting issue, is beyond the scope of this chapter.

Due to the cell-breathing phenomenon, a proper choice on the P_f is important for femtocells to enhance the downlink transmission qualities of MSes while serving reasonable number of MSes. This requires CQI reported by MSes. Thus, we propose a cell-breathing control framework, which has four phases: **Information Collection, Femtocell Cell-breathing, Cell Selection, and Capacity Allocation phases** (Fig. 2.3).

2.2.2 Information and Cell-Breathing Control Phases

In Information Collection phase, the femtocell defines the information it requires, which we denoted as θ here. All MSes in the area report their information θ_i to the femtocell then. Next, in Femtocell Cell-Breathing phase, the femtocell decides P_f in accordance with the $\{\theta_i\}$ collected in the first phase. We denote a downlink cell-breathing rule B based

on the collected $\bar{\theta} = \{\theta_i\} \in \Theta^n$ by a function B:

$$B : \Theta^n \mapsto [0, P_f^{max}] \Rightarrow B(\bar{\theta}) = B(\{\theta_i\}) = P_f,$$

where θ_i is the information reported by M_i, Θ^n is the universal set of information, and P_f^{max} is the maximum power.

Since the information is only known by the MSes themselves and unknown to the femtocell BS, MSes may "cheat" by reporting false information to mislead the femtocell's choice on P_f. Cheating not only leads to unfairness in the system but also makes the femtocell choose an improper P_f and degrades the system performance. To prevent cheating, the downlink cell-breathing rule should be truthful, that is, after all selfish MSes learned the rule, they all choose to report the true information.

In this framework, the information is reported by MSes in the first phase, and then femtocell BS chooses the downlink transmission power in second phase. If the information required is MSes' preferred downlink power, these two phases naturally formulate a **voting scheme**, and the cell-breathing rule can be considered as a **voting rule**.

Median Voter Scheme (MVS) is a popular truthful voting design. It is used to choose a public policy $r \in R$ that can be one-to-one transformed into a real value set $\bar{R} \subset [0, 1]$. The procedure of MVS is as follows:

1. The election holder announces what order of the sorted votes he will choose (the median one, for instance.)

2. All voters vote for their preferred policy v_i.

3. The election holder chooses the votes according to the rule he claimed before as the output of the election

Mathematically, given a sorted vote set $V = \{v | v_i \leq v_j \forall i < j\}$ in ascending order and a predetermined selected vote order κ, the output of MVS is v_κ. Based on MVS, we propose the **Virtual Election scheme** for cell-breathing control in this framework. Given all MSes $M_i \in S$'s vote p_i on the femtocell downlink power P_f and a predefined selected vote order

κ, we denote the Virtual Election rule as

$$B_v(\bar{p}, \kappa) = B_v(\{p | p_i \leq v_j \forall i, j \leq N, i < j\}, \kappa) = p_\kappa \qquad (2.1)$$

2.2.3 Cell Selection and Capacity Allocation Phases

The expected throughput, which is the main concern of the MSes and is denoted by γ, is then determined in Cell Selection and Capacity Allocation phases. After femtocell BS chooses the downlink power in Cell-Breathing Phase, MSes select the cell to be served in Cell Selection phase. The MS's selection on the cell is based on the expected throughput under different cells, which will be determined in the Capacity Allocation phase, where femtocell and macrocell BSes allocate their backhaul capacity to the MSes they serve. The expected throughput of an MS is under the constraints of both wireless data rate and allocated backhaul data rate. Therefore, an MS should carefully choose the cell by considering both data rates in each cell.

In this framework, we assume the backhaul data rate of macrocell BS is large enough to handle all serving MSes' downlink request since it is deployed directly through the service provider. Mathematically, its backhaul data rate, which is denoted as C_m, is larger than the sum of serving MSes' wireless data rate $\sum_{M_i \in S_m} \Gamma(\eta_{i,m})$. Hence, for M_i requiring the data from the Internet, its expected throughput, which is denoted by $\gamma_{i,m}$, is always exactly its wireless data rate, that is, $\gamma_{i,m} = \Gamma(\eta_{i,m})$.

However, in the case of the femtocell BS, the allocation of available backhaul capacity becomes an issue. The data rate C_f of a femtocell backhaul connection is usually limited because it is installed at home or the office and using a broadband connection as its backhaul. It is possible that available resources cannot meet the total wireless data rate of all serving MSes, that is, $C_f < \sum_{M_i \in S_f} \Gamma(\eta_{i,f})$. Thus, the allocated downlink data rate of M_i under femtocell, which is denoted by $\gamma_{i,f}$, is less than or equal to $\Gamma(\eta_{i,f})$. Under this circumstance, not all MSes can have downlink transmission at their maximum achievable data rate. Thus, a predefined allocation rule is required. We denote an allocation rule to

allocate C_f to all MSes served by the femtocell by

$$A(\{\Gamma(\eta_{i,f})|M_i \in S_f\}) = \{\gamma_{i,f}|M_i \in S_f\}. \tag{2.2}$$

Each MS is allocated with a backhaul data rate $\gamma_{i,j}|_{j=\{m,f\}}$ according to their wireless data rate and the total backhaul data rate. A reasonable backhaul data rate allocated to an MS should not exceed its wireless data rate. Therefore, the allocated backhaul data rate is also its expected throughput under the cell. For femtocell BS, the allocation rule $A(\cdot)$ is applied to determine all MSes' expected throughput $\gamma_{i,f}$. Since fairness is typically a desirable property in the resource allocation problem, we consider a fair allocation rule $A(\cdot)$ in this framework. We define the fairness of the allocation rule $A(\cdot)$ as follows:

Assumption 1 (Max-min Fairness). *For an allocation rule $A(\{\Gamma(\eta_{i,f})|M_i \in S_f\}) = \{\gamma_{i,f}|M_i \in S_f\} = \gamma^f$, $\forall M_i$, $M_j \in S_f$, the following assumptions must be satisfied:*

$$if \exists \gamma'^f \neq \gamma^f,\ \gamma'_{k,f} > \gamma_{k,f}\ for\ some\ M_k \in S_f, \tag{2.3}$$

$$\Rightarrow \exists M_i \in S_f, \gamma'_{i,f} < \gamma_{i,f} \leq \gamma_{k,f}.$$

A straightforward thinking of this assumption is some backhaul capacity originally allocated to the existing MSes served by the femtocell may be reallocated to the new MS in order to ensure fairness. In fact, (2.3) is a general characteristic for a allocation rule with max-min fairness constraints [22].

In addition, we assume $\forall M_i \in S,\ \frac{C_f}{N} \geq \gamma_{i,m}$, which we call the capacity assumption. This catches the characteristics of femtocell deployment in real world: femtocells mostly are installed in the environments where the macrocell cannot offer good service qualities. In addition, a service provider may support a user to install a femtocell BS by upgrading the user's broadband connection in order to make the femtocell capable of accommodating multiple MSes. In Section 2.5.1, we show that the assumption can be relaxed when our objective is maximizing overall system throughput.

2.3 Game Model Formulation and Analysis
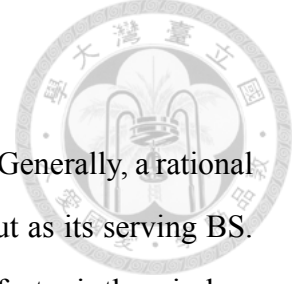
We now characterize MSes' behavior in the proposed framework. Generally, a rational MS should select the BS which offers the higher expected throughput as its serving BS. Notice that the expected throughput depends on two factors. The first factor is the wireless data rate of the serving MS, which is affected by the downlink transmission power of the BS. The second factor is the allocated backhaul data rate, which is determined by the amount of the backhaul resource that the BS will allocate to the MS. Specifically, the data rate the BS allocated to an MS depends on the channel quality under the cell and the number of MSes served by the cell. Since the expected throughput under a cell will be influence by the choice of other MSes, an MS's optimal choice will be determined by other MSes' decisions in Cell Selection phase.

These complicated interactions should be investigated in order to ensure the final operating point is the one we desire. Game Theory is an appropriate tool in formulating and analyzing such a system. We use Nash Game model to formulate the cell-breathing control problem. Nash Equilibrium of the cell-breathing control problem, which represents the stable operating point in the system, is analyzed.

In a Nash Game model, there are three components: **players**, **actions**, and **utility functions**. A player has various actions to choose from. After all players choose the actions simultaneously, the outcome of the game is decided, and their utilities are denoted by the utility functions with the outcome as input. To maximize a player's utility, he applies a **strategy** to choose specific actions under predefined conditions. Note that one's applied strategy may influence others' utilities and make them change their strategies as well,

Table 2.1: Notations

Notation	Explanation
S, S_f, S_m	The set of MSes (all, in femtocell, in macrocell)
$L_{i,\{f,m\}}$	The channel quality information (CQI) of M_i
P_f	The femtocell downlink power
$\eta_{i,\{f,m\}}$	The SINR experienced by M_i
$\Gamma(\eta_i)$	The wireless data rate of M_i under SINR η_i
$\Gamma_{i,f}(P_f)$	The wireless data rate of M_i from the femtocell under P_f
$A(\cdot)$	The femtocell's allocation rule on downlink data rate
$\gamma_{i,\{f,m\}}$	The expected throughput of M_i
$B(\cdot)$	The downlink cell-breathing rule

Figure 2.4: Two-Stage Game Model

which results in the instability of the system.

In the stable state of the game, any player should have chosen their **best response** to other players' currently applied strategies. If any single player is asked to change his strategy while others' remain unchanged, he sticks to his current strategy because changing his strategy decreases or makes no difference to his utility. This specified strategy combination forms a **Nash Equilibrium** (NE).

Definition 1 (Nash Equilibrium)**.** *In a Nash game with a player set P, each player p_i with a strategy space S_i and a utility functions u_i, a strategy combination $s^* = \{s_1^*, s_2^*, ..., s_n^*\}$ is a Nash Equilibrium if and only if $\forall p_i \in P, \forall s_i \in S_i$,*

$$u_i(s_i^*, s_{-i}^*) \geq u_i(s_i, s_{-i}^*)$$

where s_{-i}^* is the strategy combination $\{s_j^* | j \neq i\}$.

In addition, there is a special type of NE called **dominant-strategy Nash Equilibrium** (DSNE). In DSNE, given any combination of other players' strategies, a player's best response is always the same. Since a player's best response now is independent of other players' strategies, the implementation complexity is greatly reduced.

Definition 2 (Dominant-Strategy Nash Equilibrium)**.** *In a Nash game with a player set P, each player p_i with a strategy space S_i and a utility functions u_i, a strategy combination $s^* = \{s_1^*, s_2^*, ..., s_n^*\}$ is a dominant-strategy Nash Equilibrium if and only if $\forall p_i \in P, \forall s_i \in S_i, \forall s_{-i} \in S_{-i}$,*

$$u_i(s_i^*, s_{-i}) \geq u_i(s_i, s_{-i})$$

where s_{-i}^* is the strategy combination $\{s_j^*|j \neq i\}$ and S_{-i} is the strategy space of players despite p_i.

We formulate the femtocell cell-breathing control framework into a two-stage extensive-form Nash Game (Fig. 2.4). Stage 1 is Cell-Breathing stage, where we implement femtocell downlink cell-breathing mechanism in order to collect the private information (CQI, as an instance) of MSes. All MSes report their θ to the mechanism in this stage and then the mechanism chooses P_f. Stage 2 is Cell Selection stage, where MSes selecting their preferred BS. In both stages, all $M_i \in S$ are the players. Their strategy spaces are $\Theta \times \{M_i \in S_f, M_i \in S_m\}$, where Θ is the set of all possible state of private information in Stage 1, and $M_i \in S_j$ represents its choice in Stage 2. We denote the utility function of M_i by $u_i = \gamma_i$ where γ_i is M_i's expected throughput. This characterizes the MS as a selfish user seeking a higher throughput.

We follow the backward induction procedure to find the NE in the proposed two-stage Nash Game. First, we explore the NE in the Cell Selection subgame (composed of the cell selection stage only) regarding all possible outcomes of the previous stage. Then we move backward and check the NE in the game (composed of these two stages) given the NEs in the Cell Selection subgame. The NE we derive by following this procedure is a Subgame-Perfect Nash Equilibrium (SPNE).

2.4   Nash Equilibrium in Cell Selection Subgame

We first find the NE in the Cell Selection subgame. The following theorem describes the best response of M_i to select the cells under femtocell power p:

Theorem 1. *Under the allocation rule $A(\cdot)$ satisfying Assumption 1, M_i's best response in Cell Selection subgame is :*

$$\beta_i(p) = \begin{cases} M_i \in S_f, & if \, \Gamma_{i,f}(p) \geq \gamma_{i,m} \\ M_i \in S_m, & otherwise \end{cases} \tag{2.4}$$

In addition, given the MS set $S_f(p)$ under the downlink power p, $M_i \in S_f(p)$'s expected

throughput $\gamma_{i,f}$ is given below:

$$\gamma_{i,f} = \begin{cases} \Gamma_{i,f}(p), & if\, \Gamma_{i,f}(p) < \gamma_f(p) \\ \gamma_f(p), & otherwise \end{cases} \qquad (2.5)$$

where

$$\sum_{M_i \in S_f^u(p)} \Gamma_{i,f}(p) + |S_f^c(p)|\gamma_f(p) = \min\{C_f, \sum_{M_i \in S_f(p)} \Gamma_{i,f}(p)\}. \qquad (2.6)$$

$$S_f^u(p) = \{M_i | \Gamma_{i,f}(p) < \gamma_f(p)\}\, and\, S_f^c(p) = S_f(p) \setminus S_f^u(p)$$

Note that the best response of M_i is independent of other MSes' strategies. Thus, these best responses form a unique DSNE in the Cell Selection subgame: Each MS chooses to connect to the cell that offers the higher wireless data rate. This expected behavior is similar to the cell selection procedure in legacy wireless devices.

In Cell-Breathing stage, as we discussed in Section 2.2, the cell-breathing rule should be truthful in order to prevent cheating behavior in MSes.

Definition 3 (Truthful Rule). *A downlink cell-breathing rule $B(\bar{\theta})$ under $A(\{\Gamma(\eta_{i,f})|M_i \in S_f\})$ is truthful if $\forall M_i \in S_f$ with their true information $\bar{\theta}^*$, and $\forall \bar{\theta} \in \Theta^n$, $u_i(\gamma_{i,f}^*) \geq u_i(\gamma_{i,f})$, where $\{\gamma_{i,f}^{(*)}\} = A(\{\Gamma_{i,f}(B(\overline{\theta^{(*)}}))\})$.*

As shown in definition, the truthful strategies in fact construct a NE since no user will deviate from the truthful strategy.

Here we show the truthfulness of Virtual Election rule. Virtual Election rule is based on MVS, which has been shown truthful when the preferences of voters are single-peaked preferences [15].

Definition 4 (Single-Peaked Preference). *A preference $\succeq$ over $\bar{R}$ is single-peaked if and only if there exists a unique $\bar{r}_i \in \bar{R}$ that $\forall r \in \bar{R} \setminus \{\bar{r}_i\}$ and $\forall \theta \in [0, 1)$, $\theta r + (1 - \theta)\bar{r}_i \succeq r$, where $i \succeq j$ represents i is preferred or equal to j for the player.*

It has been proved by Ching [23] that all voters will vote for their peak choice $\bar{r}_i$ in MVS when their preferences are single-peaked. Thus, MVS is a truthful rule since all voters report their most preferred choices truthfully. Recalling the Virtual Election scheme

rule in (2.1), if $L_{i,j}|_{j=\{f,m\}}$ is public information among MSes, that is, all MSes know other MSes' CQI, it can be proved that the preference of MSes on the femtocell downlink power is single-peaked when the allocation rule $A(\cdot)$ satisfies Assumption 1. We first provide an insight of this preference characteristic: For $M_i \in S_f$ served by the femtocell BS, its expected throughput $\gamma_{i,f}$ is decided by the allocation rule $A(\cdot)$, which takes the MS set S_f and their wireless data rates $\{\Gamma_{i,f}(P_f)\}$ as inputs. Both inputs of $A(\cdot)$ are affected by the choice of downlink power P_f of the femtocell BS. A higher P_f will encourage more MSes connect to the femtocell and therefore share femtocell BS's backhaul capacity. This decreases the expected throughput of each MSes. Nevertheless, a higher P_f also enhances the transmission qualities of MSes by increasing the wireless data rate and therefore relaxing the expected throughput constraint. This may bring a higher expected throughput for the MS if its expected throughput is constrained by the wireless data rate. Along with the changes of P_f, these two inputs have opposite effects on the expected throughput to MSes. Note that if the macrocell and femtocell share the same spectrum, the conflicting effect of these two inputs becomes more significant. For instance, when the femtocell uses a higher downlink transmission power, the interference to the macrocell is stronger. The increased interference may encourage more MSes to choose femtocell as their serving cell. Thus, more MSes share the limited backhaul capacity, and their expected throughput under the femtocell are decreased.

Formally, we define each MS's preference over P_f:

Definition 5 (MS's preference on P_f). *M_i's preference over P_f is denoted as $\succeq_i$ which satisfies*

$$\forall p, p' \in [0, P_f^{max}], \ p \succeq_i p' \Leftrightarrow u_i(A_i(p)) \geq u_i(A_i(p')).$$

where $\{\gamma_{i,f}\} = A(\{\Gamma_{i,f}(p)\})$ and $A_i(p) = \gamma_{i,f}$.

The following theorem shows that for a given $\succeq_i$, there exists an ideal p_i^* that is preferred or equal to any other choices of $p \in [0, P_f^{max}]$. Thus, $\succeq_i$ is a single-peaked preference with a peak choice p_i^*.

Theorem 2 (Single-Peaked Preference on P_f). *When the allocation rule $A(\cdot)$ satisfies*
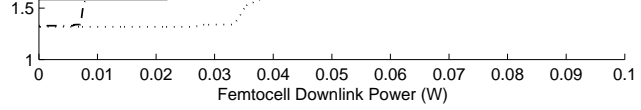
Figure 2.5: MSes' Single-Peaked Preferences over P_f

Assumption 1, $\forall M_i \in S_f$, $\succeq_i$ is single-peaked with peak p_i^*, where p_i^* is denoted as

$$p_i^* = \begin{cases} P^F, & i = \arg\max_{M_i \in S}\{L_{i,f}\} \\ P_i^M, & \textit{otherwise} \end{cases} \tag{2.7}$$
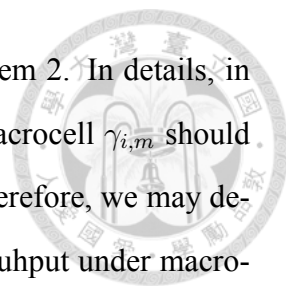
where

$$P^F = \begin{cases} \Gamma_f^{-1}(C_f), & \textit{if } \Gamma_f^{-1}(C_f) \textit{ exists} \\ p_j^{b-}, & \textit{otherwise.} \end{cases} \tag{2.8}$$

$$P_i^M = \min\{\arg_p(\Gamma_{i,f}(p) = \gamma_f(p)), P_f^{max}\}, \tag{2.9}$$

$p_i^b = \Gamma_{i,f}^{-1}(\gamma_{i,m})$, $C_f - \gamma_{j,m} < \Gamma_f(p_j^{b-}) < C_f$, and $\Gamma_f(p) = \sum_{p_i^b \leq p} \Gamma_{i,f}(p)$.

Thus, under a given allocation rule $A(\cdot)$ satisfying Assumption 1, MSes with good channel qualities prefer P^F, which is the minimum femtocell downlink power to maximizes the overall expected throughput of MSes under the femtocell. If P^f is increased, more users connect to the femtocell, and their expected throughput are strictly decreased. For those MSes with poor channel qualities, each of them prefers a femtocell downlink power that maximizes their own expected throughput. If we assume a shared spectrum model, the conflicting effect of two inputs on the allocation rule is more significant, the single-peakedness of user's preferences on P_f will be held in the shared spectrum model,

despite the peak powers are different from those described in Theorem 2. In details, in the shared spectrum model, the expected throughput of M_i under macrocell $\gamma_{i,m}$ should be decreasing with P_f due to the interference from the femtocell. Therefore, we may define a decreasing function $\Gamma_{i,m}(P_f)$ to represent M_i's expected throguhput under macrocell. Nevertheless, two important observations in the independent spectrum model are still valid: 1) the wireless data rate under femtocell $\Gamma_{i,f}(P_f)$ remains an increasing function of P_f since the macrocell does not change its transmission power and the interference from the macrocell is therefore nonincreasing with P_f. 2) There is at most one boundary point P_f^* that $\Gamma_{i,m}(P_f) = \Gamma_{i,f}(P_f)$ for every $M_i \in S$ since the former one is a decreasing function while the later one is an increasing function. Supporting by these two observations, the conclusions in Theorem 1 and Theorem 2 remain valid in the shared spectrum model.

An example of the preferences of MSes with corresponding expected throughput is shown in Fig. 2.5. Four MSes are in the overlay network, and the femtocell's backhaul data rate is 7 Mbps. Using MS 2's data rate as example, the downlink power that maximizes its expected throughput is 0.3926 Watt. Its data rate strictly decreases when the power increases or decreases. Thus, its peaked power $p_2^* = 0.3926$.

Since MSes' preferences are single-peaked, we give a corollary to conclude the truthfulness of Virtual Election rule.

Corollary 1 (Truthfulness of Virtual Election Rule). *Virtual Election rule is a truthful rule when the allocation rule $A(\cdot)$ satisfies Assumption 1.*

Proof. Returning to the Virtual Election rule, because the MSes' preferences over P_f are single-peaked, M_i will chooses to report its most preferred power p_i^* under Virtual Election rule. Therefore, the Virtual Election rule is truthful. $\square$

2.5 FEVER - A Femtocell Downlink Cell-Breathing Mechanism

Although the Virtual Election rule can make MSes truthfully report their preferences on downlink power, the NE in Virtual Election rule is not a DSNE since the peak value p_i^*

Figure 2.6: FEVER Mechanism

of M_i depends on the channel qualities of other MSes. Thus there is a serious drawback in the mechanism: all MSes and the femtocell are required to possess complete information of other MSes such as their signal loss rates and interference levels in order to derive the peak p_i^*. This requirement is undesirable in a realistic wireless network since the implementation of information sharing among MSes induces a huge overhead. The calculation on the preferred downlink power is also unrealistic considering the relatively low and scarce computational power of mobile devices. A more practical mechanism without these requirements is necessary for implementing the voting scheme in the real wireless system. Hence, we propose FEmtocell Virtual Election Rule (FEVER) mechanism for the cell-breathing control framework. FEVER is a truthful mechanism based on Virtual Election rule without the requirement of complete information. MSes are only required to report their CQI directly to the femtocell without calculating their preferred downlink power. In addition, we prove that there exists a truthful DSNE in FEVER mechanism. Therefore, the truthfulness of FEVER is guaranteed, and its implementation complexity is quite low. It only requires small changes to the existing cell selection procedures in standards.

As shown in Fig. 2.6, FEVER mechanism is composed of three levels in Cell-Breathing stage: Channel Information Harvester (CIH), Cell-Breathing Helper (CBH), and Virtual

Election Rule (VER). First, CIH requires all MSes to report their CQI $\theta_i = \{L_{i,f}, L_{i,m}\}$. Then, CBH uses the channel information harvested by CIH to calculate MSes' most preferred downlink power p_i^*. These values are derived by $H(\{\theta_i | M_i \in S\}) = H(\bar{\theta}) = \{p_i^* | M_i \in S\}$, where $H(\cdot)$ is in accordance with the results given by (2.7). Finally, VER collects $\{p_i^* | M_i \in S\}$ derived from CBH and applies Virtual Election rule to choose the femtocell downlink power P_f. Then, in Cell Selection stage there are two levels: BEst response Dynamic (BED) and Max-min Allocation Rule (MAR). According to the chosen P_f, MSes select the cell they want to be served by, which can be predicted by Theorem 1. Thus S_f and S_m is decided in this level. Since we have all CQI from CIH, we induce a cheat-proof procedure here: if an MS M_j which is not in $S_f(P_f)$ calculated by CBH selects the femtocell in this stage, we surely know this MS is cheating in Cell-Breathing stage and thus we can block this MS from using the femtocell service. Finally, the femtocell allocates the backhaul data rate according to the max-min allocation rule $A_{fever}(\cdot)$.

Then, we give the following theorem to show the truthfulness of FEVER mechanism.

Theorem 3 (Truthfulness of FEVER mechanism)**.** *All M_i report their CQI $\theta_i^* = \{{}^*_{i,f}, {}^*_{i,m}\}$ truthfully in FEVER mechanism $B_{fever}(\cdot)$. That is, $\forall M_i \in S$, $\forall \bar{\theta} \in \Theta^n = (L \times L)^n$,*

$$u_i(A_i(B_{fever}(\bar{\theta}^*))) \geq u_i(A_i(B_{fever}(\bar{\theta}))).$$

Proof. Due to page limitation, we sketch the outline of the proof here. We discuss three cases: M_i's vote v_i derived in CIH is equal to, larger than, or smaller than the selected vote v_κ. For the first case, surely M_i will just report its CQI truthfully. For the second case, the vote chosen by FEVER is larger than its most preferred downlink power v_i. Therefore, $\gamma_{i,f} = \Gamma_f(v_\kappa)$ according to Assumption 1 and Theorem 2. If M_i chooses to report $L'_{i,f} < L^*_{i,f}$, the modified vote v'_i will be larger than v_i, and the vote chosen by VER v'_κ will be no smaller than v_κ according to VER. So, $\gamma'_{i,f} = \Gamma_f(v'_\kappa) \leq \Gamma_f(v_\kappa)$. Since it eventually gets a lower downlink data rate, it has no incentive to report $L'_{i,f} < L^*_{i,f}$. However, if M_i chooses to report $L'_{i,f} > L^*_{i,f}$, since the modified vote v'_i will be smaller than v_i, and the original selected vote v_κ is larger than v_i, reporting $L'_{i,f}$ makes no difference to v_κ.

Additionally, since $\gamma_{i,f}$ is already not constrained by its wireless data rate $\Gamma_{i,f}(v_\kappa)$, its downlink data rate remains the same $\gamma'_{i,f} = \Gamma_f(v_\kappa) = \gamma_{i,f}$. Therefore, it has no incentive to report $L'_{i,f} > L^*_{i,f}$. Similarly, in the third case M_i still chooses to report $L^*_{i,f}$. For $L_{i,m}$, given $M_i \in S_j$ if v_κ is selected and $L^*_{i,m}$ is reported, it makes no difference to v_κ unless given the reported $L'_{i,m}$, M_i will make a choice of $S'_j \neq S_j|_{j=\{f,m\}}$. However, since M_i's true CQI is $L^*_{i,m}$, it will choose S_j in the Cell Selection stage, and thus the cheating will be revealed by the femtocell. Hence, FEVER mechanism is a truthful mechanism. Note that this proof requires the capacity assumption is satisfied or $\Gamma_f(p)$ may not be a decreasing function. $\qquad\square$

If the capacity assumption, that is, $\forall M_i \in S$, $\frac{C_f}{N} \geq \gamma_{i,m}$, is not satisfied, the preference on power is no longer single-peaked. However, FEVER mechanism is still truthful when the selected vote order κ is equal to 1. We show this characteristic in the following theorem.

Theorem 4 (Truthfulness without capacity assumption). *When $\exists M_i \in S$, $\frac{C_f}{N} < \gamma_{i,m}$, all M_i still report their CQI $\theta^*_i = \{^*_{i,f}, ^*_{i,m}\}$ truthfully in FEVER mechanism $B_{fever}(\cdot)$ when selected vote order $\kappa = 1$.*

Proof. Since $\kappa = 1$, $\forall M_i \in S_f$, $\gamma_{i,f} = \Gamma_{i,f}(v_1)$. For a given $M_j \in S_f$, if it chooses to report $'_{i,f} < ^*_{i,f}$, its allocated data rate $\Gamma'_{i,f}$ is strictly lower than $\Gamma_{i,f}$ because it claims a lower wireless data rate. In contrast, if it chooses to report $'_{i,f} > ^*_{i,f}$, it claims a higher wireless data rate and the CBH will decide a lower vote $v'_1 < v_1$, and thus its real downlink data rate $\gamma_{i,f} = \Gamma(v'^*_{1i,f}) < \Gamma(v'^*_{1i,f})$. Thus, it will truthfully report $_{i,f}$. For $^*_{i,m}$, a misreported $'_{i,m}$ does not affect the vote v_1 unless it is large enough that the MS will not be counted in S_f in CBH. According to the cheat-proof procedure in BED, this MS cannot return to the femtocell and its downlink data rate is $\gamma_{i,m} < \Gamma_{i,f}(v_1)$. Hence, $\forall M_i \in S_f$, they all report CQI θ^*_i. Similarly, $\forall M_j \in S_m$, they also report CQI θ^*_j. Thus FEVER mechanism is truthful even when $\exists M_i \in S$, $\frac{C_f}{N} < \gamma_{i,m}$. $\qquad\square$

The choice of $\kappa = 1$ not only relaxes the capacity assumption but also makes FEVER mechanism to choose the most capacity efficient operation point in most network scenario,

which will be shown in the following section.

2.5.1 Performance Analysis of FEVER mechanism

In FEVER mechanism, the selected vote order κ is predefined in VER to derive the κth votes as the choice of P_f. Now we discuss the influence of κ on the (throughput) efficiency and (allocation) fairness of the resulting expected throughput $\{\gamma_{i,f}|M_i \in S_f\}$ and $\{\gamma_{i,m}|M_i \in S_m\}$. We will show that there is a tradeoff between efficiency and fairness when different κ is chosen.

Price of Anarchy

First we define the price of anarchy (POA): the ratio of the maximum social utility to the social utility at NE. POA is used to measure the efficiency loss due to the selfish behavior of MSes in NE. If POA is equal to one, there is no efficiency loss at NE, and NE leads to the same performance as the social-utility maximized system. In the femtocell cell-breathing control framework, we define the social utility as $U_s = \sum_{M_i \in S} u_i$. The price of anarchy of FEVER mechanism is described as below:

Theorem 5. *The price of anarchy of FEVER mechanism $POA(\kappa)$ is one if the selected vote order $\kappa = 1$ and the social-utility maximized power P_f^* can be described as*

$$\sum_{i=1}^{j} \Gamma(P_f^* L_{i,f}) \leq C_f \text{ and } \sum_{i=1}^{j+1} \Gamma(P_f^* L_{i,f}) \geq C_f.$$

In addition, $POA(\kappa)$ is increasing with κ and bounded by 2.

Proof. First, we shortly describe how to find the optimal downlink power in the femtocell: we first sort MSes in increasing order of $\frac{L_{1,m}}{L_{1,f}}$. (This guarantees that MSes join the femtocell sequentially when the femtocell BS increases P_f.) Intuitively, the optimal power that maximizes social utility is the one that just allocates all the available backbone capacity to MSes. If the solution does not exist and the macrocell's data rate is relatively large, the optimal power will be the one that minimizes the unallocated backbone data rate before an additional MS joins S_f and uses all the capacity. Thus, the optimal

power P_f^* is given by $\sum_{i=1}^{j} \Gamma(P_f^* L_{i,f}) \leq C_f$ and $\sum_{i=1}^{j+1} \Gamma(P_f^* L_{i,f}) > C_f$, where j satisfies $P_f^* L_{i,f} \geq P_m L_{i,m}$, $\forall i \leq j$ and $P_f^* L_{i,f} < P_m L_{i,m}$ $\forall i \geq j$. If $\sum_{i=1}^{j} \Gamma(P_f^* L_{i,f}) = C_f$, the social utility $U_s^* = \sum_{M_i \in S} u_i = C_f + \sum_{i=j+1}^{N} \Gamma_{i,m}$. We observe that P_f, which is the peak value of M_1, is equal to P_F according to Theorem 2. Thus, if $\kappa = 1$, FEVER mechanism always chooses P_f^*, and thus $POA(1) = 1$.

The reason that $POA(\kappa)$ is an increasing function is intuitive. When P_f increases, there are two possible cases: one is that a new MS M_j joins S_f, and the other is that no MS changes its selection. For the former case, the social utility will decrease by $\gamma_{j,m}$ since M_j chooses to join S_f and gives up the throughput offered by the macrocell. For the latter case, there is no change in the resulting social utility. In addition, we know v_κ increases with κ, so $P_f = B_{fever}(\cdot, \kappa)$ is an increasing function of κ. Thus, $POA(\kappa)$ is an increasing function of κ.

Finally, since the worst case in FEVER mechanism will be that all users choose to join the femtocell and all macrocell's offered services are wasted under selfish behavior, we have $\gamma_{i,f}|_{\kappa=N} > \gamma_{i,m}$ $\forall M_i \in S$. In addition, we know $\sum M_i \in S \gamma_{i,f}|_{\kappa=N} = C_f$. Thus,
$$POA(\kappa) \leq POA(N) = \frac{C_f + \sum_{M_i \in S_m(P_f^*)} \gamma_{i,m}}{C_f} < \frac{C_f + C_f}{C_f} = 2. \qquad \square$$

Theorem 5 tells us that when $\kappa = 1$, FEVER mechanism always chooses the downlink power that maximizes the social utility. In addition, according to Theorem 4, even the capacity assumption is relaxed, FEVER mechanism can still maximize the social utility because all MSes truthfully report their CQI when $\kappa = 1$. For $\kappa > 1$, the social utility decreases with κ since more MSes joins S_j and waste the throughput offered by the macrocell. Thus the output becomes inefficient.

Noted that in some scenarios, the optimal power P_f^* may not be the one described in Theorem 5. This happens when $\gamma_{j+1,m} < C_f - \sum_{i=1}^{j} \Gamma(P_f^* L_{i,f})$. In this case, allowing M_{j+1} to join the femtocell is beneficial to the system since the unallocated backhaul capacity is significantly large. In this case $POA(1)$ will be slightly larger than one. The degree of efficiency loss depends on the macrocell downlink data rate of $\gamma_{j,m}$. Given $\gamma_{j,m}$, $POA(1) < \frac{C_f + \gamma_{j,m}}{C_f} = 1 + \frac{\gamma_{j,m}}{C_f}$. If capacity assumption is satisfied, $POA(1) < 1 + \frac{1}{N}$.
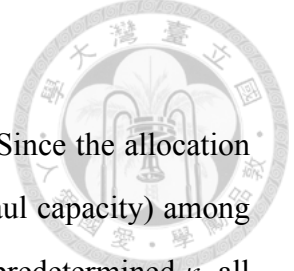
Fairness

Then, we discuss the fairness among $M_i \in S$ when κ changes. Since the allocation rule $A_{fever}(\cdot)$ follows Assumption 1, the resource allocation (backhaul capacity) among all MSes in S_f surely satisfy max-min fairness. In addition, given a predetermined κ, all MSes' utilities satisfy the max-min fairness under FEVER mechanism.

Theorem 6. *Given κ, all MSes' utilities $\{u_i | M_i \in S\}$ under FEVER mechanism satisfies max-min fairness, that is,*

$$\exists \{u_i'\} \neq \{u_i\},\ u_k' > u_k \text{ for some } M_k \in S$$

$$\Rightarrow \exists M_i \in S,\ u_i' < u_i \leq u_k.$$

Here we would like to further discuss the fairness efficiency among all MSes in the overlay system. To discuss the fairness efficiency, we apply a common fairness index: Jian fairness index $I(\{u_i\}) = \frac{(\sum_{1 \leq i \leq N} u_i)^2}{N \sum_{1 \leq i \leq N} u_i^2}$ [24] here. Jian fairness index is bounded between 0 and 1. A higher fairness index means the resource allocation is fairer. The following theorem describes the fairness efficiency of FEVER mechanism.

Theorem 7. *The fairness index $I(\{u_i\})$ of output of FEVER mechanism is an increasing function of κ.*

Proof. We use Property 1 in [24] to prove this. Before that, we define the reallocation sequence $\{(M_i^1, M_j^1, du_1), (M_i^2, M_j^2, du_2), ...\}$, where (M_i^l, M_j^l, du^l) means M_i^l's utility (downlink data rate) minus du^l while M_j^l's utility plus du^1. We also recall the notations $S_f^u(p)$ and $S_f^c(p)$ in the proof of Theorem 1 in Appendix.

According to Theorem 1, for a given p and $p' = dp + p > p$, we have $S_f(p) \subset S_f(p')$ and $\gamma_f(p) > \gamma_f(p')$. Without losing generality, we assume dp is small enough that only one of following cases happens when power is increased to p': $S_f(p') = S_f(p)$ or $S_f(p') = S_f(p) \cup \{MS_j\}$.

Since the reallocation only happens in MSes in $S_f(p')$, we focus on the effect of these users and ignore users served by the macrocell. For the first case, no new MS joins $S_f(p')$.

Since $\sum_{M_i \in S_f(p')} u_i = \sum_{M_i \in S_f(p)} u_i = C_f$ and $\gamma_f(p) > \gamma_f(p')$, there exists at least one reallocation sequence $\{(M_i^l, M_j^l, du^l)\}$, where $M_i^l \in S_f^c(p)$ and $M_j^l \in S_f^u(p')$, can realize the reallocation from $\{\gamma_{i,f}(p)\}$ to $\{\gamma_{i,f}(p')\}$.

According to the proof of Theorem 1 in Appendix, $\forall M_i \in S_f^c(p)$, $\gamma_{i,f}(p') = \gamma_f(p') < \gamma_f(p)$. And $\forall M_j \in S_f^u(p')$, $\gamma_{j,f}(p) \leq \gamma_{j,f}(p') \leq \gamma_f(p')$. Thus, for all reallocation (M_i^l, M_j^l, du^l), $du^l \leq \gamma_{i^l,f}(p) - \gamma_{i^l,f}(p') = \gamma_{i^l,f}(p) - \gamma(p') \leq \gamma_{i^l,f}(p) - \gamma_{j^l,f}(p) = u_i^l(p) - u_j^l(p)$.

According to Property 1 in [24], Jian fairness index increases when $du \leq u_i - u_j$. This means after every reallocation (M_i^l, M_j^l, du^l), Jian fairness index increases. Thus, the final output $I(\{u_i(p')\})$ is larger than $I(\{u_i(p')\})$ when $p' > p$ in the first case. Similarly, In the second case we can reach the same conclusion. Thus, the fairness index of the output of FEVER mechanism is an increasing function of femtocell downlink power p. Finally, since v_κ is increasing with κ, $I(\kappa) = I(\{u_i(v_\kappa)\})$ is increasing with κ. $\qquad\square$

Notice that when $\kappa = N$ and $p_N^* \leq P_f^{max}$, the output of FEVER mechanism has a fairness index of one.

Observed in Theorem 5 and 7, there is a tradeoff between throughput efficiency and allocation fairness. When a larger κ is chosen, the output of FEVER mechanism becomes less capacity efficient since more users give up the macrocell services. Doing so increases the allocation fairness since these users now are offered with higher expected throughput, in exchange with lower expected throughput to those users already selected by the femtocell. The choice of κ should be application-oriented. On one hand, if the service provider wants to make use of the additional backhaul data rate offered by the femtocell efficiently, he can choose a smaller κ. On the other hand, if he wants to make users share the backhaul fairly, he may choose a larger κ.

2.6 Subscriber Group Modes

We now investigate the compatibility of FEVER mechanism to subscriber group modes in femtocell system. In implementing the subscriber group modes in femtocells, two is-

sues are of concerns: access control on low-priority MSes and resource reservation for high-priority MSes. These two concerns change the access policy of femtocells and may brings some incompatibility to existing access policies for typical cell base stations.

We first apply necessary extensions into our downlink cell-breathing framework and two-stage game model. We add a new phase: Access Control Phase between Cell Breathing and Cell Selection phases into the framework. In this phase, the femtocell should decide and broadcast the allowed mobile user set S^a. Only users in S^a are allowed to access the femtocell. Notice that the choice of S^a depends on the subscriber group mode and the available resource.

To model the user behavior in the new framework, we extend the two-stage game model in Section 2.3. The Access Control Phase is included in the first stage (Cell-Breathing Stage) of our two-stage game model. In the new game model, the Cell-Breathing rule is extended to output not only the femtocell downlink power P_f but also the allowed mobile user set S_a. In addition, in the Cell-Selection stage we impose a new game rule: only users belonging to S_a have the right to access the femtocell. Mathematically, the player set in the second stage is now restricted to S^a instead of S. Other users $M_i \notin S^a$ can only select the macrocell. In the femtocell, a subscriber group $S^g \subset S$ is predetermined. Each MS $M_i \in S^g$ has a desired expected throughput γ_i^{req}. We assume their utility is maximized whenever the desired rate is satisfied. Thus, the utility function of $M_i \in S^g$ is $u_i(\gamma) = \min(\gamma, \gamma_i^{req})$. Lastly, we assume the backhaul data rate can support at least the demand of these MSes, that is, $C_f \geq \sum_{M_i \in S^g} \gamma_i^{req}$. With this assumption, we define the reserved capacity function $C^g(p)$:

$$C^g(p) = \sum_{M_i \in S^{g,a}(p)} (\min(\Gamma_{i,f}(p), \gamma_i^{req})), \tag{2.10}$$

where $M_i \in S^{g,a}(p)$ if and only if $M_i \in S^g$ and $\Gamma_{i,f}(p) \geq \Gamma_{i,m}$. $C^g(p)$ is the backhaul data rate reserved for users in S^g. Notice that the assumption and reserved data rate imply that when all users in S^g select the femtocell, they all can still have a reasonable service quality. For other users, they may have an unacceptable (lower than the one provided by macrocell) expected throughput if users in S^g have higher priority.

2.6.1 FEVER Mechanism in Subscriber Group modes
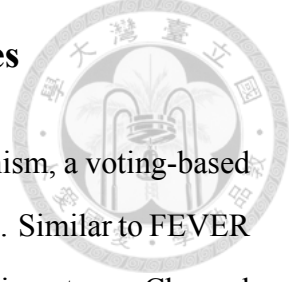
We now propose Subscriber Group FEVER (SG-FEVER) mechanism, a voting-based truthful mechanism that is compatible to three subscriber group modes. Similar to FEVER mechanism, SG-FEVER is composed of three levels in Cell-Breathing stage: Channel Information Harvester (CIH), Subscriber Group Cell-Breathing Helper (SG-CBH), and Subscriber Group Virtual Election Rule (SG-VER).

In SG-CBH, instead of directly applying max-min allocation rule to derive the peak of each user, we first define $S^{g,a}(p)$ and $C^g(p)$ according to (2.10). Then, the max-min allocation rule $A_{fever}(\cdot)$ is applied to these two groups independently: the reserved capacity $C^g(p)$ is used for users in $S^{g,a}(p)$, while the remaining capcity $C^{-g}(p) = C_f - C^g(p)$ is used for users in $S^{-g}(p)$, which is given by

$$S^{-g}(p) = \{M_i | \Gamma_{i,f}(p) \geq \Gamma_{i,m} \text{ and } M_i \notin S^g\}.$$

The peak p_i^* and the wireless data rate $\Gamma_{i,f}(p)$ of each user $M_i \in S$ are derived in this process.

Finally, SG-VER collects $\{p_i^* | M_i \in S\}$ derived from CBH and applies Virtual Election rule to choose the femtocell downlink power P_f with a predetermined selected vote order κ. In addition, SG-VER broadcasts the allowed user set S^a, which depends on the choice of subscriber group mode.

Then, in Cell Selection stage there are still two levels: BEst response Dynamic (BED) and Subscriber Group Max-min Allocation Rule (SG-MAR). In SG-FEVER mechanism, MSes select the BS they want to be served by based on their best responses given in Theorem 1 if they are in the allowed user set S^a. If not, the users have no choice but to choose the macrocell BS as their serving BS . Thus, S_f and S_m are decided in this level. The cheat-proof procedure in SG-FEVER is enhanced: if an MS is not in $S^g(P_f)$ selects the femtocell in this stage, femtocell BS blocks the MS form using femtocell services. Finally, the femtocell allocates the backhaul data rate according to the decision in SG-CBH, and the expected throughput is then determined. Since the implementation of OSG

is straightforward, we discuss the implementation of other subscriber group modes.

CSG Mode

In this mode, only users in S^g are allowed to access the femtocell. Thus $S^a = \{M_i | \Gamma_{i,f}(P_f) \geq \gamma_{i,m}\} \cap S^g$. Note that SG-FEVER promises that users in S^g will be allocated at least the wireless data rate $\Gamma_{i,f}(P_f)$ from the femtocell BS, and at most their required throughput γ_i^{req}. When $\kappa = |S^g|$, $\forall M_i \in S^g$, $\gamma_{i,f}(v_\kappa) = \gamma_i^{req}$. That is, all users derive their required throughput from the femtocell.

Corollary 2. *[Truthfulness under CSG Mode] SG-FEVER mechanism is a truthful mechanism when S^g is non-empty and $S^a = \{M_i | \Gamma_{i,f}(P_f) \geq \gamma_{i,m}\} \cap S^g$.*

Proof. We first discuss the case that $M_i \notin S^g$. If so, the MS cannot choose the femtocell whatever it reports in SG-CBH since $M_i \notin S^a \subset S^g$. Thus, any $\theta_i \in \Theta$, including θ_i^*, is M_i's best response. Then, if $M_i \in S^g$, since SG-CBH always provides the user at least its raw wireless data rate $\Gamma_{i,f}(P_f)$, its preference on P_f is single-peaked with peaks p_i^* at $\Gamma_{i,f}(p_i^*) = \gamma_i^{req}$. So, M_i will report θ_i^* in SG-FEVER mechanism. We conclude that reporting θ_i^* is the dominant strategy of any $M_i \in S$ in SG-FEVER mechanism under CSG mode, that is, SG-FEVER is a truthful mechanism. $\square$

Hybrid Mode

For Hybrid mode, the subscriber group S^g is also predefined, but other users are still allowed to access the femtocell if there are remaining resources (backhaul capacity). Given a predetermined non-empty set S^g, we define $S^a = \{M_i | \Gamma_{i,f}(P_f) \geq \gamma_{i,m}\}$ in this mode. Since we remove the restriction that all users not belonging to S^g are excluded from the femtocell, there is a chance that a user $M_i \notin S^g$ will be included in S^a. We prove that SG-FEVER mechanism is a truthful mechanism in Hybrid mode.

Corollary 3 (Truthfulness under Hybrid Mode)**.** *SG-FEVER mechanism is a truthful mechanism when S^g is non-empty and $S^a = \{M_i | \Gamma_{i,f}(P_f) \geq \gamma_{i,m}\}$.*

55

Proof. It has been shown in Corollary 2 that $\forall M_i \in S^g$, reporting θ_i^* is their dominant strategy under SG-CBH. Then, $\forall M_i \notin S^g$, the remaining capacity $C^{-g}(p)$ is allocated according to $A_{fever}(\cdot)$ in SG-CBH. Thus, according to Theorem 3, their dominant strategy is reporting θ_i^* either. So, SG-FEVER mechanism is a truthful mechanism under Hybrid mode. $\qquad\square$

2.7　Simulation Results

To evaluate the efficiency and influence of κ in FEVER mechanism, we implement a LTE overlay macrocell-femtocell simulator by extending the LTE link-level simulator [20]. We follow the settings specified by 3GPP [2] to simulate link-level SINR-throughput results, which are used to specify the wireless data rate function $\Gamma(\cdot)$ in our model. We followed IMT-Advanced 4G evaluation guidelines [1] to construct the overlay macrocell-femtocell system configuration. We apply Outdoor-to-Indoor and Indoor Small Office models as the path loss models of macrocell signal and femtocell signals respectively. In our simulations, there are 19 macrocells with a radius of 2 km in hexagonal layout. Within each macrocell, five femtocells are randomly placed. All macrocell share the same carrier which is different from the one shared by all femtocells. We chose the macrocell in the central and a femtocell at a distance of 1.6 km to the macrocell BS as our simulating overlay system. For MSes within these two cells, their locations are randomly distributed within a 50m circular house centered at the femtocell BS. All macrocells have a downlink power $P_m = 46$ dBmW, while all background femtocells have a downlink power of 23 dBmW. The AWGN noise is -132dBmW. The simulating femtocell has a maximum downlink power limit $P_{max}^f = 1$ W. The data rate of the femtocell's backhaul C_f is 25 Mbps.

2.7.1　Effect of MSes on femtocell service range

We first examine the effect of different number of MSes on the total system throughput and MSes served by the femtocell. $5 \sim 20$ MSes are randomly placed in the system ac-

cording to the parameter settings we listed before. We choose four κ settings for FEVER mechanism: $\kappa = 1$, $\kappa = 5$, $\kappa = 10$, and $\kappa = 15$. For comparison, we also sketch the results of two other mechanisms: Maximum Throughput and Maximum Power. In Maximum Throughput mechanism, the femtocell chooses the power that maximizes the overall system throughput, that is, $P_f = \arg\max_p \sum_{M_i \in S_f} \gamma_{i,f} + \sum_{M_i \in S_m} \gamma_{i,m}$. This mechanism represents the case that the femtocell's objective is maximizing the resource utilization in the system without concerns on the fairness among MSes. In the Maximum Power mechanism, the femtocell always chooses the maximum power P^f_{max} as its transmission power. This mechanism represents the case that the femtocell's objective is maximizing its coverage in this overlay system. Note that under both mechanisms the allocation rule still satisfies Assumption 1, and MSes follow the best responses stated in Theorem 1. Moreover, we assume that the MSes always report their CQI truthfully under the Maximum Throughput mechanism in order to simulate the femtocell has the perfect knowledge on the current state of wireless system. The results are shown in Fig. 2.7.

Fig. 2.7 (a) shows that when the number of MSes increases, the total system throughput also increases since more MSes are served by the femtocell or macrocell. We observe that when we choose $\kappa > 1$, the system throughput is lower than the one under $\kappa = 1$. In addition, the system throughput of Maximum Throughput is almost identical as the one under $\kappa = 1$. This observation fits the conclusion in Theorem 5 that $\kappa = 1$ maximizes the total system throughput. For other choices of κ, we observe that a larger κ leads to lower system throughput. In addition, when the number of MSes is small, FEVER mechanism under large κ chooses the same operating point as Maximum Power mechanism. This is because for those users who gives large votes, they most likely are MSes with poor channel qualities to the femtocell. Thus, they prefer the femtocell power as high as possible. When the number of MSes increases, they then hope the femtocell power is limited in order to prevent other MSes from joining the femtocell and sharing the limited backhaul capacity.

In Fig. 2.7 (b), we observe that a smaller κ indeed blocks more MSes from joining the femtocell. When the number of total MSes increases, less than 10 MSes are served by the femtocell under $\kappa = 1$. In contrast, more than 15 MSes choose to join S_f when $\kappa = 15$.

(b) Number of MSs served by femtocell
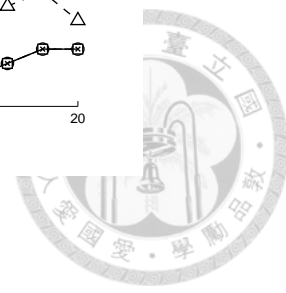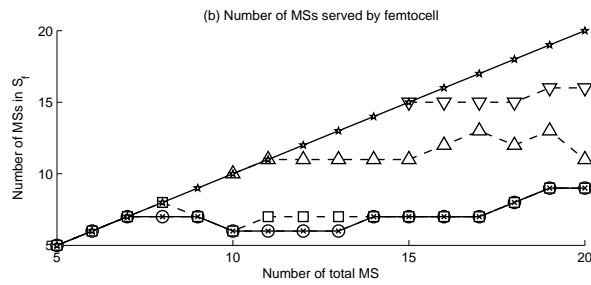
Figure 2.7: Simulation Results: FEVER Mechanism under Different Choice of κ

Note that the choice of κ does not necessary mean that only κ MSes are allowed to join the MSes, but the expected throughput of the v_κ voter is maximized.

2.7.2 Tradeoff between Efficiency and Fairness

Then, we examine the tradeoff between efficiency and fairness when different κ is chosen. 20 MSes are placed in the overlay system, and we choose $\kappa = 1 \sim 20$ in the experiments. Under each choice of κ, we calculate the system throughput efficiency (the price of anarchy of FEVER mechanism) and the fairness index of the expected throughput of all MSes. The simulation results are shown in Fig. 2.8.

The tradeoff between capacity efficiency and allocation fairness is clearly shown in Fig. 2.8, which fits the conclusion we made in Section 2.5.1. When we choose $\kappa = 1$, the efficiency becomes 1, but the fairness index is 0.7287, which is the lowest one in all operating points. Instead, if we choose $\kappa = 20$, the price of anarchy under FEVER mechanism becomes 1.2617 and fairness index becomes 1. Note that there may exist multiple choices of κ which lead to the same operating point with the efficiency of 1. This is because some MSes, most likely those near the femtocell BS, have the same votes on P^F defined in Theorem 2. In the experiment scenario, there are 9 MSes close to the

Figure 2.8: Simulation Results: Efficiency and Fairness Tradeoff

femtocell. They join the femtocell immediately when $P_f > 0$, thus they share the same vote. So, all choices of $\kappa < 10$ lead to the same performance, which is the same under Maximum Throughput mechanism.

2.7.3 Influence of Subscribe Group Modes

Finally, we evaluate the influence of different subscriber group modes in overlay system through simulations. 5 MSes, which belong to the subscriber group S^g and with required throughput of 4Mbps, are randomly placed in the range between 25m and 50m to the femtocell BS. In addition, $0 \sim 10$ MSes are randomly placed in the range between 50m and 100m. These MSes are treated as users from outside and do not belong to S^g. Then, we apply SG-FEVER mechanism with two choices of selected vote order: $\kappa = 1$ and $\kappa = \kappa^g$, where κ^g is defined as the largest vote from MSes in S^g. The choice $\kappa = \kappa^g$ is a straightforward one because all users in subscriber group should have a good service under the femtocell. The simulation results were shown in Fig. 2.9.

In Fig. 2.9 (a), we observe that $\kappa = 1$ is not a good choice in CSG and Hybrid modes. The system throughput in these two modes when $\kappa = 1$ is significantly lower than the one in OSG mode. Additionally, the system throughput is higher when $\kappa = \kappa^g$ comparing to the one with $\kappa = 1$ in all modes. The performance degradation results from the reserved resource scheme in SG-FEVER. Since the subscriber group user have reserved resources,
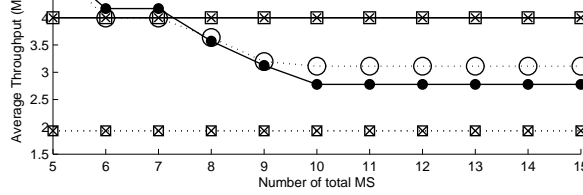
Figure 2.9: Simulation Results: SG-FEVER Mechanism under different SG modes

it is likely that the smallest vote is from the MS in subscriber group, and the MS chooses the downlink power that just meets its requirement. In this scenario it is possible that there is still unallocated backhaul data rate in the femtocell. In addition, we observd that when $\kappa = \kappa^g$, both OSG and Hybrid modes perform as well as the OSG mode with $\kappa = 1$ when there exist non-subscriber group MSes. (Note that we have prove that OSG mode with $\kappa = 1$ leads to the optimal operating points in the overlay system).

Although both OSG and Hybrid modes perform well when $\kappa = \kappa^g$ in terms of total system throughput, we have different conclusions in Fig. 2.9 (b), which shows the average subscriber group user throughput. When there are more non-subscriber group MSes in the overlay system, the average subscriber group throughput decreases to 3.112 Mbps and 2.778 Mbps when $\kappa = 1$ and $\kappa = \kappa^g$ in OSG mode. In contrast, when SG-FEVER mechanism is in Hybrid mode with $\kappa = \kappa^g$, all subscriber group MSes derive 4 Mbps downlink data rates, which are their predetermined required throughput. According to the results, among all the subscriber group modes, Hybrid mode in femtocell system is beneficial to the overlay system and the subscriber group users.

60

2.8 Related Work

Veeravalli and Sendonaris first discovered the cell-breathing phenomenon in CDMA cellular system [21]. Jalali further discussed the possibility of using cell-breathing phenomenon as a management tool on the cell capacity [25]. The fairness issue under cell-breathing was investigated by Yang and Ephremides [26]. Despite in CDMA system, researchers also observed the cell-breathing phenomenon in the coverage of WLAN AP [27] [28]. Bahl et. al. proposed various cell-breathing control algorithms under WLAN to realize power estimation and load balancing [27]. Bejerano and Han also proposed graph-based cell-breathing algorithms to realize the load-balancing [28].

For research on the femtocell subscriber group modes [18], Studies have showed that either static CSG or OSG modes may result in system inefficiency in interference management and bandwidth sharing [29] [30] [31] [32]. Hybrid mode as a balance between interference and efficiency was suggested in [31] [32]. The implementation of Hybrid mode in OFDMA system was further discussed in [33].

Some related works have focused on the issue of downlink power control in femtocell networks. Akbudak and Czylwik designed a distributed power control and scheduling algorithm to mitigate co-tier interference between femtocells. Through numerical analysis, they showed that their designed algorithm achieved sub-optimum close to global optimum [34]. Li et. al proposed both centralized and distributed solutions to reduce cross-tier interference in macrocell-femtocell overlay networks. The proposed solutions provide QoS to both macrocell and femtocell users [35]. Jorswieck and Mochaourab used game theory to analyze the non-cooperative power allocation between two cells in cellular networks. In addition, they applied AGV mechanism to guarantee MSes' truthful SINR reporting [36]. However, these works focus on the wireless capacity of the multi-cell system, while the backhaul capacity constraint in femtocell is not in their scopes.

To the best of our knowledge, the issue of cell-breathing downlink power control in backhaul-constrained overlay networks has not been covered yet.
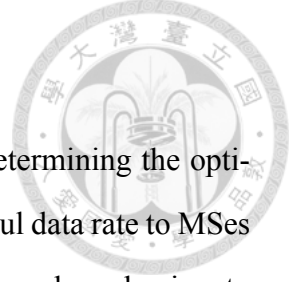
2.9 Summary

We proposed a femtocell cell-breathing control framework for determining the optimal coverage of the femtocell and allocating limited femtocell backhaul data rate to MSes fairly and efficiently. FEVER mechanism, a novel Virtual Election based mechanism to collect all MSes' channel quality information, was proposed. FEVER mechanism was shown to be truthful, and we proved that through different choice of selected vote order, the balance between system throughput and allocation fairness among MSes can be maintained. We also demonstrated the implementation of FEVER mechanism in different subscriber group modes by proposing SG-FEVER mechanism. The LTE-based realistic simulation results not only verify the performance enhancement under FEVER mechanism, but also show the benefits of Hybrid mode to the overlay system.

Appendix: Proofs of Theorems

Proof of Theorem 1 - First, we prove that the necessary and sufficient condition of M_i to join S_f is $\Gamma_{i,f}(p) \geq \gamma_{i,f}$. Given an allocation rule $A(\cdot)$ satisfying Assumption 1 and a femtocell downlink power p, we apply the water-filling algorithm and derive the below allocation:

$$\gamma_{i,f} = \min\{\Gamma_{i,f}(p), \gamma_f(p)\} \tag{2.11}$$

We denote the MSes served by the femtocell under the downlink power p by $S_f(p)$. Then, we denote $S_f^u(p) = \{M_i|\Gamma_{i,f}(p) < \gamma_f(p)\}$ and $S_f^c(p) = S_f(p) \setminus S_f^u(p)$. Thus,

$$\sum_{M_i \in S_f^u(p)} \Gamma_{i,f}(p) + |S_f^c(p)|\gamma_f(p) = \min\{C_f, \sum \Gamma_{i,f}(p)\}. \tag{2.12}$$

The (2.11) and (2.12) define a unique $r_f(p)$. In addition, we have $|S_f|\gamma_f(p) \geq \sum_{M_i \in S_f^u(p)} \Gamma_{i,f}(p) + |S_f^c(p)|\gamma_f(p)$. Thus,

$$\gamma_f(p) \geq \begin{cases} \frac{C_f}{|S_f|} \geq \frac{C_f}{|S|} = \frac{C_f}{N}, & \text{if } \sum \Gamma_{i,f}(p) \geq C_f \\ \max_{M_i \in S_f} \Gamma_{i,f}(p), & \text{otherwise} \end{cases} \tag{2.13}$$
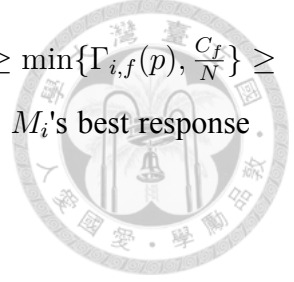
Thus, if M_i chooses to join S_j, its data rate $\gamma_{i,f}$ satisfies $\Gamma_{i,f}(p) \geq \gamma_{i,f} \geq \min\{\Gamma_{i,f}(p), \frac{C_f}{N}\} \geq \min\{\Gamma_{i,f}(p), \gamma_{i,m}\}$. In addition, we have $\forall M_i \in S$, $\frac{C_f}{N} \geq \gamma_{i,m}$. So, M_i's best response function is

$$\beta_i(p) = \begin{cases} M_i \in S_f, & \text{if } \Gamma_{i,f}(p) \geq \gamma_{i,m} \\ M_i \in S_m, & \text{otherwise} \end{cases}$$

Proof of Theorem 2 - We denote $p_i^b = \Gamma_{i,f}^{-1}(\gamma_{i,m}) = P_m \frac{L_{1,m}}{L_{1,f}}$ as M_i's boundary power. Without losing generality, given an MS set S, we assume $\frac{L_{1,m}}{L_{1,f}} \leq \frac{L_{2,m}}{L_{2,f}} \leq ... \leq \frac{L_{N,m}}{L_{N,f}}$. According to Theorem 1, $p_1^b \leq p_2^b \leq ... \leq p_N^b$. Now we discuss the relation among $\gamma_{i,f}$, p and each MS's peak. We first denote $\Gamma_f(p) = \sum_{p_i^b \leq p} \Gamma_{i,f}(p)$. Since $\Gamma(\cdot)$ is an increasing function, $\Gamma_f(p)$ is an increasing function too. Then, we denote P^F by

$$P^F = \begin{cases} \Gamma_f^{-1}(C_f), & \text{if } \Gamma_f^{-1}(C_f) \text{ exists} \\ p_j^{b-}, & \text{otherwise} \end{cases}$$

where $C_f - \gamma_{j,m} < \Gamma_f(p_j^{b-}) < C_f$. The second case occurs when M_j's joining immediately uses all the unallocated capacity and thus $\Gamma_f(p_j^{b-}) < C_f$ and $\Gamma_f(p_j^b) > C_f$. Then, we check the following two cases to show that $\gamma_f(p)$ is increasing when $p < P^F$ and decreasing when $p > P^F$:

Recalling (2.11) and (2.12), we know $\gamma_{i,f} = \Gamma_{i,f}(p) \, \forall p_i^b \leq p$. Because $\Gamma_{i,f}(p)$ is an increasing function, $\forall p_i^b \leq p, \gamma_{i,f}$ is also increasing, and so is $\gamma_f(p) = \max\{\Gamma_{i,f}(p)\}$.

Case 2: $p > P^F$. In this case, we would like to show that $\gamma_f(p)$ is strictly decreasing with p. We discuss two cases:

Case 2.A: $p_j^b < p < p' < p_{j+1}^b$. Since $p' < p_{j+1}^b$, M_{j+1} chooses not to join S_f'. Thus, $S_f' = S_f = \{M_i | i \leq j\}$. According to (2.12), we have

$$|S_f^c(p)| \gamma_f(p') + \sum_{M_i \in S_f^u(p')} \Gamma_{i,f}(p) = |S_f^c(p')| \gamma_f(p) + \sum_{M_i \in S_f^u(p')} \Gamma_{i,f}(p'). \tag{2.14}$$

We make an assumption that $\gamma_f(p) \leq \gamma_f(p')$. Since $p' > p$, $\Gamma_{i,f}(p') > \Gamma_{i,f}(p) \, \forall M_i \in S_f$. We denote $\Delta S_f^u = S_f^u(p) \setminus S_f^u(p')$. Due to (2.11), $S_f^u(p) \subset S_f^u(p')$. If $\Delta S_f^u = \emptyset$, $S_f^c(p') = S_f^c(p)$ and $S_f^u(p') = S_f^u(p)$. We check the left and right parts of (2.14) terms by

terms and find out the right part of (2.14) is strictly large than its left part, which reaches an contradiction. Thus ΔS_f^u is nonempty. For each $M_i \in \Delta S_f^u$, we find out that $\Gamma_{i,f}(p') > \Gamma_{i,f}(p) > \gamma_f(p)$. Thus, the right part of (2.14) is still strictly larger than its left part. So, according to the proof of contradiction, our assumption that $\gamma_f(p) \leq \gamma_f(p')$ is wrong. Thus we have $\gamma_f(p) > \gamma_f(p')$.

Case 2.B: $p_j^b < p < p_{j+1}^b < p_k^b < p' < p_{k+1}^b$. Since $p_k^b < p' < p_{k+1}^b$, $S_f' = S_f \cup \{M_j + 1, M_j + 2, ..., M_k\} = S_f \cup \Delta S_f$. From (2.12),

$$
\begin{aligned}
C_f &= |S_f^c(p)|\gamma_f(p) + \sum_{M_i \in S_f^u(p)} \Gamma_{i,f}(p) \qquad (2.15) \\
&= |S_f^{c'}(p')|\gamma_f(p') + \sum_{M_i \in S_f^{u'}(p')} \Gamma_{i,f}(p') \\
&\quad + |\Delta S_f^{c'}(p')|\gamma_f(p') + \sum_{M_i \in \Delta S_f^{u'}(p')} \Gamma_{i,f}(p'),
\end{aligned}
$$

where $S_f^{h'}(p') = S_f^h(p') \setminus \delta S_f$, $\delta S_f^{h'}(p') = S_f^h(p') \cap \delta S_f$ and $h = \{c, u\}$. We still make an assumption that $\gamma_f(p) \leq \gamma_f(p')$. We observe that in (2.15), the terms with $S_f^{c'}(p')$ and $S_f^{u'}(p')$ are just the right part of (2.14) in Case 2.A, which we have proved strictly larger than the left part. In addition, the third and four terms in the right part of (2.15) are strictly positive. Thus we conclude the right part of (2.15) is strictly larger than its left part. So, according to the proof of contradiction, our assumption that $\gamma_f(p) \leq \gamma_f(p')$ is wrong. Thus we have $\gamma_f(p) > \gamma_f(p')$.

Finally, we show that each M_i has its peak value p_i^*. According to (2.11), $\Gamma(\cdot)$ is increasing with p, and $\gamma_f(p)$ is decreasing with p. Thus, M_i has a unique peak value p_i^* which satisfies $\Gamma_{i,f}(p_i^*) = (\gamma_f(p_i^*))$. In addition, $\forall M_i \in S, p_i^* \geq P^F$ since $\gamma_{i,f}(p)$ is increasing when $p < P^F$.

Proof of Theorem 6 - Here we prove this theorem by contradiction. We denote the utilities of MSes under FEVER mechanism by $\{u_i\}$ and the MSes served by the femtocell by S_f. Then, we assume there exist other utilities of MSes $\{u_i'\}$ that

$$
u_k' > u_k \text{ for some } M_k \in S \text{ and } \forall u_i \leq u_k, \ u_i' \geq u_i. \qquad (2.16)
$$

We denote the MS/backhaul data rate allocation under $\{u_i'\}$ as S_f' and $\{\gamma_{i,f}' | M_i \in S_f'\}$. Then, $\{u_i'\}$ can be denoted as:

$$u_i' = \begin{cases} \gamma_{i,f}', & \text{if } M_i \in S_f' \\ \Gamma_{i,m}, & \text{otherwise.} \end{cases}$$

Notice that $S_f' \neq S_f$ must holds. Otherwise, the expected throughput of all MSes will be equal under both S_f and S_f' and we have a contradiction here. Now we examine the candidates of M_k and show the contradictions in every cases.

Case 1: $M_k \in S \setminus S_f$: We recall (2.4) in Theorem 1.

$$\beta_i(p) = \begin{cases} M_i \in S_f, & \text{if } \Gamma_{i,f}(p) \geq \gamma_{i,m} \\ M_i \in S_m, & \text{otherwise} \end{cases}$$

Given M_k in $S \setminus S_f = S_m$, we have $u_k = \Gamma_{k,m} > \Gamma_{k,f}(p) \geq \gamma_{k,f}'$. Thus, if $M_k \in S_f'$, $u_k' = \gamma_{k,f}' < \Gamma_{i,m} = u_k$. However, if $M_k \notin S_f'$, $u_k' = \Gamma_{k,f} = u_k$. Both possibilities lead to the contradiction.

Case 2: $M_k \in S_f \cap (S \setminus S_f')$: Recalling (2.4) in Theorem 1 and given $M_k \in S_f$ and $M_k \in S \setminus S_f'$, we have $u_k > \Gamma_{k,m} = u_k'$, which leads to the contradiction.

Case 3: $M_k \in S_f \cap S_f'$: We first discuss the case that $S_f \neq S_f'$. Given $M_k \in S_f' \cap S_f$, we have $u_k' = \gamma_{i,f}'$ since $M_k \in S_f'$. In addition, we have $u_k' > u_k = \gamma_{i,f}(p)$. However, recalling (2.11) in Theorem 1:

$$\gamma_{i,f} = \begin{cases} \Gamma_{i,f}(p), & \text{if } \Gamma_{i,f}(p) < \gamma_f(p) \\ \gamma_f(p), & \text{otherwise} \end{cases}$$

Since $u_k' > u_k$ and the maximum utility of M_k is $\Gamma_{i,f}(p)$, $\Gamma_{i,f}(p) > \gamma_f(p)$ and $u_k = \gamma_f(p)$. Thus, we have $\forall M_i \in S_f$, $u_k = \gamma_f(p) \geq u_i$. So, if there exists $M_i \in S_f \cap (S \setminus S_f')$, according to (2.4) its utility will be $u_i' = \Gamma_{i,m} < \gamma_{i,f} = u_i$. In addition, if there exists $M_i \in (S \setminus S_f) \cap (S_f')$, according to (2.4) its utility will be $u_i' \leq \Gamma_{i,f} < \Gamma_{i,m} = u_i$. Both cases violate (2.16) and lead to the contradiction. Since all cases has been discussed, according to the proof of contradictions, there exists no $\{u_i'\}$ satisfying (2.16) with $S_f' \neq S_f$.

Chapter 3
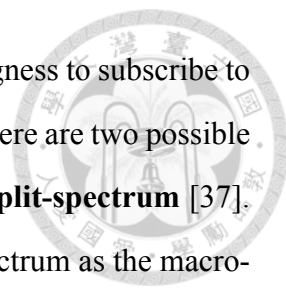
Service Price in Heterogeneous Networks: Optimal Contract Design

3.1 Introduction

Along with the growing population of mobile Internet users, the market orientation of today's mobile telecommunications has shifted from low-throughput voice traffic to high-throughput data traffic. To increase customers' interest in wireless services, most service providers offer a flat-fee pricing for unlimited data service, in which the user pays a single fixed fee for wireless service. However, variations in the service quality of wireless connections, such as signal degradation in indoor environments, present a major obstacle to telecommunications companies. As a result, customers' willingness to use these services is impaired, to the point that service providers often cut their margins, offering lower prices in order to keep the service attractive.

3.1.1 Femtocell System

One efficient way to improve wireless service instability and thereby combat these problems is to enhance the signal quality through femtocells. The femtocell, a small base station (BS) with low transmission power, can alleviate macrocell signal degradation with its lower signal loss rates and higher frequency reuse rate [17]. By introducing the femto-

cell system, service quality is enhanced, along with customers' willingness to subscribe to the wireless service. In the most state-of-the-art wireless standards, there are two possible spectrum access models for femtocell BSs : **shared-spectrum** and **split-spectrum** [37]. In the shared-spectrum model, femtocell BSs operate in the same spectrum as the macrocell BSs. This scheme is efficient when the femtocell BSs are deployed in places with poor macrocell signals, but are subject to interfere when the macrocell signals are strong. In the split-spectrum model, femtocell and macrocell BSs operate in separate spectrums, which are split according to the expected mobile station (MS) access rate, preventing the inter-system interference. Spectrum utilization may be inefficient if the cells contain unexpected loadings.

3.1.2   Contract Design

In lieu of seeking wireless system enhancements, service providers can also look to a different type of contract plan to increase their profits: the differentiated contracts. The differentiated contract method involves setting the MSs with better channel qualities apart from other users, and charging them more for their higher data-use rates. These differentiated contracts help service providers to efficiently make a higher profit from MSs according to their data usage. However, these contracts also face a significant problem: MSs tend to report low channel reception to prevent higher charges, eventually leading to an even lower profit than the flat-fee contract model. To attract users in an area with poor channel quality, service providers may offer users two contract options according to their channel quality conditions: 1) charging an average price for users with normal channel quality, and 2) charging a lower price for those with poor channel reception. Unfortunately, the latter option encourages all MSs to sign for the lower price even if their area receives normal service quality, effectively cheating the system by signing a cheaper contract. Even after the initial contract has already been signed, wireless devices can be configured or hacked by these cheating users [38], allowing them to manipulate disguised reports of poor channel quality to the service provider so that they can continue signing cheaper plans under the differentiated contract model. Thus, the differentiated contract

must be carefully designed to prevent such cheating, a problem which is known as the incentive compatible (IC) issue.

3.1.3 Contributions

In this chapter, we investigate the femtocell economic valuation and the profitability of differentiated contracts in an overlay macrocell-femtocell system, to which we make the following contributions:

1. We propose a novel wireless service differentiation framework to investigate the profit service providers make under a variety of differentiated contracts in the overlay macrocell-femtocell system. The price and maximum data rate are the differentiating factors in the contract structure. This framework addresses the differences between wireless service quality among users, which is the basis of the service differentiation developed in this chapter.

2. We show that a contract structure in our framework prevents cheating behaviors. As proved in this chapter, the existence of this contract structure is promised when the MSs experience different service qualities.

3. We draw a comparison between the shared-spectrum and split-spectrum systems in our framework and have derived the optimal (profit maximizing) contracts under three schemes: flat fee contracts, differentiated contracts without incentive compatible concerns, and incentive compatible differentiated contracts. In a split-spectrum system, it is difficult to further extract profits from MSs as the only incentive compatible contract is a flat fee one. By contrast, in a shared-spectrum system, there are differentiated contracts generating profits by raising service prices for the MSs with good service qualities in femtocells, while providing cheaper prices to other MSs with poor service qualities.
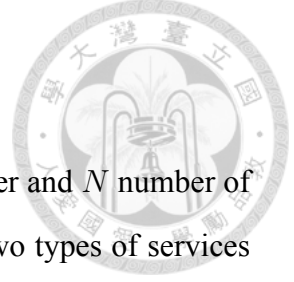
3.2 Profit Extraction Framework

In our study, we consider a wireless system with a service provider and N number of MSs, in which the service provider offers unlimited data service. Two types of services are provided in the system: one is a macrocell-only service, where MSs are only allowed to use the data service through macrocells. The other is a femtocell service, where MSs are allowed to access the data service through either the macrocells or the femtocells installed by the service provider, depending on the environment of use. In this framework, the valuation of an MS on the wireless service is based on the service quality he or she experiences. Service quality is measured by the data rate r_i, which is modeled as a random variable in this framework. Then, we denote MS i's valuation on the service with $v(r_i)$, which is an increasing function. Additionally, the MS i needs to pay a fee t_i in order to use the service. The utility of MS i is given by

$$u_i = E[v(r_i)] - t_i. \tag{3.1}$$

The data rate r_i is environmentally varied. Factors affecting the environment include location and the type of cell the user employs. In this framework, the environment is denoted as $s \in \{(out), (in, m), (in, f)\}$, where (out) represents the scheme that MS uses the macrocell service while outdoors, where (in, m) represents the macrocell service usage while indoors, and where (in, f) represents indoor use of the femtocell service. Probability of an MS being indoors or outdoors is given as p^{in} and p^{out} respectively. The wireless data rate r_i^s is determined by the channel quality MS i experienced in environment s. Due to natural characteristics of wireless transmissions, r_i^s is given by a random distribution R_i^s, which is associated with a probability density function (p.d.f.) $f_i^s(r_i^s)$ and a cumulative distribution function (c.d.f) $F_i^s(r_i^s) = \int_0^{r_i^s} f_i^s(r)dr$. When a user is in an outdoor environment, he is served by the macrocell, and his outdoor data rate p.d.f. is f_i^{out}. By contrast, if he use the service while indoors, he is served by the femtocell (if installed). In all other situations, he is served by the macrocell. In the former case, his indoor data rate p.d.f. will be $f_i^{in,f}(\cdot)$. In the latter one, the data rate p.d.f will be $f_i^{in,m}(\cdot)$.
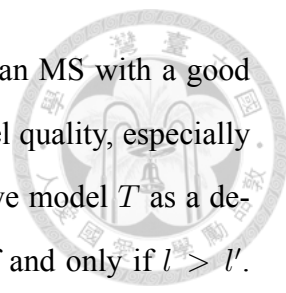
In this framework, MSs are classified according to their indoor macrocell data rate distribution $R_i^{in,m} \in \mathbf{R^{in,m}}$, where $\mathbf{R^{in,m}}$ is the universal set of $R_i^{in,m}$. The channel quality of an MS is usually modeled by propagation loss from the base station, channel fading/ shadowing, and interference from other signal sources. We assume that $\mathbf{R^{in,m}}$ is an ordered set with first-order stochastic dominance as its binary relation. A formal definition of first-order stochastic dominance is given below:

Definition 6. *[First-Order Stochastic Dominance] Given any pair of $R_l^s, R_{l'}^s \in \boldsymbol{R}^s$ associated with p.d.f $f_l^s(r)$, $f_{l'}^s(r)$ and c.d.f. $F_l^s(r)$, $F_{l'}^s(r)$, the former has first-order stochastic dominance over the latter ($R_l^s > R_{l'}^s$) if and only if $\forall r \in \mathbf{R}^+$, $F_l^s(r) < F_{l'}^s(r)$.*

Without losing generality, we let $l \in [0, 1]$ and $R_l^{in,m} > R_{l'}^{in,m}$ if and only if $l > l'$. As a result, MSs are sorted according to the indoor macrocell channel quality they experience. We define l as the type of MS in this framework. First-order stochastic dominance promises that given any increasing valuation function $v(r)$, a type l MS always has higher expected valuation than those with type l' whenever $l' < l$. Thus, MSs can be sorted according to the expected valuation on service. First-order stochastic dominance is applied because what we are tackling in this problem here is the pricing strategy of a city-wide or national-wide service provider. The differences in interference and channel fading/shadowing conditions between the huge number of MSs can be ignored on the average sense. This is because differences in channel quality can be mostly attributed to the propagation loss due to distance and walls within an indoor environment. In this case, MSs can be sorted with Definition 6. Finally, the distribution of type l is given by the p.d.f $h(l)$ and c.d.f $H(l)$. We assume $\frac{d}{dx} \frac{h(l)}{H(l)} \geq 0$, which is a common property in popular distributions (Gaussian, Poisson, Exponential, Uniform) and other single-peak densities [39].

The femtocell data rate distribution $R_i^{in,f} \in \mathbf{R^{in,f}}$ can be correlated with $R_i^{in,m}$. Correlation depends on which spectrum the femtocell is operating in. We state this relation with the function $T : \mathbf{R^{in,m}} \mapsto \mathbf{R^{in,f}}$. Again, we assume here that $\mathbf{R^{in,f}}$ is an ordered set with first-order stochastic dominance as its binary relation. The exact form of the correlation function T depends on the spectrum model, as discussed below:

1. **Shared-Spectrum** The femtocell is operating in the same spectrum as the macro-

cell. Due to interference between femtocells and macrocells, an MS with a good macrocell channel quality likely holds a poor femtocell channel quality, especially when no interference management scheme is applied. Thus, we model T as a decreasing function: $T(R_l^{in,m}) = R_l^{in,f} < R_{l'}^{in,f} = T(R_{l'}^{in,m})$ if and only if $l > l'$. Notice that this does not necessarily mean that the femtocell system is inefficient in deployment. Even though the interference exists, the femtocell may still provide some advantages such as higher channel reuse efficiency. In this framework, the higher channel reuse efficiency in indoor environments plays an important role in increasing the profit of the service provider.

2. **Split-Spectrum** The femtocell is operating in different spectrum than the macrocell. Therefore, the indoor data rates under the femtocells have no correlation to the ones under macrocells. We model T as a constant function: $T(R_l^{in,m}) = R^{in,f}$.

For $s = out$, we simply assume that all MSs share the same outdoor data rate distribution R^{out} on average.

3.2.1 Contract Design

Services can be divided into two types: the basic macrocell service and the femtocell service, where the latter deploys a femtocell at the subscriber's home or office to offer indoor coverage. We assume that the maximum data rate a femtocell supports can be controlled by the service provider. A practical method to realize this control is to simply limit the allocated backhaul capacity of the femtocells. This, in turn, limits the maximum data rate supported by the femtocells, and is an easily implemented traffic control process since service providers have full control of the backhaul of the wireless system.

The basic contract scheme for macrocell services contains only one condition for using the basic service: the price t^m. By contrast, the femtocell contract contains two conditions: the maximum data rate r and the price t. When an MS i signs a contract (r, t) with the service provider, he or she is offered a femtocell deployment at home, and the maximum data rate provided the femtocell offered will be limited to r. If the service provider offers

only one single contract (r, t) for the femtocell service, this offer is described as a flat-fee contract. On the other hand, if the service provider offers a series of contracts $\{(r_i, t_i)\}$, these types of offerings are known as **differentiated contracts**. When multiple contracts are provided, MSs have the flexibility to choose contracts that work best for them, unless additional constraints are applied.

In summary, the contract can be denoted as (y, r, t), where $y = \{m, f\}$ is the type of contract. When $y = m$, the contract has macrocell-only service. When $y = f$, the contract provides femtocell service. Note that the maximum data rate is not capped when $y = m$. Let $V(y, r, l)$ be the expected data rate of a type l MS under a signed contract (y, r, t), which is

$$V(y, r, l) = p^{out} E[v(r_l^{out})] + p^{in} (E[v(r_l^{in,y})|r_l^{in,y} < r] + v(r_i)(1 - F_l^{in,y}(r))). \quad (3.2)$$

The utility of a type l MS is

$$u(y, r, t, l) = V(y, r, l) - t. \quad (3.3)$$

When multiple contracts $\{(r, t)\}$ are provided, a rational MS will choose the contract which maximizes his or her utility.

3.2.2 Incentive Compatibility

Incentive compatibility (IC) is an issue in game theory that describes whether the players will apply the actions the designer desires. In this framework, the incentive compatibility issue arises when the MSs rationally choose the contracts. When the service provider is negotiating a contract with an MS, the channel quality distribution of the MS may not be known. That is, the data rate distribution $R_i^{in,m}$ of MS i is private information. Moreover, even after signing the contract, cheating MS may still report false channel quality measurement to the service provider, effectively disguising themselves within as another category of MSs. Experienced users may even modify their devices, reporting forged channel qualities to prevent the service provider from validating their service-quality cat-

egory. As a result, the service provider may not address the MS's service quality category as a condition for new contracts. Therefore, when multiple femtocell contracts are offered for different types of MSs, the service provider should confirm whether the targeted MSs are choosing the contracts designed for their level of service quality.

The incentive compatibility issue is resolved when the provided contracts satisfy the IC condition:

Definition 7 (Incentive compatible (IC) condition)**.** *When femtocell contracts are given by $r(l), t(l)$, where $(f, r(l), t(l))$ is the contract for a type l MS, the contracts are defined as incentive compatible for MS set **L** if they satisfy the following conditions: $\forall l, l' \in \boldsymbol{L}$*

$$u(f, r(l), t(l), l) \geq u(f, r(l'), t(l'), l), \tag{3.4}$$

$$u(f, r(l), t(l), l) \geq \underline{U}_l = u(m, \infty, t^m, l). \tag{3.5}$$

The $\underline{U}_l$ denotes the reserved utility if MSs choose not to sign the femtocell contract, which is the utility under the basic contract (m, ∞, t^m) in this framework. When the IC condition is satisfied, the utility of the target type l MS is maximized when users choose the contract $(r(l), t(l))$, which is designed for them. Therefore, the incentive to alter their choices and "cheat" to get a cheaper contract is eliminated under this contractual scheme. Femtocell contracts are considered to be **implementable** when they satisfy the IC condition. Here, we discuss three popular contract structures:

1. **Flat-fee contract**: Only one femtocell contract (r^f, t^f) is offered to all MSs. Since there is only one contract available, it is always incentive compatible.

2. **Non-IC differentiated contracts**: Multiple femtocell contracts $(r^F(l), t^F(l))$ are offered to MSs. This type of contract may not be implementable when the service type of a particular MS is unknown in advance. We apply this to show the theoretical upper bound of the overall profit when the type of MS can be validated.

3. **IC differentiated contracts**: Multiple contracts $(r^S(l), t^S(l))$ which satisfy the IC condition are offered, thereby promising implementability.

Table 3.1: Notations

Notation	Explanation
N	Total number of MSs
r_i	Data rate of MS i
$y \in \{m, f\}$	Macrocell/femtocell service
$l \in [0, 1]$	Type of MS
$s \in \{(out), (in, m), (in, f)\}$	Service environment
p^{in}, p^{out}	Probability that an MS stays indoor/outdoor
R_l^s	Data rate distribution of type l MS in environment s
$f_l^s(r), F_l^s(r)$	The p.d.f and c.d.f of type l MS's data rate r in environment s
(y, r, t)	Service contract for service y with maximum data rate r and price t
$V(y, r, l)$	The valuation of type l MS on the service y with maximum data rate r
$u(y, r, l, t)$	A type l MS's utility under contract (y,r,t)
$V^m(r), V^f(r)$	The valuation of MSs with maximum data rate r under macrocell/femtocell in split-spectrum system
$V^m(r, l), V^f(r, l)$	The valuation of type l MS with maximum data rate r under macrocell/femtocell in shared-spectrum system

The service provider aims to maximize his profits:

$$R = \int_{\mathbf{L}} (t^*(l) - c(y^*(l), r^*(l))) h(l) dl, \qquad (3.6)$$

where $\mathbf{L} \subset [0, 1]$ is the types of MSs signing contracts, $(y^*(l), r^*(l), t^*(l))$ is the contract a type l MS chooses, and $c(y, r)$ is the cost function of the service provider providing a y-type service with maximum data rate r. We assume $c(m, r) = 0$, $c(f, r) = c(r)$, $c(\infty) = \infty$, $c'(r) > 0$, and $c''(r) > 0$ for all $r \in \mathbf{R}^+$, where the latter denotes the variable cost of the femtocell deployment to a service provider.

3.3 Profit Maximization in Split-Spectrum System

Now we will show how to derive the optimal contract structure in the proposed framework. We begin with a split-spectrum system, in which no correlation exists between the channel quality under femtocell and macrocell. We assume that on average, all MSs share the same data rate distribution R^f when the femtocell is installed. If no femtocell is installed, a type l MS experienced indoor data rate distribution is $R_l^{in,m}$. We first show the optimal price of basic macrocell service. Then, we discuss the optimal contracts under three femtocell contract structures: the flat fee femtocell contract, non-IC differentiated femtocell contracts, and IC differentiated femtocell contracts.

75

3.3.1 Macrocell-Only Service

First we will discuss a case in which only the basic contract (macrocell service) under the price t^m is offered to all MSs. In this case, femtocell service is not provided, and MSs have only two options, either to sign the basic contract, or refuse to subscribe. The profit optimization problem is

$$\max N(1 - F(l^*))t^m, \quad \forall l \geq l^*, \ \underline{U}_l = u(m, \infty, t^m, l) \geq 0. \qquad (3.7)$$

The optimal basic contract price t^m and the boundary type l^* can be easily derived:

$$l^* = \begin{cases} \arg_l V(m, \infty, l) = (1 - F(l))V'(m, \infty, l), & \text{if exists,} \\ 0, & \text{else.} \end{cases} \qquad (3.8)$$

$$t^m = V(m, \infty, l^*). \qquad (3.9)$$

Notice that some MSs may refuse to sign the basic contract due to poor indoor channel quality, which holds when $l^* > 0$. In this case, the service provider simply does not offer wireless service to some MSs. In addition, for all $l > l^*$, $u(m, \infty, t^m, l) = \underline{U}_l > \underline{U}_{l^*} = 0$. That is, they all have positive utilities, which are referred to here as customer surplus. Profits can be increased by extracting customer surplus.

3.3.2 Flat Fee Femtocell Contract

Let us now discuss the flat fee femtocell contract (r^f, t^f) where only a single price and the maximum data rate option is offered. An MS will now have three options: the basic contract, femtocell contract, or no subscription. The profit maximization problem becomes

$$\max N \int_{\mathbf{L}} (t(l) - c(l))h(l)dl, \qquad (3.10)$$

where $\forall l \in \mathbf{L}$, $u(m, r(l), t(l), l) \geq 0$, and

$$(r(l), t(l), c(l)) = \begin{cases} (\infty, t^m, 0), & \text{if } u(m, \infty, t^m, l) > u(f, r^f, t^f, l), \\ (r^f, t^f, c(r^f)), & \text{otherwise.} \end{cases} \quad (3.11)$$

Notice that all MSs share the same femtocell data rate distribution R^f. Thus, they will have the same valuation $V(f, r^f, l)$ on the femtocell service. We denote $V^f(r^f) = V(f, r^f, l)$ and $V^m(l) = V(m, \infty, l)$ in the following sections.

Consider the two cases in this section: the case where t^m is adjustable and the case where it is not. We first briefly conclude that case when t^m is adjustable. In such a case, it can be shown that there always exists a t^m that is high enough to push all MSs who would potentially benefit from the femtocell turn to the femtocell contract. Let us consider that case that the femtocell service is profitable to all users, that is, $V^f(r^f) - c(r^f) - V^m(l) \geq 0$ for all $l \in [0, 1]$. In such a case, the service provider will push all MSs to use the femtocell service by increasing the basic contract price to a unreasonably high value. All customer surpluses can then be extracted from the femtocell users by setting $t^f = V^f(r^f)$ since their utilities will come out negative under the unreasonable high basic contract price t^m or zero with no subscription. The profits of service is then maximized. For other cases that only a portion of MSs are beneficial from the femtocell service, we can always choose a proper t^m to push those MSs to femtocell contract and maximize the profit by setting $t^f = V^f(r^f)$.

Let us now consider the case that t^m is given in advance and is fixed. We discuss this case because the basic contract price t^m, which represents the traditional unlimited data plan service price, is usually already determined and announced before the service provider introduces the femtocells. It may take too much inner cost to change the announced price. Without losing generality, we assume $t^m = V^m(0)$. In such a case, all MSs at least sign the basic contract since it gives them non-negative utility.

Proposition 1. *The optimal flat fee femtocell contract* (r^f, t^f) *in a split-spectrum system*

is:

$$r^f = \arg_r V^{f'}(r) = c'(r). \tag{3.12}$$

$$l^{f*} = \begin{cases} \arg_l h(l)(V^f(r^f) - c(r^f) - V^m(l) + V^m(0)) - H(l)V^{m'}(l) = 0, & \textit{if exists,} \\ 1, & \textit{otherwise,} \end{cases} \tag{3.13}$$

$$\mathbf{L^f} = [0 : l^{f*}], \ t^f = V^f(r^f) - V^m(l^{f*}) + V^m(0). \tag{3.14}$$

Please note that the proofs of all given propositions and lemmas, if not shown in the context, are provided in Appendix.

The femtocell contract is chosen by MSs with poor indoor channel quality ($l < l^{f*}$), while the basic contract is chosen by the other MSs. The femtocell service does improve the MSs' valuations on the wireless service, and the service provider's profit is increased by enhancing the channel quality of MSs. However, as shown in (3.14), t^f is strictly lower than V^f for those type l MSs that $l < l^{f*}$. This means that some customer surpluses are still left to these MSs. We may extract it with differentiated contracts.

3.3.3 Non-IC Differentiated Femtocell Contract

The customer surpluses left to MSs are due to their advantage under the flat fee contract: they are charged with the same price even if they have different service quality under the macrocell. If the service provider knows the exact type of MSs, he can charge different prices according to the MSs' types. Here we introduce the optimal non-IC differentiated contract to extract all customer surpluses from the MSs under this assumption. The maximum data rate and price now can be functions of l ($r^F(l), t^F(l)$) . If all MSs choose the corresponding contracts, the profit becomes

$$R = N(\int_0^{l^{F*}} (t^F(l) - c(r^F(l)))h(l)dl + (1 - H(l^{F*}))V^m(0)), \tag{3.15}$$

where $l^{F*} = \arg_l V^f - t^F(l) = V^m(l) - V^m(0)$.

Proposition 2. *The optimal non-IC differentiated femtocell contracts $(r^F(l), t^F(l))$ in a*

split-spectrum system are:

$$r^F(l) = r^F = \arg_r V^{f'}(r) = c'(r), \tag{3.16}$$

$$l^{F*} = \begin{cases} \arg_l V^f(r^F) - c(r^F) - V^m(l) + V^m(0) = 0, & \text{if exists,} \\ 1, & \text{otherwise,} \end{cases} \tag{3.17}$$

$$\mathbf{L^F} = [0 : l^{F*}], \ t^F(l) = V^f(r^F) - V^m(l) + V^m(0), \tag{3.18}$$

where L^f is the set of MS signing for the femtocell contracts.

The profit made from the optimal non-IC differentiated femtocell contract is
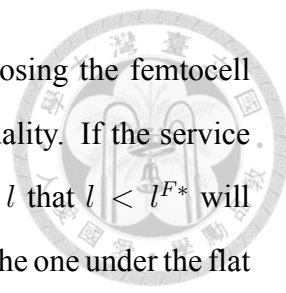
$$R = N \int_0^{l^{F*}} (V^f(r^F) - c(r^F) - V^m(l) + V^m(0))h(l)dl. \tag{3.19}$$

First, we observe that in non-IC differentiated contracts, all femtocell contracts offer the same maximum data rate r^F in (3.16), which is the same as the one offered in the optimal flat fee contract in (3.12). This is due to the fact that the channel quality under the femtocell is uncorrelated to the one under macrocells in the split-spectrum system. Then, we observe that $l^{F*} > l^{f*}$, which means that the service provider offers femtocell services to more MSs. Additionally, for those MSs already served under the flat fee femtocell contract, the price offered in non-IC differentiated contracts in (3.18) is higher than the one offered in the flat fee contract in (3.14). When the types of MSs are known, we see that the service provider may increase his profits in two directions: 1) increase the price of the femtocell service according to the MSs' type, and 2) extend the femtocell service to some MSs not served under the flat fee femtocell contract.

However, these contracts are not implementable according to our observation. We can check how much the utility of type l MS increases if he signs $(r^F, t^F(l^{F*}))$ instead of $(r^F, t^F(l))$:

$$u(f, r^F, t^F(l^{F*}), R_l) - u(f, r^F, t^F(l), R_l) = V^m(l) - V^m(l^{F*}) > 0. \tag{3.20}$$

The above equation is always positive. In other words, an MS with poor indoor macrocell

channel quality can always get a positive utility increase when choosing the femtocell contract designed for an MS with good indoor macrocell channel quality. If the service provider cannot validate the MSs' types, all rational MSs with type l that $l < l^{F*}$ will choose the contract $(r^F, t^F(l^{F*}))$. The resulting profit will be same as the one under the flat fee contract $(r^F, t^F(l^{F*})$. The profit under this contract is never larger than the optimal flat fee femtocell contract in Proposition 1 since the latter is the optimal contract. We conclude that in a split-spectrum system, the optimal non-IC differentiated femtocell contracts are neither implementable nor optimal when the types of MSs are unknown to the service provider.

3.3.4 Incentive Compatible Differentiated Femtocell Contract

For the optimal IC differentiated femtocell contracts, the only type of incentive compatible femtocell contracts are the flat fee contracts in a split-spectrum system.

Proposition 3. *The only type of IC femtocell contracts in a split-spectrum system are flat fee contracts.*

This is mainly because the femtocell service quality in a split-spectrum system is not correlated to the macrocell signals. Therefore, an IC differentiated femtocell contract does not exist in a split-spectrum system. The optimal IC contract is same as the optimal flat fee femtocell contract in Proposition 1.

3.4 Profit Maximization in Shared-Spectrum System

Next, we derive the optimal contracts in the shared-spectrum system under different contract structures. In this system, the channel quality of MSs in a femtocell deployed environment has a negative correlation with macrocells. Thus, the transform function $T(\mathbf{R})$ is modeled as a decreasing function: $T(R_l^{in,m}) = R_l^{in,f} < R_{l'}^{in,f} = T(R_{l'}^{in,m})$ if and only if $l > l'$. We denote $V^f(r,l) = V(f,r,l)$ in this section to represent the valuation of an MS with $R_l^{in,f}$ on the femtocell service. It can be checked that $V^f(r,l)$ is increasing in

r and decreasing in l. Following the previous section, we assume that the basic contract price $t^m = V^m(0)$ is fixed and announced in advance.

3.4.1 Flat Fee Femtocell Contract

The corresponding optimization problem under the flat fee contract structure is same as the one in Proposition 1 except that the utility of an MS using the femtocell service becomes $u(f, r, t, l) = V^f(r, l) - t$.

Proposition 4. *The optimal flat fee femtocell contract (r^f, t^f) in a shared-spectrum system is :*

$$r^f = \arg_r V_r^f(r, l^{f*}) = c'(r), \tag{3.21}$$

$$l^{f*} = \begin{cases} \arg_l h(l)(V^f(r^f, l) - c(r^f) - V^m(l) + V^m(0)) - H(l)V^{m'}(l) = 0, & \textit{if exists,} \\ 1, & \textit{otherwise,} \end{cases} \tag{3.22}$$

$$\mathbf{L^f} = [0 : l^{f*}], \quad t^f = V^f(r^f, l^{f*}) - V^m(l^{f*}) + V^m(0), \tag{3.23}$$

where $V_r^f(r, l^{f*}) = \frac{\partial V^f(r, l^{f*})}{\partial r}$.

Notice that t^f is strictly lower than $V^f(r^f, l)$ for all $l < l^{f*}$, which means some customer surplus is reserved to MSs. In contrast to the split-spectrum system, where all MSs have the same utility when using the femtocell service, the $u(f, r^f, t^f, l)$ is decreasing with l. Therefore, MSs with good femtocell channel quality now have higher utilities.

3.4.2 Non-IC Differentiated Femtocell Contract

We now discuss the optimal non-IC differentiated contracts $(r^F(l), t^F(l))$, under the assumption that the channel quality of an MS can be validated by the service provider. The profit maximization problem is similar to the one in the split-spectrum system except in this case, there is correlation between macrocell and femtocell channel qualities. By following the same procedure as in Proposition 2, the optimal non-IC differentiated femtocell contracts are given as follows:

Proposition 5. *The optimal non-IC differentiated femtocell contracts $(r^F(l), t^F(l))$ in a shared-spectrum system are*

$$r^F(l) = \arg_r V_r^f(r, l) = c'(r), \tag{3.24}$$

$$l^{F*} = \begin{cases} \arg_l V^f(r^F(l), l) - c(r^F(l)) - V^m(l) + V^m(0) = 0, & \text{if exists,} \\ 1, & \text{otherwise,} \end{cases} \tag{3.25}$$

$$\mathbf{L^F} = [0 : l^{F*}], \ t^F(l) = V^f(r^F(l), l) - V^m(l) + V^m(0), \tag{3.26}$$

where $V_r^f(r, l) = \frac{\partial V^f(r,l)}{\partial r}$.

Unfortunately, the above contracts are still not implementable when the channel quality cannot be validated. It can be checked that all rational MSs with $R_l^{in,m}$ that $l < l^{F*}$ will choose the contract $(r^F(l^{F*}), t(l^{F*}))$ since this contract provides a higher utility to them.

3.4.3 Incentive Compatible Differentiated Femtocell Contract

Proposition 6. *The optimal IC differentiated femtocell contracts $(r^S(l), t^S(l))$ in a shared-spectrum system:*

$$r^S(l) = \arg_r V_r^f(r^S(l), l) = c'(r^S(l)) - \frac{H(l)}{h(l)} V_{lr}^f(r^S(l'), l)|_{l'=l}, \tag{3.27}$$

$$l^{S*} = \begin{cases} \arg_l V^f(r^S(l), l) = \frac{H(l)}{h(l)}(V^{m'}(l) - V_l^f(r^S(l'), l)) + c(r^S(l)) + V^m(l)|_{l'=l}, & \text{if exists,} \\ 1, & \text{otherwise,} \end{cases} \tag{3.28}$$

$$t^S(l) = V^f(r^S(l), l) + \int_l^{l^{S*}} V_l^f(r^S(s), s)ds - (V^m(l^{S*}) - t^m), \mathbf{L^S} = [0 : l^{S*}]. \tag{3.29}$$

Now we derive the optimal IC differentiated contracts. We first discuss the sufficient condition to satisfy the IC condition in the shared-spectrum system. This can be achieved

through two methods: compensate MSs with good channel quality by offering some reserved utility, and decrease service quality of MSs with poor channel quality distribution. For femtocell contracts $(r^S(l), t^S(l))$, we denote $U(l, l') = u(f, r(l'), t(l'), l)$. Then, we show that our framework satisfies the following condition:

Lemma 1 (Differentiation Condition)**.**

$$V_{rl}^f(r, l) = \frac{\partial \left(\frac{\partial V^f(r,l)}{\partial r} \right)}{\partial l} < 0.$$

Proof. Recalling $V(y, r, l)$, we have $V_r^f(r, l) = V_r(f, r, l) = p^{in} v'(r)(1 - F_l^{in,f}(r)) > 0$. Thus,

$$
\begin{aligned}
V_{rl}^f(r, l) &= \lim_{dl \to 0} \frac{p^{in} v'(r)((1 - F_{l+dl}^{in,f}(r)) - (1 - F_l^{in,f}(r)))}{dl} \\
&= \lim_{dl \to 0} \frac{p^{in} v'(r)(F_l^{in,f}(r) - F_{l+dl}^{in,f}(r))}{dl} < 0.
\end{aligned}
\tag{3.30}
$$

The last inequality comes from the fact that $R_l^{in,f}$ has first-order stochastic dominance over the $R_{l+dl}^{in,f}$. $\qquad \square$

The differentiation condition shows that under the same maximum data rate limitation, an MS with good signal quality has higher marginal utility comparing to those with poor signal quality. This means there are service differences among MSs. With Lemma 1, we prove that the IC condition can be converted into the following form:

Lemma 2. *Femtocell contracts $(r(l), t(l))$ are implementable in $\mathbf{R^{in,f}}$, $\mathbf{R^{in,m}}$, $T(\cdot)$ if:*

$$U(l) = U(l^*) - \int_l^{l^*} V_l^f(r(s), s) ds, \tag{3.31}$$

$$U(l^*) \geq V^m(l^*) - t^m, \tag{3.32}$$

$$r'(l) \leq 0. \tag{3.33}$$

where $V_l^f(r, l) = \lim_{dl \to 0} \frac{V^f(r, l+dl) - V^f(r, l)}{dl}$ and $U(l) = u(f, r(l), t(l), l)$.

Proof. First, the (3.31) is directly converted from (3.4) when (3.33) is satisfied. This can be checked by differentiating (3.31) and applying (3.33) and Lemma 1. For (3.32), first

notice that the reserved utility $V^m(l^*) - t^m$ increases with l. Since $V_l(m, r, l) > 0$, we have $U(l) > U(l^*) > V^m(l^*) - t^m > V^m(l) - t^m$. Thus, the (3.5) is satisfied when (3.31) and (3.32) are satisfied. Since Definition 7 is satisfied, the above equations indeed describe a series of incentive compatible contracts. $\square$

Lemma 2 suggests that some utilities should be left to those MSs with good channel qualities. In addition, an MS with poor femtocell channel quality will be offered with a lower maximum data rate femtocell service to prevent other MSs having incentives to sign the same contract. Now we describe the optimal IC differentiated femtocell contracts in a shared-spectrum system in Proposition 6, while the proof is as follows:

Proof. The profit of the service provider is given by $R = \int_0^{l^{f*}} (t^S(l) - c(r^S(l)))h(l)dl + (1 - H(l^{S*}))t^m$. Recalling the definition of $u(y, r, t, l)$ in (3.3), we have

$$R = N(1 - H(l))t^m + N \int_0^{l^{F*}} (V^f(r^S(l), l) - u(f, r^S(l), t^S(l), l) - c)h(l)dl \quad (3.34)$$

Applying (3.31), (3.32), and integration by part to $u(f, r^S(l), t^S(l), l)h(l)$, we have

$$R = N \int_0^{l^{S*}} (V^f(r^S(l), l) + V_l^f(r^S(l), l)\frac{H(l)}{h(l)} - V^m(l^{S*}) - c(r^S(l)))h(l)dl + Nt^m \quad (3.35)$$

We first apply pointwise optimization over $r^S(l)$ to obtain the optimal contracts data rate $r^S(l)$ for all MSs, which is (3.27). Then, we find the optimal boundary l^{S*} by the first-order differentiation method to derive (3.28). Finally, the optimal price (3.29) is by Lemma 2 and (3.3). $\square$

Notice that (3.35) indicates l^{S*} makes two contradictory effects on the profit: when l^{S*} increases, more MSs are directed to sign the more profitable femtocell contracts $((f, r^S(l), l))$, but more utility $(V_l^f(r^S(l), l)\frac{H(l)}{h(l)} + V^m(l^{S*}))$ should be reserved for other femtocell users for maintaining IC. The profit is maximized when these two effects are balanced, which is at l^{S*}.

Figure 3.1: Negative Correlation between Macrocell and Femtocell service quality in Shared-Spectrum System

3.5 Numerical Verification

We verify the theoretical conclusions through numerical analysis. We discuss the service provider's profit and MSs' expected data rates when given certain contract structures. The settings across all simulations are as follows. The femtocell deployment cost function is $c(r) = 0.01r^2$. The valuation function of MSs is $v(r) = r$. The probability of MSs in indoor environments is $p^{in} = 0.5$. All data rates follow the Rayleigh distribution except the differences in average. The average outdoor data rate $E[R^{out}]$ is 4 Mbps, while indoor data rates vary according to simulation schemes.

3.5.1 Correlation between Macrocell and Femtocell Service Quality

We verify our assumption on the negative correlation between macrocell and femtocell service quality in a shared-spectrum system. We implement an LTE overlay macrocell-femtocell simulator by extending the link-level simulator implemented in [20]. In our simulations, there are 19 macrocells with a radius of 1.5 km in a hexagonal layout. Within each macrocell, one femtocell is randomly placed. All cells share the same carrier. We choose the macrocell in the central area and a femtocell at a random distance to the macrocell BS as our simulating overlay system. One MS is placed with a distance of 35m to the femtocell BS. The statistics of the correlation between the data rates of MSs using macrocell and femtocell are displayed in Fig. 3.1, which shows that there is a negative correlation
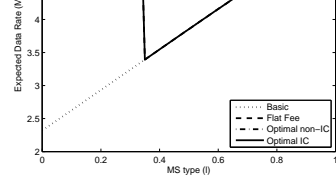
(a) Service Price

(b) Profit

(c) Expected Data Rate

Figure 3.2: Different Contract Structures in Split-Spectrum System

between the data rates under macrocell and femtocell. In addition, it suggests that a linear approximation is enough to fit the correlation. Thus, we use a linear function to model this negative correlation in our simulations.

3.5.2 Price and Profit under Split-Spectrum System

We investigate the profit and expected data rates of MSs in the split-spectrum system under different contract structures. The expected indoor macrocell data rates are uniformly distributed within $[0.1, 1]$ Mbps, and the expected femtocell data rate is 5 Mbps. The types of MSs are uniformly distributed between $[0, 1]$, that is, $\forall l \in [0, 1]$, $h(l) = 1$. A type l MS has the average indoor macrocell data rate of $0.1 + 0.9l$ Mbps.

We calculate the service prices of basic contract, flat fee femtocell contract, optimal non-IC and IC differentiated femtocell contracts. The service prices, profits, and expected data rate for type l MSs are shown in Fig. 3.2. Notice that the service provider's total revenue and profit under certain contracts is the integrated area below the contract price and profit line in each figure.

We observe that the price of optimal IC differentiated femtocell contract (3.96) is the

same as the price of the flat fee femtocell contract, which confirms Proposition 3. The optimal non-IC differentiated femtocell contracts potentially offer the largest revenue if the service provider can validate the MSs' types and force them to sign the correct corresponding contract. However, we have proved that they eventually choose the boundary contract designed for the MS with the poorest macrocell signal quality. The price of that contract is 2.92, which is lower than that of a flat fee contract. Thus, the revenue and profit are eventually lower under the non-IC differentiated contracts than the optimal flat fee contract.

However, as shown in Fig. 3.2(c), those MSs choosing the femtocell contracts indeed benefit from the data rate enhancement. However, some MSs (of the type between 0.35 to 0.69, with corresponding expected macrocell data rate 1.76 to 3.43 Mbps) refuse to sign the flat fee femtocell contract because the enhanced quality cannot cover their extra expanse. In fact, these MSs are intentionally excluded by the service provider because they cause higher service prices for others.

3.5.3 Price and Profit under Shared-Spectrum System

We create two wireless network schemes in the shared-spectrum system. The first one is the poor macrocell scheme, where the expected indoor macrocell data rates are uniformly distributed within $[0.1, 1]$ Mbps. The other is the good macrocell scheme, where the expected indoor macrocell data rates are uniformly distributed within $[0.1, 5]$. In both schemes, the femtocell data rates are distributed within $[1, 5]$, and the data rates under two cells are negatively correlated. Notice that in the poor macrocell scheme, the femtocell always provides higher data rates for all types of MSs. Therefore, service providers prefer to have all MSs use the femtocell in order to increase their valuations on the service. On the other hand, in the good macrocell scheme, some MSs may eventually have a lower data rate under the femtocell. In such a case, only those MSs with poor macrocell signals should install femtocells to increase their indoor data rates. The types of MSs are uniformly distributed between $[0, 1]$. We calculate the service price, profit, and expected data rates under different contract structures and network schemes. The results are shown in Fig.
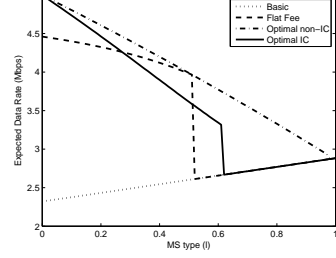
(a) Service Price with [...] M
cell Service Quality

(c) Expected Data Rat[...]
Macrocell Service Qua[...]

Figure 3.3: Different Contract Structu[...] m

(a) Service Price with Good Macro- (b) Profit within Good Macrocell
cell Service Quality   Service Quality
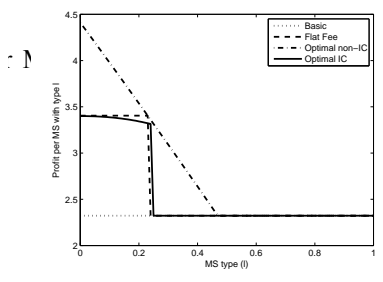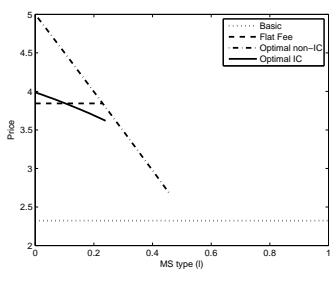
(c) Expected Data Rate within Good
Macrocell Service Quality

Figure 3.4: Different Contract Structures in Shared-Spectrum System

3.3 and 3.4.

In the poor macrocell scheme (Fig. 3.3), we observe that almost all MSs choose to sign the femtocell contracts under the non-IC differentiated contracts because the femtocell service provides better service quality (higher expected data rate) with affordable pricing to every MS. However, rational MSs are shown to still eventually choose the contract for the boundary MS ($l = 1$ in this case). Thus, though all MSs have higher expected data rates under optimal non-IC differentiated contracts, the profit of the service provider is less. For the flat free femtocell contract, only 52% of MSs choose the femtocell contracts. Although the profit under such a contract is higher, the expected data rates of those MSs not installing femtocells are less.

When the optimal IC differentiated contracts are applied, more MSs (62%) choose to sign the femtocell contracts because the service provider offers discounted choices to MSs with poor femtocell signal quality. Further, for MSs with good femtocell signal quality are charged a higher price than the flat fee contract, which returns a higher maximum data rate. Thus, the IC differentiated contracts increase the profits from two aspects: higher price for MSs with good femtocell signal qualities and discounted price for those MS not served under flat fee femtocell contract (Fig. 3.3(a)). This confirms the correctness of our conclusions in Lemma 2 and Proposition 6.

For the expected data rate (Fig. 3.3(c)), MSs with good femtocell signal qualities are offered higher expected data rate than that of the flat fee contract. However, this number is still lower than the optimal non-IC differentiated contracts. For those MSs with poor femtocell signal quality (type 0.28 to 0.52), expected data rate is lower than under the flat fee contract. This is a necessary service quality degradation to promise incentive compatibility.

We also observe that the enhancements from IC differentiated contracts is more significant when the quality difference increases. When good macrocell scheme is applied (Fig. 3.4), the profit under optimal IC differentiated contracts is almost the same as the flat fee contract ones. Since MSs now have better macrocell service quality, they also have higher reserved utilities. Thus, the service provider needs to offer more utility for
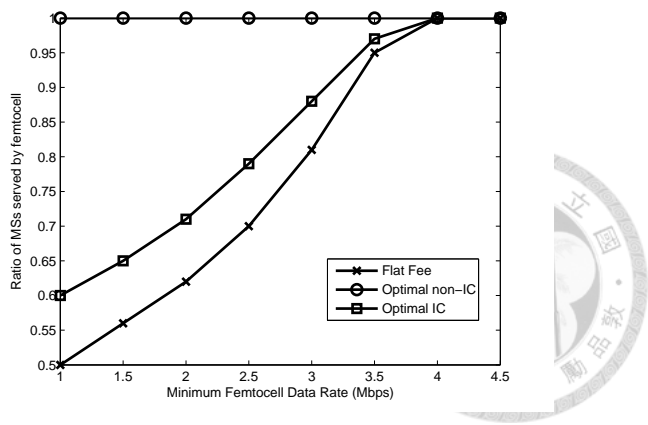
(a) Average Profit

(b) Ratio of MSs Served by Femtocell

Figure 3.5: Effect of Service Quality Difference

the incentive compatibility in IC differentiated contracts. The utility is given by offering

lower price (Compared with Fig. 3.3(b) and 3.4(b)) and higher data rate (Fig. 3.3(c) and

3.4(c)), where both are costly for the service provider when the macrocell signal quality

is generally good. Due to these two hidden costs, the IC differentiated contracts cannot

extract much more profit than with the flat fee contract in this scheme. Nevertheless, the

profits under IC differentiated contracts are never lower than the flat fee contract.

3.5.4 Effect of Service Quality Difference
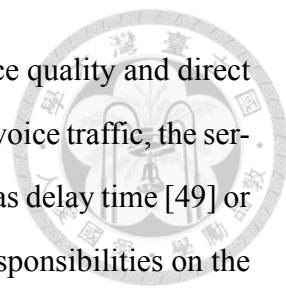
We now investigate how the service quality difference affects the profit. We reapply

the poor macrocell service quality scheme in the shared-spectrum system. We control the

minimum femtocell data rate at to fall between 1 to 4.5 Mbps in this analysis. When the

minimum femtocell data rate increases, the femtocell service quality difference among

MSs turns insignificant. We apply the four contract structures into the wireless system, and the results are shown in Fig. 3.5.

We observe that the overall profit increases with the minimum femtocell data rate under all contract structures. When the minimum femtocell data rate increases, the overall femtocell service quality also increases. Thus, the service provider can charge a higher price under all femtocell contracts. We also observe that the optimal IC differentiated contracts always derive more profits than the flat fee ones. These extra profits increases with the decrease of the minimum femtocell data rate (Fig. 3.5(a)). This is due to the increase of channel quality differences. When the minimum femtocell data rate decreases, MSs are more likely to have different channel qualities under the femtocell service. Therefore, the customer surplus, which is produced by the channel quality differences, is increased. Since the customer surplus is the source of the extra profit derived by the IC differentiated contracts, this contract structure becomes more profitable when the channel quality difference is significant. We also observe that the ratio of MSs signing the femtocell contracts increases with the minimum femtocell data rate under all contract structures (Fig. 3.5(b)). Additionally, the IC differentiated contracts indeed make more MSs choose the femtocell service comparing to the flat fee contract. In conclusion, the benefit of differentiated contracts is more significantly when the service quality difference increases. Moreover, MSs are more likely to choose the beneficial femtocell service under the differentiated contracts.

3.6   Related Work

The profits of wireless service providers have been studied extensively. One popular topic is competition [40--43]. Research shows that differentiating users according to their valuations on different service providers can mitigate competition, and therefore increase the profits of all service providers. On the other hand, when we consider a single service provider, research suggests that service differentiation can also generate more profits [41,44--48]. Service differentiation is offered either at the requests of users [41,44] or in accordance with the classification of service providers [45--47]. In the latter case, the

differentiated pricing strategy is used to classify users based on service quality and direct them to corresponding services. For instance, in research focusing on voice traffic, the service differentiation is based on measurements of service quality, such as delay time [49] or blocking probability [45, 46]. Some literature recommends mutual responsibilities on the contracts [44, 48], including pricing and quality of service (QoS) requirements. However, most of this research requires information about service quality and requirements to be reported directly by the users, which, as shown in the previous section, is susceptible to inaccuracy since users may untruthfully report their information to maximize their utilities. Service providers are in need of a truthful mechanism to guarantee expected profits.

Currently, there are several theoretical discussions on the market issues of femtocell systems [50, 51]. Claussen et al. show that an overlay macrocell-femtocell system is a better choice than a macrocell-only system in terms of increasing profits [50]. Shetty et al. discuss the effects of femtocells on the profits of service providers [51]. Results also show that femtocells can increase the profits of system operators by decreasing the loading of macrocells while charging higher for the femtocell services. However, the pricing scenario in this research applied only to the flat fee scenario in which service quality is the same on average for all MSs. Cases in which signal quality varies between the MSs under different environments have not yet been investigated. In this chapter, we show that the differentiated contract [52], which can generate profits when user's valuation on the service is varied, and has great potential to improve the overall profits of femtocell systems.

3.7 Summary

In this chapter, we demonstrate how to maximize the profit of an unlimited data plan through femtocell systems and specialized contract designs. When the service quality of an MS is verifiable, we employ the service differentiation in the differentiated contracts to maximize the service provider's profits. By contrast, when the service quality cannot be verified, the incentive compatible condition is applied to prevent MSs from cheating when signing the contract. We prove that only flat fee contracts are incentive compatible

in a split-spectrum system, and the differentiated contracts can be incentive compatible in shared-spectrum systems. We conclude that a service provider can indeed derive more profits from MSs by 1) introducing femtocell services, and 2) provide differentiated contracts. The former increases MSs' valuation on the service, while the latter derives more customer surplus from MSs using the femtocell service, while offering other MSs an affordable deal.

Appendix: Proofs of Propositions

Proof of Proposition 1: For $t^m > 0$ and $t^f < V^f$, it has been shown in previous section that if $u(f, r^f, t^f, l) > u(m, \infty, t^m, l)$, then $u(f, r^f, t^f, l') > u(m, \infty, t^m, l')$ for all $l' < l$. Thus, there exists l^{f*} that for all MS with type $l < l^{f*}$, they choose the femtocell service. Otherwise they choose the basic contract since $t^m = V^m(0) \geq V^m(l)$. Thus, the service provider's profit is given by $H(l^f)(t^f - c(r^f)) + (1 - H(l^f))(t^m)$ where $t^f \leq V^f(r^f)$. The optimal contracts are derived by optimizing this new profit function under the two constraints with respects to t^f, r^f, and l^{f*}.

Proof of Proposition 2: To make a type l MS choose the femtocell contract given the basic contract price t^m, his utility under the femtocell contract should be no less than the one under the basic contract. Thus, $V^m(l) - t^m \leq V^f(r^F) - t^m \Rightarrow t^m \leq V^f(r^F) - V^m(l) + t^m$. In addition, the profit of femtocell contract is higher than the basic contract if and only if $t^F - c(r^F) > t^m$. With the above two equations and applying pointwise optimization, we can derive the optimal contracts.

Proof of Proposition 3: Since in the split-spectrum system, all MSs share the same femtocell data rate distribution, we can denote $V(f, r, l) = V^f(r)$ for all MSs. Recalling (3.31), we have $u(f, r(l), t(l), l) = V^f(r(l)) - t(l) \geq u(f, r(l'), t(l'), l) = V^f(r(l')) - t(l') \ \forall l, l' \in \mathbf{L}$. However, the above equation is true for all l, l' if and only if $r(l) = r(l')$ and $t(l) = t(l')$ everywhere. Thus, the only incentive compatible contract is the flat fee contract.

Proof of Proposition 4: We may follow the same proof of Proposition 5 to derive the solution.

Proof of Proposition 5: The solution can be derived through point-wise optimizing each type $l \in [0, 1]$. The optimal data rate $r^F(l)$ for type l is given by

$$\frac{dV^f(r, l) - c(r)}{dr}\Big|_{r=r^F(l)} = 0 \Rightarrow V_r^f(r^F(l), l) = c'(r^F(l))$$

Then, the optimal price $t^F(l)$ is determined by how much customer surplus the MS has. The utility of MS l given the data rate $r^F(l)$ is $V^f(r^F(l), l) - V^m(l) + t^m$. Thus, we simply set the price to this in order to extract all customer surpluses. Finally, the boundary MS type l^{F*} is the one that give the service provider the same profit as the macrocell contract. Thus, it is determined by $t^F(l) - c(r^F(l)) = t^m \Rightarrow V^f(r^F(l), l) - c(r^F(l)) - V^m(l) = 0$.

Chapter 4
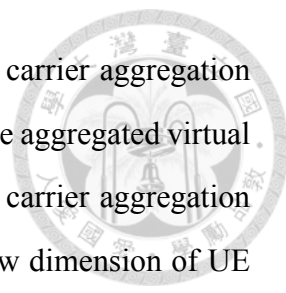
Carrier Aggregation in LTE-Advanced System: An Auction Design

4.1 Introduction

Next-generation wireless wide-area network (WWAN) standards, such as IEEE 802.16 and 3GPP LTE-Advanced, are established for achieving the 4G standard requirements proposed by ITU-R [1]. One of the most challenging requirements in 4G standard is 1Gbps peak data rate for low-mobility user equipment (UEs) and 100 Mbps peak data rate for high-mobility UEs. In theory, the data rate requirement could be achieved by expanding the carrier bandwidth to 100 MHz. Nevertheless, a contiguous spectrum with such a wide bandwidth is rarely available in developed and developing countries since most feasible spectrum has been licensed to existing wireless techniques such as TV, GSM, or 3G. The unlicensed spectrum is mostly in a non-contiguous narrowband form. Given the carriers formed by the narrowband spectrum, next-generation WWAN standards are unlikely to satisfy the peak data rate requirements if each UE is served by a single carrier.

4.1.1 Carrier Aggregation

Carrier aggregation is introduced in LTE-Advanced for aggregating non-contiguous spectrum into a virtual carrier [53]. Multiple narrowband carriers can be aggregated into

a wideband virtual carrier for better spectrum utilization. UEs with carrier aggregation capability can increase their peak data rates by transmitting through the aggregated virtual carrier that virtually provides a larger transmission bandwidth. The carrier aggregation configuration can be UE-specific, which means that it provides a new dimension of UE configurations. UEs that require high throughput or have delay constraints can be assigned with a virtual aggregated carrier for high peak data rate, while others may be assigned with the traditional carrier for energy conservation. In summary, carrier aggregation can increase UE peak data rate, enhance spectrum utilization efficiency, and provide flexible configurations on a per-UE basis.

Beside the benefits, there are challenges in the design and implementation of carrier aggregation in LTE-Advanced system. New hardware and protocol designs, for instance, are required for all LTE-Advanced infrastructure and devices to support this new function. Nevertheless, it should have minimal impacts on the existing and running LTE protocol and maintain the compatibility with the existing LTE-legacy devices. For configuration part, carrier activation on UEs is one of the key issues in carrier aggregation. Which carrier(s) should be activated for each UE is a complex problem with concerns on the diverse carrier quality, coverage, spectrum efficiency, and UE-specific data requirements [54]. Using the system we illustrated in Fig. 4.1 as an example, LTE devices with different CA capability are located at different locations in the cell. The cell is offering two carriers $C1$ and $C2$, each with different coverage in the cell. In this example, only the CA-supported device within the coverage of $C1$ can burst its throughput using both $C1$ and $C2$. For others, the choice of activated carrier for those two devices outside of $C1$ is limited to $C2$ due to carrier reception. Additionally, the legacy device within the coverage of $C1$ supports only one carrier due to device capability. In addition, it may not be necessary to enable carrier aggregation for devices within $C1$ if they are in idle state or with low data rate requirement. The carrier activation problem is complex that it deserves further studies.

Additionally, in order to make the virtual carrier function properly, one of the activated carriers should be the primary carrier, which is responsible for not only the data transmis-
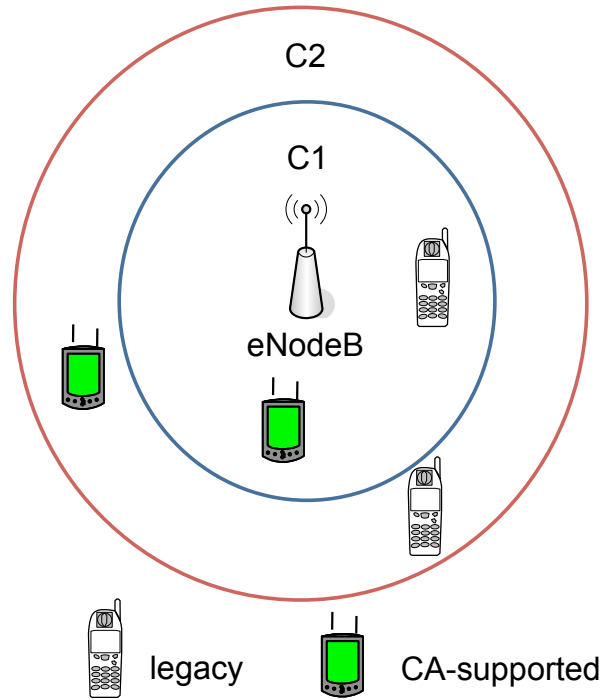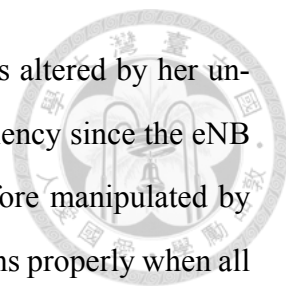
Figure 4.1: An illustration of CA-enabled LTE Cell

sion but also the delivery of control signals, which is called cross-carrier scheduling [55]. By aggregating the control signal transmission into one or several carriers, the system may prevent unnecessary interference from neighbor cells. The choice of the primary carrier further increases the complexity of the carrier activation problem. It can be seen that this problem is a NP-hard problem. Thus, an optimal solution may not be derived in a reasonable time. A practical solution with acceptable calculation time is desirable and will be one of the main objectives of this work.

4.1.2 Truth-telling

Nevertheless, most of the existing works studying cellular systems make an assumption that all infrastructure and devices will faithfully follow the designed protocol. This assumption may not be valid in real world scenario [56]. For instance, some works assume that the evolved NodeB (eNB) knows the data requirements of UEs when she is calculating the final carrier and resource block allocations. However, the data requirements of UEs should be reported by UEs themselves since only they known the information. The reporting process introduces a possibility of cheating for the UEs: A UE may report the data

requirement untruthfully if the resulting resource allocation, which is altered by her un-truthful report, increases her utility. This impairs the allocation efficiency since the eNB does not receive the correct information and the allocation is therefore manipulated by UEs under their selfish concerns. Therefore, a solution which functions properly when all devices faithfully follow the design may perform poorly when the devices (UEs) behave rationally. A detailed analysis on the rational behaviors of users in the system is neces-sary in order to understand and prevent this kind of malfunction. Game theory, which aims to analyze the rational behaviors and interactions of players under certain game rules, is suitable for this purpose.

In this work, we study the downlink carrier activation and resource block allocation in carrier aggregation capable LTE system. UEs are assumed to be rational and have different QoS requirements on the receiving data amount and delays. Their utilities are determined by the received data amount and the delay. The eNB is in charge of the carrier and re-source block allocation according to the carrier quality, coverage, and UE-specific data requirements, while its objective is two-fold: It aims to maximize the system efficiency, which is the total utility of UEs in the system, and prevent the rational UEs from reporting their information untruthfully. Our main contributions are as follows:

1. We address the heterogeneous characteristics of carrier quality, coverage, and UE QoS requirements in our proposed model and solutions. We make use of the carrier aggregation to enhance the system performance by satisfying the QoS requirements of UEs more efficiently. Specifically, we consider two type of UEs, throughput-sensitive and delay-sensitive UEs, in this work. The proposed solution effectively reduces the delay for delay-sensitive UEs while satisfying the throughput require-ments of throughput-sensitive UEs by properly triggering the carrier aggregation function of each UE accordingly.

2. To the best of our knowledge, this is the first attempt to propose and address the truth telling issue in carrier aggregation. We propose a truthful auction design specifically for the heterogeneous carrier quality and QoS requirements of UEs. We theoreti-cally prove that the proposed design indeed provides proper incentive for the UEs

to truthfully report their QoS requirements even if they selfishly behave.

3. The proposed solution is evaluated through extensive simulations in our LTE-Advances simulator, which uses the models and parameters suggested in 4G evaluation document [1] and 3GPP LTE standard [2]. The simulation results show that the proposed solution outperforms traditional implementations significantly in terms of social welfare, which represents the ability of the system satisfying the QoS requirements of UEs.

4.2 System model

We consider a LTE-Advanced cell with one eNB and a set of UEs $\mathbf{N} = \{1, 2, ..., n\}$. The eNB is assigned with a set of carriers $\mathbf{C} = \{1, 2, ..., K\}$ for serving UEs. A carrier c is divided into B_c subcarriers. In a duration of T slots, there are $T * B_c$ resource blocks in each carrier c to be allocated to UEs.

UEs are heterogeneous in their experienced carrier qualities, carrier aggregation capabilities, and QoS requirements. Specifically, the carrier quality indicator $Q_{i,c}$ indicates the expected amount of data per resource block UE i can receive if carrier c is activated for her. Notice that when $Q_{i,c} = 0$, either UE i has no reception on carrier c (out of coverage) or UE i does not support the baseband of carrier c (hardware limitation). Then, let C_i be the maximum number of aggregating carriers UE i can support. For legacy LTE devices, $C_i = 1$. For CA-capable devices, C_i is greater than one and mostly equals to two or three.

4.2.1 QoS Requirements of UEs

The QoS requirements of UE i is denoted by (M_i, k_i), where M_i is the amount of requested data in a duration of T slots, and $k_i \in \{th, delay\}$ indicates whether the UE is throughput-sensitive or delay-sensitive.

When $k_i = th$, UE i is requesting a downlink transmission service with a guaranteed average throughput of M_i/T. This type of QoS requirements can be found in file downloading or video streaming service, in which a minimum acceptable throughput is

required to maintain the quality of service to an acceptable level. In such a case, let m_i be the actually received data amount by UE i, UE i's valuation on the service quality is given by a valuation function $V^{th}(m_i, M_i)$ satisfying the following properties:

$$\frac{dV^{th}(m_i, M_i)}{dm_i} \begin{cases} \geq 0, & m_i < M_i; \\ = 0, & m_i > M_i. \end{cases} \tag{4.1}$$

$$V^{th}(M_i, M_i) \equiv 1. \tag{4.2}$$

The (4.1) indicates that UE i's valuation increases with the throughput until the requirement M_i/T is met. The (4.2) normalizes the valuations of all throughput-sensitive UE's by letting their maximum valuation on the service be one.
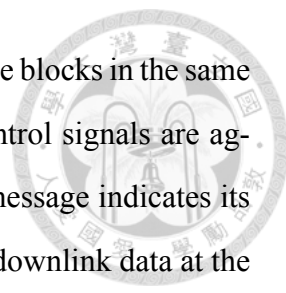
When $k_i = delay$, UE i is requesting a downlink transmission service with a delay-sensitive data of size M_i. This represents the case of search query and voice call in which small but timely response is expected. In these applications, the user will have a higher valuation when she receives the data in shorter delay. We model this requirement with the following valuation function $V^{delay}(\cdot)$. Let m_i be the actually received data amount by UE i and d_i be the delay of the last amount of received data. When $m_i \geq M_i$, UE i's valuation $V^{delay}(d_i)$ satisfy

$$\frac{dV^{delay}(d_i)}{dd_i} \leq 0 \tag{4.3}$$

For the case that $m_i < M_i$, we let $d_i = \infty$ to reflect the fact that the requested data is not completed received and therefore useless to the UE at this moment.

4.2.2 Cross-Carrier Scheduling

Cross-carrier scheduling improve the transmission quality by aggregate control signals of multiple carriers in one control channel that the UE experiences less interference from neighbor cells. Specifically, UEs not only experience different transmission quality $Q_{i,c}$ in carriers, but also the interference on the control signals. In LTE downlink transmission, physical downlink control channel (PDCCH) in the activated carrier is used to

deliver notification messages to UEs of the allocated downlink resource blocks in the same carrier. When cross-carrier scheduling is activated, all downlink control signals are aggregated into the primary carrier's PDCCH. Each downlink control message indicates its corresponding carrier, and the notified UE can listen and receive the downlink data at the indicated resource block in the indicated carrier. In such a case, the UE only needs to listen to the PDCCH in her assigned primary carrier for all the PDCCH messages.

Given the interference level on the PDCCH in each carrier experienced by UEs, the eNB should assign the primary carrier of each UE to the one with least interference among all the activated carriers. Here we denote $D_{i,c}$ as the interference level experienced by UE i in carrier c, and $c_i^p \in \mathbf{C}$ as the primary carrier used for transmitting PDCCH signals. Then, $P(D_{i,c_i^p})$ is the probability that the PDCCH signals of carrier c can be successfully decoded by UE i if the corresponding primary carrier is c_i^p. Finally, the expected received data amount per resource block of UE i in carrier c conditioning on the choice of primary carrier c_i^p is given by $P(D_{i,c_i^p})Q_{i,c}$.

4.2.3 BS Resource Allocation

The CA resource allocation works as follows. Before the time slot 1, the eNB requests UEs to report their carrier qualities and QoS requirements for the following T slot. Then, the eNB determines the carrier activation and resource block allocation for each UEs according to the received information. According to the allocation, eNB first activates each UE's carriers and assign the primary carrier for the UE. Then, at each time slot $t \in [0, T]$, the eNB notifies the UEs through PDCCH signals if their downlink data is transmitted at specific resource blocks in certain carriers at time slot t. The whole process terminates and restarts at time slot T.

4.3 Carrier Activation and Resource Block Allocation

The objective of eNB is to maximize the expected total valuation of UEs, which is given by $\sum_{i=1}^{n} v_i$. The allocation problem can be formulated as a non-linear integer opti-

mization problem. Let $\mathbf{C}_i \subset \mathbf{C}$ be the activated carriers for UE i, $x_{i,c,b,t} \in \{0,1\}$ be the assignment of carrier c's resource bock b at slot t to UE i, and $c_i^p \in \mathbf{C}_i$ be the assigned carrier for transmitting PDCCH signals of carrier c to UE i. Then, the expected received data amount of UE i in time slot t is given by

$$m_i(t) = \sum_{c \in \mathbf{C}, 1 \le b \le B_c} P(D_{i,c_i^p}) x_{i,c,b,t} Q_{i,c}. \tag{4.4}$$

Therefore, the total expected amount of received data in the following T slots is given by

$$m_i = \sum_{t=1}^{T} m_i(t) = \sum_{t=1}^{T} \sum_{c \in \mathbf{C}_i, 1 \le b \le B_c} P(D_{i,c_i^p}) x_{i,c,b,t} Q_{i,c}. \tag{4.5}$$

The expected delay d_i experienced by UE i given the allocation is

$$d_i = \begin{cases} \min \arg_t \{ \sum x_{i,c,b,t} P(D_{i,c_{i,c}^p}) Q_{i,c} \ge M_i \} \}, & \text{if exists;} \\ \infty, & \text{otherwise;} \end{cases} \tag{4.6}$$

4.3.1 Optimization problem

In this work, we consider a utility-based approach to the optimization problem. The objective of the eNB is to maximize the overall valuations of UEs, which is denoted by $V^{th}(\cdot)$ and $V^{delay}(\cdot)$ according to their types. The overall valuation also represents the ability of the system to satisfy the UE's QoS requirements. The valuation maximization problem can be formulated as follows:

$$\max_{x_{i,c,b,t}, c_i^p, \mathbf{C}_i} \sum_{k_i = \{th\}} w_i V^{th}(m_i, M_i) + \sum_{k_i = \{delay\}} w_i V^{delay}(d_i) \tag{4.7}$$

where

$$\mathbf{C}_i \subset \mathbf{C}, p_i \in \mathbf{C}_i, x_{i,c,b,t} \in \{0,1\}, \forall i, c, b, t$$

$$|\mathbf{C_i}| \leq C_i, \; \forall i \qquad \text{(CA capability constraint)}$$

$$\sum_{i \in \mathbf{N}} x_{i,c,b,t} \leq 1, \; \forall c, b, t \qquad \text{(non-overlapping constraint)}$$

$$\sum_{1 \leq t \leq T, 1 \leq b \leq B_c} x_{i,c,b,t} = 0, \; \forall i, c \notin \mathbf{C}_i \qquad \text{(assignment constraint)}$$

$$m_i = \sum_{t,c} x_{i,c,b,t} P(D_{i,p_i}) Q_{i,c}$$

$$d_i = \begin{cases} \min \arg_t \{\sum x_{i,c,b,t} P(D_{i,p_{i,c}}) Q_{i,c} \geq M_i\}\}, & \text{if exists;} \\ \infty, & \text{otherwise;} \end{cases}$$

Notice that d_i is derived through a non-linear function, which makes the optimization problem be nonlinear and hard. The difficulty of this optimization problem depends on the form of valuation function V^{th} and V^{delay}. In the following paragraph, we show that the proposed value maximization problem is NP-hard:

Theorem 8. *The proposed optimization problem in (4.7) is NP-hard.*

Proof. In order to show that the optimization problem in (4.7) is NP-hard, we will show that any arbitrary $0-1$ knapsack problem, which is NP-complete, can reduce to the proposed problem in polynomial time.

Let us consider a $0-1$ knapsack problem with a bag with maximum capacity of W and N items. Each item has a valuation of w_i and a weight of M_i. We reduce this into the proposed problem in (4.7) by considering a cell with only one carrier C containing W resource blocks. We let N items be the UEs in the system, while w_i be their weight and M_i be their requesting data amount. We then let $\forall i, c, Q_{i,c} = 1$ and $P(D_{i,c}) = 1$, and $k_i = th$. Finally, we let $V^{th}(m_i, M_i) = 1$ if $m_i = M_i$, and 0 otherwise. By this reduction, a UE will have a contribution of w_i to the overall valuation if and only if her requirement M_i is satisfied by setting an amount of M_i resource blocks to it.

The optimal solution $\{x^*_{i,c,b,t}\}$ found in this reduced problem can be transformed back to the original $0-1$ knapsack problem by putting an item i in the bag if and only if $\sum_{c,b,t} x^*_{i,c,b,t} \geq M_i$. Since the reduction and transformation can be done in a linear time, we conclude that the proposed optimization problem in (4.7) is as hard as $0-1$ knapsack problem. Therefore, the proposed optimization problem in (4.7) is NP-hard. $\qquad \square$

Since the proposed optimization problem is NP-hard, the optimal solution may be undesirable when the response time is a concern. Several heuristic approaches, such as greedy algorithm, may be applied here for finding sub-optimal solutions in an acceptable time.
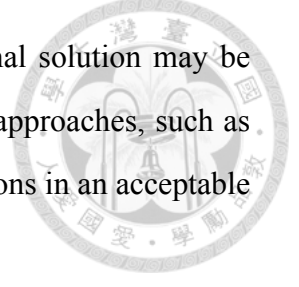
4.3.2 Sub-problem: Satisfying QoS requirement while Minimizing Allocated Resource

Here we consider a greedy approach by solving the optimization problem per UE. The basic idea is to use as few as possible resource blocks to satisfy each UE's requirement, one at a time. Formally speaking, given a UE and currently available resource blocks, we would like to minimize the number of resource blocks used to satisfy her QoS requirement.

The resource usage minimization problem for a throughput-sensitive UE i is as follows:

$$\min_{x_{i,c,b,t}, c_i^p, \mathbf{C}_i} \sum_{c,b,t} x_{i,c,b,t} \tag{4.8}$$

where

$$\mathbf{C}_i \subset \mathbf{C}, c_i^p \in \mathbf{C}_i, x_{i,c,b,t} \in \{0,1\}, \ \forall c, b, t$$

$$|\mathbf{C_i}| \leq C_i, \ \forall i \quad \text{(CA capability constraint)}$$

$$\sum_{i \in \mathbf{N}} x_{i,c,b,t} \leq 1, \ \forall c, b, t \quad \text{(non-overlapping constraint)}$$

$$\sum_{1 \leq t \leq T, 1 \leq b \leq B_c} x_{i,c,b,t} = 0, \ \forall i, c \notin \mathbf{C}_i \quad \text{(assignment constraint)}$$

$$m_i = \sum_{t,c} x_{i,c,b,t} P(D_{i,p_i}) Q_{i,c} \geq M_i \quad \text{(data amount constraint)}$$

It can be shown that the preceding optimization problem is still NP-hard due to the combinational choices on activated carriers $\mathbf{C_i}$ and primary carrier c_i^p. Nevertheless, when $\mathbf{C_i}$ and c_i^p are chosen, the optimal solution of $\{x^{i,c,b,t}\}$ can be found through greedily allocating available resource blocks from the carrier $c \in \mathbf{C_i}$ with highest $Q_{i,c}$ until $m_i \geq M_i$. Therefore, the optimal solution is still tractable in cubic time when $C_i \leq 3$.

The resource usage minimization problem for a delay-sensitive UE i is as follows:

$$\min_{x_{i,c,b,t},c_i^p,\mathbf{C}_i} d_i \tag{4.9}$$

where

$$\mathbf{C}_i \subset \mathbf{C}, c_i^p \in \mathbf{C}_i, x_{i,c,b,t} \in \{0,1\}, \ \forall c,b,t$$

$$|\mathbf{C_i}| \leq C_i, \ \forall i \qquad \text{(CA capability constraint)}$$

$$\sum_{i\in\mathbf{N}} x_{i,c,b,t} \leq 1, \ \forall c,b,t \qquad \text{(non-overlapping constraint)}$$

$$\sum_{1\leq t\leq T, 1\leq b\leq B_c} x_{i,c,b,t} = 0, \ \forall i, c \notin \mathbf{C}_i \qquad \text{(assignment constraint)}$$

$$m_i = \sum_{t,c} x_{i,c,b,t} P(D_{i,p_i}) Q_{i,c} \geq M_i \qquad \text{(data amount constraint)}$$

$$d_i = \min \arg_t \{ \sum x_{i,c,b,t} P(D_{i,p_{i,c}}) Q_{i,c} \geq M_i \}$$

Again, when $\mathbf{C_i}$ and c_i^p are chosen, the optimal solution can be found through greedily allocating available resource blocks from all carrier $c \in \mathbf{C}_i$ starting from $t = 0$ until $m_i \geq M_i$. Therefore, the optimal solution is still tractable in cubic time when $C_i \leq 3$.

These two sub-problems are useful for us to propose a greedy approach for the optimization problem in (4.7), which we will illustrate it in Section 4.5.

4.4 Game Model Formulation

The eNB requires the information of UEs to allocate the carriers and resource blocks properly. Specifically, the per-UE carrier quality $\{Q_{i,c}\}$, PDCCH interference $\{D_{i,c}\}$, and data requirements (M_i, k_i) are the information requested by eNB and reported by UEs themselves. Nevertheless, when UEs are rational, they may report the information untruthfully if the allocation manipulated by the untruthful report is beneficial to them. When UEs choose to report untruthfully, the eNB receives incorrect information from UEs, and the optimization problem in Section 4.3 will solved using incorrect constraints and parameters. As a result, the derived allocation may be inefficient or even infeasible

to the system. Thus, it is important to prevent this issue, which is called truth-telling issue in game theory terminology.

4.4.1 Game Model

We formulate the system we are investigating as a game. A game is composed of three elements: players, actions, and utility functions. In our formulation, all UEs $i \in \mathbf{N}$ are considered players in the proposed game. Each player's action $a_i \in \mathbf{A_i}$ is their reported QoS requirement $a_i = (M_i, k_i) \in \mathbf{A_i} = \mathbb{R} \times \{th, delay\}$.

In the system, each UE i are required to pay a fee p_i in order to use the service. Therefore, the utility of a UE i is given by

$$u_i(m_i, d_i, p_i) = v_i(m_i, d_i) - w_i p_i. \qquad (4.10)$$

where w_i is its weight in resource allocation priority. Given a higher weight w_i, UE i has a higher discount on its payment and higher priority in the carrier activation and resource block allocation. Notice that the expected utility of a UE is determined by the final carrier and resource block allocation, which is the solution to (4.7) and is affected by the input of all UEs. Therefore, a UE's utility is determined by not only his reported data requirement but also other UEs' reports. This complex interaction is an important characteristic in a typical game model.

The process of the proposed game is the same as the resource allocation process shown in Fig. 4.2. The eNB first requests information from all UEs. Then, all UEs report their information to the eNB. Finally, the eNB determines the carrier and resource block allocation and the corresponding payment of each UE i. The expected utility of all UEs can then be calculated accordingly.

4.4.2 Nash Equilibrium

Nash equilibrium is a solution concept for general non-cooperative game with rational players. Informally speaking, Nash equilibrium is an action profile where each player's
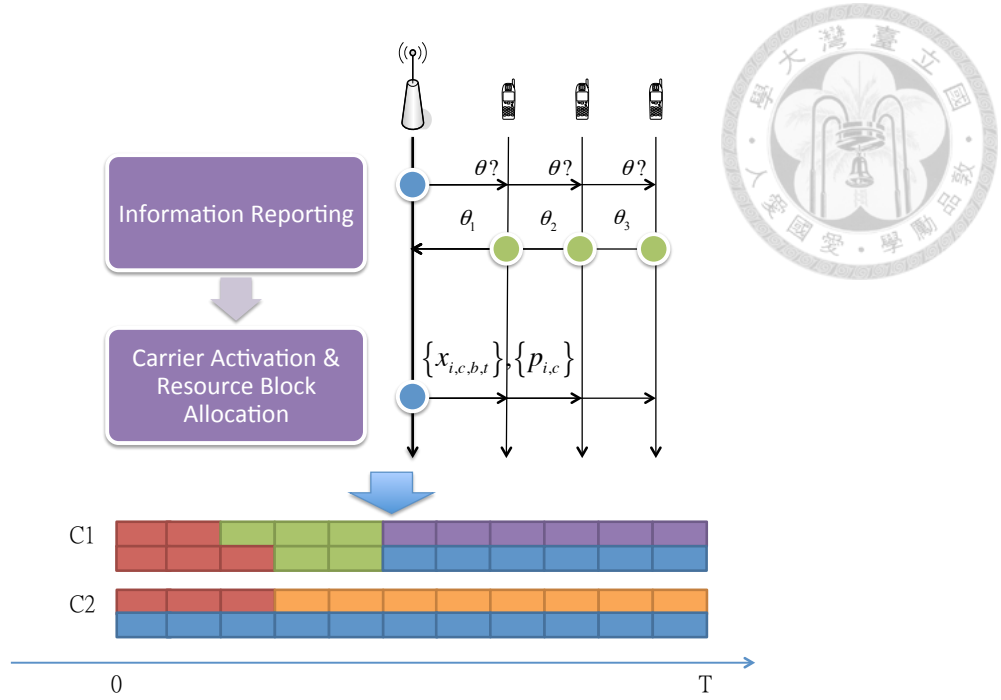
Figure 4.2: Information Reporting and Resource Allocation Process

action described in the profile is the one that maximizes his utility conditioning on the actions of other players in the profile. When the above condition is reached, no player has the incentive to deviate from their applied action, and thus the outcome remains stable. Nash equilibrium is widely used for predictions on the outcome of a game. The formal definition of Nash equilibrium is as follows:

Definition 8 (Nash Equilibrium). *An action profile* $\mathbf{a} = \{a_1, a_2, ..., a_n\}$ *is a Nash equilibrium if and only if* $\forall i \in \mathbf{N}, a_i' \in \mathbf{A_i}$,

$$u_i(a_i, \mathbf{a_{-i}}) \geq u_i(a_i', \mathbf{a_{-i}}), \tag{4.11}$$

where $\mathbf{a_{-i}}$ *denotes the actions of all players except player* i.

In this work, we focus on a specific type of Nash equilibrium, which is **truthful** Nash equilibrium.

Definition 9 (Truthful Nash Equilibrium). *Let* $a_i^* = (M_i, k_i)$ *be the true QoS requirement of UE* i. *Then, a **truthful Nash equilibrium** exists if and only if* $\mathbf{a}^* = (a_1^*, a_2^*, ..., a_n^*)$ *is a Nash equilibrium.*

107

The existence of truthful Nash equilibrium is important as players will truthfully report their private information, which is their QoS requirement, only if such equilibrium is achievable. Nevertheless, a truthful Nash equilibrium does not exist in a general non-cooperative game unless the game rule is properly designed. Therefore, our objective is implementing the truthful Nash equilibrium in the proposed game.

Algorithm 1 WINNER_DETERMINATION

Input: UE $\mathbf{N}$, Carrier $\mathbf{C}$, Carrier quality $\{Q_{i,c}\}$ and $\{D_{i,c}\}$, QoS requirement $\{k_i, M_i\}$, and weight $\{\mathbf{w}_i\}$
Output: Carrier activation $\{\mathbf{C}_i\}$, primary carrier $\{c_i^p\}$, allocation $\{x_{i,c,b,t}\}$, and first loser's utility u_{lose}
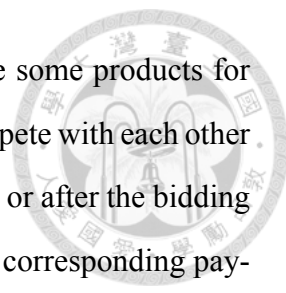
1: $\mathbf{W} = \emptyset$;
2: $u_{lose} = 0$;
3: $\forall i, c, b, t, \ x_{i,c,b,t} = 0$
4: $\mathbf{W}' = \mathbf{N}$;
5: **while** $\mathbf{W} \neq \mathbf{W}'$ and $\mathbf{N} \neq \emptyset$ **do**
6:     $\mathbf{W}' = \mathbf{W}$;
7:     **for** all i in $\mathbf{N}$ **do**
8:       **if** $k_i = th$ **then**
9:         **if** exist feasible solution to (4.8) **then**
10:           $u_i^* = 1$, and $r_i^* = \sum x_{i,c,b,t}^i$, where $\{x_{i,c,b,t}^i\}$ is the solution to (4.8) under the constraints that $d_i = \max_{\sum_{i' \neq i} x_{i',c,b,t} = 0}, t$;
11:         **end if**
12:       **else**
13:         calculate u_i^* by solving (4.9);
14:         $r_i^* = \sum x_{i,c,b,t}^i$, where $\{x_{i,c,b,t}^i\}$ is the solution to (4.9);
15:       **end if**
16:     **end for**
17:     $\mathbf{W} = \arg\max_{i \in \mathbf{N}} w_i u_i^*$;
18:     $w = \arg\min_{i \in \mathbf{W}} r_i^*$;
19:     $\{x_{i,c,b,t}\} = \{x_{i,c,b,t}^w\}$;
20:     $\mathbf{W} = \mathbf{W} \cup \{w\}$;
21:     $\mathbf{N} = \mathbf{N} \setminus \{w\}$;
22:     **if** $\mathbf{N} \neq \emptyset$ **then**
23:       $u_l = \max_{i \in \mathbf{N}} w_i u_i^*$;
24:     **else**
25:       $u_l = 0$;
26:     **end if**
27: **end while**

4.5 Auction Design

Auctions have been widely used in various domains involving resource allocations, especially on problems with concerns on private information. A typical auction has two

types of participants: auctioneers and bidders. The auctioneers have some products for sell. The bidders, who may have different valuations on products, compete with each other for the products hold by the auctioneers through a bidding process. In or after the bidding process, the auctioneers decide the allocation of the products and the corresponding payments of all participants. Notice that the valuation of a bidder on the products is private information and will not be known by the auctioneers or other bidders unless she chooses to truthfully reveal it in the bidding process. As a rational bidder, she will choose to truthfully reveal her private information only in a truthful Nash equilibrium. Therefore, the implementation of truthful Nash equilibrium is one of the main challenges in the auction theory.

Vickrey−Clarke−Groves auction (VCG auction) [57] is one of the most successful auction designs as it not only guarantees the existence of truthful Nash equilibrium, but also achieves the optimal resource allocation. Nevertheless, the implementation of VCG auction becomes impractical when the allocation problem is NP-hard since it requires the optimal allocation to be achieved eventually. This makes it an undesired choice for us since the corresponding optimization problem in our system is NP-hard, as we proved in Theorem 8.

In this section, we propose a Vickery-inspired auction to implement the truthful Nash equilibrium. The eNB is the only auctioneer, and all UEs $i \in \mathbf{N}$ are considered bidders in the auction with their reported QoS requirement (M_i, k_i) as their bids. The proposed auction is composed of two stages: winner determination and payment determination stages. The winner determination stage selects the "winners", which are the UEs selected to be fulfilled with their data requirements, according to their reports. Then, the payment determination stage determines the payment p_i each winner required to pay to the eNB. We prove that by our design, the truthful Nash equilibrium can be implemented in a low-complexity manner.
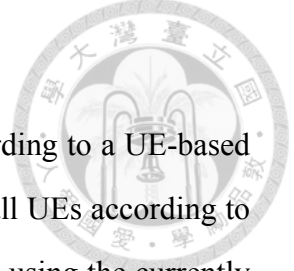
4.5.1 Winner and Payment Determination

In the winner determination stage, the winners are selected according to a UE-based greedy algorithm. The algorithm works as follows. Firstly, we sort all UEs according to their maximum weighted valuation if their requirements are satisfied using the currently available resource blocks. If two UEs have the same maximum weighted valuation, the one requires fewer resource blocks to satisfy goes first.

Then, the first UE in the list is selected as the winner and the eNB activates carriers and allocates resource blocks to the UE for satisfying its requirement M_i. The locations of the resources blocks depend on the UE's type k_i: When $k_i = delay$, the resource blocks are allocated from the beginning of the carriers ($t = 1$). When $k_i = th$, the resource blocks are allocated from the end of the carriers ($t = T$), that is, the allocation should maximize the expected delay for throughput-sensitive UEs. This promises that the delay of data for delay-sensitive type UEs is always shorter than the throughput-sensitive type UEs. Finally, the UE is excluded from the list, and all UEs in the list are sorted again following the same logic.

The routine continues until all UEs are removed from the list or the remaining resource blocks cannot satisfy the QoS requirement of the first UE remaining in the list. The algorithm terminates when one of the above conditions met. The pseudo code of Winner Determination algorithm is shown in Algorithm 1.

In the payment determination stage, the payments of all UEs are determined by a Vickery-inspired pricing rule. Firstly, we define the boundary UE $b(\mathbf{N})$ as the last winner in the winner determination stage when a set of UE $\mathbf{N}$ participates in the auction. Then, the payment of UE i is given by $V_{k_{i^b}}(M_{i^b}, d_{i^b}^b)$, where $i^b = b(\mathbf{N} \setminus \{i\})$ and $d_{i^b}^b$ be the delay of UE i^b if UE i is excluded. The pseudo code of proposed Payment Determination algorithm is shown in Algorithm 2.

4.5.2 Existence of Truthful Nash Equilibrium

By combining the proposed winner determination and payment determination rules, we now prove that there exists a truthful Nash equilibrium in the proposed auction. We

---

Algorithm 2 PAYMENT_DETERMINATION

Input: $\mathbf{N}$, $\mathbf{C}$, $\{Q_{i,c}\}$, $\{D_{i,c}\}$, $\{k_i, M_i\}$, and $\{w_i\}$
Output: Payment $\{p_i\}$
 1: **for** $i \in \mathbf{N}$ **do**
 2: $\quad$ $[\{\mathbf{C}_i\}, \{c_i^p\}, \{x_{i,c,b,t}\}, u_{lose}] \quad = \quad WINNER\_DETERMINATION(\mathbf{N} \setminus \{i\}, \mathbf{C}), \{Q_{i,c}\}, \{D_{i,c}\}, \{k_i, M_i\}, \{w_i\}$;
 3: $\quad$ $p_i = u_l$
 4: **end for**

---

start from a lemma that explains whether a delay-sensitive UE i will report its data requirement type untruthfully.

Lemma 3. *If a winner UE i reports $k_i' = th$ instead of $k_i = delay$ as its data requirement type, its experienced delay does not decrease.*

Lemma 3 is a direct result from the proposed allocation rule. It shows that a delay-sensitive UE i will never report her type untruthfully. Then, the following lemma provides a necessary condition for the existence of truthful Nash equilibrium.

Lemma 4. *If a UE wins the auction by reporting (M, k), then it can wins the action by reporting (M', k) with $M' \leq M$, but may not if reporting (M'', k) with $M'' \leq M$*

Proof. Since $M' \leq M$, the required number of resource blocks is never greater under M' than M. Therefore, the UE's order in the new list is never larger than the original list. Additionally, there are enough resource blocks to satisfy M' since the UE is a winner by reporting $M > M'$. So, the UE is still selected as a winner by reporting (M', k).

For the case of $M'' \leq M$, since the required number of resource block is never smaller under M'' than M, it is possible that the order of the UE in the new list is smaller than in the original list, according to the winner determination algorithm. This reduces the possibility of the UE to win the auction. $\square$

Lemma 4 is important as it suggests that a UE i cannot increase her probability to win in the proposed auction by increasing her requested data amount M_i. Although a UE may choose to decrease her requested data amount M_i in order to increase her probability to win, we will show that reporting $M_i' \leq M_i$ will never be beneficial to the UE i later.

Lemma 5. *a UE i's payment p_i is unrelated to her own bid (M_i, k_i).*

Proof. According to the payment determination rule, the UE i's payment is $u_{i^b}(M_{i^b}, d_{i^b}^b)$, in which UE i's bid is excluded from the winner determination stage. Since UE i's bid is excluded, it does not have any influence on the winner determination. Therefore, the UE i's bid does not have any influence on her payment. $\square$

Finally, we propose the following theorem about the existence of truthful Nash equilibrium in the proposed auction.

Theorem 9 (The existence of truthful Nash equilibrium)**.** *A truthful Nash equilibrium exists in the proposed game if the proposed auction is applied.*

Proof. Let (M_i^*, k_i^*) be the true QoS requirements of UE i, $\forall i \in \mathbf{N}$. By Lemma 4 and 5, it is guaranteed that reporting $M_i \neq M_i^*$ is never the better response of UE i if k_i^* is reported. We now need to check if report k_i' instead of k_i^* is beneficial to UE i.

Case 1: $k_i^* = th$. In this case, reporting $k_i = delay$ only reduces its weighted valuation and therefore increases its order in the list. This reduces its probability to win the auction and therefore impair its expected utility.

Case 2: $k_i^* = delay$. In this case, reporting $k_i = th$ may increase its weighted valuation and therefore decrease its order. We should discuss this under two possible cases:

Case 2.a: UE i is not a winner by reporting k_i^*. In this case, even UE i becomes a winner, its true utility will be negative since he is not a winner in the original list.

Case 2.b: UE i is a winner by reporting k_i^*. In this case, UE i is still a winner and now follows the allocation rule for throughput-sensitive type. According to Lemma 3, the delay under k_i is strictly larger than under k_i^* if the UE reports the same M_i. In such a case, the valuation of UE i is strictly lower by reporting $k_i = th$ instead of $k_i^* = delay$. Given the same payment p_i, the expected utility of UE i is strictly lower by reporting $k_i \neq k_i^*$.

Concluding from above, the truthful Nash equilibrium exists if the proposed auction is applied.

$\square$

4.6 Simulation Results

We evaluate the proposed solutions in Section 4.5 through simulations. We simulate a LTE-Advanced system with 19 cell BSs deployed in a typical 19-cell hexagonal topology. There are 5 independent carriers, each with 1.4 MHz bandwidth. According to LTE's standard, a frame is composed of 10 subframes, while a subframe is composed of 2 time slot, each with 0.5 ms. A 1.4 MHz carrier is composed of 6 resource blocks at each time slot, while a resource block has a bandwidth of 180kHz and contains 7 symbols. The number of bits contained in a symbol depends on the applied MCS. In the simulations, we apply the MCSs and link-level settings specified by 3GPP [2] according to the signal-to-interference-and-noise ratio (SINR) experienced by UEs [20]. For other settings, we follow the IMT-Advanced 4G evaluation guidelines [1]: The downlink transmission power of each cell is $23dBm$, while the cell radius is 100 m. The propagation loss model is outdoor model, while the shadow fading follows a log-normal distribution of mean $0dB$ and standard deviation $10dB$.

We assume that all cells, except the center one, are full-buffered and are treated as the neighbor cells of the center cell. Each neighbor cell activates all carriers to transmit data to their UEs, while 2 of the activated carriers are assigned as the primary carriers of their serving UEs. For the center cell, we apply the proposed auction design in order to determine the carrier activation and resource block allocations according to the QoS requests from the serving UEs. The auction holds for every 8 frames, which equal to 80 ms. This fits one of the CQI reporting rates defined in LTE-Advanced.

A fixed number of UEs are uniformly and randomly deployed in the system. These UEs request for downlink transmissions. They experience different carrier qualities due to 1) the spatial-diverse and carrier-diverse interference from neighbor cells, and 2) the propagation signal loss due to the distance from the center cell BS to the UE. Each UE supports at most 2 carriers when carrier aggregation is enabled. The QoS requirement of each UE is randomly generated. Given the average request data amount M_avg, the request data amount M_i of each UE is randomly generated from 1 kB to $2M_avg$ kB. Additionally, half of the UEs are throughput-sensitive, while others are delay-sensitive. The valuation

function of throughput-sensitive $V^{th}(m_i) = log(1 + \frac{9\min\{m_i, M_i\}}{M_i})$, while the valuation function of delay-sensitive is $V^{delay}(d_i) = log(1 + \frac{40}{d_i})$.

The carrier qualities are determined by two factors in the simulations. The first one is the expected resource block data amount ($Q_{i,c}$) in each carrier, which represents the data amount a resource block can carry under the currently applied MCS. The value can be derived through simulating the LTE wireless channel model in [20]. The second one is the PDCCH decoding probability ($P(D_{i,c})$). In LTE system, all PDCCH messages are transmitted using the BPSK modulation. Given the transmission power, resource block bandwidth and symbol rates, and the typical length of PDCCH message, we can theoretically calculate the bit-error rate and therefore the message error rate of a PDCCH message (We ignore the coding rate of PDCCH message here for simplicity).

In all simulations, we compare 5 schemes. The first one is the proposed solution, where the proposed auction design is applied. Specifically, the winner determination algorithm in Algorithm 1 is applied here for activating the carriers and allocating the resource blocks to the UEs according to their QoS requirements. We compare the proposed solution with three carrier activation schemes. One is the random scheme, where each UE randomly activates 2 carriers. Another one is the fair scheme, where each carrier is assigned with the same number of UEs (or plus/minus 1 if aliquant). The last one is the Best CQI scheme, where each UE activates two carriers that offer her the highest expected resource block data amount. In all three schemes, round-robin method is applied on the resource block allocation. These schemes represent the traditional carrier activation schemes where no QoS requirements are addressed. In the last scheme, we apply our proposed solution while limiting the number of activated carrier of each UE to 1, which simulate the case that all UEs are using legacy devices with no carrier aggregation support. This helps us to understand how carrier aggregation enhances the performance of the system.

The performance metric we choose in the simulations is the social welfare of the system, which is defined as follows:

$$SW = \sum_{i \in \mathbf{N}} V^{k_i}(\cdot),$$

114

Figure 4.3: Simulation Results: Number of UEs

which is the same as the objective function in (4.7). The social welfare represents the total

valuation of UEs on the service, which is an important indicator on the system efficiency

in game theory. Since our work focus on optimizing the service valuation based on UEs'

QoS requirements, we choose this as the performance metric in our evaluations.

4.6.1   UE Density

In the first simulation, we control the number of UEs in the center cell from 2 to 20

to evaluate the effect of UE density to the performance of proposed solution and other

schemes. The cell radius is 100m while the average request amount is 50kB. The simula-

tion results are shown in Fig. 4.3.

We observe that the proposed solution significantly outperforms other schemes. This

is because our solution properly addresses the QoS requirements of UEs, especially for the

delay-sensitive UEs. In comparison, all three traditional carrier activation schemes result

poor social welfares, while the fair scheme performs best and best CQI performs worst.

This is due to the unbalanced carrier activation resulting from best CQI and random carrier

activation. The loading on certain carriers may significantly be higher than the ones on

other carriers, which bring a negative impact on the service quality of the UEs using those

carriers.

Figure 4.4: Simulation Results: Cell Radius

For the no-CA scheme, we observe that the traditional scheme performs better than the no-CA scheme when the number of UEs is small. Nevertheless, when the number of UEs increases, our proposed solution still outperforms traditional scheme even without the help of carrier aggregation. Additionally, the social welfare significantly increases when carrier aggregation is enabled in the proposed solution. The performance boosts mostly comes from the delay reduction experienced by the delay-sensitive UEs.

4.6.2 Cell Density

Next, we control the cell radius from 100m to 1000m for investigating the effect of cell density on the system performance. The number of UEs is 10 in this simulation. The results are shown in Fig. 4.4. We observe that the proposed scheme outperforms all other schemes significantly, while all other relative performance gaps are similar to the results in the previous simulation. We also observe that the social welfare decreases when the cell radius increases to larger than 400 m. This is because when the cell radius increases, which also means the cell density decreases, the distance from the serving BS to a UE increases on average. This increases the signal propagation loss and therefore reduces the carrier qualities experienced by the UEs. In such a case, their QoS requirements are relatively harder to satisfy.

116

Figure 4.5: Simulation Results: Requested Data Amount

Nevertheless, it is interesting to note that the social welfare does not always decreases monotonically. When the cell radius is less than 400 m, the social welfare in fact increases when the radius increases. This is due to another factor influencing carrier qualities: the interference from neighbor cells. When the cell radius increases, the interference from neighbor cells decreases on average since the cell density decreases. This helps increase the carrier qualities. The results suggest that the propagation loss and neighbor cell interference are tradeoff factors in determining cell density when deploying cells.

4.6.3   QoS Requirement

Finally, we study the efficiency of the proposed solution satisfying QoS requirements under severe demands. We simulate with 10 UEs and control the average request data amount from 25kB to 250kB. The simulation results are shown in Fig. 4.5. We observe that the proposed solution again outperforms all other schemes even under severe QoS requirements. The social welfare decreases significantly when the average request data amount increases. Nevertheless, when carrier aggregation is enabled, the proposed solution can properly make use of the benefits from carrier aggregation in order to achieve higher system efficiency in terms of social welfare.
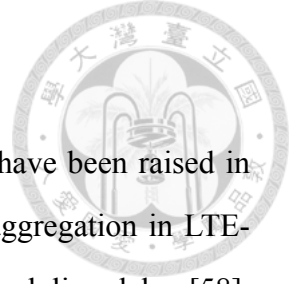
4.7 Related Work

The attentions on carrier aggregation in LTE-Advanced system have been raised in recent years. Some works focus on the implementation of carrier aggregation in LTE-Advanced system under various configurations, such as reducing scheduling delay [58], PDCCH search space design [59, 60], and aggregating TDD and FDD LTE carriers [61]. Most researchers discuss the carrier allocation and activation among multiple cells, especially in heterogeneous networks [62--65]. These works focus on the interference mitigation through properly assigning and activating the primary/secondary carriers among these cells. Nevertheless, the specific resource allocation and QoS requirements of UEs in each cell under carrier aggregation are not addressed in these works.

Some researchers therefore explore the potential of carrier aggregation to enhance the quality of LTE service through proper resource allocation, such as throughput enhancement [66], load balance [67], and utility maximization [68, 69]. Nevertheless, most existing works focus on the case that all UEs in the system share the same or similar QoS demands, such as high throughput demand or delay constraints. The study on the resource allocation in carrier aggregation given heterogeneous QoS demands from UEs are still lacking in this area. In addition, none of existing works address the potential threats from the untruthful information report from UEs, which potentially prevents all existing methods from functioning properly.

4.8 Summary

In this chapter, we study the carrier aggregation design in LTE-Advanced system through a game-theoretic perspective. We first address the heterogeneous carrier quality and QoS requirements of UEs by modeling the resource allocation problem in carrier aggregation as a utility-based non-linear optimization problem. Given that the optimization problem is NP-hard, we aim to find an efficient algorithm to find the near-optimal solution. Additionally, we address the potential threats from the selfish UEs, who may report their QoS requirements untruthfully and therefore induce an unfair and inefficient

resource allocation, by proposing a truthful auction design. The proposed auction provides an efficient greedy algorithm to satisfy the QoS requirements of UEs through carrier aggregation with reasonable computation time. Additionally, it guarantees the existence of truthful Nash equilibrium and therefore prevents the rational UEs from reporting manipulated QoS requirements. The simulation results verified that the proposed auction design for carrier aggregation enhances the LTE-Advanced system's capability to satisfy UE's QoS requirements.

Chapter 5

Device-to-Device Communications in LTE-Advanced System: A Resource Exchange Approach

5.1 Introduction

Improving the coverage and efficiency of resource utilization is one of the key challenges in the next-generation cellular systems. Device-to-Device (D2D) communication could improve the coverage and resource utilization by allowing nearby devices to communicate directly [7]. 3GPP has begun to examine the service requirement for Proximity-based Services (ProSe), which is the D2D communications for LTE-Advanced, and then has started ProSe radio access network standardization recently [9]. It allows two nearby devices to communicate with each other directly using existing WLAN or WPAN techniques in an unlicensed spectrum or an LTE-Advanced transmission technique in licensed spectrum. This approach improves the transmission quality from the proximity [8], reduces the transmission delay by utilizing one-hop direct connection instead of two-hop cellular connection, and provides an extra dimension for resource reuse in the cellar system.
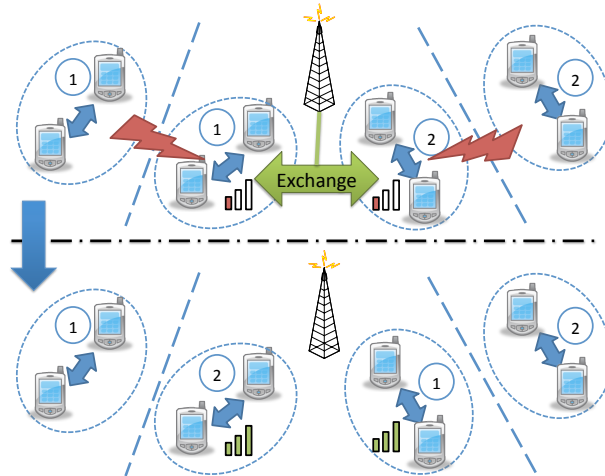
Figure 5.1: D2D Resource Exchange

5.1.1 D2D Resource Allocation

Resource allocation is one of the key challenges in D2D communications in a cellular system [7]. As specified by [7], D2D communications can be executed in unlicensed or licensed spectra. Since the former choice is relatively unreliable due to its openness to other out-of-system devices, in this chapter we study the latter choice, in which the resources utilized by D2D communications are dedicated resources (spectrum, resource blocks, etc.) licensed to the cellular system or a specific purpose (public safety, for instance) [10]. When D2D communications are utilizing a licensed spectrum, the BSs should regulate the resource allocation of D2D communications in order to 1) prevent undesired interference to existing cellular users, 2) enhance resource utilization efficiency according to (possibly frequency and spatially diverse) channel conditions, and 3) reuse resources if possible. Additionally, the BSs should be able to respond quickly to requests from the D2D devices and rapid changes in inter/intra-cell interference. Therefore, it is necessary to develop a low-complexity yet efficient algorithm for resource allocation.

The ad-hoc characteristic of D2D communication poses a new challenge to the D2D resource allocation problem: the truth-telling issue. Specifically, the BS requires the channel measurements from D2D devices in order to allocate resources efficiently. Nevertheless, the BS cannot validate these reports, since the transmissions occur only between the corresponding D2D devices. This gives the D2D devices the potential to cheat by reporting the measurements untruthfully when the untruthful reports would be advantageous to

the D2D devices in terms of the resource allocation. When D2D devices or corresponding users are rational, they will behave selfishly and therefore make use of this advantage.

To illustrate, let us assume that the BS tends to allocate the resource blocks to the devices claiming to have the highest transmission qualities (Best CQI Scheduling in LTE-Advanced, for instance). In such a case, D2D devices tend to report a forged measurement value higher than the real value of their most desired resource blocks in their reports. This forged report will increase the probability that the desired resource blocks will be allocated to them. The BS therefore cannot provide an efficient allocation, since the information she has received does not reflect the true system state. To tackle this issue, it is necessary to employ a game-theoretic analysis [56]. A strategy-proof solution, which guarantees truthful reporting, must be used to prevent untruthful reports from rational users.

5.1.2 Resource Exchange Approach

The transmission quality in D2D communications can be significantly improved when a proper resource exchange is executed. Let us consider an OFDMA-based cellular system with four D2D pairs using licensed OFDMA resource blocks. The example is illustrated in Fig. 5.1, where the two D2D pairs in the middle are using resource blocks 1 and 2, respectively. The main interference sources of these two pairs are their nearby D2D pairs using the same resource blocks. The interference can be significantly reduced if those two pairs in the middle exchange the resource blocks they have with each other. With this new allocation, all pairs experience improved transmission quality, since the interference is alleviated by the higher propagation loss from longer distances. This potentially beneficial exchange can be identified by the eNodeB or D2D pairs themselves. In addition to its simplicity, the resource exchange approach provides other benefits to D2D resource allocation: 1) the resource exchange process can be locally implemented by a simple three-way handshake signalling flow, and 2) it can be launched locally for timely response to rapid environmental changes, or globally triggered by cellular BSs for system-wide optimization. Based on these observations, we apply the resource exchange approach in our proposed D2D resource allocation framework.

5.1.3 Contributions

In this chapter, we aim to provide a comprehensive D2D resource allocation framework for an LTE-Advanced system. The framework is based on the resource exchange approach, in which a series of dedicated resource block groups (RBGs) are predefined and reserved for D2D communications. Each D2D pair possesses an RBG in a frame after a resource request is accepted by the Evolved Node B (eNodeB). [1] The eNodeB or D2D pairs may trigger a resource exchange among D2D pairs or between the eNodeB and a D2D pair if proper exchange pairs are identified. We prove that every resource exchange reduces the total system interference when it is **beneficial**. This provides a sufficient condition to guarantee the convergence of any arbitrary algorithm in our framework.

To improve the efficiency of resource utilization, the system-wide optimization can be performed by the eNodeB, in which the truth-telling issue may occur as we mentioned previously. In such a case, we provide a game-theoretic analysis for investigating the truth-telling issue in the proposed framework. We propose using the Trader-assisted Resource EXchange (T-REX) mechanism to handle the resource exchange operations. The eNodeB participates in the operations through identifying optimal exchange sequences and applying trader preference functions. We prove that the truth-telling issue can be resolved through the proposed mechanism when a proper trader preference function is chosen. Finally, we evaluate the performance of the proposed solutions through simulations using the models and parameters suggested in the latest 3GPP technical contribution [3]. In summary, we make the following contributions:

1. We propose a novel LTE-Advanced D2D resource allocation framework based on the resource exchange approach. We reuse most existing LTE-Advanced components and followed the same signalling flow logic in order to minimize the protocol impacts.

2. We theoretically prove that the resource exchange approach is equivalent to the traditional resource allocation approach in the solution feasibility. Additionally, we

---

[1]'eNodeB' and 'BS' are interchangeable in this chapter.

prove that any arbitrary algorithm, either distributed or centralized, will converge in the proposed framework whenever all exchanges are beneficial. To the best of our knowledge, we are the first group to present the resource exchange approach to the D2D resource allocation problem.

3. Based on the idea of beneficial exchange, we propose the Trader-assisted Resource Exchange (T-REX) mechanism as an efficient and flexible solution to the D2D resource allocation problem in the proposed framework. The T-REX mechanism identifies the beneficial exchanges through analysing the corresponding exchange graph. The algorithm's complexity is polynomial, which makes it a practical solution to large-scale D2D networks. In addition, the derived allocation is Pareto optimal; therefore, the efficiency is guaranteed. In addition, we prove that the T-REX mechanism is strategy-proof when the trader preference functions are properly designed; that is, all D2D pairs truthfully report their information even if they are rational and selfish. We are one of the first groups to apply game-theoretic analysis to the D2D resource allocation problem.

5.2   D2D Resource Allocation Framework for LTE-Advanced System

We design our D2D resource allocation framework according to the following principles: 1) Reuse the existing components of the LTE-Advanced standard as much as possible in order to minimize the protocol impact, and 2) maintain high flexibility in configuration and deployment for different service requirements.

The minimal transmission resource unit in LTE- Advanced is a resource block. In our framework, we define a set of resource blocks dedicated for D2D communication only. These resource blocks are grouped into resource block groups (RBGs), each with the same number of resource blocks, as illustrated in Fig. 5.2(a). The dedicated resource design has been proposed in several widely known standards, such as Terrestrial Trunked Radio (TETRA) [70], a European Telecommunications Standards Institute (ETSI) standard for

(a) Resource Block Group   (b) Resource Granting

(c) Resource Exchange
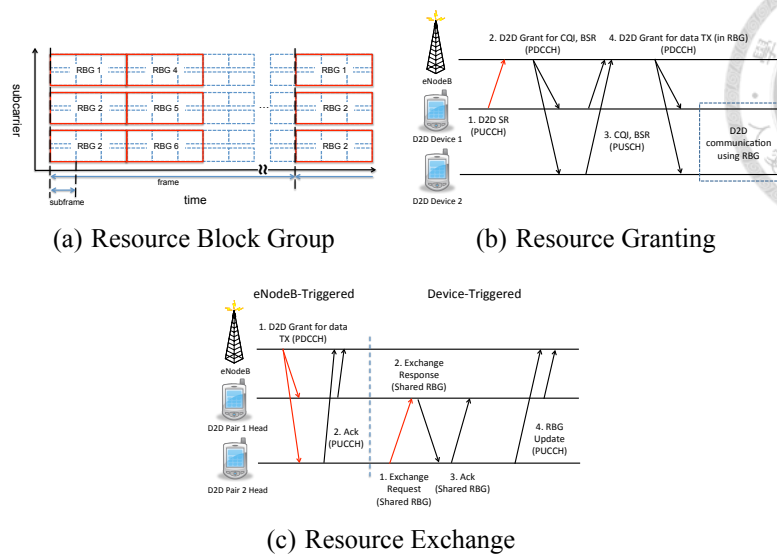
Figure 5.2: D2D Resource Allocation Framwork

public safety networks used by government agencies or emergency services. This design is especially useful for public safety service using a dedicated public safety spectrum for proximity services [10] or commercial service providers holding multiple contiguous or non-contiguous narrowband spectrum licenses.

An eNodeB governs a cell, which consists of several service areas. All RBGs are reused in every service area. D2D pairs in the same service area are allocated with different RBGs, so D2D devices suffer from only inter-area interference. This inter-area interference will be spatially diverse and changing due to device mobility or resource reallocation.

5.2.1 Resource Granting

The requesting and granting of D2D resources are realized through the following signalling flow (Fig. 5.2(b)), which is similar to the uplink resource granting signalling in LTE-Advanced system. When a potential D2D pair is identified and notified through peer discovery, one of the D2D devices triggers the resource granting procedure by sending a D2D scheduling request (D2D SR) on her dedicated SR resource in the physical uplink control channel (PUCCH) to the serving eNodeB. This device is also considered as the D2D pair head of this pair. Next, the eNodeB will send a resource grant for channel qual-

ity indicator (CQI) and buffer status report (BSR) transmission to both D2D devices if she accepts the request. The grant also indicates the corresponding resource in the physical uplink shared channel (PUSCH) for the D2D device to upload the information. Here we reuse the same CQI and BSR format in the LTE-Advanced standard.

The CQI should contain the channel measurement on all the subcarriers related to the dedicated RBGs. Therefore, the CQI reporting type should be an eNodeB-configured sub-band feedback on all the subcarriers dedicated for D2D RBGs. The BSR contains the QoS requirement of the D2D pair, which helps the eNodeB to determine the amount of RBGs reserved for this D2D pair. For instance, the eNodeB may reserve one specific RBG in several subsequent frames for the D2D pair. Finally, the resource grant for RBG is sent to both D2D devices, which indicates the RBG that this pair is granted and the corresponding leasing time. The resource granting procedure is terminated here. Notice that the eNodeB should maintain up-to-date information on each D2D pair's transmission quality, which is indicated by CQI. CQI updates can be actively requested by the eNodeB or passively triggered by some D2D pairs when necessary.

5.2.2   Resource Exchange

A resource exchange can be triggered by the eNodeB when 1) a new D2D pair joins and requests an RBG, 2) a D2D pair's RBG grant is terminated, and 3) one or more D2D pairs update their CQIs. Whenever the above situations occur, the eNodeB may identify the beneficial exchange sequence in the updated D2D pair set or CQIs. If an exchange sequence is found, the eNodeB may trigger the resource exchange among all pairs in the sequence by sending new RBG grant to the pair heads. The notified D2D pairs will then use the newly granted RBG in the subsequent transmission. Notice that an exchange may also occur between a D2D pair and the eNodeB. The eNodeB may allocate an unallocated RBG to a D2D pair in exchange for the RBG this D2D pair owns. In such a case, only one D2D pair is notified using the resource granting signalling.

Additionally, a resource exchange can also be distributively triggered by the D2D pair in delay-sensitive applications. This optimally deployed D2D-triggered mode requires a

shared RBG containing at least three subframes. This shared RBG is preserved for all D2D pairs to communicate with each other. D2D pairs that wish to communicate with others should listen to the shared RBG to receive the requests. All D2D pairs may access the shared RBG using a slotted-ALOHA mechanism in every $3n + 1$ subframe. A D2D pair head may broadcast its possessed and desired RBGs to other nearby D2D pairs in the same service area through the shared RBG. If the other D2D pair head that holds the requested RBG also prefers the exchange, she may respond to the request in the following subframe of the shared RBG. Finally, the original D2D pair head sends an acknowledgement in the third subframe, and both pairs switch to the exchanged RBGs immediately. After the exchange, both pairs notify the eNodeB about the exchange so that the eNodeB can maintain an up-to-date RBG allocation status. The above mode reduces the eNodeB's loading by offloading some responsibilities of the eNodeB to the D2D pairs themselves. It also reduces the CQI reporting signalling and eNodeB-trigger delay to perform exchanges through the eNodeB. Nevertheless, the exchange requests in the first step may be lost when multiple D2D pairs broadcast their requests simultaneously. Therefore, it is preferable to deploy this mode when the number of D2D pairs in the service area is small. The signalling flows of both modes are illustrated in Fig. 5.2(c).

5.3 System Model

The proposed framework provides necessary functions for an LTE-Advanced system to support resource allocation for D2D communications. Nevertheless, further study is required on how the service provider configures and regulates the D2D communications by the support of these functions.

Let us consider a cellular system with one BS s and a set of N D2D pairs. These D2D pairs are within the BS's service coverage. The coverage is divided into M D2D service area, while the set of D2D pairs within service area m is $\mathbf{D}_m = \{d_1^m, d_2^m, ...\}$. There is a set of RBGs $\mathbf{B} = \{1, 2, ..., L\}$ preconfigured in the system. These RBGs are reused in every service area. Each D2D pair requires an RBG to perform D2D transmissions, and all D2D pairs in the same service area use different RBGs. Let $b_i^m \in \mathbf{B}$ be the RBG allocated to

D2D pair d_i^m in service area m. Then the RBG allocation in service area m can be denoted by $\mathbf{b}_m = (b_1^m, b_2^m, ..., b_{|\mathbf{D}_m|}^m)$. Accordingly, a portion of RBGs $\mathbf{B}_m(\mathbf{b}_m) = \{j | j \in \mathbf{b}_m\} \subset \mathbf{B}$ is allocated to the D2D pairs in service area m, and other RBGs $\mathbf{B}_m^{-1}(\mathbf{b}_m) = \mathbf{B} \setminus \mathbf{B}_m$ are held by the BS in this area. Finally, the overall RBG allocation in all service areas is denoted by $\mathbf{b} = \{\mathbf{b}_m\}$

The interference experienced by a D2D pair in our framework comes from other D2D pairs using the same RBG in other service areas. Specifically, let the interference experienced by D2D pair d_i^m be I_i^m, which is

$$I_i^m(\mathbf{b}_m, \mathbf{b}_{-m}) = \sum_{j \in \mathbf{D}_{m'}, m' \neq m} \mathbf{1}(b_j^{m'} = b_i^m) P g_{j,i}^{m',m} \tag{5.1}$$

, where $\mathbf{b}_{-m}$ is the RBG allocation in all service areas except area m, P is the transmission power of D2D devices, and $g_{j,i}^{m',m}$ is the channel gain from D2D pair j in service area m' to pair i in service area m. Since D2D pairs in the same area use different RBGs, there is no intra-area interference, and we have $g_{j,i}^{m,m} = 0, \forall i, j \in \mathbf{D}_m$. Here we assume that the distance between two devices in one pair is significantly smaller than the distance between D2D pairs in different service areas. Therefore, the inter-area interference experienced by both devices in the same pair will be similar. Additionally, we assume that the channel characteristic is reciprocal, that is, $g_{j,i}^{m,m'} = g_{i,j}^{m',m}, \forall m, m', i, j$.

5.3.1 Resource Exchange Problem

Given an initial RBG allocation $\mathbf{b}^0$, our goal is to reach the optimal RBG allocation $\mathbf{b}^*$ with the lowest overall system interference through exchange operations. The objective function can be denoted as

$$\min \sum_{m, i \in \mathbf{D}_m} I_i^m(\mathbf{b}) \tag{5.2}$$

In our framework, two D2D pairs may apply an exchange operation by switching their possessed RBGs. Additionally, a D2D pair may also exchange her RBG with the BS for an RBG still unallocated to other D2D pairs. After an exchange operation is executed, a new allocation $\mathbf{b}'$ is derived.

An exchange sequence defines a series of exchanges in a service area from an initial allocation $\mathbf{b}_m^0$. For a newly arrived D2D pair, she may virtually receive a randomly-assigned RBG in the initial allocation. Notice that all exchanges are limited to devices in the same service area. For convenience, we denote s_j^m as the "holder" of RBG $j \in \mathbf{B}_m^{-1}(\mathbf{b}_m^0)$ in the BS. In addition, an exchange pair (x, y), where $x, y \in \mathbf{D}_m \cup \{s_j^m | j \in \mathbf{B}_m^{-1}(\mathbf{b}_m^0)\}$, denotes an exchange between x and y. Then, we define an exchange sequence $\mathbf{S}_m$ for service area m as

$$\mathbf{S}_m = [(x_1, y_1), (x_2, y_2), ...], \tag{5.3}$$

The new RBG allocation $\mathbf{b}_m$ is completely determined by the initial allocation $\mathbf{b}_m^0$ and the exchange sequence $\mathbf{S}_m$. We denote this process as $EX(\mathbf{b}_m^0, \mathbf{S}_m) = \mathbf{b}_m$. Thus, our objective is to find the exchange sequence $\mathbf{S}$ that minimizes the total interference in the resource exchange problem. We first show the feasibility of arbitrary RBG allocation in the resource exchange problem.

Theorem 10. *[Feasibility of Exchange Approach] Given arbitrary $\mathbf{b}_m^0$ and $\mathbf{b}_m$, there exists an exchange sequence $\mathbf{S}_m$ that $EX(\mathbf{b}_m^0, \mathbf{S}_m) = \mathbf{b}_m$. In addition, the $\mathbf{S}_m$ can be found in linear time.*

Proof. We prove this by constructing an exchange sequence that achieve $\mathbf{b}_m$. We first expand the RBG allocation vector $\mathbf{b}_m^0$ and $\mathbf{b}_m$ to $\mathbf{v}_m^0$ and $\mathbf{v}_m$ by including the holders $\{s_j^{0,m}\}$ and $\{s_j^m\}$ into the allocation. Then, we construct a resource exchange graph using all D2D pairs and holders in the BS as vertices. Then, each vertex x constructs a directed edge from herself to the vertex y with $v_x^{0,m} = v_y^m$.

Since both $\mathbf{v}_m^0$ and $\mathbf{v}_m$ are one-to-one mapping from $\mathbf{B}$ to $\mathbf{D}_m \cup \{s_j^m | j \in \mathbf{B}_m^{-1}(\mathbf{b}_m^0)\}$, each vertex in the graph has exactly one directed edge to and from another vertex. In other words, any vertex belongs to a cycle or has one directed edge pointing to herself. For the latter case, the vertex is removed from the graph. For the rest of the vertices, let $C = \{v_1, v_2, ..., v_k\}$ be a series of vertices belonging to a cycle in the graph. Then, we construct a sequence $\mathbf{S}_c = [(v_1, v_2), (v_2, v_3), ..., (v_{k-1}, v_k)]$. Finally, an exchange sequence $\mathbf{S}_m = [\mathbf{S}_c]$ is built by merging all constructed sequences together.

130

It can be verified that for every exchange (x, y) indicated in the $\mathbf{S}_m$, the vertex x possesses the desired RBG indicated in $\mathbf{b}_m$. For any vertex x that does not involve in $\mathbf{S}_m$, she has a directed edge to herself, which means $v_x^{0,m} = v_x^m$, so no exchange is required. In sum, the new allocation $\mathbf{b}_m$ is achieved through the exchange sequences $\mathbf{S}_m$ from the initial allocation $\mathbf{b}_m^0$. $\square$

Theorem 10 indicates that the resource exchange approach does not put any additional constraints on the feasible allocation. Any RBG allocation can be achieved through the exchange operations from any initial RBG allocation. Nevertheless, the allocation problem with the objective function in (5.2) is NP-hard [71]. Therefore, an optimal solution may be unachievable when a short response time is a concern. An efficient approximate method is required.

5.3.2 Beneficial Exchange

A beneficial exchange is an exchange sequences wherein all D2D pairs in the service area experience equal or less interference after the exchanges. It can be a good starting point for the approximate algorithm. We first state its formal definition:

Definition 10. *[Beneficial Exchange] A beneficial exchange is an exchange sequence* $\mathbf{S}_m$ *for an initial RBG allocation* $\mathbf{b}_m^0$ *where*

$$I_i^m(\mathbf{b}_m^0, \mathbf{b}_{-m}^0) \le I_i^m(EX(\mathbf{b}_m^0, \mathbf{S}_m), \mathbf{b}_{-m}^0), \forall i \in \mathbf{D}_m \tag{5.4}$$

A beneficial exchange can be considered as a local greedy solution to the interference minimization problem. Nevertheless, we prove that when all exchanges are beneficial, the RBG allocation of the system will converge.

Theorem 11. *[Convergence of Beneficial Exchanges] An exchange-based resource allocation algorithm in the proposed framework converges if every exchange sequences in the algorithm is a beneficial exchange.*

Proof. Without losing generality, we assume that the beneficial exchange occurs in service

area m^*. Let $I_i^{0,m}$ and I_i^m be the interference experienced by the D2D pair d_i^m before and after the beneficial exchange.

Case 1: $m = m^*$: In this case, $\sum_{\mathbf{D}_m} I_i^m < \sum_{\mathbf{D}_m} I_i^{0,m}$ is a direct result from Definition 10. We denote the interference difference as $\Delta I^{m^*} =$

$$\sum_{m \neq m^*} \sum_{j \in \mathbf{D}_m} \sum_{i \in \mathbf{D}_{m^*}} P g_{j,i}^{m,m^*} (\mathbf{1}(b_i^{m^*} = b_j^m) - \mathbf{1}(b_i^{0,m^*} = b_j^m)) < 0 \tag{5.5}$$

. **Case 2:** $m \neq m^*$: In this case, the interference difference experienced by a D2D pair d_j^m before and after the exchange is

$$\begin{aligned}
\Delta I^m &= I_j^m(\mathbf{b}_{m^*}, \mathbf{b}_{-m^*}) - I_j^m(\mathbf{b}_{m^*}^0, \mathbf{b}_{-m^*}) \tag{5.6}\\
&= \sum_{i \in \mathbf{D}_{m^*}} \sum_{j \in \mathbf{D}_m} P g_{i,j}^{m^*,m} (\mathbf{1}(b_i^{m^*} = b_j^m) - \mathbf{1}(b_i^{0,m^*} = b_j^m))\\
&= \sum_{i \in \mathbf{D}_{m^*}} \sum_{j \in \mathbf{D}_m} P g_{j,i}^{m,m^*} (\mathbf{1}(b_i^{m^*} = b_j^m) - \mathbf{1}(b_i^{0,m^*} = b_j^m))
\end{aligned}$$

Therefore, the sum of the total system interference difference is given by

$$\begin{aligned}
\sum_m \sum_{i \in \mathbf{D}_m} I_i^m(\mathbf{b}_{m^*}, \mathbf{b}_{-m^*}) &- I_i^m(\mathbf{b}_{m^*}^0, \mathbf{b}_{-m^*}) = \Delta I^{m^*} +\\
\sum_{m \neq m^*} \sum_{i \in \mathbf{D}_m} \sum_{j \in \mathbf{D}_{m^*}} & P g_{j,i}^{m,m^*} (\mathbf{1}(b_i^{m^*} = b_j^m) - \mathbf{1}(b_i^{0,m^*} = b_j^m))\\
&= \Delta I^{m^*} + \Delta I^{m^*} < 0 \tag{5.7}
\end{aligned}$$

Therefore, the total system interference is reduced when a beneficial exchange occurs. $\quad\square$

Theorem 11 is important, as it guarantees the convergences of any algorithm using beneficial exchanges in the proposed D2D resource allocation framework. Note that the convergence also holds for distributed algorithms whenever every exchanges between two D2D pairs is a beneficial exchange. In conclusion, any arbitrary beneficial-exchange-based greedy algorithm converges under either the eNodeB-assisted mode or D2D-triggered mode in the proposed framework.

5.4 eNodeB-assisted D2D Resource Allocation

A D2D-triggered resource allocation approach is suitable for small networks with few D2D pairs. In contrast, it is more desirable to have an eNodeB-assisted resource allocation approach when the D2D pairs are numerous or resource utilization efficiency is a serious concern. In this approach, the CQIs from the D2D pairs become necessary information for the eNodeB to determine the efficient allocation. Nevertheless, as we have illustrated in Section 5.1, rational D2D pairs have the incentive to report CQIs untruthfully if the allocation mechanism is not properly designed. These forged CQI reports not only give unfair advantages to these D2D pairs but also reduce the resource utilization efficiency since the eNodeB does not receive correct information. Therefore, it is necessary to address the truth-telling issue in an eNodeB-assisted resource allocation approach.

5.4.1 Game Model Formulation

We construct a Nash game model for the proposed framework in order to analyse the truth-telling issue. In a Nash game, there are three components: **players**, **actions**, and **utility functions**. We define all D2D pairs as the players. The action of a D2D pair d_i^m is the CQI ψ_i^m she reports to the BS. Her utility is defined as the experienced Carrier to Interference Ratio (CIR), which is given as follows

$$u_i^m(\mathbf{b}_m, \mathbf{b}_{-m}) = \frac{P g_i^m}{N_0 + I_i^m(\mathbf{b}_m, \mathbf{b}_{-m})}, \tag{5.8}$$

where g_i^m is the channel gain between the two devices in D2D pair d_i^m, and N_0 is the Gaussian white background noise. A D2D pair's utility is higher when she possesses an RBG with lower interference $I_i^m(\mathbf{b}_m, \mathbf{b}_{-m})$.

The RBG a D2D pair d_i^m possesses is determined by an exchange-based mechanism, which is affected by not only her reported CQI ψ_i^m but also other D2D pairs' reported CQIs, which are denoted by ψ_{-i}^m. Given the CQIs ψ_{-i}^m reported by other D2D pairs, a rational D2D pair will choose the CQI that maximizes her utility. Specifically, let the RBG allocation mechanism be $M(\psi_i^m, \psi_{-i}^m, \mathbf{b}_m^0)$, which outputs a new allocation $\mathbf{b}_m$, the

D2D pair d_i^m's best response function is

$$BE_i^m(\psi_{-i}^m, \mathbf{b}_m^0) = \arg \max_\psi u_i(M(\psi, \psi_{-i}^m, \mathbf{b}_m^0), \mathbf{b}_{-m}^0). \tag{5.9}$$

5.4.2 Nash Equilibrium

The Nash equilibrium (NE) is a solution concept for predicting the outcome of a game with rational players. Nash equilibrium is an action profile wherein each player is assigned an action, which is her best response to the other players' actions in the profile. Therefore, if all players follow this action profile, no player has incentive to deviate from the action described in the profile. A formal definition of the Nash Equilibrium in the resource exchange game is as follows:

Definition 11 (Nash Equilibrium). *In the resource exchange game in service area m with a mechanism $m(\psi_i^m, \psi_{-i}^m, \mathbf{b}_m^0)$, an action profile $\mathbf{\Psi}_m = \{\psi_1^m, \psi_2^m, ...\}$ is a Nash Equilibrium if and only if $\forall d_i^m \in \mathbf{D}_m$*

$$BE_i^m(\psi_{-i}^m, \mathbf{b}_m^0) = \psi_i^m. \tag{5.10}$$

Note that the corresponding equilibrium action ψ_i^m of a D2D pair d_i^m is not necessarily equal to its true experienced CQI ψ_i^m, i.e., it is possible that a mechanism eventually has an equilibrium where some D2D pairs choose to report their CQIs untruthfully. In such a case, since the mechanism receives forged reports, it cannot provide efficient allocation.

To prevent the undesirable untruthful reporting behaviours, the proposed mechanism should be **strategy-proof** [15]. A strategy-proof mechanism promises that the truthful action profile, i.e., that all players report their private information truthfully, is a Nash equilibrium. The formal definition of a strategy-proof mechanism in the proposed game is as follows:

Definition 12 (Strategy-proof Mechanism). *A mechanism M with an allocation function $m(\mathbf{\Psi}_m, \mathbf{b}_m^0)$ is a strategy-proof mechanism if and only if the action profile $\{\psi_i^{m,*}\}$ is a Nash equilibrium for all $\mathbf{b}_m^0$.*

If the mechanism is strategy-proof, there exists Nash equilibrium where all players

truthfully report their private information, that is, the experienced CQI in the proposed game. Therefore, the correctness of information collected by the mechanism is guaranteed, and the truth-telling issue is resolved.
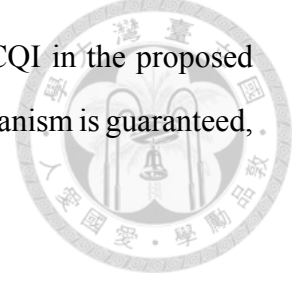
5.5 T-REX: A Trading-based Resource Exchange Mechanism

We propose the **Trading-based Resource EXchange (T-REX)** mechanism for resolving the resource exchange problem in the proposed D2D resource allocation framework. Firstly, the T-REX mechanism collects the CQIs from all D2D pairs in a service area. The **preference** of each D2D pair on RBGs is then constructed according to the reported CQIs. Then the T-REX mechanism constructs an exchange graph according to the preferences of D2D pairs. The mechanism in turn identifies the exchange sequence by searching for cycles in the exchange graph. After the exchange sequence is derived, all involved D2D pairs and traders are then requested to perform resource exchanges accordingly.

5.5.1 Preference on RBG

We define the preference of a D2D pair on the RBGs based on her expected utility in (5.8). A D2D pair experiences different level of interference in different RBGs. The less interference an RBG has, the higher utility the D2D pair has if she possesses the RBG, and thus the more preferred she is. The preference of D2D pair d_i^m can be represented as a relation $\succ_i^m$. We define RBG $j \succ_i^m k$ with RBG $j, k \in \mathbf{B}$ if and only if d_i^m prefers RBG j over RBG k. Formally speaking, the preference $\succ_i^m$ of a D2D pair d_i^m is as follows

$$j \succ_i^m k \Leftrightarrow I_i^m(\mathbf{b}_m|_{b_i^m=j}, \mathbf{b}_{-m}) < I_i^m(\mathbf{b}_m|_{b_i^m=k}, \mathbf{b}_{-m}). \tag{5.11}$$

Finally, we denote the preference profile of all D2D pairs in $\mathbf{D}_m$ as $\succ^{\mathbf{m}} = (\succ_1^m, \succ_2^m, ..., \succ_{|\mathbf{D}_m|}^m)$. Notice that the preference of a D2D pair does not affected by the preferences of other pairs in the same service area since there is no intra-area interference in the
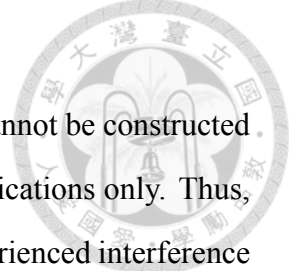
proposed framework.

The preference of the eNodeB on the RBGs, on the other hand, cannot be constructed in the same way since these RBGs are specifically for D2D communications only. Thus, it is pointless to define the eNodeB's preference according to her experienced interference in these RBGs. Instead, we propose the **trader** approach here. For each service area m, there is a set of (virtual) traders $t_i^m \in \mathbf{T}_m, i = 1 \sim |B_m^{-1}|$. The eNodeB internally assigns each unallocated RBG $j \in |B_m^{-1}|$ to a trader. A trader's preference $\succ_i^{tr,m}$ for the RBGs is given by a trader preference function $F_i^m(\cdot)$. It should be noted that these traders are not the actual players in the resource exchange game since their preferences are directly controlled by the eNodeB. The traders are tools offered by the T-REX mechanism for the eNodeB to regulate the resource exchange game.

Notice that the resource exchange game with only D2D pairs involved can be considered a variant of the house allocation problem [72], in which a strategy-proof solution called the Top-Trading Cycle Algorithm (TTCA) is illustrated. Nevertheless, when there are unallocated RBGs, TTCA only provides a locally optimal performance, as we will illustrate in Section 5.6.

5.5.2 Mechanism Design

The T-REX mechanism works as follows: a resource exchange graph is initialized with all D2D pairs and traders in a service area as vertices. For each vertex, the preference is determined by either the corresponding reported CQI ψ_i^m (D2D pair) or the trader preference function $F_i^m(\cdot)$ (trader). In addition, each vertex is also marked with an RBG according to the initial allocation $\mathbf{b_0^m}$. After the initial graph is defined, each vertex constructs a directed edge to the vertex owning her most preferred RBG in the current graph.

The T-REX mechanism then searches cycles in the graph, which always exists because each vertex has exactly one directed edge. When a cycle is found, the vertices in the cycle exchange their RBGs with each other according to their edges, and we eliminate them from the graph. It should be noted that it is possible for a vertex to have a directed edge pointing to itself, which means that the owner already possesses the most preferred

Preference	1st	2nd	3rd	4th	5th
D2D 1	2	1	3	4	5
D2D 2	4	2	1	3	5
D2D 3	2	3	1	4	5
Trader 1	1	2	3	4	5
Trader 2	2	3	4	5	1
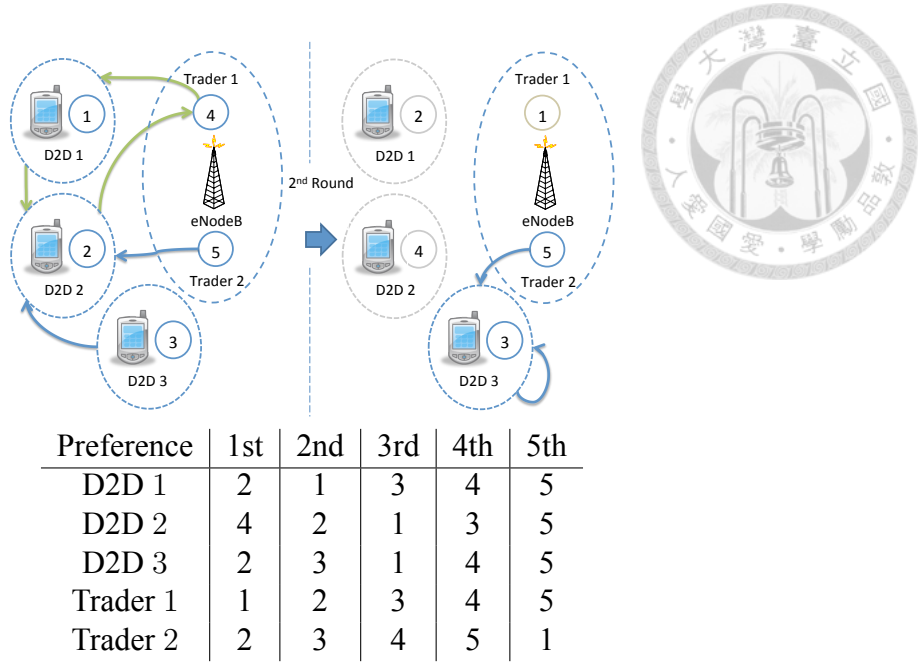
Figure 5.3: An example of the T-REX mechanism

RBG. In such a case, the vertex is simply removed from the graph. Then, the remaining edges in the graph are reconstructed according to the preference of each vertex on the RBGs held by remaining vertices, and the T-REX mechanism again identifies cycles. The exchange procedure is executed repeatedly until all vertices are removed from the graph. The pseudo-code of the T-REX mechanism is shown in Algorithm 3.

We illustrate an example of the T-REX mechanism. We consider a D2D service area with 3 D2D pairs and 5 RBGs. The preferences of D2D pairs and traders are listed in Fig. 5.3. The T-REX mechanism constructs the resource exchange graph as shown in Fig. 5.3. We can see that a cycle is formulated among D2D pairs 1, 2, and Trader 1. An exchange sequence $\{(s_1, s_2), (s_2, d_1)\}$ is then identified. Then, D2D pairs 1, 2, and Trader 1 are removed from the graph, and the edges are reconstructed. In the reconstructed graph, D2D pair 3's directed edge points to herself since her most preferred RBG in the current graph is RBG 3. Since she already possessed the desired RBG, she is directly removed from the graph. The T-REX mechanism ends at the third round since all D2D pairs are removed from the graph.

The T-REX mechanism operates in one service area. When multiple service areas exist, the T-REX mechanism can function independently in these areas. Although it is possible that the resulting RBG allocation in one area affects the preferences of D2D pairs

137
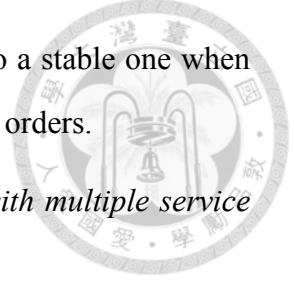
in other service areas, the overall RBG allocation $\mathbf{b}$ will converge to a stable one when the T-REX mechanism is applied sequentially in all areas in arbitrary orders.

Theorem 12. *The T-REX mechanism converges in a D2D system with multiple service areas.*

Proof. We prove the convergence of the T-REX mechanism by showing that all exchange sequences are beneficial exchanges. Let $\mathbf{b}_m^0$ be the initial RBG allocation. Then, let C be a cycle found in the resource exchange graph and $\mathbf{S}_c$ be the corresponding exchange sequence. The resulting RBG allocation is $\mathbf{b}_m = EX(\mathbf{b}_m^0, \mathbf{S}_c)$.

Case 1: $d_i^m \notin C$. In this case, the RBG allocated to D2D pair d_i^m is unaffected by the exchanges. Therefore, her experienced interference remains unchanged.

Case 2: $d_i^m \in C$. In this case, the RBG allocated to D2D pair d_i^m is changed. Let k and j be the RBG allocated to D2D pair d_i^m before and after the exchanges. Since $d_i^m \in C$, we have $j \succ_i^m k$, which means $I_i^m(\mathbf{b}_m|_{b_i^m=j}, \mathbf{b}_{-m}) < I_i^m(\mathbf{b}_m|_{b_i^m=k}, \mathbf{b}_{-m})$. Therefore, the interference experienced by D2D pair d_i^m is lower under the new allocation $\mathbf{b}_m$.

Concluding from the above two cases, all D2D pairs experience equal or higher interference after any exchange identified by the T-REX mechanism. Therefore, all exchanges in the T-REX mechanism are beneficial exchanges according to Definition 10, and the convergence of the T-REX mechanism in multiple service areas is guaranteed by Theorem 11. □

The complexity of the T-REX mechanism with a given $F_i^m(\cdot)$ is $\max\{O(|\mathbf{B}|^2), O(|\mathbf{B}|F_i^m(\cdot))\}$. This comes from the fact that at least one vertex is removed from the graph $\mathbf{G}$ at each iteration (Line 7 to 21), and it takes at most $|\mathbf{G}| \leq |\mathbf{B}|$ steps to update the edges and $O(F_i^m(\cdot))$ to update the preferences of traders in each iteration. Therefore, when $O(F_i^m(\cdot))$ is polynomial, the complexity of the T-REX mechanism is polynomial.

The key in the T-REX mechanism is the trader preference function. The eNodeB regulates the resource allocation through defining the trader preference function in the T-REX mechanism. Different choices on trader preference functions will result in different RBG allocations even if the eNodeB receives same CQI reports from D2D pairs. Next, we provide some trader preference function candidates.

Algorithm 3 T-REX Mechanism
___
Input: $\Psi_m = \{\psi_i^m\}$, $\{F_i^m\}$, and $\mathbf{b}_m^0$
Output: Exchange Sequence $\mathbf{S}_m$ and Allocation $\mathbf{b}_m$
 1: $\mathbf{b}_m = \mathbf{b}_m^0$;
 2: $\mathbf{S}_m = [\,]$;
 3: **for** all d_i^m in $\mathbf{D}_m$ **do**
 4:      constructs $\succ_i^m$ based on ψ_i^m;
 5: **end for**
 6: constructs a resource exchange graph G with each $d_i^m \in \mathbf{D}_m$ and $t_i^m \in \mathbf{T}_m$ as vertices;
 7: **while** G is not empty **do**
 8:      **for** all v in $\mathbf{T}_m$ **do**
 9:          constructs $\succ_v^m$ according to $F_v^m(x)$;
 10:     **end for**
 11:     **for** all vertices v in G **do**
 12:         constructs a directed edge $e(v, v')$ where $a(v') \succ_v^m a(v'') \forall v'' \in G$;
 13:     **end for**
 14:     find a cycle C in G;
 15:     **for** all vertices v in C with edge $e(v, v')$ **do**
 16:         **if** $v \neq v'$ **then**
 17:             append (v,v') to $\mathbf{S}_m$;
 18:         **end if**
 19:     **end for**
 20:     exclude all vertices in C from G;
 21: **end while**
 22: $\mathbf{b}_m = EX(\mathbf{b}_m^0, \mathbf{S}_m)$;
___

5.5.3   Cycle-Complete Preference

First, we propose a cycle-complete preference (CYC), which enhances the allocation of RBGs according to the preferences of D2D pairs. First, we define an <u>incomplete cycle</u> in the resource exchange game.

Definition 13 (Incomplete Cycle). *An incomplete cycle ω is an open, directed path with no repeated vertex in the graph; i.e., a path that could be closed into a cycle only if there is an additional directed edge connected from the tail to the head vertex.*

The primary operation of the CYC preference is to ensure that when an incomplete cycle ω with trader t_i^m as the tail vertex exists, the trader t_i^m always chooses the RBG possessed by the head D2D pair of the incomplete cycle ω as her most preferred RBG in that round. A new directed edge is connected from the trader t_i^m to the head D2D pair, and the incomplete cycle ω is now complete. With the CYC addition, all D2D pairs in the incomplete cycle will derive their most preferred RBGs. In cases where there is no
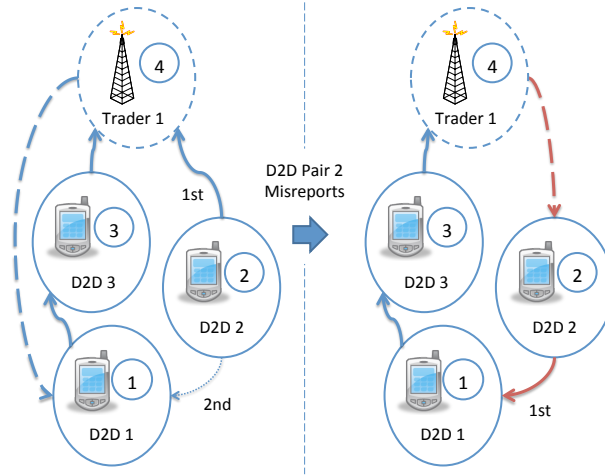
Figure 5.4: Cheating in CYC preference

incomplete cycle with tail vertex as t_i^m, the trader t_i^m just randomly chooses a RBG $j \in \mathbf{B}_m$ as her preferred RBG.

When multiple incomplete cycles end at the same trader, a reasonable choice for the CYC preference is to choose the largest incomplete cycle. With this choice, we greedily maximize the number of D2D pairs receiving their preferred RBGs. We define the set of incomplete cycles with tail vertex t_i^m in round l as $\mathbf{\Omega}_{t_i^m,l}$, and the set of incomplete cycles with n vertices as $\mathbf{\Omega}_{t_i^m,l}^n \subset \mathbf{\Omega}_{t_i^m,t}$. The trader preference function $F_{i,CYC}^m$ is given by

$$F_{i,CYC}^m(\mathbf{\Omega}_{t_i^m,l}) = \{head(RAND(\omega)) \succ_i^{tr,m} b_j, \forall b_j \neq head(\omega), \omega \in \mathbf{\Omega}_{t_i^m,l}^{n_l}, n_l = \max_{\mathbf{\Omega}_{t_i^m,l}^j \neq \emptyset} j\},$$

(5.12)

where the head vertex of ω is $head(\omega)$.

Unfortunately, a T-REX mechanism with CYC preference is not strategy-proof. An example of cheating is shown in Fig. 5.4. In this D2D service area, D2D pair 2 prefers RBG 4 most, which is held by Trader 1. Her second preferred RBG is RBG 1, which is held by D2D pair 1. However, the largest incomplete cycle ending at Trader 1 is $\{d_1, d_3, t_1\}$. According to the CYC preference, Trader 1 will choose RBG 1 as her most preferred RBG. D2D pair 2 does not have the chance to exchange with either Trader 1 or D2D pair 1. Nevertheless, it can be seen that if D2D pair 2 sends a forged CQI report to choose RBG 1 as her most preferred RBG, a new incomplete cycle $\omega' = \{d_2, d_1, d_3, t_1\}$ is formed. In the manipulated resource exchange graph, Trader 1 will choose RBG 2 as her most

140

preferred RBG, and D2D pair 2 can exchange with D2D pair 1 to get her second preferred RBG, which is better than the results in the original resource exchange graph. Therefore, D2D pair 2 has the incentive to cheat when CYC preference is applied. In conclusion, the T-REX mechanism with CYC preference is not strategy-proof.
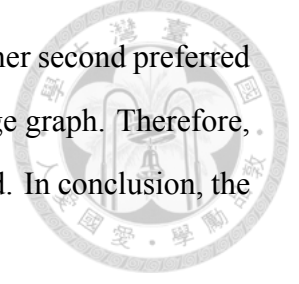
5.5.4 Sufficient Conditions of Strategy-proofness

We now discuss the sufficient conditions of the trader preference function to make the T-REX mechanism strategy-proof. As observed in the previous section, the primary problem with the CYC preference is that the preferences of traders are related to the preferences of D2D pairs. This results in the possibility for that D2D pairs could cheat in the game by influencing the preferences of traders. Based on this observation, we now propose the sufficient conditions for a strategy-proof T-REX mechanism.

Theorem 13. *When the preferences of traders are unrelated to the preferences of D2D pairs, the T-REX mechanism with the implemented trader preference function is strategy-proof.*

Proof. Since the trader preferences are not related to the preferences of D2D pairs, the problem is equivalent to an allocation problem with $\mathbf{D}'_m = \{\mathbf{D}_m, \mathbf{T}_m\}, \mathbf{B}_m = \mathbf{B}$. In this equivalent problem, all nodes are considered as D2D pairs with independent preferences.

We first denote the cycle found in round k of the procedure as C_k, the D2D pair set in C_k as N_k, and the set of RBGs exchanged in this round as B_k. Assume that a D2D pair d_i^m has a CQI ψ_i. Without losing generality, we assume $d_i^m \in N_k$ when reporting ψ_i.

Let $\mathbf{b}_m$ and $\mathbf{b}'_m$ be the allocation return by the T-REX mechanism when d_i^m reports ψ_i and $\psi'_i \neq \psi_i$, respectively. Also, let $N_1, N_2, ...$ and $N'_1, N'_2, ...$ be the corresponding cycles formed in round $1, 2, ...$ given d_i^m reporting ψ_i and ψ'_i. First we show that it is not possible for a $d_i^m \in N_k$ to break into $C_r, r = 1, 2, ..., k-1$ by reporting ψ'_i. Since $d_i^m \in N_k$, no edge $e(j, i)$ exists $\forall d_j^m \in \cup_{0<r<k} N_r$. Thus, given any $\psi'_i \in R^l$, $N_r = N'_r \forall r < k$ and $d_i^m \notin \cup_{0<r<k} N'_r$. So d_i^m cannot derive any RBG in $\cup_{0<r<k} B_r$ by reporting ψ'_i. However, since b_i^m is the RBG d_i^m derived by reporting ψ_i, the constructed preference $\succ_i$ has already

141

chosen the most preferred RBG in $B - \cup_{0<r<k} B_r$. Thus $b_i^m \succeq_i b_i'^m$. This completes the proof for strategy-proofness. □

In addition to the strategy-proofness, we see that the final RBG allocation of Algorithm 3 is Pareto optimal.

Theorem 14 (Pareto Optimal). *Given the trader preference $\succ^{\mathbf{tr}}$, the allocation returned by Algorithm 3 is Pareto optimal when $\succ_i$ is strict for all $d_i^m \in \mathbf{D}_m$.*

Proof. We prove this by contradiction. Let $\mathbf{b}_m$ be the output allocation of Algorithm 3. We assume that there exists a set of D2D pairs $\mathbf{D}_b \subset \mathbf{D}_m$ which can form an exchange sequence and derive a new allocation $\mathbf{b}'_m$ that $\forall d_j^m \in \mathbf{D}_b$, $b_j'^m \succeq_i b_j^m$, and $\exists d_i^m \in \mathbf{D}_b$, $b_i'^m \succ_i b_i^m$. Without losing generality, let $i = 1, 2, ..., |\mathbf{D}_b|$, $d_i^m \in N_{k_i}$, $k_i \geq k_j$ when $i \geq j$.

We check each D2D pair's possessed RBG in $\mathbf{b}_m$. For d_1^m, since it belongs to N_{k_i}, it has chosen the most preferred RBG in $\{b_i^m | \forall d_i^m \in \cup_{r=k_i,k_i+1,...} N_r\}$. In addition, $\forall d_i^m \in \mathbf{D}'_m$, $\succ_i$ is strict. Thus, $b_1'^m = b_1^m$. We can repeat this statement from d_2^m to $d_{|\mathbf{D}_b|}^m$ and conclude that $b_i'^m = b_i^m$, $\forall d_i^m \in \mathbf{D}'_m$. We reach a contradiction here. Thus, there exists no D2D pairs that can get better RBGs than in the allocation $\mathbf{b}_m$ without harming others. In short, the allocation $\mathbf{b}_m$ is Pareto optimal. □

5.5.5 Strategy-proof Preference Designs

In the following, we propose three trader preference functions which are strategy-proof.

Randomized Preference

We now propose a strategy-proof trader preference function: RANdomized preference (RAN). In the RAN preference, each trader randomly generates her preference on RBGs. Let the set that contains all possible preferences on RBG set $\mathbf{B}$ be $P(\mathbf{B})$. The trader preference function of the RAN preference is defined as:

$$F_{i,RAN}^m(\mathbf{B}) = RAND(P(\mathbf{B})). \tag{5.13}$$

142

Theorem 13 guarantees that the RAN preference is strategy-proof, since the preferences of traders are not related to the preferences of traders.

Nevertheless, since the preferences of traders are randomly chosen, it is possible that traders may choose each other's RBGs as their most preferred RBGs. In such a case, an inter-trader exchange will occur. But it is meaningless to the system because both traders in fact belong to the same eNodeB. This also eliminates the possibility of D2D pairs exchanging with these traders, leading to an inefficient RBG allocation
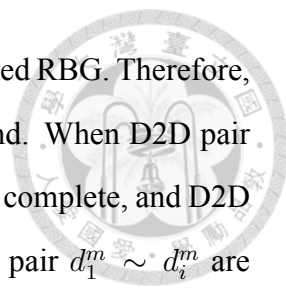
To enhance the efficiency while maintaining strategy-proofness, we propose the modified RAN algorithm, which we call D2D-preferred RANdomized preference (DRAN). Recall that $\mathbf{B}_m(\mathbf{b}_m^0)$ represents the RBGs allocated to D2D pairs in the initial allocation $\mathbf{b^0}_m$. We use these RBGs to determine the first n^{th} highest preferred RBGs for all traders. The rest of the unallocated RBGs are then randomly chosen as the $(n+1)^{th}$ to L^{th} highest preferred RBGs for all traders. With this modified preference, we eliminate the possibility of traders exchanging RBGs with each others. The trader preference function of DRAN is

$$F_{i,DRAN}^m(\mathbf{b}_m^0, \mathbf{B}) = \{RAND(P(\mathbf{B}_m(\mathbf{b}_m^0))) \succ_i^{tr,m} RAND(P(\mathbf{B}_m^{-1}(\mathbf{b}_m^0)))\}.\text{(5.14)}$$

Prioritized Preference

Finally, it remains to illustrate how the T-REX mechanism can be configured for different objectives, such as D2D pair prioritization. We consider the case that D2D pairs are prioritized. Some D2D pairs should be granted priority to receive an allocated RBGs with greater transmission quality. We can realize the prioritization with the proposed PRIoritized preference (PRI). Without losing generality, we assume the priority order is the same as the D2D pair's numbering. Recalling that the RBG allocated to D2D pair d_i^m in b_i^m, the trader preference function of the PRI preference is

$$F_{i,PRI}^m(\mathbf{b}_m) = \{\{b_i^{0,m} \succ_i^{tr,m} b_j^{0,m} \text{ iff } i < j\} \succ_i^d RAND(P(\mathbf{B}_m^{-1}(\mathbf{b}_m)))\}. \quad \text{(5.15)}$$

At the first round, all traders choose the RBG $b_1^{0,m}$ as their most preferred RBG. Therefore, all traders will have direct edges to the D2D pair d_1^m in the first round. When D2D pair d_1^m belongs to an incomplete cycle ending at a trader, the cycle will be complete, and D2D pair d_1^m receives her most preferred RBG. Additionally, when D2D pair $d_1^m \sim d_i^m$ are removed from the graph, all traders construct directed edges to D2D d_{i+1}^m according to PRI preference, and D2D pair s_{i+1} now has a higher probability to receive her preferred RBG. In such a design, D2D pairs with higher priority are more likely to get the RBGs they prefer. Plus, Theorem 13 again ensures that the PRI preference is strategy-proof.

5.6 Simulation Results

We study a D2D communication scenario to examine the efficiency of the proposed framework and the T-REX mechanism in allocating RBGs. We consider a system with one BS governing a typical 19 hexagonal service area topology. The length of the service area edge is 100m. The system has M dedicated RBGs. Each service area has N D2D pairs using a transmission power of 23dBm. Their locations are uniformly given with in the area. We initiate the RBG assignment by randomly allocating N RBGs to those N D2D pairs in each service area. For the signal loss model, we apply the D2D outdoor-to-outdoor path loss model and antenna gain suggested in 3GPP LTE-Advanced Release 12 contributions [3].

The preference of RBGs is based on the D2D pairs' measurements on the interference in each RBG. The interference is mainly caused by those D2D pairs served in different areas. We assume that the D2D pairs in the same area measure the interference at the same time. Therefore, their measurements do not include the interference from the D2D pairs in the same area.

Then, we simulate the system in multiple rounds. In each round, we randomly choose a service area and apply the simulating resource allocation mechanism. If the applied mechanism does not alter the allocation in all service areas, the simulation goes to the next round and the process repeats. The loop process terminates when there exists no service area that would like to alter its allocation under the simulating mechanism.
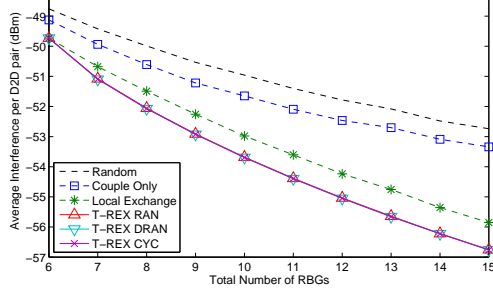
(a) Number of D2D Pairs per Area

(b) Total Number of RBGs

Figure 5.5: Simulation Results: Interference

5.6.1 Interference Mitigation

We measure the average system interference experienced by D2D pairs under the T-REX mechanism with two strategy-proof preferences (RAN and DRAN), as well as the greedy cycle-complete preferences (CYC). We compare the T-REX mechanism with the Random, Local Exchange, and Couple Only mechanisms. The Random mechanism, in which all RBGs are randomly assigned to D2D pairs, is considered as a baseline with no optimization applied. In Local Exchange mechanism, D2D pairs exchange with the RBGs held by other D2D pairs only. This can be implemented in a distributed way through the D2D-Tirggered mode in our framework or by using TTCA algorithm. It represents the case that the eNodeB generally is not involved in the resource re-allocation. In the Couple Only mechanism, an exchange occurs only when both pairs have lower interference immediately after the exchange. This mechanism represents the case that D2D pairs have very limited information about the preferences of other pairs and therefore it is not possible to have an exchange sequence with more than two pairs involved. We measure the efficiency of each mechanism with the interference experienced by D2D pairs in their

possessed RBGs.

We first evaluate the impact of number of D2D pairs on the efficiency of the T-REX mechanism. We preserve 15 RBGs and adjust the number of D2D pairs from 6 to 15 in the simulation. The simulation results are shown in Fig. 5.5(a). We first observe that the T-REX mechanism significantly outperforms the Random, Local Exchange, and Couple Only mechanisms in terms of average interference. The Couple Only mechanism has a little improvement in interference compared to the Random mechanism, while the Local Exchange mechanism has better performance than the Couple Only one.

Nevertheless, all T-REX mechanisms perform much better because of the granting of unallocated RBGs from the BSs to the D2D pairs through traders. We also observe that all T-REX RAN, DRAN, and CYC mechanisms perform similarly. This suggests that when the T-REX mechanism converges, the resulting allocation is very close to (or is) the optimal one. Additionally, the strategy-proof T-REX RAN and DRAN mechanisms perform equally well with non-strategy-proof T-REX CY mechanism in terms of interference. We also observe that when the number of D2D pairs increases, there is an increase in the interference level under all T-REX mechanisms. The increase is due to the decrease of RBGs preserved by the BS. Since there are fewer RBGs for exchange, the room for improvements through the exchange is smaller. Additionally, we also observe that as the number of D2D pairs increases, the effect of trader preference functions becomes insignificant. This result comes from the decrease in available RBGs in the BS.

Finally, we simulate with 6 D2D pairs and adjust the number of available RBGs from 6 to 15. The results are shown in Fig. 5.5(b). We observe that when the number of available RBGs increases, the interference decreases in all schemes, and the interference mitigation of the T-REX mechanism from the Random scheme increases.

5.6.2 Convergence Rounds

Next, we compare the average convergence rounds of different mechanisms in the simulations. The results are shown in Fig. 5.6. First, the Couple Only mechanism converges in less than 15 rounds in all simulations since there is only a limited number of D2D pairs
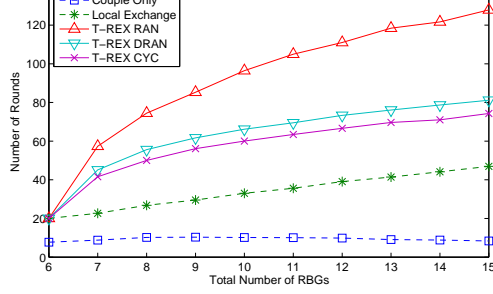
(a) Number of D2D pairs per Area

(b) Total Number of RBGs

Figure 5.6: Simulation Results: Convergence

that can exchange with this mechanism. For the Local mechanism, on the other hand, the convergence rounds increase to around $40 \sim 60$ rounds, which is significantly higher than those of the Couple Only mechanism. In return, her performance is also much better than that of the Couple Only mechanism, as we have seen in Fig. 5.5.

Then, we observe that T-REX mechanisms with different trader preference functions have different numbers of convergence rounds even if they perform similarly in terms of interference mitigation (Fig. 5.5). T-REX RAN has the largest number of convergence rounds in all simulations. This is due to the fact that inter-trader exchanges, which only occur in RAN, reduces the probability that a D2D pair possesses her desired RBG from the BS. This significantly slows down the convergence speed. For others, the T-REX DRAN and T-REX CYC mechanisms have similar numbers of convergence rounds. Additionally, the greedy cycle-complete method in T-REX CYC mechanism leads to less number of convergence rounds since no random process is involved in the T-REX CYC mechanism.

Figure 5.7: Simulation Results: Prioritization
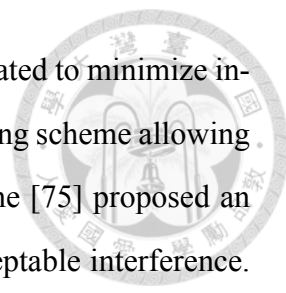
5.6.3 Prioritization using T-REX PRI mechanism

Finally, we illustrate the prioritization effect when using PRI preference in the T-REX mechanism. We simulate the D2D system with 8 D2D pairs per area and 15 available RBGs. We assume that the D2D pairs in each area are prioritized according to their numbering, that is, D2D pair 1 has the highest priority while D2D pair 8 has the lowest priority in their area. We simulate with T-REX DRAN and PRI mechanisms, and the average interference experienced by D2D pairs with different priorities are shown in Fig. 5.6.3.

We observe that those D2D pairs with higher priorities (lower numbers) indeed experience lower average interference when T-REX PRI mechanism is applied. For T-REX DRAN mechanism, there is no significant difference between D2D pairs in terms of average interference. In conclusions, the T-REX mechanism with PRI preference indeed prioritized the D2D pairs by offering better RBGs to D2D pairs with higher priorities.

5.7 Related Work

Regarding resource allocation in D2D communications within a cellular system, Yu [73] proposed resource sharing modes and the corresponding closed form solutions to determine the optimized resource allocation for D2D communication underlying cellular networks. Fodor [7] demonstrated the major difficulties in D2D transmission design, in view of peer discovery and resource allocation. When D2D devices co-exist with traditional

cellular ones, the resources for D2D devices should be carefully allocated to minimize interference. In such an approach, Wang [74] presented a resource sharing scheme allowing D2D UEs to reuse resources from multiple cellular users. Zulhasnine [75] proposed an algorithm to assign D2D devices to shared resource blocks with acceptable interference. Zhu [76] presented an algorithm to maintain tolerable interference among D2D UEs sharing different RBGs. Chen [77] investigated the coexistence of D2D and cellular users given partial frequency reuse. The interference limited area is proposed to limit mutual interference.

In addition, the D2D transmission may be virtual, relayed by the eNodeB, or direct. The mode selection further complicates the problem. Janis [78] proposed a method to allocate resources and assign transmission modes to D2D devices with limited interference to cellular ones. Belleschi [79] proposed a single-cell formulation for D2D communication, in which a D2D device may adopt the D2D or cellular modes to minimize the overall power. A load-control algorithm was introduced to approximate the optimal solution for the NP-hard formulation. Nevertheless, most existing works only consider centralized schemes with eNodeB assigning the radio resource for D2D devices. In such an approach, periodic or on-demand report of channel status from D2D devices to eNodeB are required, since the interference perceived by D2D devices is unknown to eNodeB. However, most of theexisting literature does not address the issues caused by the rationality of D2D devices and users, such as truth-telling. As we have illustrated in Section 5.1, rational D2D devices and users may untruthfully report their information and behave maliciously in order to achieve better performance for themselves. When rationality is a concern, the mechanisms proposed above may receive forged information from the D2D devices and therefore be unable to make correct decisions.

There exist few works on tackling the truth-telling problem in D2D communications. Xu [80] formulated a sequential second-price auction for the D2D resource allocation. Users' payoff is maximized and the system sum rate is improved using the proposed resource allocation algorithm. Nevertheless, such approaches require a monetary transfer process, which significantly increases the complexity of implementation in the cellular

network. It may be preferable to have a direct mechanism involving no payment process.

5.8 Summary

In this chapter, we proposed a novel resource-exchange-based D2D resource allocation framework for an LTE - Advanced system. We showed that the convergence of any algorithm in the framework is guaranteed when all performed exchanges are beneficial. Based on the idea of beneficial exchange, we proposed the Trader-assisted Resource Exchange (T-REX) mechanism. The T-REX mechanism identifies the beneficial exchanges through analysing the corresponding exchange graph. The eNodeB participates in the exchange process through designing the trader preference functions. This design is critical to the convergence speed, as has been shown in the simulations. Through game-theoretic analysis, we also proved that when the trader preference functions are properly designed, the T-REX mechanism is strategy-proof. This prevents the eNodeB from receiving forged CQI reports from rational D2D devices and users. Finally, we evaluated the performance of the T-REX mechanism through simulations. The simulations with the parameters suggested in the latest 3GPP technical contribution showed that the T-REX mechanism significantly mitigates the interference experienced by D2D devices.

Chapter 6
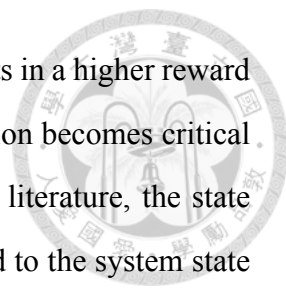
Chinese Restaurant Game: Social Learning vs. Network Externality

6.1 Introduction

How agents in a network learn and make decisions is an important issue in numerous research fields, such as social learning in social networks, machine learning with communications among devices, and cognitive adaptation in cognitive radio networks. Agents make decisions in a network in order to achieve certain objectives. However, the agent's knowledge on the system may be limited due to the limited ability in observations or the external uncertainty in the system. This impaired his utility since he does not have enough knowledge to make correct decisions. The limited knowledge of one agent can be expanded through learning. One agent may learn from some information sources, such as the decisions of other agents, the advertisements from some brands, or his experience in previous purchases. In most cases, the accuracy of the agent's decision can be greatly enhanced by learning from the collected information.

6.1.1 Traditional Social Learning

The learning behavior in a social network is a popular topic in the literature. Let us consider a social network in an uncertain system state. The state has an impact on the
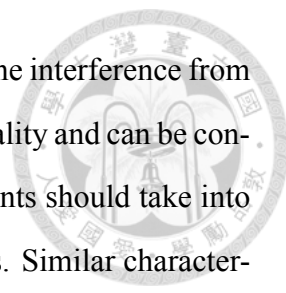
agents' rewards. When the impact is differential, i.e., one action results in a higher reward than other actions in one state but not in all states, the state information becomes critical for one agent to make the correct decision. In most social learning literature, the state information is unknown to agents. Nevertheless, some signals related to the system state are revealed to the agents. Then, the agents make their decisions sequentially, while their actions/signals may be fully or partially observed by other agents. Most of existing works [81--84] study how the believes of agents are formed through learning in the sequential decision process, and how accurate the believes will be when more information is revealed. One popular assumption in traditional social learning literature is that there is no network externality, i.e., the actions of subsequent agents do not influence the reward of the former agents. In such a case, agents will make their decisions purely based on their own believes without considering the actions of subsequent agents. This assumption greatly limits the potential applications of these existing works.

6.1.2 Network Externality

The network externality, i.e., the influence of other agents' behaviors on one agent's reward, is a classic topic in economics. How the relations of agents influence an agent's behavior is studied in coordinate game theory [85]. When the network externality is positive, the problem can be modeled as a coordination game: When one agent makes a decision, the subsequent agents are encouraged to make the same decision in two aspects: the probability that this action has the positive outcome increases due to this agent's decision, and the potential reward of this action may be large according to the belief of this agent.

When the externality is negative, it becomes an anti-coordination game, where agents try to avoid making the same decisions with others [86--88]. The negative network externality plays an important rule in many applications in different research fields. One important application is spectrum access in cognitive radio networks. In spectrum access problem, secondary users accessing the same spectrum need to share with each other. The more secondary users access the same channel, the less available access time or higher interference for each of them. In this case, the negative network externality degrades the

utility of the agents making the same decision. As illustrated in [89], the interference from other secondary users will degrade a secondary user's transmission quality and can be considered as the negative network externality effect. Therefore, the agents should take into account the possibility of degraded utility when making the decisions. Similar characteristics can also be found in other applications, such as service selection in cloud computing and deal selection in Groupon website.

The combination of negative network externality with social learning is difficult to analyze. When the network externality is negative, the game becomes an anti-coordination game, where one agent seeks the strategy that differs from others' to maximize his own reward. Nevertheless, in such a scenario, the agent's decision also contains some information about his belief on the system state, which can be learned by subsequent agents through social learning algorithms. Thus, subsequent agents may then realize that his choice is better than others, and make the same decision with the agent. Since the network externality is negative, the information leaked by the agent's decision may impair the reward the agent can obtain. Therefore, rational agents should take into account the possible reactions of subsequent players to maximize their own rewards.

6.1.3 Chinese Restaurant Game

Chinese restaurant process, which is a non-parametric learning methods in machine learning [90], provides an interesting non-strategic learning method for unbounded number of objects. In Chinese restaurant process, there exists infinite number of tables, where each table has infinite number of seats. There are infinite number of customers entering the restaurant sequentially. When one customer enters the restaurant, he can choose either to share the table with other customers or to open a new table, with the probability being predefined by the process. Generally, if a table is occupied by more customers, then a new customer is more likely to join the table, and the probability that a customer opens a new table can be controlled by a parameter [91]. This process provides a systematic method to construct the parameters for modeling unknown distributions. Nevertheless, the behavior of customers in Chinese restaurant game is non-strategic, which means they

follow predefined rules without rational concerns on their own utility. We observe that if we introduce the strategic behaviors into Chinese restaurant process, the model can be a general framework for analyzing the social learning with negative network externality. To the best of our knowledge, no effort has been made to bring rationality concerns into such a decision making structure in the literature.

By introducing the strategic behavior into the non-strategic Chinese restaurant process, we propose a new game, called **Chinese Restaurant Game**, to formulate the social learning problem with negative network externality In our previous work [92], we have studied the simultaneous Chinese restaurant game without social learning where customers make decisions simultaneously. In this chapter, we will study the sequential Chinese restaurant game with social learning where customers make decisions sequentially. Let us consider a Chinese restaurant with J tables. There are N customers sequentially requesting for seats from these J tables for having their meals. One customer may request one of the tables in number. After requesting, he will be seating in the table he requested. We assume that all customers are rational, i.e., they prefer bigger space for a comfortable dining experience. Thus, one may be delighted if he has a bigger table. However, since all tables are available to all customers, he may need to share the table with others if multiple customers request for the same table. In such a case, the customer's dining space reduces, due to which the dining experience is impaired. Therefore, the key issue in the proposed Chinese restaurant game is how the customers choose the tables to enhance their own dining experience. This model involves the negative network externality since the customer's dining experience is impaired when others share the same table with him. Moreover, when the table size is unknown to the customers, but each of them receives some signals related to the table size, this game involves the learning process if customers can observe previous actions or signals.

In the rest of this chapter, we first provide detailed descriptions on the system model of Chinese restaurant game in Section 6.2. Then, we study the sequential game model with perfect information to illustrate the advantage of playing first in Section 6.3. In Section 6.4, we show the general Chinese restaurant game framework by analyzing the learning

behaviors of customers under the negative network externality and uncertain system state. We provide a recursive method to construct the best response for customers, and discuss the simulation results in Section 6.5. In Section 6.6, we illustrate how the traditional spectrum access problem can be formulated as a Chinese restaurant game. Finally, we summarize this chapter in Section 6.8.

6.2 System Model

Let us consider a Chinese restaurant with J tables numbered $1, 2, ..., J$ and N customers labeled with $1, 2, ..., N$. Each customer requests for one table for having a meal. Each table has infinite seats, but may be in different size. We model the table sizes of a restaurant with two components: the restaurant state θ and the table size functions $\{R_1(\theta), R_2(\theta), ..., R_J(\theta)\}$. The state θ represents an objective parameter, which may be changed when the restaurant is remodeled. The table size function $R_j(\theta)$ is fixed, i.e., the functions $\{R_1(\theta), R_2(\theta), ..., R_J(\theta)\}$ will be the same every time the restaurant is remodeled. An example of θ is the order of existing tables. Suppose that the restaurant has two tables, one is of size L and the other is of size S. Then, the owner may choose to number the large one as table 1, and the small one as table 2. The decision on the numbering can be modeled as $\theta \in \{1, 2\}$, while the table size functions $R_1(\theta)$ and $R_2(\theta)$ are given as $R_1(1) = L$, $R_1(2) = S$, and $R_2(1) = S$, $R_2(2) = L$. Let Θ be the set of all possible state of the restaurant. In this example, $\Theta = \{1, 2\}$.

6.2.1 Chinese Restaurant Game

We formulate the table selection problem as a game, called **Chinese Restaurant Game**. We first denote $\mathcal{X} = \{1, ..., J\}$ as the action set (tables) that a customer may choose, where $x_i \in \mathcal{X}$ means that customer i chooses the table x_i for a seat. Then, the utility function of customer i is given by $U(R_{x_i}, n_{x_i})$, where n_{x_i} is the number of customers choosing table x_i. According to our previous discussion, the utility function should be an increasing function of R_{x_i}, and a decreasing function of n_{x_i}. Note that the decreasing character-

istic of $U(R_{x_i}, n_{x_i})$ over n_{x_i} can be regarded as the negative network externality effect since the degradation of the utility is due to the joining of other customers. Finally, let $\mathbf{n} = (n_1, n_2, ..., n_J)$ be the numbers of customers on the J tables, i.e., the **grouping** of customers in the restaurant.

As mentioned above, the restaurant is in a state $\theta \in \Theta$. However, customers may not know the exact state θ, i.e., they may not know the exact size of each table before requesting. Instead, they may have received some advertisements or gathered some reviews about the restaurant. The information can be treated as some kinds of signals related to the true state of the restaurant. In such a case, they can estimate θ through the available information, i.e., the information they know and/or gather in the game process. Therefore, we assume that all customers know the prior distribution of the state information θ, which is denoted as $\mathbf{g_0} = \{g_{0,l}|g_{0,l} = Pr(\theta = l), \forall l \in \Theta\}$. The signal each customer received $s_i \in \mathcal{S}$ is generated from a predefined distribution $f(s|\theta)$. Notice that the signal quality may vary, depending on how accurate the signal can reflect the state. A simple example is given as follows. Considering a signal space $\mathcal{S} = \{1, 2\}$ and the system state space $\Theta = \{1, 2\}$. Then, we define the signal distribution as follows:

$$Pr(s = \theta|\theta) = p \, , \; Pr(s \neq \theta|\theta) = 1 - p, \; 0.5 \leq p \leq 1. \tag{6.1}$$

In such a case, the parameter p is the signal quality of this signal distribution. When p is higher, the signal is more likely to reflect the true system state.

6.2.2 Belief on System State

We introduce **belief**, which is well-known in the Bayesian game literature [83], to describe how a customer estimates the system state θ. Since customers make decisions sequentially, it is possible that the customers who make decisions later learn the signals from those customers who make decisions earlier. Let us denote the signals customer i learned, excluding his own signal s_i, as $\mathbf{h_i} = \{s\}$. With the help of these signals $\mathbf{h_i}$, his own signal s_i, the prior distribution $\mathbf{g_0}$, and the conditional distribution $f(s|\theta)$, each

customer i can estimate the current system state in probability with the belief being defined as

$$\mathbf{g_i} = \{g_{i,l} | g_{i,l} = Pr(\theta = l | \mathbf{h_i}, s_i, \mathbf{g_0}), \ \forall l \in \Theta\} \ \forall i \in N. \tag{6.2}$$

According to the above definition, $g_{i,l}$ represents the probability that system state θ is equal to l conditioning on the collected signals $\mathbf{h_i}$, received signal s_i, the prior probability $\mathbf{g_0}$, and the conditional distribution $f(s|\theta)$. Notice that in the social learning literature, the belief can be obtained through either non-Bayesian updating rule [81, 82] or fully rational Bayesian rule [83]. For the non-Bayesian updating rule, it is implicitly based on the assumption that customers are only limited rational and follows some predefined rules to compute their believes. Their capability to maximize their utilities is limited not only by the game structure and learned information, but also by the non-Bayesian updating rules. In the fully rational Bayesian rule, customers are fully rational and have the potential to optimize their actions without the restriction on the fixed belief updating rule. Since the customers we considered here are fully rational, they will follow the Bayesian rule to update their believes as follows:

$$g_{i,l} = \frac{g_{0,l} Pr(\mathbf{h_i}, s_i | \theta = l)}{\sum_{l' \in \Theta} g_{0,l'} Pr(\mathbf{h_i}, s_i | \theta = l')}. \tag{6.3}$$

Notice that the exact expression for belief depends on how the signals are generated and learned, which is generally affected by the conditional distribution $f(s|\theta)$ and the game structure.

6.3 Perfect Signal: Advantage of Playing First

We first study the perfect signal case, where the system state θ is known by all customers. Let us consider a Chinese restaurant game with J tables and N customers. Since θ is known, the exact sizes of tables $R_1(\theta), R_2(\theta), ..., R_J(\theta)$ are also known by customers.

In Chinese restaurant game, customers make decisions sequentially with a predetermined order known by all customers, e.g., waiting in a line of the queue outside of the

restaurant. Without loss of generality, in the rest of this chapter, we assume the order is the same as the customer's number. We assume every customer knows the decisions of the customers who make decisions before him, i.e., customer i knows the decisions of customers $\{1, ..., i-1\}$. Let $\mathbf{n_i} = (n_{i,1}, n_{i,2}, ..., n_{i,J})$ be the current grouping, i.e., the number of customers choosing table $\{1, 2, ..., J\}$ before customer i. The $\mathbf{n_i}$ roughly represents how crowded each tables is when customer i enters the restaurant. Notice that $\mathbf{n_i}$ will not be equal to $\mathbf{n}$, which is the final grouping that determines customers' utilities. A table with only few customers may eventually be chosen by many customers in the end.

A strategy describes how a player will play given any possible situation in the game. In Chinese restaurant game, the customer's strategy should be a mapping from other customers' table selections to his own table selection. Recalling that n_j stands for the number of customers choosing table j. Let us denote $\mathbf{n_{-i}} = (n_{-i,1}, n_{-i,2}, ..., n_{-i,J})$ with $n_{-i,j}$ being the number of customers except customer i choosing table j. Then, given $\mathbf{n_{-i}}$, the best response of a rational customer i should be

$$BE_i(\mathbf{n_{-i}}, \theta) = \arg\max_{x \in \mathcal{X}} U(R_x(\theta), n_{-i,x} + 1). \tag{6.4}$$

Notice that given $\mathbf{n_{-i}}$, $n_j = n_{-i,j} + 1$ if $x = j$. However, the $\mathbf{n_{-i}}$ may not be completely observable by customer i since customers $i + 1 \sim N$ make decisions after customer i. Therefore, as shown in the next subsection, customer i should predict the decisions of the subsequent customers given the current observation $\mathbf{n_i}$ and state θ.

6.3.1 Equilibrium Grouping

We first study the possible equilibria of Chinese restaurant game. Nash equilibrium is a popular concept for predicting the outcome of a game with rational customers. Informally speaking, Nash equilibrium is an action profile, where each customer's action is the best response to other customers' actions in the profile. Since all customers use their best responses, none of them have the incentive to deviate from their actions. We observe that in Chinese restaurant game, the Nash equilibrium can be translated into the equilibrium

grouping, which is defined as follows
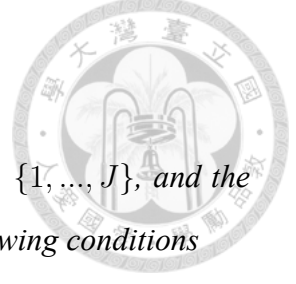
Definition 14. *Given the customer set $\{1, ..., N\}$, the table set $\mathcal{X} = \{1, ..., J\}$, and the current system state θ, an **equilibrium grouping** $\mathbf{n}^*$ satisfies the following conditions*

$$U(R_x(\theta), n_x^*) \geq U(R_y(\theta), n_y^* + 1), \; if \; n_x^* > 0, \forall x, y \in \mathcal{X}. \qquad (6.5)$$

Obviously, there will be more than one Nash equilibrium since we can always exchange the actions of any two customers in one Nash equilibrium to build a new Nash equilibrium without violating the sufficient and necessary condition shown in (6.5). Nevertheless, the equilibrium grouping $\mathbf{n}^*$ may be unique even if there exist multiple Nash equilibria. The sufficient condition to guarantee the uniqueness of equilibrium grouping is stated in the following Theorem.

Theorem 15. *If the inequality in (6.5) strictly holds for all $x, y \in \mathcal{X}$, then the equilibrium grouping $\mathbf{n}^* = (n_1^*, ..., n_J^*)$ is unique.*

Proof. We would like to prove this by contradiction. Suppose that there exists another Nash equilibrium with equilibrium grouping $\mathbf{n}' = (n_1', ..., n_J')$, where $n_j' \neq n_j^*$ for some $j \in \mathcal{X}$. Since both $\mathbf{n}^*$ and $\mathbf{n}'$ are equilibrium groupings, we have $\sum_{j=1}^{J} n_j' = \sum_{j=1}^{J} n_j^* = N$. In such a case, there exists two tables x and y with $n_x' > n_x^*$ and $n_y' < n_y^*$. Then, since $\mathbf{n}^*$ is an equilibrium grouping, we have

$$U(R_y(\theta), n_y^*) > U(R_x(\theta), n_x^* + 1). \qquad (6.6)$$

Since $n_x' > n_x^*$, $n_y' < n_y^*$, and $U(\cdot)$ is a deceasing function of n, we have

$$U(R_x(\theta), n_x^*) > U(R_x(\theta), n_x^* + 1) \geq U(R_x(\theta), n_x'), \qquad (6.7)$$

$$U(R_y(\theta), n_y') > U(R_y(\theta), n_y' + 1) \geq U(R_y(\theta), n_y^*). \qquad (6.8)$$

Since $\mathbf{n}'$ is also an equilibrium grouping, we have

$$U(R_x(\theta), n'_x) \geq U(R_y(\theta), n'_y + 1). \qquad (6.9)$$

According to (6.7), (6.8), and (6.9) we have

$$U(R_x(\theta), n^*_x + 1) \geq U(R_x(\theta), n'_x) \geq U(R_y(\theta), n'_y + 1) \geq U(R_y(\theta), n^*_y), (6.10)$$

which contradicts with (6.6). Therefore, the equilibrium grouping $\mathbf{n}^*$ is unique when the inequality in (6.5) strictly holds. $\qquad \square$

A concrete example that the equilibrium grouping is and is not unique is as follows. Consider a Chinese restaurant with 3 customers and 2 tables with size R_1 and R_2. When $R_1 = R_2$, we have two equilibrium grouping, which are $\mathbf{n^1} = (1, 2)$ and $\mathbf{n^2} = (2, 1)$. The equilibrium grouping is not unique in this case is because the inequality in (6.5) does not strictly hold, which means that one customer may have the same utility if he choose another table given the decisions of others. In contrast, when $R_1 > R_2$ and $U(R_1, 3) < U(R_2, 1)$, we have a unique equilibrium grouping $\mathbf{n^3} = (2, 1)$ since all other grouping cannot be the equilibrium output as we proved in Theorem 15.

The equilibrium grouping can be found through a simple greedy algorithm. In the algorithm, customers choose their actions in the myopic way, i.e., they choose the tables that can maximize their current utilities purely based on what they have observed. Let $\mathbf{n_i} = (n_{i,1}, n_{i,2}, ..., n_{i,J})$ with $\sum_{j=1}^{J} n_{i,j} = i - 1$ be the grouping observed by customer i. Then, customer i will choose the myopic action given by

$$BE_i^{myopic}(\mathbf{n_i}, \theta) = \arg\max_{x \in \mathcal{X}} U(R_x(\theta), n_{i,x} + 1). \qquad (6.11)$$

We check if the greedy algorithm indeed outputs an equilibrium grouping. Let $\mathbf{n}^* = (n^*_1, n^*_2, ..., n^*_J)$ be the corresponding grouping. For a table j with $n^*_j > 0$, suppose cus-

160

tomer k is the last customer choosing table j. According to (6.11), we have

$$U(R_j(\theta), n_{k,j} + 1) \geq U(R_{j'}(\theta), n_{k,j'} + 1) \geq U(R_{j'}(\theta), n_{j'}^* + 1), \forall j' \in \mathcal{X}. \quad (6.12)$$

Note that (6.12) holds for all $j, j' \in \mathcal{X}$ with $n_j^* > 0$, i.e., $U(R_j(\theta), n_j^*) \geq U(R_{j'}(\theta), n_{j'}^* + 1)$, $\forall j, j' \in \mathcal{X}$ with $n_j^* > 0$. According to Definition 14, the output grouping $\mathbf{n}^*$ from the greedy algorithm is an equilibrium grouping.

6.3.2 Subgame Perfect Nash Equilibrium

In a sequential game, we will study the subgame perfect Nash equilibrium. Subgame perfect Nash equilibrium is a popular refinement to the Nash equilibrium under the sequential game. It guarantees that all players choose strategies rationally in every possible subgame. A subgame is a part of the original game. In Chinese restaurant game, any game process begins from player i, given all possible actions before player i, could be a subgame.

Definition 15. *A subgame in Chinese restaurant game is consisted of two elements: 1) It begins from customer i; 2) The current grouping before customer i is $\mathbf{n_i} = (n_{i,1}, ..., n_{i,J})$ with $\sum_{j=1}^{J} n_{i,j} = i - 1$.*

Definition 16. *A Nash equilibrium is a subgame perfect Nash equilibrium if and only if it is a Nash equilibrium for any subgame.*

We would like to show the existence of subgame perfect Nash equilibrium in Chinese restaurant game by constructing one. Basically, as a rational customer, customer i should predict the final equilibrium grouping according to his current observation on the choices of previous customers $\mathbf{n_i}$ and the system state θ. Then, he may choose the table with highest expected utility according to the prediction. Following from this idea, we derive the best response of customers in a subgame.

We first implement the prediction part through two functions as follows. First, let $EG(\mathcal{X}^s, N^s)$ be the function that generates the equilibrium grouping for a table set $\mathcal{X}^s$ and number of customers N^s. The equilibrium grouping is generated by the greedy algorithm

shown in previous section with $\mathfrak{X}$ being replaced by $\mathfrak{X}^s$ and N being replaced by N^s. Notice that $\mathfrak{X}^s$ could be any subset of the total table set $\mathfrak{X} = \{1, ..., J\}$, and N^s is less or equal to N.

Then, let $PC(\mathfrak{X}^s, \mathbf{n^s}, N^s)$, where $\mathbf{n^s}$ denotes the current grouping observed by the customer, be the algorithm that generates the set of available tables given $\mathbf{n^s}$ in the subgame. The algorithm removes the tables that already occupied by more than the expected number of customers in the equilibrium grouping. This helps the customer remove those unreasonable choices and correctly predict the final equilibrium grouping in every subgame. The basic flow of this algorithm is shown as follows 1) calculate the equilibrium grouping $\mathbf{n^e}$ given the table set $\mathfrak{X}^s$ and number of customers N^s, 2) check if there is any overly occupied table by comparing $\mathbf{n^s}$ with $\mathbf{n^e}$. If so, 3) remove these tables from $\mathfrak{X}^s$ and the customers occupying these tables from N^s, and go back to 1). Otherwise, the algorithm terminates. The procedures of implementing $PC(\mathfrak{X}^s, \mathbf{n^s}, N^s)$ are described as follows:

1. Initialize: $\mathfrak{X}^o = \mathfrak{X}^s$, $N^t = N^s$

2. $\mathfrak{X}^t = \mathfrak{X}^o$, $\mathbf{n^e} = EG(\mathfrak{X}^t, N^t)$, $\mathfrak{X}^o = \{x | x \in \mathfrak{X}^t, n_j^e \geq n_j^s\}$, $N^t = N^s - \sum_{x \in \mathfrak{X}^s \setminus \mathfrak{X}^o} n_x^s$.

3. If $\mathfrak{X}^o \neq \mathfrak{X}^t$, go back to step 2.

4. Output $\mathfrak{X}^o$.

Now, we propose a method to construct a subgame perfect Nash equilibrium. This equilibrium also satisfies (6.5). For each customer i, his strategy in a subgame is

$$BE_i^{se}(\mathbf{n_i}, \theta) = \arg \max_{x \in \mathfrak{X}^{i,cand}, n_{i,x} < n_x^{i,cand}} U(R_x(\theta), n_x^{i,cand}), \qquad (6.13)$$

where $\mathfrak{X}^{i,cand} = PC(\mathfrak{X}, \mathbf{n_i}, N)$, $N^{i,cand} = N - \sum_{x \in \mathfrak{X} \setminus \mathfrak{X}^{i,cand}} n_{i,x}$, and $\mathbf{n^{i,cand}} = EG(\mathfrak{X}^{i,cand}, N^{i,cand})$. The proposed best response $BE_i^{se*}(\mathbf{n_i}, \theta)$ chooses the table with the highest utility according to the predicted equilibrium grouping $\mathbf{n^{i,cand}}$ and candidate table set $\mathfrak{X}^{i,cand}$. The equilibrium grouping $\mathbf{n^{i,cand}}$ is obtained by $EG(\mathfrak{X}^{i,cand}, N^{i,cand})$, where the candidate table set $\mathfrak{X}^{i,cand}$ is derived by $PC(\mathfrak{X}, \mathbf{n_i}, N)$. In Lemma 6, we show that the above strategy results in the equilibrium grouping in any subgame.

Lemma 6. *Given the available table set* $\mathcal{X}^s = PC(\mathcal{X}, \mathbf{n^s}, N)$, $N^s = N - \sum_{x \in \mathcal{X} \setminus \mathcal{X}^s} n_x^s$, *the proposed strategy shown in (6.13) leads to an equilibrium grouping* $\mathbf{n}^* = EG(\mathcal{X}^s, N^s)$ *over* $\mathcal{X}^s$.

Proof. We prove this by contradiction. Let $\mathbf{n} = (n_j | j \in \mathcal{X}^s)$ be the final grouping after all customers choose their tables according to (6.13). Suppose that $\mathbf{n} \neq \mathbf{n}^* = EG(\mathcal{X}^s, N^s)$, then there exists some tables j that $n_j > n_j^*$. Let table j be the first table that exceeds n_j^s in this sequential subgame. Since $n_j > n_j^*$, there are at least $n_j^* + 1$ customers choosing table j. Suppose the $n_j^* + 1$-th customer choosing table j is customer i. Let $\mathbf{n_i} = (n_{i,1}, n_{i,2}, ..., n_{i,J})$ be the current grouping observed by customer i before he chooses the table. Since customer i is the $n_j^* + 1$-th customer choosing table j, we have $n_{i,j} = n_j^*$. Since table j is the first table exceeding $\mathbf{n}^*$ after customer i's choice, we have $n_{i,x} \leq n_x^* \ \forall x \in \mathcal{X}^s$.

According to the definition of $PC(\cdot)$, none of the tables will be removed from candidates. Thus, $\mathcal{X}^{i,cand} = \mathcal{X}^s$ and $N^{i,cand} = N^s$. We have

$$\mathbf{n^{i,cand}} = EG(\mathcal{X}^{i,cand}, N^{i,cand}) = EG(\mathcal{X}^s, N^s) = \mathbf{n}^*. \tag{6.14}$$

However, according to (6.13), the customer i should not choose table j since $n_{i,j} = n_j^* = n_j^{i,cand}$. This contradicts with our assumption that customer i is the n_j^*+1-th customer choosing table j. Thus, the strategy (6.13) should lead to the equilibrium grouping $\mathbf{n}^* = EG(\mathcal{X}^s, N^s)$. $\square$

Note that Lemma 6 also shows that the final grouping of the sequential game should be $\mathbf{n}^* = EG(\mathcal{X}, N)$ if all customers follow the proposed strategy in (6.13). In the following Lemma, we show that $PC(\mathcal{X}^s, \mathbf{n^s}, N^s)$ removes the tables that are dominated by other tables if all customers follow (6.13).

Lemma 7. *Given a subgame with current grouping* $\mathbf{n^s}$, *if table* $j \notin \mathcal{X}^s = PC(\mathcal{X}, \mathbf{n^s}, N)$, *then table* j *is never the best response of the customer if all other customers follow (6.13).*

Proof. Let $\mathbf{n}' = EG(\mathcal{X}, N)$, and $\mathbf{n}^*$ be the final grouping. We first show that for every table under the final grouping $\mathbf{n}^*$, there always exists a table providing a less or equal utility

under the grouping $\mathbf{n}'$. According to Lemma 6, the final grouping $\mathbf{n}^*$ is an equilibrium grouping over $\mathcal{X}^s$ if all customers follow (6.13). Additionally, $n_j^* = n_j^s$ since no customers will choose table j. Assuming that there exists a table $k \in \mathcal{X}^s$ with $n_k' < n_k^*$. Since $n_j^* = n_j^s > n_j'$, we have $\sum_{x \in \mathcal{X} \setminus \{j\}} n_x^* < \sum_{x \in \mathcal{X} \setminus \{j\}} n_x'$. Therefore, $\exists k' \in \mathcal{X}^s$ that $n_{k'}' > n_{k'}^*$. Since $\mathbf{n}'$ and $\mathbf{n}^*$ are equilibrium groupings over $\mathcal{X}^s$, similar to (6.10), we have

$$U(R_k(\theta), n_k' + 1) \geq U(R_k(\theta), n_k^*) \geq U(R_{k'}(\theta), n_{k'}^* + 1) \geq U(R_{k'}(\theta), n_{k'}') \geq U(R_k(\theta), n_k' + 1) \tag{6.15}$$

The first and third inequalities are due to $n_k' < n_k^*$ and $n_{k'}' > n_{k'}^*$, and the second and fourth ones come from the equilibrium grouping condition in (6.5). The equation is valid only when all equalities hold. Thus, if $n_k' < n_k^*$, $\exists k' \in \mathcal{X}^s$ that $U(R_k(\theta), n_k^*) = U(R_{k'}(\theta), n_{k'}')$, which means that we can always find a table k' providing the same utility as $U(R_k(\theta), n_k^*)$ under grouping $\mathbf{n}'$. When $n_k' \geq n_k^*$, we have $U(R_k(\theta), n_k^*) \geq U(R_k(\theta), n_k')$. Therefore, $\forall k \in \mathcal{X}^s$, $\exists k' \in \mathcal{X}^s$ that $U(R_k(\theta), n_k^*) \geq U(R_{k'}(\theta), n_{k'}')$.

Then, we show that table j is dominated by all other tables under $\mathbf{n}^*$. Since table j is removed by $PC(\mathcal{X}, \mathbf{n}^s, N)$, we have $n_j^s > n_j'$. Therefore, according the above discussion and the fact that $\mathbf{n}'$ is an equilibrium grouping, we have $\forall k \in \mathcal{X}^s$,

$$U(R_k(\theta), n_k^*) \geq \min_{k' \in \mathcal{X}^s} U(R_{k'}(\theta), n_{k'}') \geq U(R_j(\theta), n_j' + 1) > U(R_j(\theta), n_j^s + 1). \tag{6.16}$$

Since $U(R_j(\theta), n_j^s + 1)$ is the highest utility that can be offered by table j, it is dominated by all other tables in $\mathcal{X}^s$ under the final grouping $\mathbf{n}^*$. So, table j is never the best response of the customer. $\qquad\square$

Theorem 16. *There always exists a subgame perfect Nash equilibrium with the corresponding equilibrium grouping $\mathbf{n}^*$ satisfying (6.5) in a sequential Chinese restaurant game.*

Proof. We would like to show that the proposed strategy in (6.13) forms a Nash equilibrium. Suppose customer i chooses table j in his round according to (6.13). Then, customer i's utility is $u_i = U(R_j(\theta), n_j^*)$ since based on Lemma 6, the equilibrium grouping $\mathbf{n}^*$ will be reached at the end.

Now we show that table j is indeed customer i's best response. Let's assume that customer i is the last customer, i.e, $i = N$, and chooses another table $j' \neq j$ in his round, then his utility becomes $U(R_{j'}(\theta), n_{j'}^* + 1)$. However, according to (6.5), we have

$$u_j^* = U(R_j(\theta), n_j^*) \geq U(R_{j'}(\theta), n_{j'}^* + 1). \tag{6.17}$$

Thus, choosing table j is never worse than choosing table j' for customer N.

For the case that customer i is not the last customer, we assume that he chooses table j' instead of table j in his round. Since all customers before customer i follows (6.13), we have $n_{i,j} \leq n_j^* \ \forall j \in \mathcal{X}$. Otherwise, $\mathbf{n}^*$ cannot be reached, which contradicts with Lemma 6.

If $n_{i,j'} < n_{j'}^*$, we have $n_{i+1,j'} \leq n_{j'}^*$. In addition, we have $n_{i+1,j} = n_{i,j} \leq n_j^* \ \forall j \in \mathcal{X} \setminus \{j'\}$, since other tables are not chosen by customer i. Thus, $\mathcal{X}^{i+1,cand} = PC(\mathcal{X}, \mathbf{n_{i+1}}, N)$ and $N^{i,cand} = N$. According to Lemma 6, the final grouping should be $\mathbf{n}^* = EG(\mathcal{X}, N)$. Thus, the new utility of customer i becomes $u_i' = U(R_{j'}(\theta), n_{j'}^*)$. However, according to (6.13), we have

$$u_i = U(R_j(\theta), n_j^*) = \arg\max_{x \in \mathcal{X}, n_{i,x} < n_x^*} U(R_x(\theta), n_x^*) \geq U(R_{j'}(\theta), n_{j'}^*) = u_i'. \tag{6.18}$$

Thus, choosing table j' never gives customer i a higher utility.

If $n_{i,j'} = n_{j'}^*$, and the final grouping is $\mathbf{n}' = (n_1', n_2', ..., n_J')$. Since customer i chooses table j' when $n_{i,j'} = n_{j'}^*$, we have $n_{j'}' \geq n_{i+1,j'} = n_{i,j'} + 1 = n_{j'}^* + 1$. Thus, we have

$$u_i = U(R_j(\theta), n_j^*) \geq U(R_{j'}(\theta), n_{j'}^* + 1) \geq U(R_{j'}(\theta), n_{j'}') = u_i', \ \forall j' \in X, \tag{6.19}$$

where the first inequality comes from the equilibrium grouping condition in (6.5), and the second inequality comes from the fact that $U(R, n)$ is decreasing over n and $n_{j'}' \geq n_{j'}^* + 1$. Thus, under both cases, choosing table j' is never better than choosing table j. We conclude that $\{BE_i^{se}(\cdot)\}$ in (6.13) forms a Nash equilibrium, where the grouping being the equilibrium grouping $\mathbf{n}^*$.

Finally, we show that the proposed strategy forms a Nash equilibrium in every subgame. In Lemma 7, we show that if the table j is removed by $PC(\mathfrak{X}, \mathbf{n^s}, N)$, it is never the best response of all remaining customers. Thus, we only need to consider the remaining table candidates $\mathfrak{X}^s = PC(\mathfrak{X}, \mathbf{n^s}, N)$ in the subgame. Then, with Lemma 6, we show that for every possible subgame with corresponding $\mathfrak{X}^s$, the equilibrium grouping $\mathbf{n}^* = EG(\mathfrak{X}^s, N^s)$ will be achieved at the end of the subgame. Moreover, the above proof shows that if the equilibrium grouping $\mathbf{n^s}$ will be achieved at the end of the subgame, $BE_i^{se}(\cdot)$ is the best response function. Therefore, the proposed strategy forms a Nash equilibrium in every subgame, i.e., we have a subgame perfect Nash equilibrium. $\qquad\square$

In the proof of Theorem 16, we observe that the sequential game structure brings advantages for those customers making decisions early. According to (6.13), customers who make decisions early can choose the table providing the largest utility in the equilibrium. When the number of customers choosing that table reaches equilibrium number, the second best table will be chosen until it is full again. For the last customer, he has no choice but to choose the worst one.

6.4 Imperfect Signal: How Learning Evolves

In Section 6.3, we have showed that in the Chinese restaurant game with perfect signal, customers choosing first have the advantages for getting better tables and thus higher utilities. However, such a conclusion may not be true when the signals are not perfect. When there are uncertainties on the table sizes, customers who arrive first may not choose the right tables, due to which their utilities may be lower. Instead, customers who arrive later may eventually have better chances to get better tables since they can collect more information to make the right decisions. In other words, when signals are not perfect, learning will occur and may result in higher utilities for customers choosing later. Therefore, there is a trade-off between more choices when playing first and more accurate signals when playing later. In this section, we would like to study this trade-off by discussing the imperfect signal model.

In the imperfect signal model, we assume that the system state $\theta \in \Theta = \{1, 2, ..., L\}$ is unknown to all N customers. The sizes of J tables can be expressed as functions of θ, which are denoted as $R_1(\theta), R_2(\theta), ..., R_J(\theta)$. The prior probability of θ, $\mathbf{g_0} = \{g_{0,1}, g_{0,2}, ..., g_{0,J}\}$ with $g_{0,l} = Pr(\theta = l)$, is assumed to be known by all customers. Moreover, each customer receives a private signal $s_i \in \mathcal{S}$, which follows a p.d.f $f(s|\theta)$. Here, we assume $f(s|\theta)$ is public information to all customers. When conditioning on the system state θ, the signals received by the customers are uncorrelated.

In Chinese restaurant game with imperfect signal model, the customers make decisions sequentially with the decision orders being their numbers. After a customer i made his decision, he cannot change his mind in any subsequent time and his decision and signal are revealed to all other customers. Since signals are revealed sequentially, the customers who make decisions later can collect more information for better estimations of the system state. We assume customers are fully rational, which means they should apply Bayesian learning rule in their decision making process [83]. Therefore, when a new signal is revealed, all customers follow the Bayesian rule to update their believes based on their current believes. Derived from (6.3), we have the following belief updating function

$$g_{i,l} = \frac{g_{i-1,l} f(s_i|\theta = l)}{\sum_{w \in \Theta} g_{i-1,w} f(s_i|\theta = w)}. \tag{6.20}$$

6.4.1 Best Response of Customers

Since the customers are rational, they will choose the action to maximize their own expected utility conditioning on the information they collect. Let $\mathbf{n_i} = (n_{i,1}, n_{i,2}, ..., n_{i,J})$ be the current grouping observed by customer i before he chooses the table, where $n_{i,j}$ is the number of customers choosing table j before customer i. Then, let $\mathbf{h_i} = \{s_1, s_2, ..., s_{i-1}\}$ be the history of revealed signals before customer i. In such a case, the best response of customer i can be written as

$$BE_i(\mathbf{n_i}, \mathbf{h_i}, s_i) = \arg \max_j \mathbb{E}[U(R_j(\theta), n_j)|\mathbf{n_i}, \mathbf{h_i}, s_i]. \tag{6.21}$$

From (6.21), we can see that when estimating the expected utility in the best response function, there are two key terms needed to be estimated by the customer: the system state θ and the final grouping $\mathbf{n} = (n_1, n_2, ..., n_J)$. The system state θ is estimated using the concept of belief denoted as $\mathbf{g_i} = \{g_{i,1}, g_{i,2}, ..., g_{i,L}\}$ with $g_{i,l} = Pr(\theta = l | \mathbf{h_i}, s_i)$. Since the information on the system state θ in $\mathbf{n_i}$ is fully revealed by $\mathbf{h_i}$, given $\mathbf{h_i}$, $\mathbf{g_i}$ is independent with $\mathbf{n_i}$. Therefore, given the customer's belief $\mathbf{g_i}$, the expected utility of customer i choosing table j becomes

$$\mathbb{E}[U(R_j(\theta), n_j) | \mathbf{n_i}, \mathbf{h_i}, s_i, x_i = j] = \sum_{w \in \Theta} g_{i,w} \mathbb{E}[U(R_j(w), n_j) | \mathbf{n_i}, \mathbf{h_i}, s_i, x_i = j, \theta] \quad (6.22)$$

Note that the decisions of customers $i + 1, ..., N$ are unknown to customer i when customer i makes the decision. Therefore, a close-form solution to (6.22) is generally impossible and impractical. In this chapter, we purpose a recursive approach to compute the expected utility.

6.4.2 Recursive Form of Best Response

Let $BE_{i+1}(\mathbf{n_{i+1}}, h_{i+1}, s_{i+1})$ be the best response function of customer $i+1$. Then, the signal space $\mathcal{S}$ can be partitioned into $\mathcal{S}_{i+1,1}, ..., \mathcal{S}_{i+1,J}$ subspaces with

$$\mathcal{S}_{i+1,j}(\mathbf{n_{i+1}}, \mathbf{h_{i+1}}) \quad (6.23)$$
$$= \{s | s \in \mathcal{S}, BE_{i+1}(\mathbf{n_{i+1}}, \mathbf{h_{i+1}}, s) = j\}, \forall j \in \{1, ..., J\}.$$

Based on (6.23), we can see that, given $\mathbf{n_{i+1}}$ and $\mathbf{h_{i+1}}$, $BE_{i+1}(\mathbf{n_{i+1}}, \mathbf{h_{i+1}}, s_{i+1}) = j$ if and only if $s_{i+1} \in \mathcal{S}_{i+1,j}$. Therefore, the decision of customer $i + 1$ can be predicted according to the signal distribution $f(s | \theta)$ given by

$$Pr(x_{i+1} = j | \mathbf{n_{i+1}}, \mathbf{h_{i+1}}) = \int_{s \in \mathcal{S}_{i+1,j}(\mathbf{n_{i+1}}, \mathbf{h_{i+1}})} f(s)ds. \quad (6.24)$$

Let us define $m_{i,j}$ as the number of customers choosing table j after customer i (including customer i himself). Then, we have $n_j = n_{i,j} + m_{i,j}$, where n_j denotes the final

number of customers choosing table j at the end of the game. Moreover, according to the definition of $m_{i,j}$, we have

$$m_{i,j} = \begin{cases} 1 + m_{i+1,j}, & x_i = j; \\ m_{i+1,j}, & \text{else.} \end{cases}$$
(6.25)

The recursive relation of $m_{i,j}$ in (6.25) will be used in the following to get the recursive form of the best response function. We first derive the recursive form of the distribution of $m_{i,j}$, i.e., $Pr(m_{i,j} = X | \mathbf{n_i}, \mathbf{h_i}, s_i, x_i, \theta)$ can be expressed as a function of $Pr(m_{i+1,j} = X | \mathbf{n_{i+1}}, \mathbf{h_{i+1}}, s_{i+1}, x_{i+1} = j, \theta = l)$, $\forall l \in \Theta$, $0 \leq j \leq J$, as follows:

$$Pr(m_{i,j} = X | \mathbf{n_i}, \mathbf{h_i}, s_i, x_i, \theta = l) = \begin{cases} Pr(m_{i+1,j} = X-1 | \mathbf{n_i}, \mathbf{h_i}, s_i, x_i, \theta = l), & x_i = j, \\ Pr(m_{i+1,j} = X | \mathbf{n_i}, \mathbf{h_i}, s_i, x_i, \theta = l), & x_i \neq j, \end{cases}$$
(6.26)

$$= \begin{cases} \sum_{u \in \{1,\ldots,J\}} \int_{s \in \mathcal{S}_{i+1,u}(\mathbf{n_{i+1}}, \mathbf{h_{i+1}})} Pr(m_{i+1,j} = X-1 | \mathbf{n_{i+1}}, \mathbf{h_{i+1}}, s_{i+1} = s, x_{i+1} = u, \theta = l) f(s | \theta = l) ds, & x_i = j, \\ \sum_{u \in \{1,\ldots,J\}} \int_{s \in \mathcal{S}_{i+1,u}(\mathbf{n_{i+1}}, \mathbf{h_{i+1}})} Pr(m_{i+1,j} = X | \mathbf{n_{i+1}}, \mathbf{h_{i+1}}, s_{i+1} = s, x_{i+1} = u, \theta = l) f(s | \theta = l) ds, & x_i \neq j, \end{cases}$$

where $\mathbf{h_{i+1}}$ and $\mathbf{n_{i+1}}$ can be obtained using

$$\mathbf{h_{i+1}} = \{h_i, s_i\} \text{ and } \mathbf{n_{i+1}} = (n_{i+1,1}, \ldots, n_{i+1,J}),$$
(6.27)

with

$$n_{i+1,k} = \begin{cases} n_{i,k} + 1, & \text{if } x_i = k, \\ n_{i,k}, & \text{otherwise.} \end{cases}$$
(6.28)

Based on (6.26), $Pr(m_{i,j} = X | \mathbf{n_i}, \mathbf{h_i}, s_i, x_i, \theta = l)$ can be recursively calculated. Therefore, we can calculate the expected utility $\mathbb{E}[U(R_j(\theta), n_j) | \mathbf{n_i}, \mathbf{h_i}, s_i]$ by

$$\mathbb{E}[U(R_j(\theta), n_j) | \mathbf{n_i}, \mathbf{h_i}, s_i] = \sum_{l \in \Theta} \sum_{x=0}^{N-i+1} g_{i,l} Pr(m_{i,j} = x | \mathbf{n_i}, \mathbf{h_i}, s_i, x_i = j, \theta = l) U(R_j(l), n_{i,j}+x).$$
(6.29)

Finally, the best response function of customer i can be derived by

$$BE_i(\mathbf{n_i}, \mathbf{h_i}, s_i) = \arg\max_j \sum_{l \in \Theta} \sum_{x=0}^{N-i+1} g_{i,l} Pr(m_{i,j} = x | \mathbf{n_i}, \mathbf{h_i}, s_i, x_i = j, \theta = l) U(R_j(l), n_{i,j}+x).$$
(6.30)

With the recursive form, the best response function of all customers can be obtained using backward induction. The best response function of the last customer N can be found

169

as

$$BE_N(\mathbf{n_N}, h_N, s_N) = \arg\max_j \sum_{l \in \Theta} g_{N,l} u_N(R_j(l), n_{N,j} + 1). \tag{6.31}$$

Note that $Pr(m_{N,j} = X | \mathbf{n_N}, \mathbf{h_N}, s_N, x_N, \theta)$ can be easily derived as follows:

$$Pr(m_{N,j} = 1 | \mathbf{n_N}, \mathbf{h_N}, s_N, x_N, \theta) = \begin{cases} 1, & \text{if } x_N = j, \\ 0, & \text{otherwise.} \end{cases} \tag{6.32}$$

As of the convergence of the recursive best response, which is based on the traditional backward induction technique, it definitely converges since this game has finite players. As a Chinese restaurant game with N players, only N recursive calls are required to derive all the best responses.

6.5   Simulation Results

In this section, we verify the proposed recursive best response and corresponding equilibrium. We simulate a Chinese restaurant with two tables $\{1, 2\}$ and two possible states $\theta \in \{1, 2\}$. When $\theta = 1$, the size of table 1 is $R_1(1) = 100$ and the size of table 2 is $R_2(1) = 100r$, where r is the ratio of table sizes. When $\theta = 2$, $R_1(2) = 100r$ and $R_2(2) = 100$. The state is randomly chosen with $Pr(\theta = 1) = Pr(\theta = 2) = 0.5$. The number of customers is fixed. Each customer receives a randomly generated signal s_i at the beginning of the simulation. The signal distribution $f(s|\theta)$ is given by $Pr(s = 1|\theta = 1) = Pr(s = 2|\theta = 2) = p$, $Pr(s = 2|\theta = 1) = Pr(s = 1|\theta = 2) = 1 - p$, where $p \geq 0.5$ can be regarded as the quality of signals. When the signal quality p is closer to 1, the signal is more likely to reflect the true state θ. With the signals, customers make their decisions sequentially. After the i-th customer makes his choice, he reveals his decision and signal to other customers. The game ends after the last customer made his decision. Then, the utility of the customer i choosing table j is given by $U(R_j(\theta), n_j) = \frac{R_j}{n_j}$, where n_j is the number of customers choosing table j in the end.
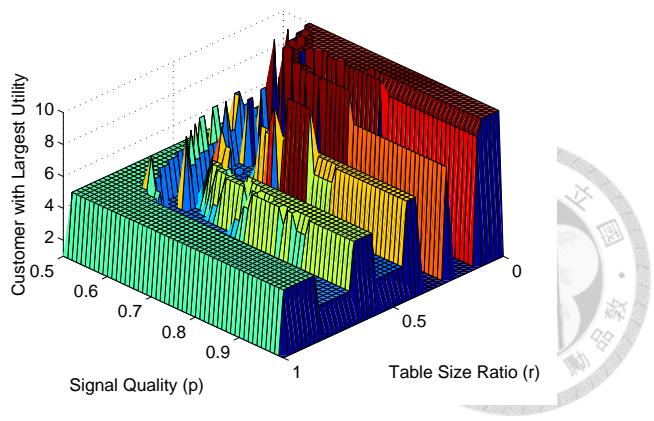
(a) 5 Customers
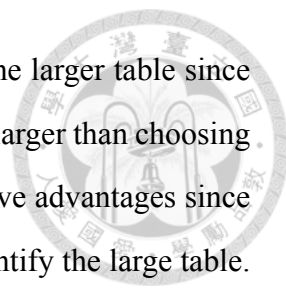
(b) 10 Customers

Figure 6.1: The effect of different Table Size Ratio and Signal Quality

6.5.1 Advantage of Playing Positions vs. Signal Quality

We first investigate how the decision order and quality of signals affect the utility of customers. We fix the size of one table as 100. The size of the other table is $r \times 100$, where r is the ratio of the table sizes. In the simulations, we assume the ratio $r \in [0, 1]$. When the ratio $r = 1$, two tables are identical, but the utility of choosing each table may have different utility since we may have odd customers. When $r = 0$, one table has a size of 0, which means a customer has a positive utility only when he chooses the correct table.

Due to the complicated game structure in Chinese restaurant game, the effect of signal quality and table size ratio is generally non-linear. As shown in Fig. 6.1(a), when the number of customers is 5, customer 5 has the largest utility when the signal quality is high and the table size ratio is low, while customer 1 has the largest utility when the signal quality is low and the table size ratio is high. This phenomenon can be explained

171

as follows. When the table size ratio is lower, all customers desire the larger table since even all of them select the larger one, each of them still have a utility larger than choosing the smaller one. In such a case, customers who choose late would have advantages since they have collected more signals and have a higher probability to identify the large table. Nevertheless, when the signal quality is low, even the last customer cannot form a strong belief on the true state. In such a case, the expected size of each table becomes less significantly, and customers' decisions rely more on the negative network externality effect, i.e., how crowded of each table. In such a case, the first customer has the advantage to choose the table with fewer customers in expectation.

However, we observe that in some cases, customer 3 becomes the one with largest utility. The reasons behind this phenomenon is as follows. In these cases, the expected number of customers in the larger table is 3, and this table provides the customers a larger utility at the equilibrium. Therefore, customers would try to identify this table and choose it according to their own believes. Since customer 3 collects more signals than customers 1 and 2, he is more likely to identify the correct table. Moreover, since he is the third customer, this table is always available to him. Therefore, customer 3 has the largest expected utility in these cases.

Note that the expected table size is determined by both the signal quality and the table size ratio. Generally, when the signal quality is low, a customer is less likely to construct a strong belief on the true state, i.e., the expected table sizes of both tables are similar. This suggests that a lower signal quality has a similar effect on the expected table size as a higher table size ratio. Our arguments are supported by the concentric-like structure shown in Fig. 6.1(a). The same arguments can be applied to the 10-customer scheme, which is shown in Fig. 6.1(b). We can observe the similar concentric-like structure. Additionally, we observe that when the table size ratio increases, the order of customer who has the largest utility in the peaks decreases from 10 to 5. This is consistent with our arguments since when the table size ratio increases, the equilibrium number of customers in the large table decreases from 10 to 5. This also explains why customer 1 does not have the largest utility when the table size ratio is high. In this case, the equilibrium number of customers

172
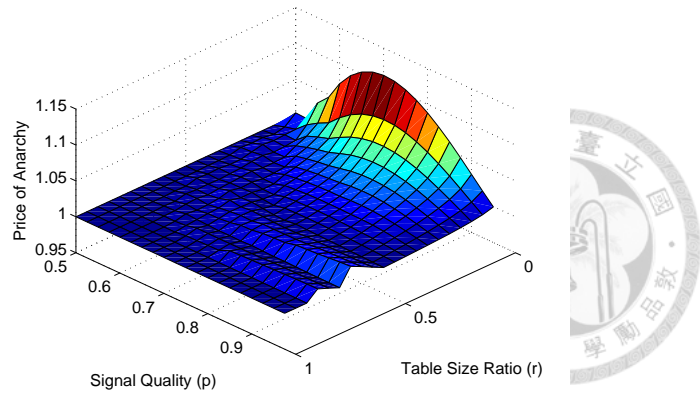
(a) $U(R,n) = R/n$

(b) $U(R,n) = log(\frac{R}{n+10})$

Figure 6.2: Price of Anarchy with Different Utility Functions

in the large table is 5, and the large table provides higher utilities to customers in the equilibrium. Since customer 5 can collect more signals than previous customers, he has better knowledge on the table size than customer 1 to 4. Moreover, since customer 5 is the fifth one to choose the table, he always has the opportunity to choose the large table. In such a case, customer 5 has the largest expected utility when the table size ratio is high.

6.5.2 Price of Anarchy

We then investigate the efficiency of the equilibrium grouping in Chinese restaurant game using price of anarchy, which is a popular measurement in game theory on the degradation of the system efficiency due to rational behaviors of players. Basically, the price of anarchy in a game-theoretic system is defined as the ratio of the social welfare under worst equilibrium in the system to the one under the centralized-optimal solution. There-

fore, when the price of anarchy is close or equal to 1, the rational behaviors generally do not incur efficiency loss to the system.

We first define the social welfare function $W(\mathbf{B})$ in Chinese restaurant game as the sum of customers expected utilities, that is, $W(\mathbf{B}) = \mathbb{E}[\sum_{i=1}^{N} U(R_{x_i}(\theta), n_{x_i})|\mathbf{B}]$, where $\mathbf{B}$ denotes the strategies of customers applied in Chinese restaurant game. Let $\mathcal{B}^{\mathcal{U}}$ be the universal set of all possible strategies and $\mathcal{B}^{\mathcal{E}}$ be the set of all equilibria in Chinese restaurant game, then the price of anarchy is defined as follows:

$$PoA = \frac{\max_{\mathbf{B} \in \mathcal{B}^{\mathcal{U}}} W(\mathbf{B})}{\min_{\mathbf{B}' \in \mathcal{B}^{\mathcal{E}}} W(\mathbf{B}')}. \tag{6.33}$$

We simulate a 5-customer restaurant with two tables and two states. All other settings are the same as the ones in Section 6.5.1 except the utility function. In this simulation, we apply two utilities functions: $U(R, n) = R/N$ and $U(R, n) = log(\frac{R}{n+10})$. The former represents the case that the resource is equally shared, while the latter roughly represents the SINR-throughput in wireless networks. The centralized-optimal solution is found through exhaustive search. The prices of anarchy under all combinations of signal quality and table size ratio are shown in Fig. 6.2.

As shown in Fig. 6.2(a), when the utility function is set as R/n, the price of anarchy is equal to one under most combinations except when the table size ratio is close to 0. The reason that the price of anarchy is larger than 1 at these points is that the smaller table is so small that all customers have a higher utility even sharing the larger one. In such cases, the small table will not be chosen, and the resource provided by this table is lost due to the rational behaviors of customers. For the scenario that the utility function is set as $U(R, n) = log(\frac{R}{n+10})$, the price of anarchy never exceeds 1.06 (Fig. 6.2(b)). This is because in such a scenario, a proper balance in loadings on tables will greatly increase the social welfare, which is automatically achieved by the rational choices of customers due to their concerns on negative network externality. Therefore, the rational behaviors in Chinese restaurant game generally does not harm much on the system efficiency, and the equilibrium we found is efficient even compared with the centralized-optimal solution.

(a) 5 Customers   (b) 3 Customers

Signals	Best Response	
s_1, s_2, s_3	$p = 0.9$	$p = 0.6$
2,2,2	2,2,1	1,2,2
1,2,2	1,2,2	2,1,2
2,1,2	2,1,2	1,2,2
1,1,2	1,1,2	2,1,1
2,2,1	2,2,1	1,2,2
1,2,1	1,2,1	2,1,1
2,1,1	2,1,1	1,2,1
1,1,1	1,1,2	2,1,1

(c) Best Response when N=3

Figure 6.3: Average utility of Customers in Resource Pool scenario when $r = 0.4$

6.5.3   Case Study: Resource Pool and Availability scenarios

Finally we discuss two specific scenarios: the resource pool scenario with $r = 0.4$ and available/unavailable scenarios with $r = 0$. In resource pool scenario, the table size of the second table is 40. Users act sequentially and rationally to choose these two tables to maximize their utilities. In available/unavailable scenario, the second table size is 0, which means that a customer has positive utility only when he chooses the right table. For both scenarios, we examine the schemes with $N = 3$ and $N = 5$.

From Fig. 6.3, we can see that in the resource pool scenario with $r = 0.4$, customer 1 on average has significant higher utility, which is consistent with the result in Fig. 6.1(a). Using 5-customer scheme shown in Fig. 6.3(a) as an example, the advantage of playing first becomes significant when signal quality is very low ($p < 0.6$), or the signal quality is high ($p > 0.7$). We also find that customer 5 has the lowest average utility for most signal quality p. We may have a clearer view on this in the 3-customer scheme. We list the best response of customers given the received signals in Fig. 6.3(c). We observe that when signal quality p is large, both customer 1 and 2 follow the signals they received to choose the tables. However, customer 3 does not follows his signal if the first two customers

175

(a) 5 Customers　　　　　　　(b) 3 Customers

Signals	Best Response		
s_1, s_2, s_3	$p = 0.9$	$p = 0.7$	$p = 0.55$
2,2,2	2,2,2	2,2,2	1,2,2
1,2,2	1,2,2	1,2,2	2,1,2
2,1,2	2,1,2	2,1,2	1,2,2
1,1,2	1,1,1	1,1,2	2,1,1
2,2,1	2,2,2	2,2,1	1,2,2
1,2,1	1,2,1	1,2,1	2,1,1
2,1,1	2,1,1	2,1,1	1,2,1
1,1,1	1,1,1	1,1,1	2,1,1

(c) Best Response when $N = 3$

Figure 6.4: Average utility of Customers in Available/Unavailable scenario when $r = 0$

choose the same table. Instead, customer 3 will choose the table that is still empty. In this case, although customer 3 may know which table is larger, he does not choose that table if it has been occupied by the first two customers. The network externality effect dominates the learning advantage in this case.

However, when p is low, the best response of customer 1 is opposite, i.e., he will choose the table that is indicated as the smaller one by the signal he received. At the first glance, the best response of customer 1 seems to be unreasonable. However, such a strategy is indeed customer 1's best response considering the expected equilibrium in this case. According to Theorem 16, if perfect signals ($p = 1$) are given, the large table should be chosen by customer 1 and 2 since the utility of large table is $100/2 = 50$ is larger than the that of the small table, which is $40/1 = 40$, in the equilibrium. However, when the imperfect signals are given, customers choose the tables based on the expected table sizes. When signal quality is low, the uncertainty on the table size is large, which leads to similar expected table sizes for both tables. In such a case, customer 1 favors the smaller table because it can provide a higher expected utility, compared with sharing with another customer in the larger table.

In the available/unavailable scenario, as shown in Fig. 6.4, the advantage of customer 1 in playing first becomes less significant. Using 5-customer scheme shown in Fig. 6.4(a)

as an example, when signal quality p is larger than 0.6, customer 5 has the largest average utility and customer 1 has smallest average utility. Such a phenomenon is because customers should try their best on identifying the available table when $r = 0$. Learning from previous signals gives the later customers a significant advantage in this case.

Nevertheless, we observe that the best responses of later customers are not necessary always choosing the table that is more likely to be available. We use the 3-customer as an illustrative example. We list the best response of all customers given the received signals in Fig. 6.4(c). When the signal quality is pretty low ($p = 0.55$), we have the same best response as the one in resource pool scenario, where the network externality effect still plays a significant role. Using $(s_1, s_2, s_3) = (2, 2, 1)$ as an example, even customer 3 finds that table 2 is more likely to be available, his best response is still choosing table 1 since table 2 is already chosen by both customer 1 and 2, and the expected utility of choosing table 1 with only himself is higher than that of choosing table 2 with other two customers. As the signal quality p becomes high, e.g., $p = 0.9$, customer 3 will choose the table according to all signals s_1, s_2, s_3 he collected since the belief constructed by the signals is now strong enough to overcome the loss in the network externality effect.

6.6 Application: Cooperative Spectrum Access in Cognitive Radio Networks

We would like to illustrate an important application of Chinese restaurant game: cooperative spectrum access in cognitive radio networks. Traditional dynamic spectrum access methods focus on identifying available spectrum through spectrum sensing. Cooperative spectrum sensing is a potential scheme to enhance the accuracy and efficiency of detecting available spectrum [93--95]. In cooperative spectrum sensing, the sensing results from the secondary users are shared by all members within the same or neighboring networks. These secondary users then use the collected results to make spectrum access decision collaboratively or individually. If the sensing results are independent from each other, the cooperative spectrum sensing can significantly increase the accuracy of detecting the

(a) Channel Sensing   (b) Channel Selection and Signal Broadcast

(c) Data Transmission

Figure 6.5: Sequential Cooperative Spectrum Sensing and Accessing

primary user's activity. Secondary users can learn from others' sensing results to improve their knowledge on the primary user's activity. After the available spectrum is detected, secondary users need to share the spectrum following some predetermined access policy. In general, the more secondary users access the same channel, the less available access time for each of them, i.e., a negative network externality exists in this problem. Therefore, before making decision on spectrum access, a secondary user should estimate both the primary user's activity and the possible number of secondary users accessing the same spectrum.

6.6.1 System Model

We consider a cognitive radio system with J channels, N secondary transmitter-receiver pairs, and one primary user. We assume that the spectrum access behavior of secondary users is organized by an access point through a control channel. Through the organization, the secondary users can synchronize their channel sensing and selection time. Suppose that the primary user is always active and transmitting some data on one of the channels. In addition, the primary user's access time is slotted. At each time slot, each channel has equal probability of $1/J$ to be selected by the primary user for transmission. The secondary users' activities are shown in Fig. 6.5. At the beginning of each time slot, secondary users (transmitters) individually perform sensing on all channels $1 \sim J$. Then, they follow a predefined order to sequentially determine which channel they are going to

178

access in this time slot. Without loss of generality, we assume they follow the same order as their indices. When making a decision, a secondary user i reports his decision and the sensing result to the access point through a pre-allocated control channel. At the same time, all secondary users also receive this report by overhearing. After all secondary users have made their decisions, the access point announces the access policy of each channel through the control channel: secondary users choosing the same channel equally share the slot time. However, if the channel is occupied by the primary user, their transmission will fail due to the interference from primary user's transmission.

Such a cognitive radio system can be modeled as a Chinese restaurant game. Let H_j be the hypothesis that channel j is occupied by the primary user. Then, let the sensing results of secondary user $i \in \{1, 2, ..., N\}$ on channel $j \in \{1, 2, ..., J\}$ be $s_{i,j}$. We use a simple binary model on the sensing result in this example, where $s_{i,j} = 1$ if the secondary user detected some activities on channel j and $s_{i,j} = 0$ if no activity is detected on channel j. For secondary user i, his own sensing results are denoted as $\mathbf{s_i} = (s_{i,1}, s_{i,2}, ..., s_{i,J})$. In addition, the results he collected from the reports of previous users are denoted as $\mathbf{h_i} = \{\mathbf{s_1}, \mathbf{s_2}, ... \mathbf{s_{i-1}}\}$.

We define the belief of a secondary user i on the occupation of channels as $\mathbf{g_i} = \{g_{i,1}, g_{i,2}, ..., g_{i,J}\}$, where $g_{i,j} = Pr(H_j|\mathbf{h_i}, \mathbf{s_i})$. Let the probability of false alarm and miss detection of the sensing technique on a single channel be p_f and p_m, respectively. The probability of $\mathbf{s_i}$ conditioning on H_j is given by

$$Pr(\mathbf{s_i}|H_j) = p_m^{1-s_{i,j}}(1-p_m)^{s_{i,j}} \prod_{k \in \{1,...,J\}\setminus\{j\}} p_f^{s_{i,k}}(1-p_f)^{1-s_{i,k}}. \qquad (6.34)$$

Thus, we have the following belief updating rule

$$g_{i,j} = \frac{g_{i-1,j}Pr(\mathbf{s_i}|H_j)}{\sum_{k=1}^{J} g_{i-1,k}Pr(\mathbf{s_i}|H_k)}. \qquad (6.35)$$

With this rule, the belief of secondary user i is updated when a new sensing result is reported to the access point. The available access time of a channel j within a slot is its slot time, which is denoted as T. However, if the channel occupied by primary user, its

access time becomes 0. Thus, we define the access time of channel j as

$$R_j(H_k) = \begin{cases} 0, & j = k. \\ T, & \text{otherwise.} \end{cases} \tag{6.36}$$

Then, let x_i be secondary user i's choice on the channels, and n_j be the number of secondary users choosing channel j. We define the utility of a secondary user i as

$$u_i = U(x_i) = \frac{Q_{x_i} R_{x_i}(\theta)}{n_{x_i}}, \tag{6.37}$$

where $\theta \in \{H_j\}$ is the hypothesis to be true and Q_{x_i} is the channel quality of channel x_i. Here we assume that the secondary users are close to each other and share the similar channel conditions that are mainly determined by the external interference and background noise. The differences in channel gains are mainly influenced by the frequency or time-dependent external interference. If the channel has higher quality, the secondary users choosing the channel have higher data rates, and thus higher utility. Then, the best response of secondary user i is as follows,

$$BE_i(\mathbf{n_i}, \mathbf{h_i}, \mathbf{s_i}) = \arg\max_x \sum_{k \in \{1,2,\dots,J\} \setminus \{x\}} g_{i,k} E\left[\frac{Q_x T}{n_x} | \mathbf{n_i}, \mathbf{h_i}, \mathbf{s_i}, H_k\right]. \tag{6.38}$$

This best response function can be solved recursively through the recursive equations in (6.26) and (6.30).

6.6.2 Simulation Results

We simulate a cognitive radio network with 3 channels, 1 primary user, and 7 secondary transmitter-receiver pairs. When the channel is not occupied by the primary user, the available access time for secondary users in one time slot is $100ms$. Secondary users (transmitters) sense the primary user's activity in all three channels at the beginning of the time slot. We assume that the primary user has equal probability to occupy one of three channels. Conditioning on the primary user's occupation of the channel, the probabilities

of miss detection and false alarm in sensing one channel are 0.1. The channel quality factor of channel 1 is $Q_1 = 1$, while channel 2 and 3 are $1 - d$ and $1 - 2d$. The d is the degraded factor, which is within $[5\%, 50\%]$ in the simulations.

We compare our best response strategy in (6.30) with the following four strategies: random, signal, learning, and myopic strategies. In the random strategy, customers choose their strategies randomly and uniformly, i.e., all J tables have equal probability of $\frac{1}{J}$ to be chosen under the random strategy. In the signal strategy, customers make their decisions purely based on their own signal. Information from other customers, including the revealed signals and their choices on tables, is ignored. The objective of signal strategy is to choose the largest expected table size conditioning on his signal given by

$$x_i^{signal} = \arg \max_x \sum_{l \in \Theta} Pr(\theta = l | \mathbf{s_i}) Q_x R_x(l). \tag{6.39}$$

The learning strategy is an extension of the signal strategy. Under this strategy, the customer learns the system state not only by his own signal but also by the signals revealed by the previous customers. Therefore, the learning strategy can be obtained as

$$x_i^{learn} = \arg \max_x \sum_{l \in \Theta} g_{i,l} Q_x R_x(l), \tag{6.40}$$

where $g_{i,l} = Pr(\theta = l | \mathbf{h_i}, \mathbf{s_i}, \mathbf{g_0})$ is the belief of the customer on the state.

Finally, the myopic strategy simulates the behavior of a myopic player. The objective of a customer under myopic strategy is maximizing his current utility, i.e., the customer makes the decision according to his own signal, all revealed signals, and the current grouping $\mathbf{n_i}$ as follows,

$$x_i^{myopic} = \arg \max_x \sum_{l \in \Theta} g_{i,l} \frac{Q_x R_x(l)}{n_{i,x} + 1}. \tag{6.41}$$

From (6.41), we can see that the myopic strategy is similar to the proposed best response strategy except the Bayesian prediction of the subsequent customers' decisions. The performance of all these four strategies will be evaluated in all simulations in the following applications. They will be treated as the baseline of the system performance without fully rational behaviors of customers.
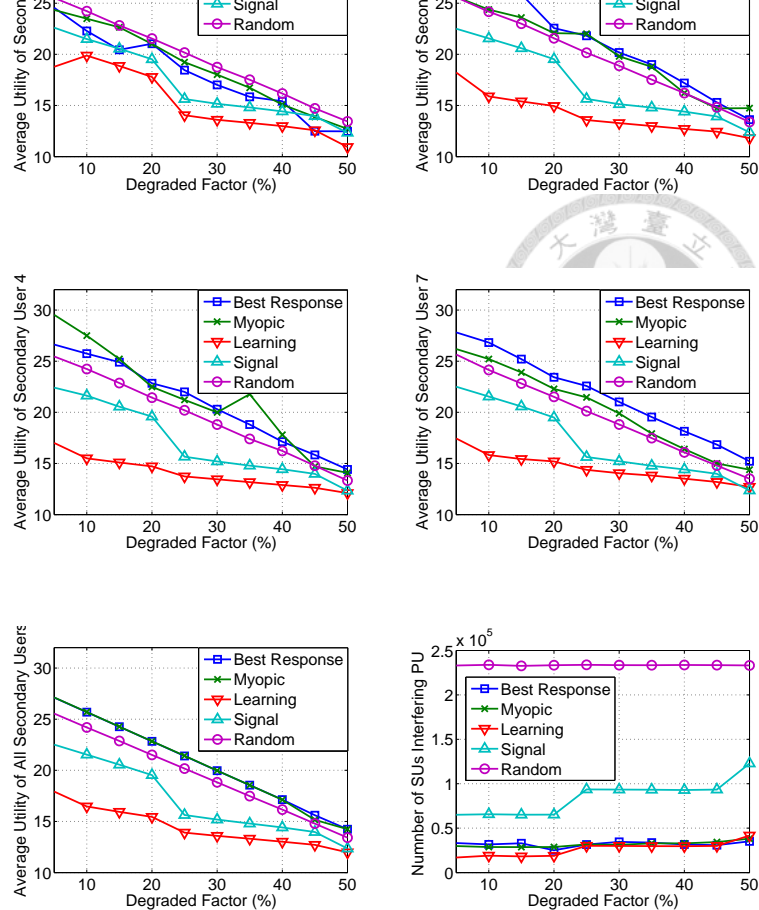
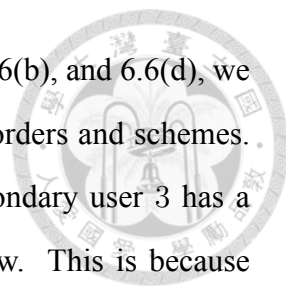(a) Secondary User 1   (b) Secondary User 3

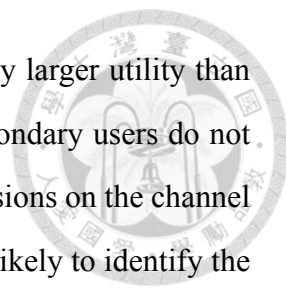(c) Secondary User 4   (d) Secondary User 7

(e) Average Utility   (f) SUs Interfering PU

Figure 6.6: Spectrum Accessing in Cognitive Radio Network under Different Schemes

The simulation results are shown in Fig. 6.6. From Fig. 6.6(a), 6.6(b), and 6.6(d), we can see that secondary users have different utilities under different orders and schemes. For both the myopic and the proposed best response schemes, secondary user 3 has a larger utility than secondary user 1 when the degraded factor is low. This is because secondary user 3 has the advantages in collecting more signals than secondary 1 to identify the channel occupied by the primary user. Moreover, the loadings of the other two channels are still far from their expected equilibrium loadings since only two secondary users have made choices. Therefore, secondary user 3 has a larger utility than secondary user 1. Nevertheless, when the degraded factor is high, we can see that secondary user 1's utility is larger than that of secondary user 3. This is because when the degraded factor increases, the quality difference among channels increases. In such a case, even secondary user 3 successfully identify the occupied channel, the channel that offers a higher utility in the equilibrium is usually the one with fewer number of secondary users. The expected number of secondary users accessing such a channel is generally 2 or even 1, and secondary user 3 can no longer freely choose those channels. For secondary user 7, he usually has no choice since there are six secondary users making decisions before him. Therefore, he has the smallest utility.

Generally, the myopic scheme provides an equal or lower utility than the best response scheme for secondary users making decisions early, such as secondary user 1, since secondary users in the myopic scheme do not predict the decisions of subsequent users. However, some secondary users eventually benefit from the mistakes made by early secondary users. We can see from Fig. 6.6(b)and Fig. 6.6(c) that for some cases, customer 3 and 4 has a higher utility under the myopic scheme than under the best response scheme due to the mistakes made by customer 1 and 2. We can also see from Fig. 6.6(e) that both best response and myopic schemes provides the same average utilities of all secondary users. In such a case, the utility loss of some secondary users in the myopic scheme will lead to the utility increase of some other secondary users. For random and signal schemes, there is no difference among the average utilities of secondary user 1, 3, and 7 since secondary users do not learn from other agents' actions and signals under these two schemes. For the

learning scheme, we can see that secondary user 1 has a significantly larger utility than secondary user 3 and 7. This is because in the learning scheme, secondary users do not take the negative network externality into account when making decisions on the channel selection. Since secondary users who made decisions later are more likely to identify the primary user's activity, they are more likely to choose the same channels, and their utilities are degraded due to the negative network externality.

Let us take a deeper look at the average utility of all secondary users shown in Fig. 6.6(e). On one hand, we can see that both best response and myopic schemes achieve highest average utilities of all secondary users. The network externality effects in spectrum access force strategic secondary users to access different channels instead of accessing the same high quality channels. On the other hand, learning and signal schemes lead to poor average utilities since they do not consider the network externality in their decision processes. All secondary users tend to access the same available high quality channel, and therefore the spectrum resource in other available channels is wasted. This also explains the phenomenon that learning scheme leads to poorer performance than signal scheme. Under the learning scheme, secondary users are more likely to reach a consensus on the primary user's activity and make the same choice on the channels, which degrades the overall system performance.

Finally, we show the number of secondary users causing interference to the primary user in Fig. 6.6(f). We can see that those schemes involving learning, which are best response, myopic, and learning schemes, have low interference to the primary user. Secondary users who learn from others' signals efficiently avoid the channel occupied by the primary user.

6.7 Related Work

A closely-related strategic game model to our work is the global game [96, 97]. In the global game, all agents, with limited knowledge on the system state and information held by other agents, make decisions simultaneously. The agent's reward in the game is determined by the system state and the number of agents making the same decision

with him. The influence may be positive or negative depending on the type of network externality. An important characteristics of global game is that the equilibrium is unique, which simplifies the discussion on the outcome of the game. It draws great attentions in various research fields, such as financial crisis [98], sensor networks [99] and cognitive radio networks [100]. Since all players in the global game make decisions simultaneously, there is no learning involved in the global game.

In recent years, several works [101--105] make efforts to introduce the learning and signaling into the global game. Dasgupta's first attempt was investigating a binary investment model, while one project will succeed only when enough number of agents invest in the project in [101]. Then, Dasgupta studied a two-period dynamic global game, where the agents have the options to delay their decisions in order to have better private information of the unknown state in [105].

Angeletos et. al. studied a specific dynamic global game called regime change game [102,103]. In the regime change game, each agent may propose an attack to the status quo, i.e., the current politic state of the society. When the collected attacks are large enough, the status quo is abandoned and all attackers receive positive payoffs. If the status quo does not change, the attackers receive negative payoffs. Angeletos et. al. first studied a signaling model with signals at the beginning of the game in [102]. Then, they proposed a multiple stages dynamic game to study the learning behaviors of agents in the regime change game in [103].

Costain provided a more general dynamic global game with an unknown binary state and a general utility function in [104]. However, the positions of the agents in the game are assumed to be unknown to simply the analysis. Nevertheless, most of these works study the multiplicity of equilibria in dynamic global game with simplified models, such as binary state, binary investment model, or lacking of position information. Moreover, the network externality they considered in their models are mostly positive. By proposing Chinese restaurant game, we hereby provides a more general game-theoretic framework on studying the social learning in a network with negative network externality, which has many applications in various research fields.

6.8 Summary

In this chapter, we proposed a new game, called Chinese Restaurant Game, by combining the strategic game-theoretic analysis and non-strategic machine learning technique. The proposed Chinese restaurant game can provide a new general framework for analyzing the strategic learning and predicting behaviors of rational agents in a social network with negative network externality. By conducting the analysis on the proposed game, we derived the optimal strategy for each agent and provided a recursive method to achieve the equilibrium. The tradeoff between two contradictory advantages, which are making decisions earlier for choosing better tables and making decisions later for learning more accurate believes, is discussed through simulations. We found that both the signal quality of the unknown system state and the table size ratio affect the expected utilities of customers with different decision orders. Generally, when the signal quality is low and the table size ratio is high, the advantage of playing first dominates the benefit from learning. On the contrary, when the signal quality is high and the table size ratio is low, the advantage of playing later for better knowledge on the true state increases the expected utility of later agents. Our simulations also showed that the price of anarchy under Chinese restaurant game is close to one, which suggests that the efficient loss due to the rational behaviors of customers is close to zero. The small price of anarchy is achieved by the loading balance among tables, which is automatically achieved in Chinese restaurant game. Finally, we illustrated a specific application of Chinese restaurant game in wireless networking: the cooperative spectrum access problem in cognitive radio networks. We showed that the overall channel utilization can be improved by taking the negative network externality into account in secondary users' decision process. The interference from secondary users to the primary user can also be reduced through learning from the sensing results of others.

Chapter 7

Stochastic SVC Multicasting model using Chinese Restaurant Game

7.1 Introduction

With the development of multimedia compression and the advance of wireless networking techniques, multimedia content delivery over wireless networks becomes more and more popular, e.g., mobile video download/upload, live video streaming [11] and Internet Protocol TV (IPTV) [12, 13]. One challenging issue in such wireless multimedia delivery systems is how to maintain the quality of service due to the scare resource in wireless networks and heavy loading from heterogeneous demands.
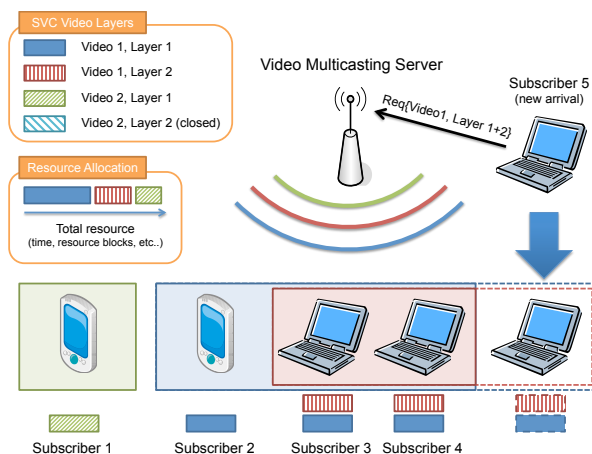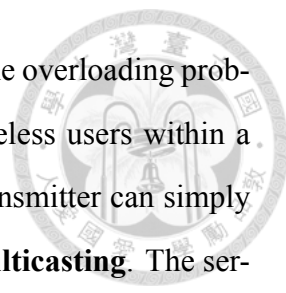

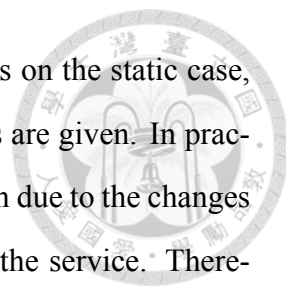Figure 7.1: A SVC multicasting platform offering two 2-layer videos

Multicasting in wireless communications is a natural solution to the overloading problem in wireless live video streaming and IPTV. When multiple wireless users within a certain range are requesting for the same multimedia content, the transmitter can simply broadcast one copy of the content to all receivers, which is called **multicasting**. The service provider may categorize users into several multicasting groups according to their demands in contents, and then perform multicasting in delivering. However, challenges still exist in such a group-based multicast approach since each multicast group still requires resource to function. How the limited resource should be allocated to each group is an important issue. Moreover, heterogeneous users may use devices with different computational capabilities. A device with low computation capability may not be able to decode the received high-quality content. Therefore, the service provider needs to deliver the same content in multiple qualities, such as in standard resolution (SD) and high resolution (HD), to satisfy these heterogeneous demands. This introduces serious redundancy in the delivery and therefore further aggravates the overloading issue.

Scalable video coding (SVC) is a promising technique to resolve the content redundancy issue [14]. It provides a flexible design to encode the videos into a series of data streams, each of which represents a layer of the video. The base layer (layer 1) can be decoded independently without the information stored in other data streams. It also has a low decoding requirement in computation capability. Other layers are called enhancement layers, which contain extra information to reconstruct a higher quality video. A receiver may derive a higher quality video by decoding the base layer and subsequent enhancement layers. Therefore, the redundancy in delivery can be greatly reduced with such a technique. By combining multicasting and SVC techniques, the cross-layer design shows great potentials in enhancing the quality of multimedia delivery service. An example is illustrated in Fig. 7.1, where a video multicasting server is offering two SVC videos, each with two layers. Four users are already using the service, while subscriber 2~4 request for video 1 and subscriber 1 requests for video 2. Three multicasting groups, each for a specific layer of a video, are formed according to their requests for the video and layers. Notice that the transmission of video 2's layer 2 is suspended because no users are request-

ing it. Notice that when subscriber 5 arrives the system, he sends a request to the video server for the video 1 with both layers. If the video server accepts the request, subscriber 5 will join the multicasting groups for video 1's layer 1 and layer 2. The resource allocation of each multicasting group will then be determined according to the channel conditions and demands of users.

7.1.1 Scalable Video Coding Multicasting System

The cross-layer design of SVC multicasting system has been discussed in the literature. A popular approach is the utility-based approach [106], where users are assumed to have some utilities if they receive and decode the demanding videos correctly. Under such an approach, the objective of the system is maximizing the total users' utilities given the current demands and the channel conditions. Generally, given a snapshot of the multicasting system, the multiple multicast resource allocation problem can be reduced to a 0-1 Knapsack problem if the selectable resource allocation pattern is not continuous, e.g., finite set of modulation and coding schemes. Since the 0-1 Knapsack problem is NP-hard, approximated algorithms are required to efficiently solve the resource allocation problem. Several approximated algorithms with different objectives for the snapshot optimization have been proposed in the literature. A straightforward greedy algorithm is proposed in [107] while a pseudo-polynomial algorithm for minimizing the total energy consumption is proposed in [13]. In [12], the authors proposed an envelop-based approximated algorithm and gave a tight error bound. Dynamic programming approaches, which make use of the sequential utility increment structure in SVC technique, are introduced in [11, 108, 109]. This problem becomes more challenging when it comes to cognitive radio [110]. In [111] the authors illustrate how to jointly consider the availability of channels with the video multicasting decisions. A similar opportunistic multicasting approach is shown in [112] to enhance the QoS in WiMAX system. Pricing has been shown to be a powerful tool for regulating the subscribers' actions in a video streaming service [113]. In [114], a pricing approach is proposed to transform the utility into the immediate revenue with different priorities in layers.
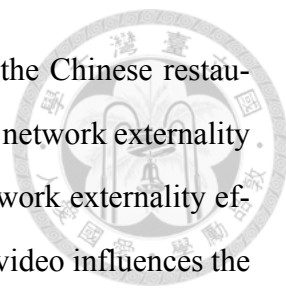
However, most existing works on SVC multicasting system focus on the static case, i.e., considering the snapshot scenario where the demands from users are given. In practice, the SVC multicasting system will be highly dynamic in a long run due to the changes of channel conditions, user demands, and the reserved resource for the service. Therefore, there is a need of stochastic analysis to find a policy that can regulate the demands of users to maintain QoS. In the literature, there are works investigating the policy design of stochastic multicasting system in wired networks [115]. However, to the best of our knowledge, there is no existing work on the stochastic analysis on the SVC multicasting system over wireless networks.

7.1.2 Economic Value of SVC Multicasting System

In addition, from the service provider's perspective, the economic value of a SVC multicasting system may be the most important factor. A commercial service provider will provide such a service only when significant economic value can be achieved [113]. Taking into account such a factor, we discuss a subscription-based economic model with different pricing schemes, where we involve rational users' selfish nature. Researchers have discovered that the rational behaviors of users should be seriously considered in designing any system with users applying actions and making decisions [56, 116]. A system works well in a centralized-control system may fail in a user-oriented system since the rational users focus on their own utilities instead of overall system performance. The selfish behaviors of users may eventually degrade the system efficiency or service provider's revenue [113]. Some incentive designs may be required to regulate the behaviors of users in order to improve the system efficiency [117]. By considering rational users' selfish nature, we propose to use game theory to analyze how users react under different pricing schemes.

In light of these concerns, we study a dynamic SVC multicasting system with stochastic user arrival and heterogeneous user demand in this chapter. Specifically, we propose a Multi-dimensional Markov Decision Process (M-MDP) framework to analyze the optimal load balancing and economic efficient policies for the dynamic SVC multicasting
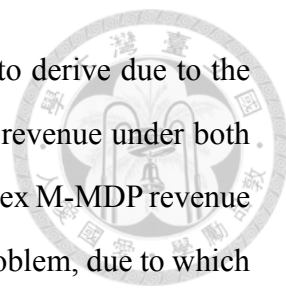
system. The M-MDP framework is a stochastic extension [118] to the Chinese restaurant game [92, 119], in which the authors investigate how the negative network externality and social learning influence the decisions of rational users. The network externality effect also exists in our framework, as the amount of demands on each video influences the resource allocation and thus differentiates the quality of services to the users requesting different videos.

In this chapter, we introduce a subscription system to help the service provider to regulate the subscription requests from the heterogeneous users. We consider two subscription pricing schemes: one-time charge and per-slot charge scheme. We prove that both pricing schemes achieve the same optimal revenue. In addition, we prove that the complex M-MDP optimization problem can be reduced to the traditional average MPD problem when the optimal pricing strategy is adopted, and the solution can be effectively derived through the proposed approximate algorithms.

7.1.3 Contributions

In summary, our main contributions are shown as follows:

1. We develop a Markov decision process based stochastic framework to analyze the resource allocation in a SVC multicasting system with heterogeneous user demands. By considering the stochastic user arrival, such a framework is more general than the existing snapshot-based approaches in the literature.

2. We propose a game-theoretic model to analyze the behaviors of heterogeneous users. We study how rational and intelligent users submit their demands, i.e., subscriptions, under two pricing schemes: one-time charge scheme and per-slot charge scheme, and derive the equilibrium conditions of the game. To the best of our knowledge, this chapter is the first work bringing game theoretic analysis to the SVC multicast system.

3. We theoretically evaluate the economic value of the SVC multicasting system. Specifically, we investigate the revenue-maximized policy and pricing strategies in both

one-time charge and per-slot charge schemes, which are hard to derive due to the coupling effects in both terms. By proving that the maximum revenue under both schemes is equivalent under all policies, we transform the complex M-MDP revenue maximization problem to a traditional average-reward MDP problem, due to which we can derive the optimal policy and pricing strategies in an efficient way. Both theory and simulation results confirm that the derived solution not only maximizes the expected revenue but also optimizes the social welfare.

The rest of the chapter is organized as follows. In Section 7.2, we describe a general SVC multicasting system where users have heterogeneous preferences and computation capabilities. In Section 7.3, we formulate the system as a game-theoretic M-MDP framework for investigating the rational behaviors of users under such a subscription-based SVC multicasting system. Then, the equilibrium conditions of the system are derived in Section 7.4, where the expected subscription requests from users under certain pricing scheme strategies are analyzed. In Section 7.5, the optimal pricing strategies that maximize the revenue of the service provider under both pricing schemes are derived. By applying optimal pricing strategies, we reduce the complex M-MDP problem into a traditional average MDP problem and derive the revenue-maximized subscription regulation policy in Section 7.6. Finally, the simulation results are discussed in Section 7.7, and we summarize this chapter in Section 7.8.

7.2 System Model

We consider a video multicasting service with one video server and multiple potential users who arrive and depart stochastically. The service is offering multiple choices of a SVC video. Given the limited resource (time, bandwidth, etc..), the service provider needs to determine the video server's resource allocation given the current demands for videos. In addition, the provider also determines the prices of the video multicasting services, which may be dynamically adjusted. On the other hand, the potential users request for the service when they arrive the system. Their requests are based on their preferences,

computation capabilities, and the price of the service. The objective of the service provider is maximizing its revenue, while the users aim to seek for best experience, i.e., highest utility, in the video multicasting service.

7.2.1 Video Server

Let us consider a video server which is capable of serving at most N subscribers. The server provides videos denoted by $\mathcal{J} = \{1, 2, ..., J\}$. Each video is encoded by SVC and an encoded video steam contains K layers. The server transmits the layers of each video periodically on the same channel. All layers are transmitted with the same interval but at different time period so they do not interfere with each other.

A subscriber can decode a video if he receives at least the base layer (layer 1), while the quality of the video will be enhanced if he successfully decodes more subsequent layers. Let layer k be the k-th layer of the video, a subscriber may decode the video up to layer k only when all layer $1 \sim k$ are successfully received. In Fig. 7.1, we illustrate a SVC multicasting server with 5 subscribers, while the server is offering $J = 2$ videos, each with $K = 2$ layers.

The reception of the layer is determined by two factors: the supported modulation and coding scheme (MCS) at the subscriber side and the MCS applied on the layer at the video server side. On the subscriber side, let $g_i \in \mathcal{G}$ be the maximum MCS supported by subscriber i, where $\mathcal{G}$ is the universe set of the MCSs. In this chapter, we assume that g_i is a random variable with a probability density function $f(g_i)$.

On the video server side, the video server needs to determine the MCS applied on each layer of each video. Let $g_{j,k}$ be the MCS applied on layer k of video j. When a video stream is transmitted with the MCS $g_{j,k}$, all users with channel quality $g \geq g_{j,k}$ can successfully receive this stream.

The applied MCS $g_{j,k}$ determines the required resource (transmission time) to transmit the layer. We denote $R_{j,k}(g_{j,k})$ as the required resource to transmit layer k of video j to users with MCS $g_{j,k}$. The $R_{j,k}(g_{j,k})$ should be a decreasing function of $g_{j,k}$ since a layer can be transmitted in a shorter time if a higher-level MCS with higher throughput is applied.

The video server may choose to stop transmitting layer k. We define $R_{j,k}(\underline{g^c}) \equiv 0$. The $\underline{g^c}$ represents the case that the transmission of this layer is disabled and therefore no users can receive this layer. Finally, let R^{total} be the total available resource, which is the total transmission time in our system. As the overall resource is limited to R^{total}, we have a firm constraint that $R^{total} \geq \sum_{j,k} R_{j,k}(\underline{g_{j,k}})$.

Notice that the resource should be dynamically allocated according to the current realization of users' channel qualities in order to maximize the delivery efficiency. Let $\mathbf{s} = \{n_{j,k}^s\}$ be the current **system state**, where $n_{j,k}$ be the number of users requesting video j's layer k stream. The state $\mathbf{s}$ represents the current loading of the video server. Then, we denote the dynamic resource allocation rule as $\mathbb{D}(\mathbf{s}) = \{\underline{g_{j,k}} | \forall j, k\}$. The allocation rule takes the current system state $\mathbf{s}$ as input and outputs the corresponding MCS for each layer. The $\mathbb{D}(\mathbf{s})$ may be implemented with different objectives, such as efficiency maximization or fairness constraints. In a utility-based system [12, 107], a common and reasonable choice of $\mathbb{D}$ is the overall utility maximization, that is,

$$\mathbb{D}(\mathbf{s}) = \arg \max_{\underline{g_{j,k}}} \mathbb{E}[u_i(\{\underline{g_{j,k}}\})] \tag{7.1}$$

under the resource constraint $R^{total} \geq \sum_{j,k} R_{j,k}(\underline{g_{j,k}})$, where u_i is the utility of user i. In a wireless system with finite choices of the lowest channel quality, e.g., limited choices of MCS in WiMAX, this problem has been shown to be NP-hard [12]. Therefore, heuristic approaches are required and can be found in the literature [11, 12, 107--109].

7.2.2 User Valuation

In our system, users with different preferences arrive stochastically. In general, there are some users who have strong preference on a certain type of videos, e.g., sport fans always subscribe to the sport news channels. On the other hand, there are also some users that may not have a strong preference on the type of videos. They can enjoy all videos they successfully receive and decode.

Users with similar preferences usually have similar valuations on video content and

quality. However, their devices may have different capabilities in receiving and decoding the videos. For instance, users who prefer the sport news may subscribe to the same channels, but some of them are only equipped with mobile phones. With such a limited capability device, only base layer can be decoded and displayed correctly. Therefore, users' abilities to have better video quality may be limited.

We model all the aforementioned properties with the following notations. Users are categorized into types, which is denoted by $t \in \{1, 2, .., , T\} = \mathcal{T}$. A type $t = (\mathcal{J}^t, k^t)$ user prefers videos $j^t \in \mathcal{J}^t$ and is equipped with a device capable of decoding the SVC-encoded video up to layer k^t. We denote the valuation function on video $j \in \mathcal{J}$ with maximum decoded layer k as $v_j(k)$. Then, a type t user's valuation on video j with maximum consecutively received layer k is denoted as

$$
v^t(j, k) = \begin{cases} v_j(k), & j \in \mathcal{J}^t, k \le k^t; \\ v_j(k^t), & j \in \mathcal{J}^t, k > k^t; \\ 0, & \text{else.} \end{cases} \tag{7.2}
$$

Note that a user has positive valuations on the service only if he receives and decodes his preferred video $j^t \in \mathcal{J}^t$ successfully. In addition, when $|\mathcal{J}^t| = 1$, the type t user prefers only one video, we call them as **concentrated users**. Otherwise, we call them **casual users**. Finally, as a stochastic model, we assume users with different types arrive independently. We describe the arrival process of type t users with a Poisson process with the average arrival rate $\bar{\lambda}^t$.

7.2.3 Payment System

We consider a subscription-based payment system as the revenue source of the service provider. We assume that the video service is private and all transmissions are encrypted. Therefore, users who enter the system should subscribe to one of the videos in order to correctly decrypt the corresponding data streams. A subscription contains two terms: the subscribed video j and the desired maximum layer k. When a subscription is accepted by the video server, the decryption keys of video j's layer $1 \sim k$ streams are delivered

to the user. However, the receiving of these streams is not guaranteed due to the natural instability characteristics of the channel quality g. This is characterized by $f(g)$. We assume the channel qualities of all users are independent from each other and among time slots.

The price for a subscription, which is determined by the service provider, should be properly chosen in order to maximize its expected revenue. We model it as a function of the current state $\mathbf{s} = (n_{1,1}^s, n_{1,2}^s, ..., n_{J,K}^s)$. In this chapter, two pricing schemes are considered.

1. One-time charge: a payment $P_{j,k}^e(\mathbf{s}^a)$ is charged as soon as the user's subscription (j, k) is accepted, and no further payments are required. The $\mathbf{s}^a$ denotes the system state when the user arrives at the system.

2. Per-slot charge: At each time slot, as long as the user stays in the system with a valid subscription, he is charged with a price of $P_{j,k}(\mathbf{s})$, where $\mathbf{s}$ is the current state of the system.

Notice that a subscription can be canceled by a user at any time. In this model, we assume the time period of a user staying in the system is an exponential process with the average departure rate $\bar{\mu}$. The subscription is canceled immediately when the user leaves the system.

7.3 Game Theoretic Formulation

In our model, we assume that users are rational and thus naturally selfish. Therefore, we need to consider users' selfish behaviors when evaluating and designing the pricing schemes and strategies, and game theory is powerful mathematical tool that analyzes the strategic interactions among multiple selfish decision makers [56].

We consider a subscription game where the players are the potential subscribers and the service provider. The service provider determines and announces at the beginning of the game the service price, $\{P_{j,k}^e(\mathbf{s})\}$ for one-time charge scheme or $\{P_{j,k}(\mathbf{s})\}$ for per-slot

charge scheme, while the potential subscribers submit their requests after receiving the announcements from the service provider.

The objective of the service provider is to maximize the expected revenue in the system. Notice that users are rational with the objective of maximizing their own utility under the rules given by the service provider. As a result, the service provider needs to carefully determine the pricing strategy by taking into account the response of selfish users.

A user's objective is to maximize its own utility by choosing the best subscription. As described in Section 7.2, users arrive stochastically. When a type t user arrives, he determines whether to subscribe to the service with a specific video at certain layers. To subscribe to the service, the user sends a subscription request and will receive the corresponding video stream if the server accepts the request. Note that since the system state and the channel quality are changing over time, the service quality is dynamic.

The expected utility of the user with subscription (j, k) is conditioned on the system state $\mathbf{s}$ when he arrives. Let the system state at time slot l be $\mathbf{s}^l$. A type t user with a valid subscription (j, k) has an immediate valuation on the service, $v^t(j, \overline{k})$, where $\overline{k} \leq k^t$ is the maximum successfully decoded layer at current time slot. In addition, there is a cost of using the service, which is the charged payment determined by the pricing scheme. Given the state and costs, the expected utility of a type t user if he submits a subscription (j, k) is as follows

$$\mathbb{E}[u^t(j, k)|\mathbf{s}] = -c(\mathbf{s}, j, k, 0) \tag{7.3}$$
$$+ \sum_{l=l_a}^{l_d} (\mathbb{E}[v^t(j, \overline{k})|\mathbf{s} = \mathbf{s}^l, \overline{k} \leq k] - c(\mathbf{s}^l, j, k, 1)),$$

where $c(\mathbf{s}, j, k, e)$ is a common pricing function depending on the pricing scheme, $\mathbf{s}$ is the state when the user arrives the system, and l_a and l_d are the user's arrival and departure time indices, respectively. Specifically, $c(\mathbf{s}, j, k, 0)$ is the entrance fee to request a subscription (j, k) before using the service, which will be zero under the per-slot charge scheme. The $c(\mathbf{s}, j, k, 1)$ is the per-slot charge when the user is in the system, which will be zero under the one-time charge scheme. A rational user will choose the subscription that maximizes

the expected utility in (7.3) when arriving at the system.

7.4 Equilibrium Conditions

Nash equilibrium is a solution concept for predicting the outcomes of a game with the assumption that all players are fully-rational. Nash equilibrium describes an action profile, where each player's action is the best response to other players' actions in the profile. Since all players apply their best responses, none of them has the incentive to deviate from their actions described in the profile.

The Nash equilibrium of the proposed video subscription game can be analyzed through the following procedures. We first model the selfish users' behaviors through a multi-dimensional Markov decision process (MDP) by fixing the pricing function $c(\cdot)$. The steady state and the expected utilities can then be calculated, and therefore the users' equilibrium conditions can be derived. With the equilibrium conditions of users, we then derive the equilibrium conditions for the service provider to maximize the revenue.

7.4.1 Users' Behavior Modeling Using Multi-Dimensional Markov Decision Process

The video subscription game, when the pricing function $c(\cdot)$ is given, can be formulated as a multi-dimensional Markov decision process (M-MDP) [118]. A Markov decision process describes a stochastic system where the transition between states is partially or fully determined by a decision maker [120]. The objective of the decision maker, the subscriber in our model, is to maximize his expected reward. In a traditional MDP, there is only one decision maker and the optimal solution that maximizes the unique expected reward can be found using dynamic programming [120]. However, since there are multiple decision makers with their own utility functions in our game, the traditional MDP cannot be directly applied here.

In the proposed M-MDP framework, we consider a discrete-time Markov system where a time slot has a duration of T_s. The arrival and departure probability of each type t of

subscribers can be approximate to $\lambda^t = \bar{\lambda}^t T_s$ and $\mu = \bar{\mu} T_s$, respectively, when T_s is sufficient small. The system state is $\mathbf{s} = (n_{j,k}^s | j \in \{1...J\}, k \in \{1...K\}) \in \mathcal{S}$, where $n_{j,k}^s$ denotes the number of users subscribing video j with maximum subscribed layer k. The server can serve up to N users, therefore we have the boundary constraints $\sum_{j,k} n_{j,k}^s \leq N$ on the states.

The action of a user is the subscription request $a = (j, k)$. Different types of users may have different action space due to the limitation in computation capability. The action space of a type t user is $\mathcal{A}^t = \mathcal{J}^t \times \mathcal{K}^t \bigcup \{(0,0)\}$, where $(0,0)$ represents that he does not subscribe to any video and leaves the system immediately. Note that users will not subscribe the unpreferred videos since their valuations on those videos are zero. Therefore, we denote $V(j,k) \equiv v_j(k)$ to describe any subscriber's valuation on the video if he indeeds submit a request (j,k). Therefore, after taking the action $a = (j, k)$, the user can obtain an immediate reward as follows

$$R(\mathbf{s}, j, k) = \mathbb{E}[U(j,k)|\mathbf{s}] = V_{j,k}(\mathbf{s}) - c(\mathbf{s}, j, k, 1). \tag{7.4}$$

where $U(j,k)$ is the common utility function of any subscriber in the system if he indeeds request for (j,k). In general, the immediate reward is the expected valuation of the successfully decoded video $V_{j,k}(\mathbf{s})$ minus the subscription payment, which happens to be the expected utility of a type t user with subscription $(j \in \mathcal{J}^t, k)$ in state $\mathbf{s}$. For the case that $(j,k) = (0,0)$, we let $R(\mathbf{s}, 0, 0) = 0, \forall \mathbf{s}$.

Policy is an important concept in Markov decision process. A policy is an action profile which describes a decision of the decision maker at a certain state in the stochastic system. In our model, a policy is denoted as a function $\pi(\mathbf{s}, t) : \mathcal{S} \times \mathcal{T} \mapsto \mathcal{A}^t$, which describes the subscription decision of type t user arriving in state $\mathbf{s}$.

7.4.2 Expected Reward under Transition Probability

A rational user will make the decision to maximize the expected reward defined as follows

$$W(\mathbf{s}, j, k) = \mathbb{E}[\sum_{l=l^e}^{\infty}(1-\mu)^{t-1}R(\mathbf{s}^l, j, k)|\mathbf{s}] \qquad (7.5)$$

where μ is the departure rate, and thus $1 - \mu$ is the probability that the user will stay at next time slot. Note that $1 - \mu$ can also be considered as the discount factor of the future utility. In the steady state, the Bellman equation of the expected reward can be written as follows

$$W(\mathbf{s}, j, k) = R(\mathbf{s}, j, k) + (1-\mu)\sum Pr(\mathbf{s}'|\mathbf{s}, \pi, j, k)W(\mathbf{s}', j, k) \qquad (7.6)$$

where $Pr(\mathbf{s}'|\mathbf{s}, \pi, j, k)$ denotes the transition probability from $\mathbf{s}$ to $\mathbf{s}'$ when the user takes the action (j, k) under the policy π. Notice that this transition probability is conditioned on the fact that he is not leaving the system at next time slot. Otherwise he will not receive the rewards from next time slot. Let $\mathbf{e}_{j,k}$ be a standard basis vector. Then, the transition probability of a user with a subscription (j, k) is given as follows:

$$
Pr(\mathbf{s}'|\mathbf{s}, \pi, j, k) \qquad (7.7)
$$
$$
= \begin{cases}
\sum_{t\in\mathbf{T}, \mathbf{s}'=\mathbf{s}+\mathbf{e}_{\pi(\mathbf{s},t)}} \lambda^t, & \exists t \in \mathbf{T}, \mathbf{s}' = \mathbf{s} + \mathbf{e}_{\pi(\mathbf{s},t)} \\
& \text{and } \pi(\mathbf{s}, t) \neq (0, 0); \\
(n^s_{j',k'})\mu, & \mathbf{s}' = \mathbf{s} - \mathbf{e}_{j',k'}; \\
(n^s_{j,k} - 1)\mu, & \mathbf{s}' = \mathbf{s} - \mathbf{e}_{j,k}, n^{s'}_{j,k} \neq 0; \\
1 - \mu(N(\mathbf{s}) - 1) - \lambda(\mathbf{s}, \pi), & \mathbf{s} = \mathbf{s}', n^{s'}_{j,k} \neq 0; \\
1 - \mu N(\mathbf{s}) - \lambda(\mathbf{s}, \pi), & \mathbf{s} = \mathbf{s}', n^{s'}_{j,k} = 0; \\
0, & \text{else.}
\end{cases}
$$

where $N(\mathbf{s}) = \sum_{j,k} n^s_{j,k}$ and $\lambda(\mathbf{s}, \pi) = \sum_{t\in\mathcal{T}} \mathbf{1}(\pi(\mathbf{s}, t) \neq (0, 0))\lambda^t$.

Since users are assumed to be rational, a type t user should choose the subscription that

maximizes his expected utility when he arrives at the system. Recalling that $c(\mathbf{s}, j, k, 0)$ is the initial subscription fee for (j, k), which will be zero under the per-slot charge scheme and non-negative under the one-time charge scheme, the optimal policy under the expected reward $W(\mathbf{s}, j, k)$ is given by

$$\pi(\mathbf{s}, t) \in \arg\max_{(j,k) \in \mathcal{A}^t} W(\mathbf{s} + \mathbf{e}_{j,k}, j, k) - c(\mathbf{s}, j, k, 0), \tag{7.8}$$

Notice that when the server is full, new users will not be allowed to enter, i.e., $\forall N(\mathbf{s}) = N$, $\pi(\mathbf{s}, t) = (0, 0)$, $\forall t \in \mathcal{T}$.

The Nash equilibrium is achieved when (7.6) and (7.8) are satisfied, which are denoted as the equilibrium conditions. When the equilibrium conditions are met, each type of users has chosen the subscription that maximizes the expected utility. Therefore, they have no incentive to deviate, and a Nash equilibrium is achieved.

7.4.3 Average Revenue Maximization for Service Provider

The objective of the service provider is to maximize his revenue in the system under the rational response of subscribers. Let π and W be the policy and expected rewards derived in (7.6) and (7.8) under the pricing function $c(\cdot)$. Then, let $Q(\mathbf{s})$ be the expected revenue in state $\mathbf{s}$. The best response of the service provider is the solution to the following optimization problem:

$$\max_{c(\cdot)} \lim_{N \to \infty} \frac{1}{N} \mathbb{E}[\sum_{l=1}^{N} Q(\mathbf{s}^l)], \tag{7.9}$$

under the constraints

$$W^*(\mathbf{s} + \mathbf{e}_{\pi^*(\mathbf{s},t)}, \pi^*(\mathbf{s}, t)) - c(\mathbf{s}, j, k, 0) \geq 0, \ \forall \mathbf{s}, t, \tag{7.10}$$

where π^* and W^* satisfy the equilibrium conditions in (7.6) and (7.8).

Note that the state transition probability in this problem is different from the one ob-
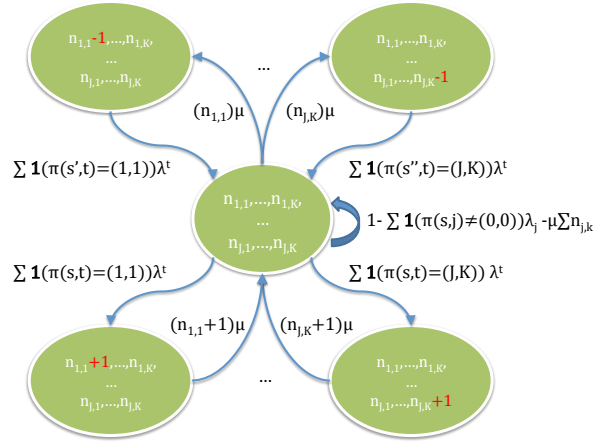
Figure 7.2: An illustration of State Transition in the proposed M-MDP system

served by users in (7.7), and can be written as follows

$$Pr(\mathbf{s}'|\mathbf{s}, \pi) = \tag{7.11}$$

$$
\begin{cases}
\sum_{t \in \mathbf{T}, \mathbf{s}' = \mathbf{s} + \mathbf{e}_{\pi(\mathbf{s},t)}} \lambda^t, & \exists t \in \mathbf{T}, \mathbf{s}' = \mathbf{s} + \mathbf{e}_{\pi(\mathbf{s},t)} \\
& \text{and } \pi(\mathbf{s}, t) \neq (0, 0); \\
(n_{j,k}^s)\mu, & \mathbf{s}' = \mathbf{s} - \mathbf{e}_{j,k}; \\
1 - N(\mathbf{s})\mu - \lambda(\mathbf{s}, \pi), & \mathbf{s} = \mathbf{s}'; \\
0, & \text{else.}
\end{cases}
$$

An illustration of the state transition is shown in Fig. 7.4.3.

With primal-dual transformation [120], the expected average revenue can be given as follows:

$$g(\pi) = \sum_{\mathbf{s} \in \mathcal{S}} Pr(\mathbf{s}|\pi) Q(\mathbf{s}), \tag{7.12}$$

where $Pr(\mathbf{s}|\pi)$ is the stationary distribution of the states under policy π.

7.5 Optimal Pricing Strategies

In this section, we would like to discuss the optimal pricing strategy that maximizes the expected revenue under a given policy while satisfying the user equilibrium conditions in (7.6) and (7.8). Since the policy is given and fixed, the optimization problem is sim-

plified. This helps us to have an initial understanding on how the service provider should determine the price in order to maximize its expected revenue given a known pattern on the subscription requests from users and constraints from the corresponding equilibrium conditions.
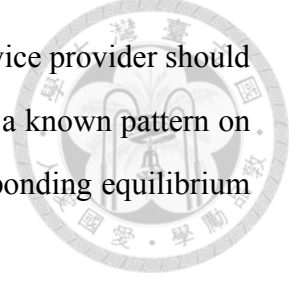
7.5.1 Optimal Pricing in One-time Charge Scheme

In one-time charge scheme, a user is charged with a state-dependent subscription fee $P^e_{j,k}(\mathbf{s})$ when his subscription (j,k) is accepted, and no future payments are required. Therefore, we have $c(\mathbf{s}, j, k, 1) = 0$ and $c(\mathbf{s}, j, k, 0) = P^{\mathrm{e}}_{j,k}(\mathbf{s}) \geq 0$ for all $\mathbf{s}, j, k$. Let $W(\mathbf{s}, j, k)$ be the expected reward derived by solving (7.6) through dynamic programming or matrix operations. Since the policy π is fixed, the transition probability is fixed. Therefore, the original revenue optimization problem can be solved in a state-wise way.

Since the server can serve at most N users, we have $N(\mathbf{s}) \leq N$ for all $\mathbf{s}$. When $N(\mathbf{s}) = N$, all requests will be rejected, which leads to zero revenue. When $N(\mathbf{s}) < N$, the revenue maximization problem can be written as follows

$$\max_{\{P^e_{j,k}(\mathbf{s})\}} Pr(\mathbf{s}|\pi) \sum_{t \in \mathcal{T}, \pi(\mathbf{s},t) \neq (0,0)} \lambda^t P^e_{\pi(\mathbf{s},t)}(\mathbf{s}), \tag{7.13}$$

under the constraint in (7.6) and (7.8). We first relax the constraint set by letting all subscribers derive non-negative expected rewards if they follow the policy $\pi(\mathbf{s}, t)$ and ignore (7.8). We then have the following relaxed constraint set

$$W(\mathbf{s} + \mathbf{e}_{\pi(\mathbf{s},t)}, \pi^*(\mathbf{s}, t)) - P^e_{\pi(\mathbf{s},t)}(\mathbf{s}) \geq 0, \ \forall \mathbf{s}, t. \tag{7.14}$$

Clearly, the solution to the relaxed optimization problem is $\forall t \in \mathcal{T}$, $P^e_{\pi(\mathbf{s},t)}(\mathbf{s}) = W(\mathbf{s} + \mathbf{e}_{\pi(\mathbf{s},t)}, \pi^*(\mathbf{s}, t))$. By applying the solution to all $\mathbf{s} \in \mathcal{S}$, we have the optimal pricing strategy for the relaxed problem:

$$\forall \mathbf{s}, t, \ N(\mathbf{s}) < N, \ P^e_{\pi(\mathbf{s},t)}(\mathbf{s}) = W(\mathbf{s} + \mathbf{e}_{\pi(\mathbf{s},t)}, \pi^*(\mathbf{s}, t)). \tag{7.15}$$

Then, we derive the following theorem.

Theorem 17. *A policy* $\pi(s, j)$ *with the pricing strategy* $P_{j,k}^e(\mathbf{s}) = W(\mathbf{s}+\mathbf{e}_{j,k}, j, k) \, \forall \mathbf{s}, N(\mathbf{s}) < N, \; j \in \mathcal{J}, \; k \in \mathcal{K}$ *satisfies (7.8) for all* $\mathbf{s} \in \mathcal{S}$.

Proof. Notice that the expected utility from a subscription (j, k), which is $W(\mathbf{s}+\mathbf{e}_{j,k}, j, k) - P_{j,k}^e(\mathbf{s})$, becomes zero under every state, every type, and every subscription when $P_{j,k}^e(\mathbf{s}) = W(\mathbf{s} + e_{j,k}, j, k) \, \forall \mathbf{s}, N(\mathbf{s}) < N, \; j \in \mathcal{J}, \; k \in \mathcal{K}$. Therefore, the (7.8) is always satisfied. □

From Theorem 17, we can see that there is always a solution to the optimization problem in (7.13) and the solution can be described as

$$P_{j,k}^e(\mathbf{s}) = W(\mathbf{s} + \mathbf{e}_{j,k}, j, k) \,, \forall \mathbf{s} \in \mathcal{S}, N(\mathbf{s}) < N. \tag{7.16}$$

7.5.2 Optimal Pricing in Per-slot Charge Scheme

In per-slot charge scheme, a user is charged with a state-dependent $P_{j,k}(\mathbf{s})$ at each slot he stays, and no entrance fee is required. Therefore, we have $c(\mathbf{s}, j, k, 1) = P_{j,k}(\mathbf{s}) \geq 0$ and $c(\mathbf{s}, j, k, 0) = 0$ for all $\mathbf{s}, j, k$. We would like to derive the optimal pricing strategy under the constraints in (7.8).

Let $Pr(\mathbf{s}|\pi)$ be the stationary probability that the system is in state $\mathbf{s}$ under policy π. Since the policy π is fixed, the transition probability is fixed. Therefore, the original revenue maximization problem can be written as

$$\max_{\{P_{j,k}(\mathbf{s})\}} \sum_{\mathbf{s}\in\mathcal{S}} Pr(\mathbf{s}|\pi) \sum_{j\in\mathcal{J},k\in\mathcal{K}} n_{j,k}^s P_{j,k}(\mathbf{s}) \tag{7.17}$$

under the constraints in (7.8).

Let $\mathcal{R}_{j,k}$, $\mathcal{W}_{j,k}$, $\mathcal{V}_{j,k}$, and $\mathcal{P}_{j,k}$ be the $1-$by$-|\mathcal{S}|$ matrix representation of $R(\mathbf{s}, j, k)$, $W(\mathbf{s}, j, k)$ $V_{j,k}(\mathbf{s})$, and $P_{j,k}(\mathbf{s})$ over $\mathcal{S}$. Then, let $\mathcal{L}(\pi)$ be the state transition probability matrix under policy π, which is a $|\mathcal{S}|-$by$-|\mathcal{S}|$ matrix with terms $Pr(\mathbf{s}'|\mathbf{s}, \pi)$ over $\mathcal{S}$. From

(7.4) and (7.6), we have

$$(I - (1 - \mu)\mathcal{L}(\pi))\mathcal{W}_{j,k} = \mathcal{R}_{j,k} = \mathcal{V}_{j,k} - \mathcal{P}_{j,k}, \ \forall j, k$$

Therefore, the constraints in (7.8) can be re-written as

$$(I - (1 - \mu)\mathcal{L}(\pi))^{-1}(\mathcal{V}_{j,k} - \mathcal{P}_{j,k}) = \mathcal{W}_{j,k}, , \ \forall j, k \tag{7.18}$$

$$W(\mathbf{s} + \mathbf{e}_{\pi(\mathbf{s},t)}, \pi(\mathbf{s}, t)) \geq 0, \ \forall \pi(\mathbf{s}, t) \neq (0, 0) \tag{7.19}$$

$$W(\mathbf{s} + \mathbf{e}_{\pi(\mathbf{s},t)}), \pi(\mathbf{s}, t)) - W(\mathbf{s} + \mathbf{e}_{j,k}, j, k) \geq 0,$$

$$\forall \pi(\mathbf{s}, t) \neq (0, 0), (j, k) \in \mathcal{A}^t \tag{7.20}$$

$$W(\mathbf{s} + \mathbf{e}_{\pi(\mathbf{s},t)}, \pi(\mathbf{s}, t)) \leq 0,$$

$$\forall \pi(\mathbf{s}, t) = (0, 0), (j, k) \in \mathcal{A}^t \tag{7.21}$$

which is a set of linear constraints over $\mathcal{P} = \{P_{j,k}(\mathbf{s})|\mathbf{s} \in \mathcal{S}, j \in \mathcal{J}, k \in \mathcal{K}\}$. Therefore, the original maximization problem is equivalent to the following linear programming problem:

$$\max_{\mathcal{P}} \sum_{\mathbf{s} \in \mathcal{S}} Pr(\mathbf{s}|\pi) \sum_{j \in \mathcal{J}, k \in \mathcal{K}} n_{j,k}^s P_{j,k}(\mathbf{s}) \tag{7.22}$$

with the constraints in (7.18) - (7.21), which can be solved by standard linear programming methods.

7.6 Revenue-Maximized Policy

Finding revenue-maximized policy is challenging since the policy, revenue function and the pricing strategy couple together as discussed in previous sections. In such a case, the traditional MDP solvers cannot be directly applied for the revenue-maximization MDP problem. Therefore, there is a need for a more efficient approach. In this section, we will first prove that the maximum revenue under both pricing schemes is equal for any given policy. Then, we will show that there exists an optimal pricing strategy in per-slot charge scheme which always satisfies the equilibrium conditions while maximizing the

expected revenue. Moreover, such an optimal pricing strategy makes the per-state revenue independent from the policy. In such a case, we can reduce the original complex revenue maximization problem to a traditional average-reward MDP problem that can be solved efficiently.
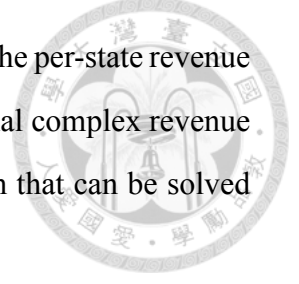
7.6.1 Revenue-Maximization Problem

In this subsection, we discuss how to formulate the revenue-maximization problem. We will use the one-time charge scheme for illustration. However, the per-slot charge scheme can be formulated in a similar way. From (7.16), we can see that the optimal price is equal to users' expected reward, which means that the revenue is maximized when the expected rewards are maximized. Let $\mathcal{L}(\pi)$ be the state transition matrix and $\mathcal{Q}^*(\mathbf{s}, \pi)$ be the revenue vector over states, which is

$$Q^*(\mathbf{s}, \pi) = \sum_{t \in \mathcal{T}, \pi(\mathbf{s},t) \neq (0,0)} \lambda^t W(\mathbf{s} + \mathbf{e}_{\pi(\mathbf{s},t)}, \pi(\mathbf{s}, t)), \tag{7.23}$$

where $W(\mathbf{s}, j, k)$ satisfies (7.6). Then, the revenue optimization problem becomes

$$\max_{\pi} \lim_{N \to \infty} \frac{1}{N} \sum_{l=1}^{N} \mathcal{L}(\pi)^{l-1} Q^*(\mathbf{s^0}, \pi), \tag{7.24}$$

which is a Markov decision process concerning the average expected reward. Unfortunately, the immediate reward $\mathcal{V}^*$ depends on the policy π, due to which, the linear programming or the traditional iteration-based algorithms cannot be directly applied here. A dynamic approach may be applied by iteratively updating the $\mathcal{V}^*$ and π. However, the convergence cannot be guaranteed.

7.6.2 Equality in Optimal Revenue and Policy

Here we state one of our main results in the revenue optimization problem.

Theorem 18. *Let $Rev^{one,*}$ and $Rev^{per,*}$ be the optimal revenue of the proposed system under one-time charge and per-slot charge schemes. Then, $Rev^{one,*} = Rev^{per,*}$.*

Proof. The proof contains two parts. In the first part, we prove that given any pricing strategy under the one-time charge scheme with a given policy π, we can always find a feasible solution under the per-slot charge scheme reaching the same revenue. In the second part, we prove vice versa. When these two directions hold for any policy, we can conclude that the optimal revenue under per-slot charge scheme is never larger or lower than under the one-time charge scheme and therefore $Rev^{one,*} = Rev^{per,*}$.

Part I: Let $\{P_{j,k}^e(\mathbf{s})\}$ be the solution to the optimization problem in (7.13). From (7.16), we have

$$P_{\pi(\mathbf{s},t)}^e(\mathbf{s}) = W^{one}(\mathbf{s} + \mathbf{e}_{\pi(\mathbf{s},t)}, \pi^*(\mathbf{s},t)), \ \forall \pi(\mathbf{s},t) \neq (0,0).$$

Then we construct the per-slot charge prices that reaches the same revenue. Let $P_{j,k}'(\mathbf{s}) = V_{j,k}(\mathbf{s}), \forall \mathbf{s}, j, k$. With such a price, we have $R^{per}(\mathbf{s},j,k) = V_{j,k}(\mathbf{s}) - P_{j,k}'(\mathbf{s}) = 0$ and therefore $W^{per}(\mathbf{s},j,k) = 0$, which satisfies (7.6) and (7.8) under any given policy. Moreover, as $\mathcal{W}^{per}$ is a linear transform of $R^{per}(\mathbf{s},j,k) = V_{j,k}(\mathbf{s}) - P_{j,k}'(\mathbf{s})$, there exists a transform matrix $A(\pi)$ with $\mathcal{W}^{per} = A(\pi)\mathcal{R}^{per} = A(\pi)\mathcal{V} - A(\pi)\mathcal{P}' = 0$. Notice that since $\mathcal{W}^{one}$ is a linear transform of $\mathcal{V}$ with the same transform matrix $A(\pi)$, we have $\mathcal{W}^{one} = A(\pi)\mathcal{V}$, which leads to $\mathcal{W}^{one} = A(\pi)\mathcal{P}'$.

The expected total payment by a user with subscription (j,k) under the per-slot charge scheme can be written using Bellman equation as follows:

$$P_{j,k}^{total,per}(\mathbf{s}) = P_{j,k}'(\mathbf{s}) + (1-\mu) \sum_{\mathbf{s}' \in \mathcal{S}} Pr(\mathbf{s}'|\mathbf{s}, \pi) P_{j,k}^{total,per}(\mathbf{s}') \qquad (7.25)$$

Let $\mathcal{P}^{t'}$ be the matrix form of $P_{j,k}^{total,per}(\mathbf{s})$. The solution $\mathcal{P}^{t'}$ to the above Bellman equation function is $\mathcal{P}^{t'} = A(\pi)\mathcal{P}' = \mathcal{W}^{one}$. Finally, a type t user that arrives in state $\mathbf{s}$ submits the subscription $\pi(\mathbf{s},t)$ to the system. The per-slot charge payment starts as soon as he enters the system, where the state becomes $\mathbf{s} + \mathbf{e}_{\pi(\mathbf{s},t)}$. Therefore, the expected revenue generated from the type t user under π with $P_{j,k}'(\mathbf{s})$ is

$$P^{total,per,t} = P_{\pi(\mathbf{s},t)}^{total,per}(\mathbf{s} + \mathbf{e}_{\pi(\mathbf{s},t)}) = W^{one}(\mathbf{s} + \mathbf{e}_{\pi(\mathbf{s},t)}, \pi^*(\mathbf{s},t)), \qquad (7.26)$$

which is exactly the same as the optimal one-time charge price $P_{j,k}^e(\mathbf{s})$. Therefore, the expected revenue Rev^{per} under the per-slot charge scheme with price $\{P'_{j,k}(\mathbf{s}) = V_{j,k}(\mathbf{s})\}$ should be equal to the one under the one-time charge scheme with price $\{P_{j,k}^e(\mathbf{s})\}$. As a result, $Rev^{per,*} \geq Rev^{per} = Rev^{one,*}$.

Part II: Let $\{P_{j,k}(\mathbf{s})\}$ be a feasible solution to the optimization problem in (7.22) and $\mathcal{P}$ is its matrix form. Since it is a feasible solution, it should satisfy (7.18) - (7.21). Recalling the Bellman equation in (7.25) and let $\mathcal{P}^t$ be the matrix form of the expected revenue generated by a type t user under $\{P_{j,k}(\mathbf{s})\}$, we have $\mathcal{P}^t = A(\pi)\mathcal{P}$. In addition, the expected reward $W_{j,k}^{per}(\mathbf{s})$ in matrix form is

$$\mathcal{W}^{per} = A(\pi)\mathcal{R}^{per} = A(\pi)\mathcal{V} - A(\pi)\mathcal{P} = W^{one} - A(\pi)\mathcal{P}. \qquad (7.27)$$

According to the above discussion and (7.18), we have

$$P^{total',per,t} \leq W^{one}(\mathbf{s} + \mathbf{e}_{\pi(\mathbf{s},t)}, \pi^*(\mathbf{s},t)), \ \forall \pi(\mathbf{s},t) \neq (0,0)$$

which means that the expected revenue from user t is bounded by $W^{one}(\mathbf{s}+e_{\pi(\mathbf{s},t)}, \pi^*(\mathbf{s},t))$. Therefore, the expected overall revenue is

$$
\begin{aligned}
Rev^{per} &= Pr(\mathbf{s}|\pi)\sum_{t\in\mathcal{T}} \lambda^t P_{\pi^*(\mathbf{s},t)}^{total,per}(\mathbf{s}) \\
&\leq Pr(\mathbf{s}|\pi)\sum_{t\in\mathcal{T}} \lambda^t W^{one}(\mathbf{s} + \mathbf{e}_{\pi(\mathbf{s},t)}, \pi^*(\mathbf{s},t)) \\
&= Rev^{one,*}.
\end{aligned}
$$

Therefore, we have $Rev^{one,*} \geq Rev^{per}$ for all feasible $\{P_{j,k}(\mathbf{s})\}$, which means $Rev^{one,*} \geq Rev^{per,*}$. Combining the results in Part I and II, we conclude that $Rev^{one,*} = Rev^{per,*}$. $\square$

From Theorem 18, we can see that both pricing schemes have the same maximum expected revenue when the optimal pricing strategies are applied. In other words, these two schemes are equivalent in terms of revenue optimization. Moreover, in the Part I of the proof, we observe that a simple pricing strategy under the per-slot charge scheme leads

to the same optimal revenue under the one-time charge scheme, which is

$$P^*_{j,k}(\mathbf{s}) = V_{j,k}(\mathbf{s}), \ \forall \mathbf{s} \in \mathcal{S}, j \in \mathcal{J}, k \in \mathcal{K}. \tag{7.28}$$

Since the revenue under such a pricing strategy reaches the same optimal value of the one-time charge scheme, it is also the optimal solution to the per-slot charge scheme. Such a pricing strategy is very useful since the price and per-state revenue is now independent from the policy. The optimal policy can then be derived by formulating the problem as a traditional average-reward MDP with $V(\mathbf{s}) = \sum_{j,k} n^s_{j,k} P^*_{j,k}(\mathbf{s})$ as its immediate reward.

7.6.3 Algorithm for Finding Revenue-Maximized Policy

In Algorithm 4, we propose a value iteration method to find the ϵ-optimal solution. Since both pricing schemes share the same optimal revenue under the same policy, the policy found through Algorithm 4 is optimal under both pricing schemes.

Algorithm 4 Value Iteration for Revenue-Maximization Solution

1: Initialize $\pi^o, W^{v,o}$
2: **while** 1 **do**
3:     $\forall \mathbf{s} \in \mathcal{S}, \pi^n \leftarrow \arg\max_{\pi(\mathbf{s})}\{V(\mathbf{s}) + \sum_{\mathbf{s}' \in \mathcal{S}} Pr(\mathbf{s}'|\mathbf{s}, \pi(s))W^{v,o}(\mathbf{s}')\}\}$
4:     $\forall \mathbf{s} \in \mathcal{S}, W^{v,n}(\mathbf{s}) \leftarrow V(\mathbf{s}) + \sum_{\mathbf{s}' \in \mathcal{S}} Pr(\mathbf{s}'|\mathbf{s}, \pi^n)W^{v,o}(\mathbf{s}')$
5:     $W^{v,d} \leftarrow W^{v,n} - W^{v,o}$
6:     **if** $\max W^{v,d} - \min W^{v,d} < \epsilon$ **then**
7:        Break
8:     **else**
9:        $W^{v,o} \leftarrow W^{v,n}$
10:    **end if**
11: **end while**
12: Output π^n and $W^{v,n}$

The convergence and optimality of such an algorithm is guaranteed as shown in [120]. Notice that under the optimal pricing strategy $P^*_{j,k}(\mathbf{s})$, the per-state revenue is

$$V(\mathbf{s}) = \sum_{j \in \mathcal{J}, k \in \mathcal{K}} n^s_{j,k} P^*_{j,k}(\mathbf{s}) = \sum_{j \in \mathcal{J}, k \in \mathcal{K}} V_{j,k}(\mathbf{s}), \tag{7.29}$$

which is the overall user's valuation on the system, i.e., social welfare, in state $\mathbf{s}$. Therefore, the solution to the revenue-maximization problem also maximizes the social welfare of the

system. As a result, we have the following corollary.

Corollary 4. *When $\epsilon \to 0$, the revenue-maximized policy derived in Algorithm 4 is equivalent to a socially-optimal policy.*

Nevertheless, the value-iteration algorithm 4 converges slowly as $\epsilon \to 0$ since the revenue-optimization problem is an average-reward MDP system. Next, we will propose an approximate algorithm based on a discounted MDP model.

7.6.4 Approximate Optimal Policy

Here we propose a discounted MDP model as an approximation to the average-reward MDP. By modeling the revenue-optimization problem as a discounted MDP system, we propose an approximate algorithm which converge to the optimal policy in significantly less rounds.

We first model the revenue-optimization problem as a γ-discounted Markov decision process. We introduce γ as a discounted factor for the service provider on the future revenue, where $1 > \gamma > 0$. Then, let $W^\gamma(\mathbf{s})$ be the expected total revenue if the current state is $\mathbf{s}$, then we have

$$W^\gamma(\mathbf{s}) = \sum_{l=0}^{\infty} \mathbb{E}[(1-\gamma)^l V(\mathbf{s^l})|\mathbf{s^0} = \mathbf{s}], \tag{7.30}$$

Notice that when γ is close to 0, the expected reward is arbitrarily close to the average expected reward. Given the γ, we can derive the γ-optimal policy through the following process. According to the Bellman equation, the expected total revenue can be written as follows:

$$W^\gamma(\mathbf{s}) = V(\mathbf{s}) + (1-\gamma) \sum_{\mathbf{s'} \in \mathcal{S}} Pr(\mathbf{s'}|\mathbf{s}, \pi) W(\mathbf{s'}), \tag{7.31}$$

where transition probability $Pr(\mathbf{s'}|\mathbf{s}, \pi)$ is given in (7.11).

For the optimal policy, the service provider should choose the action that maximizes

its expected total revenue at every state, which is as follows:

$$\pi^\gamma(\mathbf{s}) = \arg \max_\pi \sum_{t \in \mathcal{T}} \lambda^t W^\gamma(\mathbf{s} + e_{\pi(s,t)}).$$

(7.32)

Notice that both (7.31) and (7.32) are coupling together. These two equations describes the optimality conditions of the proposed γ-discounted MDP.

7.6.5 Policy Iteration γ-Optimal Algorithm

As shown in literature [120], the γ-optimal policy π^γ and expected reward W^γ can be solved by policy iteration algorithm. We provide such an algorithm in Algorithm 5.

Algorithm 5 Policy Iteration for γ-Optimal Solution

1: Initialize π^o
2: **while** 1 **do**
3:     Solve W^n using (7.31) with $\pi = \pi^o$
4:     Solve π^n using (7.32) with $W = W^n$
5:     **if** $\pi^n = \pi^o$ **then**
6:         Break
7:     **else**
8:         $\pi^o \leftarrow \pi^n$
9:     **end if**
10: **end while**
11: Output π^n and W^n

Notice that the convergence of Algorithm 5 is guaranteed as this is a traditional discounted MDP problem with a fixed discounted factor [120]. In addition, the algorithm terminates in polynomial time, which is much faster than Algorithm 4. In all of our simulations, the approximated algorithm converges in less than ten rounds with the resulting revenue loss less than 1% when the discounted factor γ is 0.01. We provide further discussions on this through simulations in Section 7.7.

7.7 Simulation Results

We evaluate the efficiency of the proposed approach through simulations. We consider a SVC multicasting service over a WiMAX network. The wireless system parameters

Table 7.1: Transmission Throughput

Quality	Modulation	Data Rate (Mbps)
1	BPSK 1/2	3.8768
2	QPSK 1/2	7.7552
3	QPSK 3/4	11.6336
4	QAM32 1/2	15.512
5	QAM32 3/4	23.2688
6	QAM64 2/3	31.0256
7	QAM64 3/4	34.904

follow the WiMAX standard, in which 7 level of MCSs are chosen and given in Table 7.1. Then, let each MCS's lowest required SINR be $g_1 \sim g_7$. According to the requirements, the channel quality is quantized to seven levels $\mathcal{G} = \{1, 2, 3, 4, 5, 6, 7\}$. A user with the channel quality $g \in \mathcal{G}$ can receive data streams transmitted by up to g-th MCS. In all simulations, we assume g is uniformly distributed in these seven levels in every time slot. Let the data rates offered by the MCSs be $r_1 \sim r_7$, where the exact values are given in Table 7.1. A data stream with a bit-rate of R requires R/r_m time to transmit at each slot if MCS m is chosen.

We simulate a SVC multicasting server which provides two videos, MOBCAL and STOCKHOLM, recorded by SVT Sveriges Television AB [121]. We use JSVM reference software [122] to encode each video into a three-layer spatial-scaled H.264 SVC video stream. The resulting video bit-rates, resolutions, and peak-signal-to-noise-ratio (PSNR) of each video with different layers can be found in Table 7.2.

The server can serve up to 12 users, while the total available service time per second is a ratio between 0% and 100%. There are four types of users with their preferences on videos with different computation capabilities, which are specified in Table 7.3. The user's valuations on each layer of each video are shown in Table 7.2. Finally, the user arrival and departure parameters are set to be 0.04 and 0.01.

The resource allocation rule $\mathcal{D}$, which determines the applied MCS $\{g_{j,k}\}$ in each state, is maximizing the expected overall valuation given the current demands of videos and corresponding layers from the users. The optimal solution is derived through exhaustive search in the simulations. Notice that any approximated approach to the snapshot-based

Table 7.2: Video Specifications
MOBCAL

Layer	Bit-Rate (kbps)	Resolution	PSNR	User Valuation
1	315.33	360i	29.74	0.5
1,2	1660.83	720i	33.38	0.75
1,2,3	10719.41	1080i	33.80	1

STOCKHOLM

Layer	Bit-Rate (kbps)	Resolution	PSNR	User Valuation
1	319.75	360i	29.70	0.8
1,2	1480.32	720i	33.68	0.9
1,2,3	6806.29	1080i	34.01	1

Table 7.3: User Specifications

Type	Preferred Video(s)	Maximum Layer
1	MOBCAL	2
2	STOCKHOLM	2
3	STOCKHOLM	3
4	MOBCAL,STOCKHOLM	3

optimization problem in the literature is applicable to our system.

We evaluate the system efficiency through two performance metrics: average social welfare, which is the total users' valuations on the service, and average revenue of the proposed SVC multicasting system. For the social welfare performance, we compare two policies: revenue-maximized policy and free subscription policy. The revenue-maximized policy is given by Algorithm 4 with $\epsilon = 0.0001$. The free subscription policy is the solution to (7.6) and (7.8) without payment, i.e., $P_{j,k}^e = P_{j,k} = 0, \forall j, k$. Free subscription represents the case that all users that are capable of evaluating the expected service quality are free to subscribe any video without any payment. By comparing these two policies, we can evaluate the efficiency loss when no pricing scheme is applied.

For the performance of the average revenue, we compare three pricing schemes: optimal one-time charge pricing, optimal per-slot charge pricing, and maximum fixed entrance fee. The first two schemes are the proposed pricing schemes as discussed in Section 7.6, while the third one is the pricing scheme with a fixed entrance fee, which is widely adopted in current video subscription services. In the simulation, the entrance fee for the maximum
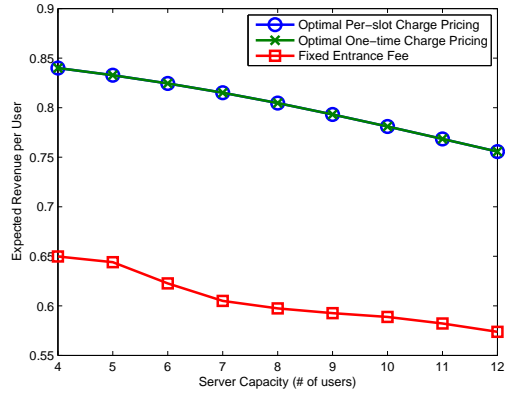
(a) Social Welfare per Capacity

(b) Revenue per Capacity

Figure 7.3: System Performance under Different Server Capacity

fixed entrance fee scheme is chosen as $P^e = \min_{\mathbf{s},t,\pi(\mathbf{s},t)\neq(0,0)} W^{indv}(\mathbf{s} + \mathbf{e}_{\pi(\mathbf{s},t)}, \pi(\mathbf{s},t))$, where W^{indv} is the expected reward under the free subscription policy. Note that with such a fixed payment, the free subscription policy still satisfies (7.8).

7.7.1 Effect of Server Capacity

We first study how the server capacity influences the social welfare and the revenue by adjusting the server capacity N from 4 to 12 while keeping all other settings unchanged. The simulation results are shown in Fig. 7.3.

From Fig. 7.3(a), we can see that the proposed revenue-maximized policy achieves better average social welfare performance compared with the free subscription policy under all server capacities, which verifies that there will be an efficiency loss if no pricing scheme is applied. Notice that under both policy the social welfare per capacity decreases
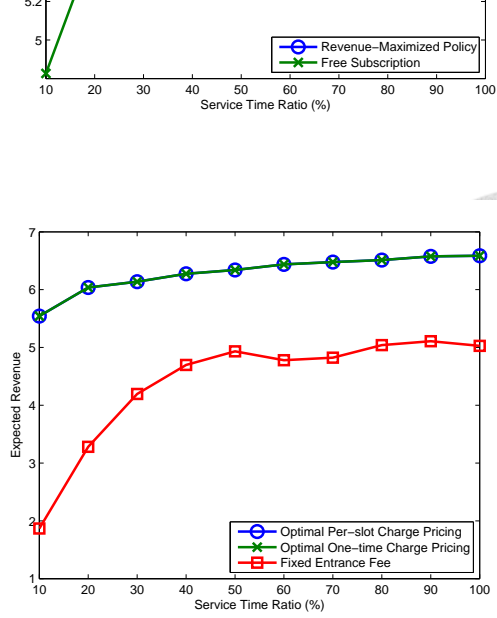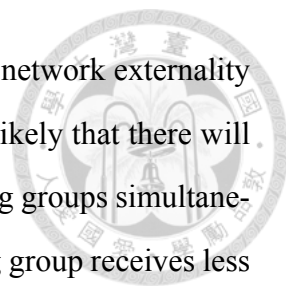
(a) Social Welfare

(b) Revenue

Figure 7.4: System Performance under Different Available Service Time Ratio

Table 7.4: Expected revenue under different discounted factor γ

γ	0.10	0.09	0.08	0.07	0.06	0.05	0.04	0.03	0.02	0.01	0.001	0
Convergence round	4	4	4	4	4	5	5	5	5	4	3	1080
Revenue	5.1838	5.3158	5.3887	5.3887	5.3888	5.4000	5.4987	5.4987	5.5394	5.5421	5.5424	5.5425
Efficiency	0.9353	0.9591	0.9723	0.9723	0.9723	0.9743	0.9921	0.9921	0.9995	0.9999	1	1

with the expansion of the server capacity. This is due to the negative network externality effect in this system. When the server capacity increases, it is more likely that there will be more users with different demands, which means more multicasting groups simultaneously. Given the fixed amount of service time ratio, each multicasting group receives less service time. This generally impairs all users' utilities in this system and therefore reduces the social welfare per user.

From Fig. 7.3(b), we can see that both optimal per-slot charge pricing and one-time charge pricing result in the same revenue under all scenarios, which verifies our conclusion in Theorem 18. Moreover, the revenue under both optimal pricing schemes is significantly higher than the fixed entranced fee as the later one loses a large amount of revenue from users with higher valuations on the service. Again, both pricing schemes have lower revenue per capacity when the server capacity expands. The negative network externality in this system also has a negative effects on the revenue in this case.

7.7.2 Effect of Service Time Ratio

Then, we investigate how the amount of service time affects the efficiency of the SVC multicasting system under different policies. We control the service time ratio in the system from 0 to 100% with other settings unchanged. The simulations results are shown in Fig. 7.4.

From Fig. 7.4(a), we observe that the revenue-maximized policy always achieves better performance than the free subscription policy. For the performance of the average revenue shown in Fig. 7.4(b), we again observe that both optimal pricing schemes have higher revenue than the fixed entrance fee. Notice that the revenue under fixed entrance fee does not always increase when the service time ratio increases. This phenomenon comes from the fact that the optimal resource allocation problem in (7.1) is nonlinear. When the service time increases, it is possible that some streams eventually get less resource in order to improve the transmission quality of other streams along with the increased resource under the optimal allocation. In such a case, the fixed entrance fee scheme has a lower revenue since the price under this scheme is constrained by the video stream with

lowest expected reward. Nevertheless, our proposed pricing schemes are resistant to this effect since the expected revenue under our pricing schemes are equal to the overall social welfare, which is maximized and nondecreasing with the increases of service time when the optimal solution in (7.1) is applied.
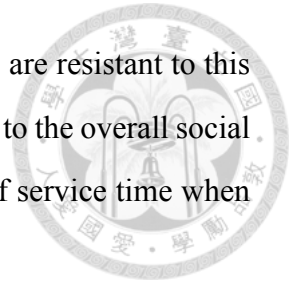
7.7.3 Efficiency of Approximate Algorithm

Finally, we evaluate the convergence speed and solution quality of the proposed $\gamma-$optimal algorithm. We set the maximum number of users as 8 and the service time ratio as 10% with other settings unchanged. Then, we control the discounted factor γ in Algorithm 5 from 0.1 to 0.001, and compare it with the $\epsilon-$optimal solution derived in Algorithm 4 with $\epsilon = 0.00001$. The simulation results are shown in Table 7.4.

We observe that when the discounted factor γ decreases, the resulting expected revenue with Algorithm 5 is closer to the optimal one with Algorithm 4. When γ is 0.01, there is only 0.01% revenue loss from Algorithm 5. When γ decreases to 0.001, the derived policy is the same as the one from Algorithm 4, and the expected revenue is equal under both algorithms. In addition, the convergence round never exceeds 5 under any simulated γ. In contrasts, Algorithm 4 requires 1080 rounds to converge. We conclude that the proposed $\gamma-$optimal algorithm provides efficient approximate solutions to the revenue-maximization problem with much less computational complexity.

7.8 Summary

In this chapter, we proposed a novel framework to study a general stochastic SVC multicasting system. This framework supports stochastic user arrival and heterogeneous user preferences and is applicable to existing resource allocation algorithms in the literature. A subscription-based payment system was studied in this framework for exploring the economic value of the system with rational users. The responses of selfish users under two pricing schemes, one-time charge scheme and per-slot charge scheme, were discussed and the equilibrium conditions were derived as the constraints of the corresponding rev-

enue optimization problem for the service provider. We theoretically proved that both pricing schemes reach the same optimal revenue under all policies, and the optimal pricing strategies and policies which maximize the expected revenue of the system can be efficiently derived by reducing the M-MDP problem to a traditional average-reward MDP problem. Moreover, we showed that the revenue-maximized policy is a socially-optimal policy, which means that the proposed optimal policy also maximizes the social welfare.

Chapter 8

Conclusions and Future Work

8.1 Conclusions

In this dissertation, we propose novel game-theoretic approaches to several resource management problems in the state-of-the-art wireless systems, which are heterogeneous networks, D2D communication, and multicasting system. All the studied systems share the same characteristic that devices may selfishly compete for the limited resource in the wireless system, as we illustrated in each chapter. In such systems, we observe undesired operations which are unexpected from traditional perspectives. The system performance is also degraded due to fierce competitions among participants. Therefore, we propose novel game-theoretic solutions for each problem to tackle in order to regulate the selfish behaviors of participants while keeping reasonable efficiency and practicability.
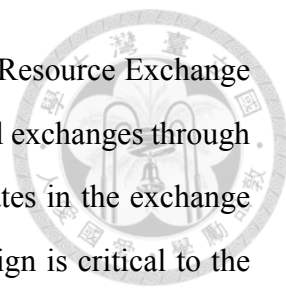
In Chapter 2, we proposed a femtocell cell-breathing control framework for determining the optimal coverage of the femtocell and allocating limited femtocell backhaul data rate to MSes fairly and efficiently. FEVER mechanism, a novel Virtual Election based mechanism to collect all MSes' channel quality information, was proposed. FEVER mechanism was shown to be truthful, and we proved that through different choice of selected vote order, the balance between system throughput and allocation fairness among MSes can be maintained. We also demonstrated the implementation of FEVER mechanism in different subscriber group modes by proposing SG-FEVER mechanism. The LTE-based realistic simulation results not only verify the performance enhancement under FEVER

mechanism, but also show the benefits of Hybrid mode to the overlay system.

In Chapter 3, we demonstrate how to maximize the profit of an unlimited data plan through femtocell systems and specialized contract designs. When the service quality of an MS is verifiable, we employ the service differentiation in the differentiated contracts to maximize the service provider's profits. By contrast, when the service quality cannot be verified, the incentive compatible condition is to prevent MSs from cheating when signing the contract. We prove that only flat fee contracts are incentive compatible in a split-spectrum system, and the differentiated contracts can be incentive compatible in shared-spectrum systems. We conclude that a service provider can indeed derive more profits from MSs by 1) introducing femtocell services, and 2) provide differentiated contracts. The former increases MSs' valuation on the service, while the latter derives more customer surplus from MSs using the femtocell service, while offering other MSs an affordable deal.

In Chapter 4, we study the carrier aggregation design in LTE-Advanced system through a game-theoretic perspective. We first address the heterogeneous carrier quality and QoS requirements of UEs by modeling the resource allocation problem in carrier aggregation as a utility-based non-linear optimization problem. Given that the optimization problem is NP-hard, we aim to find an efficient algorithm to find the near-optimal solution. Additionally, we address the potential threats from the selfish UEs, who may report their QoS requirements untruthfully and therefore induce an unfair and inefficient resource allocation, by proposing a truthful auction design. The proposed auction provides an efficient greedy algorithm to satisfy the QoS requirements of UEs through carrier aggregation with reasonable computation time. Additionally, it guarantees the existence of truthful Nash equilibrium and therefore prevents the rational UEs from reporting manipulated QoS requirements. The simulation results verified that the proposed auction design for carrier aggregation enhances the LTE-Advanced system's capability to satisfy UE's QoS requirements.

In Chapter 5, we proposed a novel resource-exchange-based D2D resource allocation framework for an LTE - Advanced system. We showed that the convergence of any algorithm in the framework is guaranteed when all performed exchanges are beneficial. Based

on the idea of beneficial exchange, we proposed the Trader-assisted Resource Exchange (T-REX) mechanism. The T-REX mechanism identifies the beneficial exchanges through analysing the corresponding exchange graph. The eNodeB participates in the exchange process through designing the trader preference functions. This design is critical to the convergence speed, as has been shown in the simulations. Through game-theoretic analysis, we also proved that when the trader preference functions are properly designed, the T-REX mechanism is strategy-proof. This prevents the eNodeB from receiving forged CQI reports from rational D2D devices and users. Finally, we evaluated the performance of the T-REX mechanism through simulations. The simulations with the parameters suggested in the latest 3GPP technical contribution showed that the T-REX mechanism significantly mitigates the interference experienced by D2D devices.

In Chapter 6, we proposed a new game, called Chinese Restaurant Game, by combining the strategic game-theoretic analysis and non-strategic machine learning technique. The proposed Chinese restaurant game can provide a new general framework for analyzing the strategic learning and predicting behaviors of rational agents in a social network with negative network externality. By conducting the analysis on the proposed game, we derived the optimal strategy for each agent and provided a recursive method to achieve the equilibrium. The tradeoff between two contradictory advantages, which are making decisions earlier for choosing better tables and making decisions later for learning more accurate believes, is discussed through simulations. We found that both the signal quality of the unknown system state and the table size ratio affect the expected utilities of customers with different decision orders. Generally, when the signal quality is low and the table size ratio is high, the advantage of playing first dominates the benefit from learning. On the contrary, when the signal quality is high and the table size ratio is low, the advantage of playing later for better knowledge on the true state increases the expected utility of later agents. Finally, we illustrated a specific application of Chinese restaurant game in wireless networking: the cooperative spectrum access problem in cognitive radio networks. We showed that the overall channel utilization can be improved by taking the negative network externality into account in secondary users' decision process. The inter-
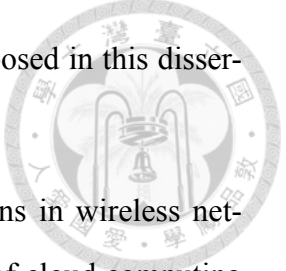
ference from secondary users to the primary user can also be reduced through learning.

In Chapter 7, we proposed a novel framework to study a general stochastic SVC multicasting system. This framework supports stochastic user arrival and heterogeneous user preferences and is applicable to existing resource allocation algorithms in the literature. A subscription-based payment system was studied in this framework for exploring the economic value of the system with rational users. The responses of selfish users under two pricing schemes, one-time charge scheme and per-slot charge scheme, were discussed and the equilibrium conditions were derived as the constraints of the corresponding revenue optimization problem for the service provider. We theoretically proved that both pricing schemes reach the same optimal revenue under all policies, and the optimal pricing strategies and policies which maximize the expected revenue of the system can be efficiently derived by reducing the M-MDP problem to a traditional average-reward MDP problem. Moreover, we showed that the revenue-maximized policy is a socially-optimal policy, which means that the proposed optimal policy also maximizes the social welfare.

8.2   Future Work

Along with the development of heterogeneous network and device-to-device communications, there exists a trend on next-generation wireless networking system favoring a more open, distributed and user-oriented network scenario, such as liquid cell and local IP access (LIPA) in LTE-Advanced. Assisted by some existing infrastructure such as base stations and backhaul, a distributed network can be more flexible in resource allocation, while a user-oriented network responds to the user's demands and requirements more suitably and rapidly. Nevertheless, such a scenario increases the participant ratio and power of users in the network configuration and deployments. As we illustrated in this dissertation, these potentially rational and selfish users may perform unexpected and undesired operations in the wireless network. These selfish operations, if not regulated, may decrease the system performance or even harm the system stability. How an open, distributed, and user-oriented wireless system could regulate these powerful and selfish users is a serious challenge in next-generation wireless networks. This challenge potentially could be well

addressed by game theory through extending the approaches we proposed in this dissertation.

Additionally, the security and privacy become important concerns in wireless networks. People rely on the Internet in their daily life. The advances of cloud computing make individuals and enterprises tend to store, access, and compute their valuable information on the Internet. All the information should be securely processed, especially for the access part, since they may be confidential and critical to the owners. Additionally, popular online social networks such as Facebook and Twitter become one of the main mediums for people to interact with their friends and relatives. These interactions are conducted through the Internet, while most of them are private and should not be known by others. As a result, people demand for always-online, secure, and privacy-preserving Internet service, which could be achieved only by wireless networking services. The next-generation wireless networks should not only provide high-speed and stable Internet connections, but also let users access their requested contents securely. However, the threats from malicious attackers and hackers grow significantly in recent years. The future wireless network service is expected to be more distributed, complex, and user-oriented. These characteristics make the system much more difficult to defend itself from the attackers, or requires a significant high cost to provide secure wireless communications. How the system should defend those malicious attackers considering the corresponding cost and loss is also a critical issue. Potentially, this issue could also be addressed by game theory. We may take both attackers and networks as players, while their attack/defense operations as their actions. The corresponding cost and loss can be formulated as the utility of the players. In such an approach, we can investigate how network and attackers interact with each other through game theory. Base on the results, we may apply various solution concepts in game theory to find a desirable solution which maintains the security requirement in a rational and cost efficient way.
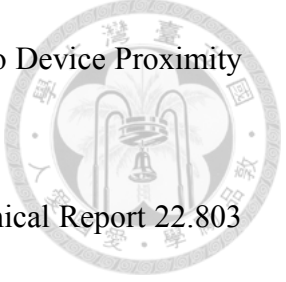
In sum, we have explored the potentials of game theory to regulate the selfish behaviors of participants in the resource allocation problems in next-generation wireless networks in our previous work. In the future, we would like to extend the proposed resource allocation
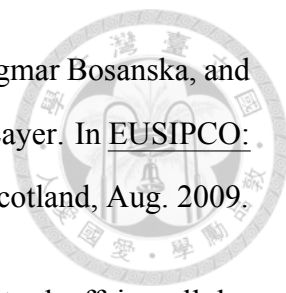
approaches to more advanced transmission techniques and novel network scenarios, such as CoMP, liquid cell, and LIPA. Additionally, we may explore the potentials of game theory in addressing the security design in wireless networks, especially for the attack/counterattack interactions between attackers and networks. We believe that game theory can be powerful tools to address these on-the-rise issues. Our ultimate goal is to establish a general game-theoretic framework that includes both the resource allocation and security aspects of the wireless network system in order to have a comprehensive view on the challenges next-generation wireless network.
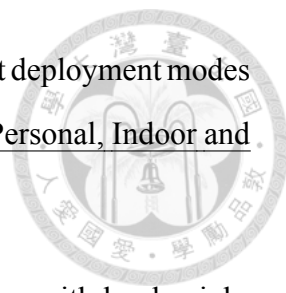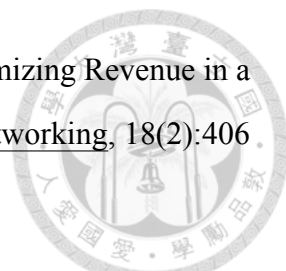
Bibliography

[1] ITU-R. Guidelines for evaluation of radio interface technologies for IMT-Advanced. Technical Report ITU-R M. 2135, ITU, 2008.

[2] Alcatel-Lucent. DL E-UTRA performance checkpoint. Technical Report R1-071967, 3GPP TSG-RAN1, 2007.

[3] Alcatel-Lucent. R1-130469: LTE device to device evaluation methodology. 3GPP TSG-RAN1 Meeting #72, Jan. 2013.

[4] S. Parkvall, A. Furusk□ andr, and E. Dahlman. Evolution of LTE toward IMT-advanced. IEEE Communications Magazine, 49(2):84 --91, Feb. 2011.

[5] D. Lopez-Perez, I. Guvenc, G. de la Roche, M. Kountouris, T.Q.S. Quek, and Jie Zhang. Enhanced intercell interference coordination challenges in heterogeneous networks. IEEE Wireless Communications, 18(3):22 --30, June 2011.

[6] D. Lopez-Perez, A. Valcarce, G. de la Roche, and Jie Zhang. OFDMA femtocells: A roadmap on interference avoidance. IEEE Communications Magazine, 47(9):41 --48, Sep. 2009.

[7] G. Fodor, E. Dahlman, G. Mildh, S. Parkvall, N. Reider, G. Miklos, and Z. Turanyi. Design aspects of network assisted Device-to-Device communications. IEEE Communications Magazine, 50(3):170 --177, March 2012.

[8] Marcel Groβsmann. Proximity enhanced mobile d2d video streaming. New York, NY, USA, Aug. 2012. ACM.

[9] Qualcomm Incorporated. RP-122009: Study on LTE Device to Device Proximity Services. 3GPP TSG RAN Meeting #58, Dec. 2012.

[10] 3GPP. Feasibility Study on Proximity Services (ProSe). Technical Report 22.803 v12.0.0, 3GPP Service and System Aspects WG 1, Dec. 2012.

[11] P. Li, H. Zhang, B. Zhao, and S. Rangarajan. Scalable Video Multicast With Adaptive Modulation and Coding in Broadband Wireless Data Systems. IEEE-ACM Trans. on Networking, 20(1):57--68, Feb. 2012.

[12] W.-H. Kuo, W. Liao, and T. Liu. Adaptive Resource Allocation for Layer-Encoded IPTV Multicasting in IEEE 802.16 WiMAX Wireless Networks. IEEE Trans. on Multimedia, 13(1):116--124, Feb. 2011.

[13] Y. Yu, P. Hsiu, and A. Pang. Energy-Efficient Video Multicast in 4G Wireless Systems. IEEE Trans. on Mobile Computing, to appear.

[14] H. Schwarz, D. Marpe, and T. Wiegand. Overview of the Scalable Video Coding Extension of the H.264/AVC Standard. IEEE Trans. on Circuits and Systems for Video Technology, 17(9):1103 --1120, Sep. 2007.

[15] N. Nisan, T. Roughgarden, and V. V. Vazirani. Algorithmic Game Theory. Cambridge University Press, 2007.

[16] Holger Claussen, Lester T. W. Ho, and Louis G. Samuel. An Overview of the Femtocell Concept. Bell Labs Technical Journal, 13(1):221--245, 2008.

[17] V. Chandrasekhar, J. Andrews, and A. Gatherer. Femtocell networks: a survey. IEEE Communications Magazine, 46(9):59--67, Sep. 2008.

[18] A. Golaup, M. Mustapha, and L. B. Patanapongpibul. Femtocell access control strategy in UMTS and LTE. IEEE Communications Magazine, 47(9):117--123, Sep. 2009.

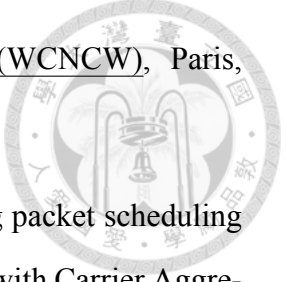[19] R. Farquharson. Theory of voting. Blackwell Oxford, 1969.

[20] Christian Mehlführer, Martin Wrulich, Josep Colom Ikuno, Dagmar Bosanska, and Markus Rupp. Simulating the Long Term Evolution Physical Layer. In EUSIPCO: The 17th European Signal Processing Conference, Glasgow, Scotland, Aug. 2009.

[21] V.V. Veeravalli and A. Sendonaris. The coverage-capacity tradeoff in cellular CDMA systems. IEEE Trans. on Vehicular Technology, 48(5):1443 --1450, Sep. 1999.

[22] J.Y. Le Boudec. Rate adaptation, congestion control and fairness: A tutorial. 2005.

[23] S. Ching. Strategy-proofness and !'§median voters!¨. International Journal of Game Theory, 26(4):473--490, 1997.

[24] R. Jain, A. Durresi, and G. Babic. Throughput fairness index: an explanation. In ATM Forum Contribution 99, volume 45, 1999.

[25] A. Jalali. On cell breathing in CDMA networks. In IEEE International Conference on Communications (ICC), Jun. 1998.

[26] Shih-Tsung Yang and A. Ephremides. Resolving the CDMA cell breathing effect and near-far unfair access problem by bandwidth-space partitioning. In IEEE Vehicular Technology Conference (VTC Spring), May 2001.

[27] P. Bahl, MT Hajiaghayi, K. Jain, SV Mirrokni, L. Qiu, and A. Saberi. Cell breathing in wireless lans: Algorithms and evaluation. IEEE Trans. on Mobile Computing, 6(2):164--178, 2007.

[28] Y. Bejerano and Seung-Jae Han. Cell breathing techniques for load balancing in Wireless LANs. IEEE Trans. on Mobile Computing, 8(6):735 --749, Jun. 2009.

[29] Shu-ping Yeh, S. Talwar, Seong-choon Lee, and Heechang Kim. WiMAX femtocells: a perspective on network architecture, capacity, and coverage. IEEE Communications Magazine, 46(10):58--65, Oct. 2008.
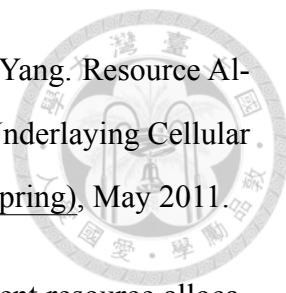
[30] H. A. Mahmoud and I. Guvenc. A comparative study of different deployment modes for femtocell networks. In *IEEE International Symposium on Personal, Indoor and Mobile Radio Communications (PIMRC)*, Sep. 2009.

[31] D. Choi, P. Monajemi, Kang Shinjae, and J. Villasenor. Dealing with loud neighbors: The benefits and tradeoffs of adaptive femtocell access. In *IEEE Global Communications Conference (GLOBECOM)*, Nov. 2008.

[32] A. Valcarce, D. Lopez-Perez, G. De La Roche, and Zhang Jie. Limited access to OFDMA femtocells. In *IEEE International Symposium on Personal, Indoor and Mobile Radio Communications (PIMRC)*, Tokyo, Japan, Sep. 2009.

[33] G. de la Roche, A. Valcarce, D. Lopez-Perez, and Zhang Jie. Access control mechanisms for femtocells. *IEEE Communications Magazine*, 48(1):33--39, Jan. 2010.

[34] T. Akbudak and A. Czylwik. Distributed power control and scheduling for decentralized OFDMA networks. In *IEEE International ITG Workshop on Smart Antennas (WSA)*, pages 59 --65, Bremen, Germany, Feb. 2010.

[35] Xiangfang Li, Lijun Qian, and D. Kataria. Downlink power control in co-channel macrocell femtocell overlay. In *43rd Annual Conference on Information Sciences and Systems (CISS)*, pages 383 --388, Baltimore, Maryland, USA, March 2009.

[36] E. Jorswieck and R. Mochaourab. Power control game in protected and shared bands: Manipulability of Nash Equilibrium. In *International Conference on Game Theory for Networks (GameNets)*, Istanbul, Turkey, May 2009.

[37] J. D. Hobby and H. Claussen. Deployment Options for Femtocells and Their Impact on Existing Macrocellular Networks. *Bell Labs Technical Journal*, 13(4):145--160, 2009.

[38] Ravishankar Borgaonkar, Kevin Redon, and Jean-Pierre Seifert. Security Analysis of a Femtocell Device. In *SIN '11*, Nov. 2011.
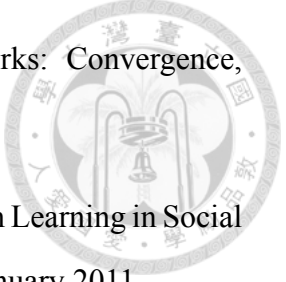
[39] T. Bergstrom and M. Bagnoli. Log-concave Probability and its Applications. Economic theory, 26:445--469, 2005.

[40] S. Ren, J. Park, and M. Schaar. Subscription Dynamics and Competition in Communications Markets. ACM NetEcon '10, Oct. 2010.

[41] S. Das, H. Lin, and M. Chatterjee. An Econometric Model for Resource Management in Competitive Wireless Data Networks. IEEE Network, 18(6):20 -- 26, 2004.

[42] M.C. Mozer, R. Wolniewicz, D.B. Grimes, E. Johnson, and H. Kaushansky. Predicting Subscriber Dissatisfaction and Improving Retention in the Wireless Telecommunications Industry. Neural Networks, Jan. 2002.

[43] A. Aram, C. Singh, S. Sarkar, and A. Kumar. Cooperative Profit Sharing in Coalition based Resource Allocation in Wireless Networks. IEEE INFOCOM '09, Jan. 2009.

[44] G. L. Bodic, J. Irvine, and J. Dunlop. Resource Cost and QoS Achievement in a Contract-based Resource Manager for Mobile Communications Systems. IEEE/AFCEA EUROCOMM, May 2000.

[45] O. Yilmaz and I.R. Chen;. Utilizing Call Admission Control to Derive Optimal Pricing of Multiple Service Classes in Wireless Cellular Networks. IEEE ICPADS '06, July 2006.

[46] E. Viterbo and C. Chiasserini. Dynamic Pricing for Connection-oriented Services in Wireless Networks. IEEE International Symposium on Personal, Indoor and Mobile Radio Communications (PIMRC), Sep. 2001.

[47] S. Sengupta, M. Chatterjee, and K. Kwiat. Pricing-based Service and Network Selection in Overlaid Access Networks. IEEE ICICS '07, Dec. 2007.

[48] J. Delicado and J. Gozalvez. User Satisfaction Based CRRM Policy for Heterogeneous Wireless Networks. IEEE ISWCS '09, Sep. 2009.
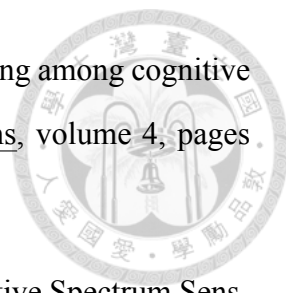
[49] L. Huang and M. Neely. The Optimality of Two Prices: Maximizing Revenue in a Stochastic Communication System. *IEEE/ACM Trans. on Networking*, 18(2):406 -- 419, 2010.

[50] H. Claussen, L. T. W. Ho, and L. G. Samuel. Financial Analysis of a Pico-Cellular Home Network Deployment. In *IEEE International Conference on Communications (ICC)*, Glasgow, Scotland, June 2007.

[51] N. Shetty, S. Parekh, and J. Walrand. Economics of Femtocells. In *IEEE Global Communications Conference (GLOBECOM)*, Dec. 2009.

[52] L.A. Stole. Nonlinear pricing and oligopoly. *Journal of Economics & Management Strategy*, 4(4):529--562, 1995.

[53] Guangxiang Yuan, Xiang Zhang, Wenbo Wang, and Yang Yang. Carrier aggregation for LTE-advanced mobile communication systems. *IEEE Communications Magazine*, 48(2):88--93, 2010.

[54] M. Iwamura, K. Etemad, Mo-Han Fong, R. Nory, and R. Love. Carrier aggregation framework in 3GPP LTE-advanced. *IEEE Communications Magazine*, 48(8):60--67, 2010.

[55] Zukang Shen, A. Papasakellariou, J. Montojo, D. Gerstenberger, and Fangli Xu. Overview of 3GPP LTE-advanced carrier aggregation for 4G wireless communications. *IEEE Communications Magazine*, 50(2):122--130, 2012.

[56] B. Wang, Y. Wu, and K. J. R. Liu. Game Theory for Cognitive Radio Networks: An Overview. *Computer Networks*, 54(14):2537--2561, Oct. 2010.

[57] N. Nisan, T. Roughgarden, and V. V. Vazirani. *Algorithmic Game Theory*. Cambridge University Press, 2007.

[58] G Galaviz, D H Covarrubias, and A G Andrade. On a Spectrum Resource Organization Strategy for Scheduling Time Reduction in Carrier Aggregated Systems. *IEEE Communications Letters*, 15(11):1202--1204, 2011.

[59] Anxin Li, K Takeda, N Miki, Yuan Yan, and Hidetoshi Kayama. Search Space Design for Cross-Carrier Scheduling in Carrier Aggregation of LTE-Advanced System. In IEEE International Conference on Communications (ICC), Kyoto, Japan, June 2011.

[60] Yuan Yan, Anxin Li, A Harada, and H Kayama. Enhanced Downlink Control Channel Resource Allocation Algorithm for Cross-Carrier Scheduling in LTE-Advanced Carrier Aggregation System. In IEEE Vehicular Technology Conference (VTC Spring), Budapest, Hungary, May 2011.

[61] Yong Li, Qin Mu, Liu Liu, Lan Chen, Mugen Peng, and Wenbo Wang. Control Channel Design for Carrier Aggregation between LTE FDD and LTE TDD Systems. In IEEE Vehicular Technology Conference (VTC Spring), Yokohama, Japan, May 2012.

[62] L G U Garcia, I Z Kovacs, K I Pedersen, G W O Costa, and P E Mogensen. Autonomous Component Carrier Selection for 4G Femtocells --- A Fresh Look at an Old Problem. IEEE Journal on Selected Areas in Communications, 30(3):525--537, 2012.

[63] Yong Xiao, Tim Forde, Irene Macaluso, Luiz A DaSilva, and Linda Doyle. Spatial spectrum sharing-based carrier aggregation for heterogeneous networks. In IEEE Global Communications Conference (GLOBECOM), Anaheim, California, USA, Dec. 2012.

[64] L. G. U. Garcia, G. W. O. Costa, A. F. Cattoni, K. I. Pedersen, and P. E. Mogensen. Self-Organizing Coalitions for Conflict Evaluation and Resolution in Femtocells. In IEEE Global Telecommunications Conference (GLOBECOM), Miami, Florida, USA, Dec. 2010.

[65] G W O Costa, A F Cattoni, I Z Kovacs, and P E Mogensen. A fully distributed method for dynamic spectrum sharing in femtocells. In IEEE Wireless

Communications and Networking Conference Workshops (WCNCW), Paris, France, Apr. 2012.

[66] Yao-Liang Chung and Zsehong Tsai. A quantized water-filling packet scheduling scheme for downlink transmissions in LTE-Advanced systems with Carrier Aggregation. In IEEE International Conference on Software, Telecommunications and Computer Networks (SoftCOM),, Split, Dubrovnik, Croatia, Sep. 2010.

[67] Yuanye Wang, K I Pedersen, T B Sorensen, and P E Mogensen. Carrier load balancing and packet scheduling for multi-carrier systems. IEEE Trans. on Wireless Communications, 9(5):1780--1789, 2010.

[68] Yuanye Wang, K I Pedersen, T B Sorensen, and P E Mogensen. Utility Maximization in LTE-Advanced Systems with Carrier Aggregation. In IEEE Vehicular Technology Conference (VTC Spring), Budapest, Hungary, May 2011.

[69] Fan Wu, Yuming Mao, Xiaoyan Huang, and Supeng Leng. A joint resource allocation scheme for OFDMA-based wireless networks with carrier aggregation. In IEEE Wireless Communications and Networking Conference (WCNC), Paris, France, Apr. 2012.

[70] EN ETSI. 300 392-2:" terrestrial trunked radio (tetra). Voice plus Data, 500(Part 2).

[71] D.C. Cox and D.O. Reudink. Dynamic Channel Assignment in High-capacity Mobile Communications Systems. Bell System Technical Journal, 50:1833--1857, 1971.

[72] L. Shapley and H. Scarf. On Cores and Invisibility. Journal of Mathematical Economics, 1(1):23--37, 1974.

[73] Chia-Hao Yu, K. Doppler, C.B. Ribeiro, and O. Tirkkonen. Resource sharing optimization for device-to-device communication underlaying cellular networks. IEEE Trans. on Wireless Communications, 10(8):2752 --2763, Aug. 2011.

[74] Bin Wang, Li Chen, Xiaohang Chen, Xin Zhang, and Dacheng Yang. Resource Allocation Optimization for Device-to-Device Communication Underlaying Cellular Networks. In IEEE Vehicular Technology Conference (VTC Spring), May 2011.

[75] M. Zulhasnine, Changcheng Huang, and A. Srinivasan. Efficient resource allocation for device-to-device communication underlaying lte network. In IEEE WiMob, Oct. 2010.

[76] Xiaoyue Zhu, Si Wen, Gen Cao, Xin Zhang, and Dacheng Yang. QoS-based resource allocation scheme for Device-to-Device (D2D) radio underlaying cellular networks. In ICT, April 2012.

[77] Xiaohang Chen, Li Chen, Mengxian Zeng, Xin Zhang, and Dacheng Yang. Downlink resource allocation for Device-to-Device communication underlaying cellular networks. In IEEE International Symposium on Personal, Indoor and Mobile Radio Communications (PIMRC), Sep. 2012.

[78] P. Janis, V. Koivunen, C. Ribeiro, J. Korhonen, K. Doppler, and K. Hugl. Interference-Aware Resource Allocation for Device-to-Device Radio Underlaying Cellular Networks. In IEEE Vehicular Technology Conference (VTC Spring), April 2009.

[79] M. Belleschi, G. Fodor, and A. Abrardo. Performance analysis of a distributed resource allocation scheme for D2D communications. In IEEE GLOBECOM Workshops, Dec. 2011.

[80] Chen Xu, Lingyang Song, Zhu Han, Qun Zhao, Xiaoli Wang, and Bingli Jiao. Interference-aware resource allocation for Device-to-Device communications as an underlay using sequential second price auction. In IEEE International Conference on Communications (ICC), June 2012.

[81] V. Bala and S. Goyal. Learning from neighbours. The Review of Economic Studies, 65(3):595, 1998.

[82] B. Golub and M.O. Jackson. Naïve learning in social networks: Convergence, influence, and the wisdom of crowds. Working Paper, 2007.

[83] D. Acemoglu, M.A. Dahleh, I. Lobel, and A. Ozdaglar. Bayesian Learning in Social Networks. LIDS report 2780, Review of Economic Studies, January 2011.

[84] Daron Acemoglu and Asuman Ozdaglar. Opinion dynamics and learning in social networks. Dynamic Games and Applications, 1:3--49, 2011.

[85] R.W. Cooper. Coordination games: Complementarities and macroeconomics. Cambridge University Press, 1999.

[86] M.L. Katz and C. Shapiro. Technology adoption in the presence of network externalities. The journal of political economy, pages 822--841, 1986.

[87] W.H. Sandholm. Negative externalities and evolutionary implementation. Review of Economic Studies, 72(3):885--915, 2005.

[88] G. Fagiolo. Endogenous neighborhood formation in a local coordination model with negative network externalities. Journal of Economic Dynamics and Control, 29(1-2):297--319, 2005.

[89] Seung-Jun Kim and G.B. Giannakis. Optimal resource allocation for mimo ad hoc cognitive radio networks. IEEE Trans. on Information Theory, 57(5):3117 --3131, May 2011.

[90] D. Aldous, I. Ibragimov, J. Jacod, and D. Aldous. Exchangeability and related topics. In Lecture Notes in Mathematics, volume 1117, pages 1--198. Springer Berlin / Heidelberg, 1985.

[91] J. Pitman. Exchangeable and partially exchangeable random partitions. Probability Theory and Related Fields, 102(2):145--158, 1995.

[92] C.-Y. Wang, Y. Chen, and K. J. R. Liu. Chinese Restaurant Game. IEEE Signal Processing Letters, 19(12):898 --901, Dec. 2012.

[93] S.M. Mishra, A. Sahai, and R.W. Brodersen. Cooperative sensing among cognitive radios. In IEEE International Conference on Communications, volume 4, pages 1658--1663, 2006.

[94] B. Wang, K. J. R. Liu, and T.C. Clancy. Evolutionary Cooperative Spectrum Sensing Game: How to Collaborate? IEEE Trans. on Communications, 58(3):890--900, Mar. 2010.

[95] K.J.R. Liu and B. Wang. Cognitive Radio Networking and Security: A Game-theoretic View. Cambridge University Press, 2010.

[96] H. Carlsson and E. Van Damme. Global games and equilibrium selection. Econometrica: Journal of the Econometric Society, pages 989--1018, 1993.

[97] S. Morris and H. Shin. Global games: theory and applications. Cowles Foundation Discussion Paper No. 1275R, 2001.

[98] G.M. Angeletos and I. Werning. Crises and prices: Information aggregation, multiplicity, and volatility. The American economic review, pages 1720--1736, 2006.

[99] V. Krishnamurthy. Decentralized activation in sensor networks-global games and adaptive filtering games. Digital Signal Processing, 2011.

[100] V. Krishnamurthy. Decentralized Spectrum Access Amongst Cognitive Radios: An Interacting Multivariate Global Game-Theoretic Approach. IEEE Trans. on Signal Processing, 57(10):3999 --4013, Oct. 2009.

[101] A. Dasgupta. Social learning with payoff complementarities. Working Paper, 2000.

[102] G.M. Angeletos, C. Hellwig, and A. Pavan. Signaling in a global game: Coordination and policy traps. Journal of Political Economy, 114(3):452--484, 2006.

[103] G.M. Angeletos, C. Hellwig, and A. Pavan. Dynamic global games of regime change: Learning, multiplicity, and the timing of attacks. Econometrica, 75(3): 711--756, 2007.

[104] J.S. Costain. A herding perspective on global games and multiplicity. The BE Journal of Theoretical Economics, 7(1):22, 2007.

[105] A. Dasgupta. Coordination and delay in global games. Journal of Economic Theory, 134(1):195--225, 2007.

[106] S.-F. Chang and A. Vetro. Video Adaptation: Concepts, Technologies, and Open Issues. Proceedings of the IEEE, 93(1):148 --158, Jan. 2005.

[107] S. Deb, S. Jaiswal, and K. Nagaraj. Real-Time Video Multicast in WiMAX Networks. In IEEE International Conference on Computer Communications (INFOCOM), Phoenix, AZ, USA, Apr. 2008.

[108] S. Chuah, Z. Chen, and Y. Tan. Energy-Efficient Resource Allocation and Scheduling for Multicast of Scalable Video over Wireless Networks. IEEE Trans. on Multimedia, (4):1324--1336, Aug. 2012.

[109] W. Ji, Z. Li, and Y. Chen. Joint Source-Channel Coding and Optimization for Layered Video Broadcasting to Heterogeneous Devices. IEEE Trans. on Multimedia, 14(2):443--455, Apr. 2012.

[110] Y. Chen, Y. Wu, B. Wang, and K. J. R. Liu. Spectrum Auction Games for Multimedia Streaming over Cognitive Radio Networks. IEEE Trans. on Communications, 58(8):2381--2390, August 2010.

[111] P. Polacek, T.-Y. Yang, and C.-W. Huang. Joint Opportunistic Spectrum Access and Scheduling for Layered Multicasting over Cognitive Radio Networks. In IEEE MMSP, Hangzhou, China, Oct. 2011.

[112] C.-W. Huang, S.-M. Huang, P.-H. Wu, S.-J. Lin, and J-N Hwang. OLM: Opportunistic Layered Multicasting for Scalable IPTV over Mobile WiMAX. IEEE Trans. on Mobile Computing, 11(3):453 --463, Jan. 2012.

[113] W.S. Lin and K. J. R. Liu. Game-Theoretic Pricing for Video Streaming in Mobile Networks. IEEE Trans. on Image Processing, 21(5):2667 --2680, May 2012.

[114] P.-H. Wu and Y.H. Hu. Optimal Layered Video IPTV Multicast Streaming Over Mobile WiMAX Systems. IEEE Trans. on Multimedia, 13(6):1395--1403, Dec. 2011.

[115] A. Dan, D. Sitaram, and P. Shahabuddin. Dynamic Batching Policies for an On-demand Video Server. Multimedia Systems, 4:112--121, 1996.

[116] Y. Chen and K. J. R. Liu. Understanding Microeconomic Behaviors in Social Networking: An engineering view. IEEE Signal Processing Magazine, 29(2):53 --64, Mar. 2012.

[117] W.S. Lin, H.V. Zhao, and K. J. R. Liu. Incentive Cooperation Strategies for Peer-to-Peer Live Multimedia Streaming Social Networks. IEEE Trans. on Multimedia, Special Issues on Community and Media Computing, 11(3):396 --412, April 2009.

[118] C. X. Jiang, Y. Chen, Y.H. Yang, C.Y. Wang, and K. J. R. Liu. Dynamic Chinese Restaurant Game in Cognitive Radio Networks. In IEEE International Conference on Computer Communications (INFOCOM), Turin, Italy, April 2013.

[119] C.-Y. Wang, Y. Chen, and K. J. R. Liu. Sequential Chinese Restaurant Game. IEEE Trans. on Signal Processing, 61(3):571 --584, Feb. 2013.

[120] Martin L. Puterman. Markov Decision Processes: Discrete Stochastic Dynamic Programming. John Wiley & Sons, Inc., 1st edition, 1994.

[121] Lars Haglund. SVT Video Test Sequence. SVT Sveriges Television AB, 2001.

[122] Haris Al Qodri Maarif, Teddy Surya Gunawan, and Othman Omran Khalifa. JSVM Reference Software.